Evolution equations for systems governed by social interactions

Evolution Equations for Systems Governed by Social Interactions

Joep Evers

Evolution Equations for Systems Governed by Social Interactions

Joep Evers

Cover: Sculpture based on the work of M.C. Escher (Houtrustweg 120, The Hague).
Photo by the author, used with kind permission of the M.C. Escher Company.

A catalogue record is available from the Eindhoven University of Technology Library

ISBN: 978-90-386-3851-5

Evolution Equations for Systems Governed by Social Interactions

PROEFSCHRIFT

ter verkrijging van de graad van doctor aan de Technische Universiteit Eindhoven, op gezag van de rector magnificus prof.dr.ir. F.P.T. Baaijens, voor een commissie aangewezen door het College voor Promoties, in het openbaar te verdedigen op maandag 1 juni 2015 om 16:00 uur

door

Joseph Hubertus Marianne Evers

geboren te Roermond

Dit proefschrift is goedgekeurd door de promotoren en de samenstelling van de promotiecommissie is als volgt:

voorzitter:	prof.dr. E.H.L. Aarts
1^{e} promotor:	prof.dr. M.A. Peletier
copromotor:	dr.habil. A. Muntean
leden:	prof.dr. J.A. Carrillo de la Plata (Imperial College London)
	dr. R.C. Fetecau (Simon Fraser University)
	prof.dr.ir. B. Koren
adviseurs:	dr. S.C. Hille (Universiteit Leiden)
	dr. H.M. Wyss

[Percy enters, wearing an extremely wide new neckruff]

Blackadder: "You look like a bird who's swallowed a plate. What do you think of Percy's ruff, Baldrick?"

Baldrick: "I think he looks like a bird who's swallowed a plate, my Lord."

Blackadder: "No, that's what *I* think. What do *you* think? Try to have a thought of your own, Baldrick; thinking is so important. What do *you* think?"

Baldrick: "I think thinking is so important, my Lord."

– *Blackadder II 2*

Abstract

In this thesis we consider mathematical models for systems of individuals that interact in a social way. Typical examples of such systems are crowds of pedestrians, flocks of birds or schools of fish. The models that we use are similar in spirit to descriptions of non-living particles and their physical interactions.
We consider the anisotropy that follows from the fact that people and animals have a field of vision: the influence a reference person experiences from another individual is weighted according to the direction in which he perceives the other. We obtain a model with implicitly defined velocity from which we deduce unique solutions via a regularization of the underlying ODE.
Measure theory provides a generalized framework that incorporates several perspectives ranging from ODEs for particle positions to PDEs for particle densities. We use this framework to derive systematically particle schemes for continuum equations and to prove their convergence in the Wasserstein distance.
We derive flux boundary conditions for measure-valued evolutions on bounded domains in the context of semigroups. First, we obtain the result for prescribed velocity field. Afterwards we use this result as a building block to deal with measure-dependent velocities. Finally, we quantify the error related to the approximation of a finite-size mass-emitting object by a point source.
The tools and techniques used are a combination of concepts taken from partial differential equations, measure theory, semigroup theory, continuum mechanics, functional analysis, probability theory, singular perturbation theory and numerical analysis.

Keywords: Measure-valued equations; mild solutions; particle systems; conservation laws; regularization; singular perturbation; convergence rate; pedestrian flows.

MSC 2010: 46E27; 28A33; 35Q91; 70Fxx; 34A12; 35L65; 65L11; 91Cxx.

PACS 2010: 02.30.Cj; 89.65.-s; 45.50.-j; 47.10.ab.

Contents

Chapter 1

Introduction

Underlying the work presented in this thesis is the very broad question:

How can we describe and predict
the behaviour of living, social individuals?

The attempt to capture social phenomena in (mathematical) formalism is not new. Scientists have had this idea ever since the Renaissance, in particular concerning human behaviour, as is described elaborately by Philip Ball in [Bal04]. In the scope of this thesis, we understand the word 'behaviour' primarily as meaning 'motion'. That is, we model how groups of social individuals move (in space) as the result of inter-individual interactions.

This work is relevant, because nowadays more and more large-scale events take place, where huge crowds gather. A combination of overcrowding, badly designed infrastructure and human emotions might lead to uncomfortable or even life-threatening situations. A clear example of how things can go wrong is the Love Parade that took place on the 24th of July 2010 in the German city of Duisburg: 21 people lost their lives in a stampede. More information can be found e.g. in [Gua, Sue, Tag]. For me personally, the events in Duisburg are significant too, since this drama happened around the time when I first started studying models for crowd behaviour.

There are other important, but less dramatic reasons for modelling social individuals:

- Civil engineers need to be sure at the design stage that train stations, airports and other public buildings can cope with the expected flow of people.
- In biological aggregations often complex dynamic patterns arise. Can such patterns form without a 'leader' or 'mastermind'?
- To be able to 'fluidize' motion in traffic jams, understanding of the basic mechanisms of vehicular traffic is required.
- Related to the two previous points: Self-organizing biological groups have been a source of inspiration for designing interacting robots. Based on the same ideas

smart self-driving cars are built. Such cars can be used e.g. to regulate traffic on highways.

Over the last decades, mathematical models inspired by biology, social sciences and life sciences have become a substantial area of interest for researchers working in the fields of (partial) differential equations, functional analysis and measure theory. Formerly, the associated problems were mostly treated heuristically and only by means of numerical simulations. This research has a broad variety of applications, while the mathematics involved is challenging in its own right.

It is exactly this combination of societal relevance and modern mathematics that was the main motivation for the work presented here. However, before we can solve any major real-world problem, we need to understand the pieces that make up the whole. In this thesis, we contribute to a better understanding of those pieces. The approach we take travels along and across the borders between partial differential equations, measure theory, semigroup theory, continuum mechanics, functional analysis, probability theory, singular perturbation theory and numerical analysis.

We use the following mathematical question as a guide:

Can ideas from mathematical physics provide inspiration when modelling and analyzing systems of socially interacting individuals?

We focus on models in which the solutions are measure-valued. More specifically, we consider trajectories in the space of measures parameterized by time, where the measure represents the distribution of our individuals in space.

Why do we choose to work in this measure-theoretical setting?

- Measure-valued evolutions provide a useful framework for unifying in a single formalism several points of view ranging from ODEs for particle positions to PDEs for particle densities, and from stochastic equations to equations for statistical data of low regularity. Such unification moreover facilitates the transition between perspectives, e.g. in discrete-to-continuum limits.
- Measure-valued equations allow for solutions that concentrate on lower-dimensional manifolds, e.g. on curves in two-dimensional space. Additionally, point masses and contributions with a density may be present. Models with 'hybrid' solutions of this type have the advantage that keeping track of the individual parts in an explicit, artificial way is not necessary.

This chapter is an introduction to the main ideas of this thesis with particular emphasis on the measure-theoretical concepts we use. We explain in Sections 1.1 and 1.2 the two basic ingredients of the title of this thesis: 'evolution equations' and 'social interactions'. The remainder of the chapter describes the wider context of the topics treated in the individual chapters and the connections between them. Also, references to the relevant literature are provided. Since we focus on the general message, many details are omitted here or postponed to the coming chapters. A chapter-wise overview of the thesis is given in Section 1.7.

1.1 Evolution equations

The central equation of this thesis is the formal expression

$$\boxed{\frac{\partial \mu}{\partial t} + \nabla \cdot (\mu\, v) = 0,} \tag{1.1}$$

which closely resembles the well-known continuity equation. Here, μ is a measure describing the distribution of mass in space, t is the time variable and v is a velocity field to be specified. The continuity equation is omnipresent in mathematical physics; it is the mathematical formulation of the concept of local conservation of mass. The evolution in time of a solution to (1.1) is dictated by v. Choosing v is a crucial step in the modelling process.

In (1.1) the continuity equation is written in terms of measures, which should merely be interpreted as a short-hand notation for its weak formulation. Let $\mathcal{M}^+(\mathbb{R}^d)$ be the space of positive, finite Borel measures on $\mathbb{R}^d$ and let $T > 0$ be some fixed final time. Then $\mu \in C([0,T]; \mathcal{M}^+(\mathbb{R}^d))$ is a continuous trajectory (in an appropriate metric) in $\mathcal{M}^+(\mathbb{R}^d)$ parameterized by $t \in [0,T]$. It is said to be a *weak solution* of (1.1) with initial condition $\nu_0 \in \mathcal{M}^+(\mathbb{R}^d)$ if it satisfies

$$\int_{\mathbb{R}^d} \psi(T,x)\, d\mu_T(x) - \int_{\mathbb{R}^d} \psi(0,x)\, d\nu_0(x) = \int_0^T \int_{\mathbb{R}^d} \frac{\partial \psi}{\partial t}(t,x) + \nabla \psi(t,x) \cdot v(x)\, d\mu_t(x)\, dt \tag{1.2}$$

for all $\psi : [0,T] \times \mathbb{R}^d \to \mathbb{R}$ in a class of test functions. A typical choice is $\psi \in C_c^\infty([0,T] \times \mathbb{R}^d)$, the space of infinitely continuously differentiable functions with compact support, or $\psi \in C_b^1([0,T] \times \mathbb{R}^d)$, the space of bounded and continuous functions with bounded and continuous first derivatives. The exact space of test functions is usually problem-dependent. See e.g. [Tai04], pp. 62–64, for an overview of how the modelling of different kinds of boundaries leads to different boundary conditions on the test functions.

For simplicity, we assume for the moment that the velocity field v is a Lipschitz continuous function on $\mathbb{R}^d$. Whenever we write 'Lipschitz continuous' without further specification, we mean '*globally* Lipschitz continuous'. Hence, by the Picard-Lindelöf Theorem, the initial value problem

$$\begin{cases} \dfrac{dx}{dt} = v(x(t)); \\ \\ x(0) = x_0, \end{cases} \tag{1.3}$$

has a unique global solution $x(\,\cdot\,; x_0) : [0,\infty) \to \mathbb{R}^d$ for all $x_0 \in \mathbb{R}^d$. We associate to this solution a mapping Φ_t that maps the initial position x_0 to the solution of (1.3) at time t:

$$\Phi_t(x_0) := x(t; x_0),$$

for all $t \in [0,\infty)$ and $x_0 \in \mathbb{R}^d$. The family of mappings $(\Phi_t)_{t \geqslant 0}$, often called *motion mapping*, is a semigroup. That is, it satisfies the property that Φ_0 is the identity, and

$\Phi_s\Phi_t = \Phi_{s+t}$ for all $s, t \geqslant 0$. For each t and $\mu \in \mathcal{M}(\mathbb{R}^d)$, we call the object $\Phi_t\#\mu$, the *push-forward measure* of μ by Φ_t if

$$\int_{\mathbb{R}^d} f(x)\, d(\Phi_t\#\mu)(x) = \int_{\mathbb{R}^d} f(\Phi_t(x))\, d\mu(x) \tag{1.4}$$

holds for all measurable, bounded functions f on $\mathbb{R}^d$. The measure $\Phi_t\#\mu$ represents the distribution of mass after a transformation of all material points by the motion mapping Φ_t, if mass was originally distributed according to μ. Essentially, what we see in (1.4) is a coordinate transform.

We use the push-forward operator to lift the semigroup $(\Phi_t)_{t\geqslant 0}$ on $\mathbb{R}^d$ to the space of measures $\mathcal{M}(\mathbb{R}^d)$, and we define $P_t : \mathcal{M}(\mathbb{R}^d) \to \mathcal{M}(\mathbb{R}^d)$ for each $t \geqslant 0$ by

$$P_t\mu := \Phi_t\#\mu \tag{1.5}$$

for all $\mu \in \mathcal{M}(\mathbb{R}^d)$. The fact that $(\Phi_t)_{t\geqslant 0}$ is a semigroup implies that $(P_t)_{t\geqslant 0}$ is a semigroup. Moreover, $(P_t)_{t\geqslant 0}$ preserves positivity.

We now present an alternative solution concept for (1.1) that is closely related to the semigroup defined in (1.5). A *mild solution* of (1.1) is defined as a trajectory $\mu \in C([0,T];\mathcal{M}^+(\mathbb{R}^d))$ that satisfies

$$\mu_t = P_t\nu_0 \tag{1.6}$$

for all $t \in [0,T]$, where $\nu_0 \in \mathcal{M}^+(\mathbb{R}^d)$ is the given initial condition. Equation (1.6) explicitly *defines* the measure μ_t for all t. It is a simplified example of a more involved concept that is introduced in (1.10). Let us show first that mild solutions are weak solutions.

Let $\nu_0 \in \mathcal{M}^+(\mathbb{R}^d)$ be given and assume that $\mu \in C([0,T];\mathcal{M}^+(\mathbb{R}^d))$ satisfies $\mu_t = P_t\nu_0$ for all $t \in [0,T]$. Then a simple calculation shows that

$$\begin{aligned}
&\int_0^T\int_{\mathbb{R}^d}\left[\frac{\partial\psi}{\partial t}(t,x) + \nabla\psi(t,x)\cdot v(x)\right] d\mu_t(x)\, dt \\
&\qquad \overset{(1.4)}{=} \int_0^T\int_{\mathbb{R}^d}\left[\frac{\partial\psi}{\partial t}(t,\Phi_t(x)) + \nabla\psi(t,\Phi_t(x))\cdot v(\Phi_t(x))\right] d\nu_0(x)\, dt \\
&\qquad \overset{(1.3)}{=} \int_0^T\int_{\mathbb{R}^d}\frac{d}{dt}\left[\psi(t,\Phi_t(x))\right] d\nu_0(x)\, dt \\
&\qquad = \int_{\mathbb{R}^d}\psi(T,x)\, d\mu_T(x) - \int_{\mathbb{R}^d}\psi(0,x)\, d\nu_0(x),
\end{aligned} \tag{1.7}$$

for all $\psi \in C_b^1([0,T]\times\mathbb{R}^d)$. Hence μ is a weak solution.

Remark 1.1.1. Weak solutions, however, are not necessarily mild solutions.

The definition of a mild solution becomes more involved if we introduce a source or sink term in (1.1):

$$\frac{\partial \mu}{\partial t} + \nabla \cdot (\mu\, v) = F(t, \mu), \tag{1.8}$$

where $F : [0,T] \times \mathcal{M}(\mathbb{R}^d) \to \mathcal{M}(\mathbb{R}^d)$. The weak formulation corresponding to (1.8) is:

$$\int_{\mathbb{R}^d} \psi(T,x)\, d\mu_T(x) - \int_{\mathbb{R}^d} \psi(0,x)\, d\nu_0(x) = \int_0^T \int_{\mathbb{R}^d} \frac{\partial \psi}{\partial t}(t,x) + \nabla \psi(t,x) \cdot v(x)\, d\mu_t(x)\, dt + \int_0^T \int_{\mathbb{R}^d} \psi(t,x)\, d\mu_{F,t}(x)\, dt, \tag{1.9}$$

for all $\psi : \mathbb{R}^d \to \mathbb{R}$ in the same class of test functions as in (1.2), say $\psi \in C_b^1([0,T] \times \mathbb{R}^d)$. The measure $\mu_{F,t}$ is for all $t \in [0,T]$ defined as $\mu_{F,t} := F(t, \mu_t)$.

Mild solutions satisfy, by definition, a generalized variant of (1.6). Recall that $(P_t)_{t \geqslant 0}$ is the semigroup on $\mathcal{M}(\mathbb{R}^d)$ associated to the flow induced by v. A trajectory $\mu \in C([0,T]; \mathcal{M}^+(\mathbb{R}^d))$ is called a mild solution of (1.8) if it satisfies

$$\mu_t = P_t \nu_0 + \int_0^t P_{t-s} F(s, \mu_s)\, ds \qquad \text{for all } t \in [0,T]. \tag{1.10}$$

This equation is referred to as the *variation of constants formula*; cf. e.g. Chapter 6 of [Paz83].[1] The integral in (1.10) is itself a measure and should be understood in the sense of Bochner integrals. Further details about integration of measure-valued maps are given in Chapter 2 of [DU77] and in Appendix B of this thesis. One can prove, in the spirit of (1.7), that mild solutions in the sense of (1.10) are weak solutions in the sense of (1.9). See also the proof of Proposition 3.7 in [Hoo13] that treats a comparable case.

We have now introduced the basic ingredients that are used in the remainder of this thesis in the following way:

(i) We consider a particle system in Chapter 2; that is, we consider a *discrete measure* ν_0 in (1.6). This implies that we only need to trace the positions of the corresponding point masses. The underlying equation for the mapping Φ occurs in Chapter 2 first as a system of coupled first-order (in time) ODEs, secondly as an implicit equation for $\dot{\Phi}$, and thirdly as a second-order ODE. The third formulation is used as a tool to approximate the implicit expression by means of a small parameter. A more extensive introduction to Chapter 2 is given in Section 1.7.1.

(ii) In Chapter 3, Φ follows from a second-order equation which is derived from physical considerations. The resulting measure-valued evolution follows from (1.6). This

[1] The concept of a mild solution can be defined in the same way for general differential operators A, such that $-A$ generates a (strongly continuous) semigroup. This is done in Chapter 6 of [Paz83]. Compare this also to *Duhamel's principle*; [Eva10], p. 49.

chapter focusses on approximating the initial data and proves that the corresponding solutions converge. A special case is the approximation of a continuum by a particle system. More details are provided in Section 1.7.2 and in Chapter 3.

(iii) Chapter 4 starts from (1.10). The semigroup $(P_t)_{t\geqslant 0}$ however follows from the evolution restricted to a bounded domain (the interval $[0,1]$). We derive flux boundary conditions at 0 and 1 by means of a vanishing absorption zone near the boundary. In this zone, mass is taken away at a certain rate according to F that is non-Lipschitz in μ. Due to the fact that F lacks sufficient regularity, a non-standard approach is required in the analysis. In Chapter 5 we proceed along the lines of Chapter 4 and we introduce a procedure that resembles the forward-Euler method for ODEs (see Chapter 2 in [But03]), to define mild solutions when v depends on the solution itself; see also Section 1.7.3.

(iv) We treat the diffusion equation with a measure-valued point source in Chapter 6. Mild solutions to this equation are defined via the variation of constants formula (1.10) with $(P_t)_{t\geqslant 0}$ replaced by the *diffusion semigroup*. For more details, see Section 1.7.4.

The extension from $v : \mathbb{R}^d \to \mathbb{R}^d$ to measure-dependent velocity fields in Chapter 5 enables us to incorporate mutual interactions that influence individuals' motion. This is what the words 'social interactions' in the title of this thesis refer to. In (i) and (ii) above, these interactions play a role too, although they were not mentioned explicitly.

1.2 Social interactions

In the previous section we used the velocity field $v : \mathbb{R}^d \to \mathbb{R}^d$ for simplicity of presentation. Much more interesting are those cases in which v is also time-dependent or even depends on the solution itself. In this thesis, one of the central choices for v is of the form

$$v[\mu_t](x) := (\mathcal{K} * \mu_t)(x) = \int_{\mathbb{R}^d} \mathcal{K}(x-y)\, d\mu_t(y). \tag{1.11}$$

This expression represents interactions between the 'individuals' that are described by μ_t. Typically, $\mathcal{K}$ includes a short-range repulsion zone and a long-range attraction zone. These are natural mechanisms in social groups: on the one hand an individual (person, bird, fish,...) wants to avoid collisions, but on the other hand he/she does not want to lose contact with the rest of the group.
Often, $\mathcal{K}$ arises from an *interaction potential*, i.e. there is a function $K : \mathbb{R}_0^+ \to \mathbb{R}$ such that $\mathcal{K}(\xi) := -\nabla_\xi K(|\xi|) = -K'(|\xi|)\frac{\xi}{|\xi|}$. A common choice for K is the *Morse potential* [LTB09, CDM$^+$07]. In this thesis we will only occasionally be concerned with issues about the regularity of $\mathcal{K}$, such as boundedness or differentiability in the origin. In [BCL09] such issues are addressed for particle solutions based on (1.3) and (1.11) with attractive interaction kernels. Depending on the behaviour of the kernel around the origin (cf. in particular the so-called *Osgood condition*) collisions and collapse into a single point can happen in finite or infinite time; see Theorem 2.1 in [BCL09]. See also [CDF$^+$11] for

further results. To avoid these degeneracy problems, one needs to choose an appropriate interaction potential such that particle collisions do not happen.

A particular feature that makes living individuals different from non-living particles is that most species have a restricted zone of social perception, defined by the limitations of their field of vision or of other perception senses [SK81, KH12]. We assume that vision is the most important factor in the decision-making process that leads to an individual's motion and we disregard all other senses. Due to anatomy, i.e. the position of the eyes, the amount of information received is not the same for each direction. In the models that are studied in this thesis, this is reflected by incorporating weights (see Chapter 2) to the influence one reference individual experiences from another, depending on the direction in which he/she perceives the other. See Figure 1.1 for a schematic illustration. We use a function $\bar{g} : (-\pi, \pi] \to [0, 1]$ to relate these weights, $\bar{g}(\phi_{ik})$, to the angle ϕ_{ik} as defined in Figure 1.1.

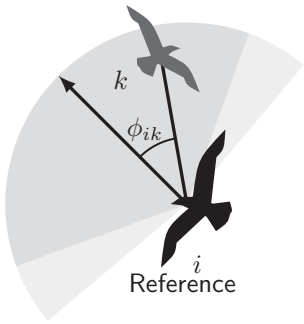

Figure 1.1: Illustration of the angle-dependent visual perception of the individual i. Individual i perceives individual k under an angle ϕ_{ik} with respect to the velocity of i. We distinguish between three basic regions: the field of vision (dark grey), the zone of peripheral vision (light grey) and the blind zone (white).

Sometimes the word *cone of vision* is used in this context. We avoided this word up to now, because it suggests that inside this cone (say, the dark grey area in Figure 1.1) there is full vision, while outside there is none. We opt for an approach in which there is a more gradual transition from full vision in the direction of motion to (nearly) no vision: the function $\bar{g}$ is continuous. In Figure 1.1, three zones are indicated: the dark grey field of vision, the light grey periphery and the white blind zone. The function $\bar{g}$ is a continuous representation of these zones. In the field of vision $\bar{g}$ is nearly 1, in the periphery there is a sharp but smooth transition, and in the blind zone $\bar{g}$ is nearly 0; see also Figure 2.2a and the corresponding graph in Figure 2.2b.

The field of vision as introduced in this section is the central topic of Chapter 2 where our main concern is to guarantee existence and uniqueness of solutions (see also Section 1.7.1). Velocity fields of the form (1.11) appear in a first-order model in Chapters 2 and 5. Moreover, a convolution term resembling (1.11) is used in Chapter 3 where it repres-

ents mutual interactions in a force balance. This force balance is given as a second-order in time evolution equation. In the next section, Section 1.3, we explain how first- and second-order models relate.

1.3 First- and second-order equations

Note that (1.1) is an equation written (formally) as a PDE in Eulerian coordinates. By introducing the concept of mild solutions, in some sense we made a transition to a Lagrangian formulation, in which the transport of mass is linked via (1.6) and (1.5) to an underlying ODE (1.3) that defines the trajectories of individual material points. Let us now place this underlying equation (1.3) in a slightly broader perspective.

In Section 1.1, the measure-valued trajectory μ is induced by the motion mapping $(\Phi_t)_{t\geqslant 0}$ that is in turn the solution of the simple equation of motion

$$\dot{\Phi}_t(x) = \mathcal{F}(\Phi_t(x)), \tag{1.12}$$

for each $x \in \mathbb{R}^d$, where $\mathcal{F} : \mathbb{R}^d \to \mathbb{R}^d$ is *given*. As explained in Section 1.2, ultimately we are interested in systems that have the structure

$$\begin{cases} \dot{\Phi}_t(x) = \mathcal{F}[\mu_t](\Phi_t(x)); & \text{(1.13a)} \\ \mu_t = \Phi_t \# \nu_0, & \text{(1.13b)} \end{cases}$$

where $\mathcal{F}$ is of the form (1.11). We introduce the symbol $\mathcal{F}$ instead of the symbol v used in (1.3), since this term will be interpreted as a *force* in (1.14). If the initial measure ν_0 is discrete or absolutely continuous, then (1.13) reduces to a system of coupled ODEs for the positions of the point masses, or a PDE for the density, respectively. The density of an absolutely continuous measure is also called *Radon-Nikodym derivative*; see Sections 30 and 31 in [Hal59] for more details.

Remark 1.3.1 (Existence and uniqueness of solutions)**.** At the level of ODEs (with or without interactions) existence and uniqueness are typically proved using the Picard-Lindelöf Theorem (also called Cauchy-Lipschitz Theorem, see [Tes12], Theorem 2.2). Such arguments are used in Chapters 2, 3 and 4 of this thesis. In Chapter 4, the Picard-Lindelöf Theorem is used to derive well-posedness for the underlying motion mapping with prescribed velocity (before a restriction to $[0, 1]$ is imposed and mass decay is considered). At the PDE level, the well-posedness of the model with interactions was studied in [BV06, BL07, BLR11], and its long-time behaviour in [BDF08, LTB09, FHK11, FH13]. One focus of the analytical investigations was on the possibility of the blow-up of the solutions via mass concentration into one or several Dirac measures when the potential K is attractive [FR10, BCL09, HB10, CDF$^+$11].
For *general* measures however (i.e. without any prior knowledge about whether the measure is discrete or absolutely continuous), the solution concept related to (1.13) is not as straightforward as in Section 1.1. There, the procedure is unidirectional in the sense that Φ_t does not depend on μ_t, and μ_t is simply defined by the variation of constants formula. More effort is needed to obtain well-posedness of the system if the equation for Φ_t does depend on the measure μ_t, like in (1.13). This issue will be addressed in Chapter 3, in particular in Part 1 of Theorem 3.3.10, and throughout Chapter 5.

The discrete and continuum formulations appear (in several different ways) in many places in literature, for instance in the context of mathematical models for biological aggregations; see e.g. the list of references in [MEK99, TBL06]. In Section 1.4, we take a closer look at discrete and continuum views (and what lies in between).

The first-order ODE (1.12) is closely related to a second-order damped Newton-like equation of the form

$$m\ddot{\Phi}_t(x) = -\dot{\Phi}_t(x) + \mathcal{F}(\Phi_t(x)), \tag{1.14}$$

where m is a particle's (read: material point's) mass. We see that the choice for the symbol $\mathcal{F}$ in (1.14) is appropriate, because this term refers to (external) forces. Depending on the specific setting we are considering, $\mathcal{F}$ may be of the form $\mathcal{F} = \mathcal{F}[\mu_t]$. Formally, (1.12) follows from (1.14) in the limit $m \downarrow 0$. In literature, different terms are used to describe this and closely related procedures, and they occur in several distinct settings. We discuss the terminology and context now.

In [BV05], (1.13a) is used with $\mathcal{F}$ of the form (1.11). In comparison with the second-order equation, (1.12) is described from a mechanical point of view as a situation in which mass is negligible (cf. the limit $m \downarrow 0$ in the above) and motion is dominated by friction. Changes in velocity occur instantaneously as a reaction to external and interaction forces. The authors of [BV05] concentrate on cell movement and also provide a biological interpretation. Equation (1.12) reflects the absence of persistence (or: inertia [FS14]) of cells. Rigorous results about the convergence of solutions in the limit $m \downarrow 0$ are given in e.g. [Tik52, Vas63, FS14]. In opposite direction, (1.14) follows from (1.12) by the introduction of a small response time for the individuals; see [EFR14] (or Chapter 2 of this thesis), which elaborates on this point.

Furthermore, the passage from second- to first-order equations is well-established in the context of *stochastic* differential equations (SDE). The Langevin equation (see e.g. [Pav14, Sch02]) is the stochastic counterpart of (1.14), that follows from the particular choice $\mathcal{F} = -\nabla V$ for some $V : \mathbb{R}^d \to \mathbb{R}$, and the incorporation of a noise term. Analogously to taking the limit $m \downarrow 0$ in (1.14), a first-order equation can be obtained from the Langevin equation by sending a friction coefficient to infinity; cf. [Nel67], Chapter 10 and [LRS10], Remark 2.16. This procedure is called the (highly) overdamped limit [Nel67, LRS10, Pav14], Smoluchowski limit [Pav14], high friction limit [GPK12], or large viscosity limit [Kra40]. The resulting first-order equation is called the Smoluchowski SDE [Nel67], or simply overdamped Langevin equation. Note that (1.14) and (1.12) are the deterministic counterparts of the Langevin and Smoluchowski SDEs, respectively.

Both the Langevin equation and the Smoluchowski equation are SDEs for a random variable. They each have an associated PDE for the corresponding probability density, which we refer to as the *kinetic equation* and the *Fokker-Planck equation*, respectively. One can pass from the kinetic to the Fokker-Planck equation in a way that is compatible with the overdamped limit. This procedure was described first by [Kra40]; see also e.g. [LRS10], Proposition 2.15. The kinetic equation associated to a deterministic second-order ODE is usually interpreted via the many-particle limit. Further details are given in Section 1.4. Performing the overdamped limit is also possible in this determi-

nistic setting. A rigorous result is given in [FS14] for those $\mathcal{F}$ that are of convolution type.

In Chapter 2 (and [EFR14]) we explicitly exploit the relation between (1.13a) and (1.14) for the vanishing inertia term. A result by Tikhonov, see [Tik52, Vas63], shows that the limit $m \downarrow 0$ can be performed in the smooth regime, provided that the solutions of the first-order equation are asymptotically stable in a certain sense (further details are delayed until Section 1.7.1 and Chapter 2). Typically, the solution of the second-order equation for any $m > 0$ fixed is a 'smoothed' version of the solution of the first-order equation.

1.4 Modelling perspectives

In the previous section, Section 1.3, we have mentioned discrete and continuum descriptions as special cases associated to (1.13) or, more generally, associated to (1.1). Let us now discuss more elaborately the level at which our systems are described. To facilitate the exposition we use the overview presented in Figure 1.2, in which we also incorporate some of the ideas mentioned in Section 1.3.

Let the initial measure ν_0 be a discrete measure; that is, a weighted sum of N Dirac measures: $\nu_0 := \sum_{i=1}^N \alpha_i \delta_{x_{i,0}}$. Here, the set of prefactors $(\alpha_i)_{i=1}^N \subset \mathbb{R}^+$ is fixed and the set $(x_{i,0})_{i=1}^N \subset \mathbb{R}^d$ denotes the initial configuration. In Chapter 3 we treat *probability measures* of this kind, which satisfy the constraint $\sum_{i=1}^N \alpha_i = 1$. The space of all probability measures is denoted by $\mathcal{P}(\mathbb{R}^d)$. The so-called *empirical measure* is an example of such measure for which $\alpha_i = 1/N$ for all i.

Assume that the (possibly measure-dependent) equation of motion for Φ, see e.g. (1.12) or (1.13a), is well-posed and yields a unique trajectory $(\Phi_t(x_0))_{t\geqslant 0}$ for each $x_0 \in \mathbb{R}^d$, or at least if $x_0 = x_{i,0}$, for any $i \in \{1, \dots, N\}$. Then the corresponding solution is a discrete measure for all time $t \geqslant 0$ and is of the form

$$\mu_t = \sum_{i=1}^N \alpha_i \delta_{\Phi_t(x_{i,0})}. \tag{1.15}$$

We are now in a *microscopic setting*: we follow individual material points (or simply: individuals). The term 'microscopic' typically refers *only* to situations in which we have a discrete measure and hence a system of (coupled) ODEs describing particle positions. The way in which we defined mass evolution (by means of a push-forward) implies however that the motion mapping (and thus the ODE, or SDE) is also present if we have a mass density or general mass distribution. The second- and first-order equations in the two blocks at the top of Figure 1.2 are underlying all our approaches; they are however only called 'microscopic equations' if we consider a particle system.

In Section 1.3 we have discussed the blocks in Figure 1.2 named 'kinetic' and 'Fokker-Planck' in the context of the Langevin and Smoluchowski SDEs and their related PDE for probability densities. In [BV05], the authors perform (formally) the transition between the first-order ODE/SDE and the macroscopic PDE (Fokker-Planck) both in the presence

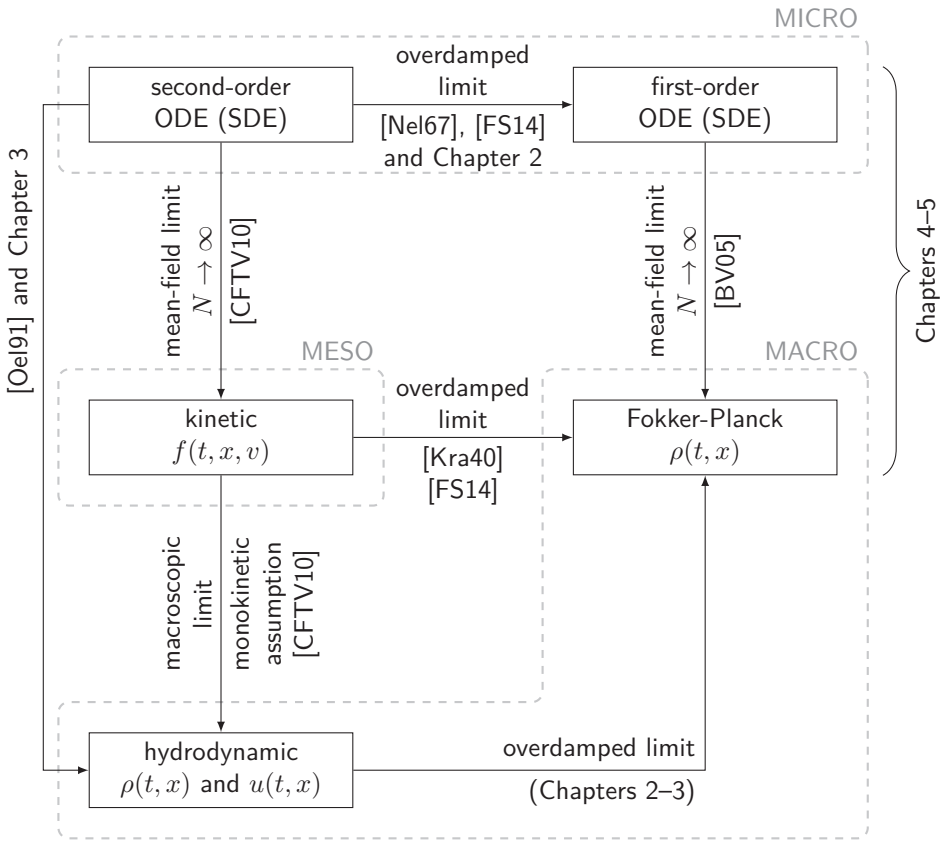

Figure 1.2: Schematic overview of model perspectives and the relation between first- and second-order equations of motion. The given references are indicative and certainly not exhaustive. Chapter numbers refer to chapters of this thesis.

and in the absence of the stochastic term. A stochastic interpretation of this transition between equations is that we take the limit $N \to \infty$ of N independent realizations $(X_i(t))_{t \geqslant 0}$, $i \in \{1, \dots, N\}$, of the dynamics dictated by the SDE. Random effects are present in each realization both via the randomness of the initial position and via the stochastic noise term. The result obtained by taking the limit $N \to \infty$ is closely related to the *law of large numbers*. This approach is demonstrated in [MCO05], in which the authors show (weak) convergence of the aforementioned empirical measure (or empirical distribution)

$$\rho_t^N = \frac{1}{N} \sum_{i=1}^{N} \delta_{X_i(t)}. \tag{1.16}$$

with $X_i(t)$ the independent realizations according to the Smoluchowski SDE. The limit equation is called the *mean-field* equation. In the deterministic case, the limit object ρ is considered as a mass density rather than as a probability measure. Nevertheless, it

is possible to use (1.16) as some approximating discrete measure, still called empirical measure, but without the stochastic interpretation of $X_i(t)$. Rigorous results regarding the convergence as $N \to \infty$ were given in [Oel90] using the empirical measure. Well-posedness for (a specific form) of the limit equation was proved in [BV06].

The *kinetic* equation follows from the Langevin SDE in a law of large numbers-like procedure called *mean-field limit*[2]. There is an underlying equation for $\ddot{X}_i(t)$, $i \in \{1, \dots, N\}$, in terms of $\dot{X}_i(t)$ and $X_i(t)$. The crucial point is now to consider the empirical measure not just on the space of positions (i.e. $\mathbb{R}^d$) but on the product space of positions and velocities: $\mathbb{R}^d \times \mathbb{R}^d$. The empirical measure to approximate the limit density $f_t \in \mathcal{P}(\mathbb{R}^d \times \mathbb{R}^d)$ is given by

$$f_t^N = \frac{1}{N} \sum_{i=1}^{N} \delta_{X_i(t)} \otimes \delta_{\dot{X}_i(t)}, \tag{1.17}$$

for each $t \geqslant 0$. Equation (1.17) is the counterpart of (1.16). The limit equation for f_t is derived formally in the context of weak formulations in [CFTV10] for two specific microscopic equations. The rigorous statements (in terms of the *1-Wasserstein distance* between measures) are also given; see also [CCR11]. The Wasserstein distance is introduced in Chapter 3, Definition 3.3.3. In [FS14] the formal limit is derived in a similar fashion for an equation with the same structure as (1.14). The resulting equation is a PDE for $f : [0, \infty) \to \mathcal{P}(\mathbb{R}^d \times \mathbb{R}^d)$ with partial derivatives in both the x and v variables. The kinetic equation describes what is called the *mesoscopic* level (as indicated in Figure 1.2). This is an intermediate level: in one position the velocity is not prescribed but distributed according to a certain probability density.

The next step, called 'macroscopic limit' in Figure 1.2, is to lose the v-dependency. To this aim, we redefine ρ_t as

$$\rho_t := \int_{\mathbb{R}^d} f_t(\cdot, dv), \tag{1.18}$$

i.e. we integrate out the velocity. The quantity ρ_t is called the *macroscopic density* of f_t.

Similarly, the mean velocity u is defined by

$$\rho_t \, u_t := \int_{\mathbb{R}^d} v \, f_t(\cdot, dv). \tag{1.19}$$

The limit equations (for ρ and u) are called *hydrodynamic equations* – cf. the terminology in Figure 1.2 – and are obtained by integrating the kinetic equation over the velocity coordinate, as we will show now. Note that we deliberately did not show the kinetic equation to avoid an overabundance of notation, but we refer to the examples given in e.g. [CFTV10, FS14]. If we integrate the kinetic equation over v then we obtain the continuity equation

$$\frac{\partial \rho}{\partial t} + \nabla \cdot (\rho \, u) = 0, \tag{1.20}$$

[2]The word 'mean-field' is also used e.g. in [MCO05] for the limit of the first-order equation.

for the macroscopic density. The second step is to multiply the kinetic equation by v and integrate afterwards. A term of the form $\int_{\mathbb{R}^d} |v|^2 \, f_t(\cdot, dv)$ will appear, which cannot be readily expressed in terms of ρ and u. Instead, an extra assumption (closure relation) is needed. We use here the *monokinetic assumption*, which states that all material points at the same position move according to the mean velocity:

$$\int_{\mathbb{R}^d} |v - u_t|^2 \, f_t(\cdot, dv) = 0, \tag{1.21}$$

or

$$f_t(x, v) = \rho_t(x) \, \delta_{v - u_t(x)}. \tag{1.22}$$

The equation that results from multiplication by v and integration, followed by application of the monokinetic assumption, is a PDE that reflects the conservation of momentum. It is a vector-valued equation for which the kth component has the form

$$\frac{\partial}{\partial t}(\rho u_k) + \nabla \cdot (\rho u u_k) = \mathfrak{f}_k[\rho, u], \tag{1.23}$$

cf. (16) in [CDM$^+$07] and (2.4) in [CC08]. The right-hand side $\mathfrak{f}$ in (1.23) is model-dependent and includes a (functional) dependence on ρ and u. See the exposition in [CFTV10] for more details.

In view of the limit object ρ, the hydrodynamic limit (1.20)–(1.23) resembles the mean-field limit for first-order dynamics. Both reflect the macroscopic perspective – cf. Figure 1.2. Note that an alternative for the introduction of the monokinetic assumption is to multiply by $|v|^2$, integrate and use a different closure relation in the equation for the second moment. This yields an additional equation representing conservation of energy.

Formulated *in terms of measures*, the transition from the second-order ODE to the kinetic equation and, subsequently, to the hydrodynamic limit, is treated in Chapter 8 of [CPT14]. In Chapter 3 of this thesis we perform the discrete-to-continuum limit immediately from a second-order ODE to the hydrodynamic limit. This is in fact a special case of the more general result presented in Chapter 3 involving the convergence of general measure-valued solutions in the 1-Wasserstein distance. The special case holds for measures of the form (1.15), hence also for the empirical measure. In [Oel91] convergence of the *empirical measure* is proven, using weak convergence. The equation of motion is simpler than the one used in Chapter 3. Both approaches are represented by an extra arrow in Figure 1.2.

Assume that $\mathfrak{f}$ in (1.23) is of the form $\rho(-u + \tilde{\mathfrak{f}}[\rho])/\varepsilon$ for some $\varepsilon > 0$. Then (1.20) and (1.23) yield

$$\varepsilon \left(\frac{\partial u}{\partial t} + (u \cdot \nabla) u \right) = -u + \tilde{\mathfrak{f}}[\rho]. \tag{1.24}$$

Compare the part on 'isentropic Euler equations' on p. 2523 of [DPZ14], in particular (27). Note that in brackets on the left-hand side the Eulerian formulation of Lagrangian (material) acceleration $\ddot{\Phi}_t$ appears. Taking the limit $\varepsilon \downarrow 0$ thus resembles taking the

overdamped limit in (1.14). Indeed, in the limit we obtain (at least formally) that $u = \tilde{\mathfrak{f}}[\rho]$ which, substituted in (1.20), yields

$$\frac{\partial \rho}{\partial t} + \nabla \cdot (\rho \tilde{\mathfrak{f}}[\rho]) = 0. \tag{1.25}$$

This is a Fokker-Planck equation. In Figure 1.2, we indicate this transition by the arrow from 'hydrodynamic' to 'Fokker-Planck' again labelled 'overdamped limit'. Existing approaches in literature regarding this transition are mainly formal. One example is the work by Chavanis, see Section III.A of [Cha03]. Note that the hydrodynamic equations are derived in [Cha03] using a closure relation different from (read: more general than) the monokinetic assumption. We mention Chapters 2–3 in brackets in Figure 1.2 because we refer in their respective discussion sections to the transition from hydrodynamic to Fokker-Planck; rather than results we give comments and ideas for further research there.

As briefly mentioned in Section 1.1, Chapters 4 and 5 treat measure-valued evolutions with boundary conditions. The underlying equation of motion is first-order in time. The modelling perspective depends on whether the initial measure is for instance discrete (microscopic perspective) or absolutely continuous (macroscopic perspective). This explains the depiction of Chapters 4 and 5 in Figure 1.2.

Remark 1.4.1 (Scaling in N)**.** When going from the microscopic level to a higher level of description (meso- or macroscopic, cf. Figure 1.2) via the passage to the limit $N \to \infty$, the exact form of the limit equation depends on the way in which space, time, interaction lengths (and possibly other quantities) are scaled with respect to N. The issue of finding proper, meaningful scalings is beyond the scope of this thesis. However, we indicate here concisely where and how this aspect is addressed in the literature related to the models mentioned above. In [BV05], the average distance between particles (cells) is compared to the average interaction length. The structure of the limit equation is determined by both the nature of the interaction kernel and the asymptotic relation between these two length scales. An explicit distinction between three scaling regimes is made in [MCO05], p. 53. These regimes are described in terms of the typical number of interactions with others that each individual is involved in. In [Oel91], where a second-order equation of motion is treated, it is explicitly mentioned that the range of the interactions is large compared to the typical distance between individuals.

1.5 First-order models: gradient flows and pattern formation

Let us return to the ODE (1.14) with $\mathcal{F}$ containing interactions of convolution type – cf. (1.11). To simplify the notation, we write

$$\begin{cases} \dfrac{dx_i}{dt} = v_i, & \text{(1.26a)} \\ m\,\dfrac{dv_i}{dt} = -v_i - \dfrac{1}{N}\displaystyle\sum_{j \neq i} \nabla K(|x_i - x_j|), & \text{(1.26b)} \end{cases}$$

for each $i \in \{1, \dots, N\}$. Here, x_i and v_i are to be understood as mappings $t \mapsto x_i(t)$ and $t \mapsto v_i(t)$, respectively, for each t. We define the corresponding total energy (i.e. the sum of kinetic and potential parts) as

$$E_2^N(x_1, \dots, x_N, v_1, \dots, v_N) := \frac{m}{2N} \sum_i |v_i|^2 + \frac{1}{2N^2} \sum_i \sum_{j \neq i} K(|x_i - x_j|). \tag{1.27}$$

We add the subscript 2 to indicate that this is the energy corresponding to a second-order model. Let $E_2^N(t)$ denote (1.27) evaluated along solutions of (1.26). It follows that

$$\frac{dE_2^N}{dt} = -\frac{1}{N} \sum_i |v_i|^2, \tag{1.28}$$

which is independent of m. The right-hand side is often called *dissipation*. In case the friction term $-v_i$ is absent in (1.26b), then the energy is conserved in time. If we set $m = \varepsilon$ and perform the overdamped limit $\varepsilon \downarrow 0$ (see Section 1.3), we obtain the first-order equation

$$\begin{cases} \dfrac{dx_i}{dt} = v_i, & \text{(1.29a)} \\ v_i = -\dfrac{1}{N} \displaystyle\sum_{j \neq i} \nabla K(|x_i - x_j|), & \text{(1.29b)} \end{cases}$$

for each i; cf. (1.13a). We define the corresponding energy as

$$E_1^N(x_1, \dots, x_N) := \frac{1}{2N^2} \sum_i \sum_{j \neq i} K(|x_i - x_j|), \tag{1.30}$$

evaluate it along solutions of (1.29) to obtain the quantity $E_1^N(t)$ and calculate its time-derivative, which is

$$\frac{dE_1^N}{dt} = -\frac{1}{N} \sum_i |v_i|^2. \tag{1.31}$$

We see that the definition of E_1^N follows naturally from (1.27), with $m = 0$ substituted. As the right-hand side of (1.28) is independent of m, an expression for dE_1^N/dt is formally obtained from the limit $m \downarrow 0$ in (1.28). This coincides with (1.31).

However, the structure of the system has changed drastically by the overdamped limit. From Hamiltonian systems with damping we have entered the research area of gradient flows. For a general introduction to gradient flows we refer to the standard work [AGS08]. Without going into too many details, we point out here some properties that are especially relevant in the context of this thesis.

Gradient flows are characterized by the combination of an energy and a mechanism according to which this energy is dissipated. The key characteristic is that solutions go down the energy landscape in a *steepest-descent* fashion. The evolution in (1.29b) represents,

together with the energy defined in (1.30), a gradient flow in the Euclidean space $\mathbb{R}^{Nd}$. See e.g. [KSUB11]. For the vector $\mathbf{x} := (x_1, \dots, x_N)^T \in \mathbb{R}^{Nd}$ we can write

$$\frac{d\mathbf{x}}{dt} = -N \nabla E_1^N(\mathbf{x}), \tag{1.32}$$

where ∇ denotes the gradient on $\mathbb{R}^{Nd}$. Due to (1.31), E_1^N can be used as a Lyapunov functional to characterize equilibria of the system. Asymptotically, the solution tends to a minimizer of (1.30). First, assume that $K : \mathbb{R}_0^+ \to \mathbb{R}$ is a convex function, that is

$$K(\alpha\,\xi + (1-\alpha)\,\zeta) \leqslant \alpha\,K(\xi) + (1-\alpha)\,K(\zeta), \tag{1.33}$$

for all $\xi, \zeta \in \mathbb{R}_0^+$ and all $\alpha \in [0,1]$. If K is moreover strictly increasing, then E_1^N is strictly convex[3] and has (for each initial configuration) exactly one minimizer: the configuration in which all individuals are in the same position. The corresponding interactions are purely attractive, hence it is intuitively clear that all mass will accumulate in one point. When defining what 'uniqueness' of a steady state means in this setting, one has to take into account that the energy (1.30) depends on pairwise distances only. Hence the set of all minimizers of the energy is invariant e.g. under translations (and rotations, which are irrelevant in this specific case). One should consider all of these configurations as instances of *the same* steady state, though. Note that the specific initial configuration determines the exact limit configuration. Furthermore, the evolution dictated by (1.29) is such that the centre of mass is preserved. One can therefore rule out the translation invariance of steady states by restricting to initial configurations with centre of mass in the origin.

If K is strictly decreasing, then the energy is not convex, and the particles tend to a (rather trivial) 'configuration' in which they are 'infinitely far' apart. This is not a genuine steady state of the system or minimizer of the energy as this limit state is not actually attained by any $\mathbf{x} \in \mathbb{R}^{Nd}$. There are no other steady states.

Remark 1.5.1. Steady states are also invariant under permutations of the particles' indices. This issue is one of the reasons to introduce a formulation in terms of measures.

Of much interest are the situations in which the interaction potential is non-monotonic and non-convex; cf. [McC97]. These are cases in which the interplay between repulsion and attraction results in very diverse steady states: uniform densities in a ball, uniform densities on a co-dimension one manifold (ring in 2D, sphere in 3D), annuli, soccer balls, etc. See e.g. [FHK11, FH13, vBUKB12, KSUB11, LTB09, vBU12, BCLR13a]; the pattern that arises depends on the exact form of K. Many of these patterns are observed experimentally in self-assembled biological aggregations [PK99, BCC$^+$08, CDF$^+$03, TGCD03], which gives practical ground and motivation to study this model.

Remark 1.5.2. The steady states (patterns) discussed here are also relevant for second-order models. Consider a possible steady state of (1.26) such that all velocities and accelerations are zero. It follows from (1.26b) that the corresponding configuration of

[3] The definition of *strict convexity* is (1.33) with '$\leqslant$' replaced by '$<$'. Note that convexity of K is not sufficient to deduce convexity of the energy, even though the Euclidean distance is convex itself (triangle inequality). The composition of the two, that appears in (1.30), is only (strictly) convex under the extra assumption that K is (strictly) increasing.

the positions must be a stationary point of (1.30). The same observation was made in [CFTV10], be it that for their equations dynamic patterns can arise: spatial minimizers of (1.30) that move with nonzero velocity.

In Chapter 2, we 'destroy' the gradient flow structure by inclusion of a field of vision in the model. The long-time behaviour of the resulting model is even much more challenging and is subject of ongoing work. Preliminary results on a related approach were presented in [EMvdV13], where the field of vision is taken with respect to a fixed direction. There we focus on Lyapunov-like functionals to obtain an equation compatible with (1.31). Also here, the study of equilibria is work in progress.

There are two features that make the description of the evolution as a gradient flow in Euclidean space not completely satisfactory: the explicit appearance of a prefactor N in (1.32); and the issue about permutations in particle indices mentioned in Remark 1.5.1. A more sophisticated approach involves a lift to the space of probability measures (i.e. the empirical measure) and the introduction of *Wasserstein gradient flows*. Their relevance and the associated literature are both vast. Wasserstein gradient flows are introduced here mainly to show the broader context of the systems in this thesis, while they are not studied explicitly in the rest of this thesis. Therefore we only mention the main points and do not go into the technicalities. For more information the reader is referred to Chapter 8 of [Vil03] and Section 8.1 of [AGS08]. In the latter reference also the link with the underlying ODE is treated.

Assume that we have an energy functional $\mathcal{E} : \mathcal{P}(\mathbb{R}^d) \to \mathbb{R}$. In simplistic language, the Wassertein gradient flow of this energy is the evolution equation

$$\dot{\mu}_t = -\operatorname{grad}_{\mathrm{W}} \mathcal{E}(\mu_t),$$

where $\operatorname{grad}_{\mathrm{W}}$ denotes a gradient concept that depends on the 2-Wasserstein distance, hence the subscript W. We remark that, in fact, this is an evolution equation on the space of probability measures with bounded second moment. Further details about the background and interpretation of this equation are deliberately omitted. For our setting, it is important that $\operatorname{grad}_{\mathrm{W}}$ can be expressed in the following way

$$-\operatorname{grad}_{\mathrm{W}} \mathcal{E}(\mu) = \nabla \cdot \left(\mu \nabla \left(\frac{\delta \mathcal{E}}{\delta \mu} \right) \right),$$

see [Vil03], Chapter 8, or [Ren13], Section 1.7. By $\delta\mathcal{E}/\delta\mu$ we denote the *variational derivative* (or L^2-gradient of a functional). The empirical measure associated to the solution of (1.32) satisfies the general equation for measures

$$\frac{\partial \mu}{\partial t} - \nabla \cdot \left(\mu \nabla \left(\frac{\delta \mathcal{E}}{\delta \mu} \right) \right) = 0, \tag{1.34}$$

with

$$\mathcal{E}(\mu) := \frac{1}{2} \int_{\mathbb{R}^d} \int_{\mathbb{R}^d} K(|x-y|)\, d\mu(y)\, d\mu(x). \tag{1.35}$$

See [BCLR13b] for more information. Note that $\delta\mathcal{E}/\delta\mu = K(|\cdot|) * \mu$, and compare (1.34) to (1.1) with $v = -\nabla(\delta\mathcal{E}/\delta\mu)$.

In (1.29b) and (1.30) the diagonal terms (self-interactions) are explicitly excluded, while in (1.35) this is not the case. This is quite a subtle issue, which is however solved if $K(|\cdot|) \in C^2(\mathbb{R}^d)$. The system does not change if we add a constant to or subtract it from the energy; in this case the constant is $N \cdot K(0)$. Namely, the requirement $K(|\cdot|) \in C^2(\mathbb{R}^d)$ implies automatically that $K'(0) = 0$. Hence, the explicitly excluded diagonal terms in (1.29b) are all zero.

Other choices for $\mathcal{E}$ are provided in [CMV03, CMV06, Vil03]. For us, the most relevant ones are

$$\mathcal{E}(\mu) := \int_{\mathbb{R}^d} V \, d\mu, \tag{1.36}$$

and, if μ is absolutely continuous with density ρ,

$$\mathcal{E}(\rho) := \int_{\mathbb{R}^d} U(\rho) \, dx,$$

which lead to

$$\frac{\partial \mu}{\partial t} - \nabla \cdot (\mu \nabla V) = 0,$$

and

$$\frac{\partial \rho}{\partial t} - \nabla \cdot (\rho \nabla U'(\rho)) = 0,$$

respectively. The latter example yields the diffusion equation for $U(\rho) = \rho \log(\rho)$. The structure is preserved under addition of such energies.

The aforementioned advantages of setting models in a measure space should be stressed here once more. The structure of the equations is independent of the perspective (micro/macro) that we choose, and hence linking the two (e.g. by many-particle limits) is easier. The relevance of this link lies – for example – in the fact that doing analysis about equilibria and their stability is more convenient in a setting of PDEs and measure theory, see e.g. [BCLR13b], while from the point of view of numerical implementation, treating particle systems is advantageous[4]; see e.g. [vBUKB12].

1.6 Related work

Before giving a chapter-wise introduction to the content of the thesis in Section 1.7, let us point out some related work done by others.

[4] In a personal communication, Razvan Fetecau told me that a numerical strategy sometimes used to find equilibria is to evolve that particle system with large timestep and simply accept the update if the energy decreases. Accurate approximation of the dynamics is not aimed for. This strategy is based on the central idea in gradient flows.

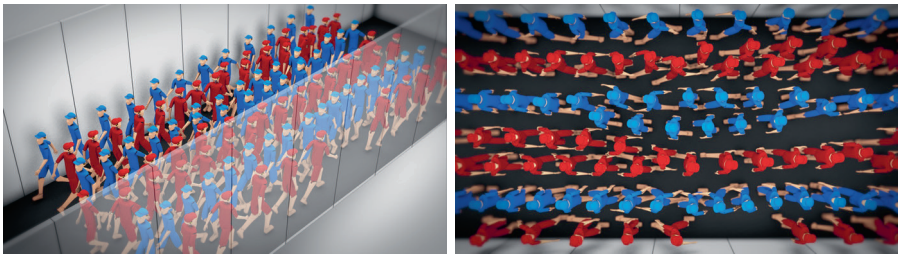

(a) (b)

Figure 1.3: Illustration of pattern emergence in a first-order model for pedestrians: *lane formation*. Dynamics in a corridor are imitated by periodic boundary conditions (left and right in Figure 1.3b) and repulsive walls (top and bottom in Figure 1.3b). The images are based on our simulation results. See also `www.youtube.com/watch?v=Txrs4ssiAz0`. Visualization: ICMS Animation Studio, TU/e.

Both the discrete and the continuous versions of the first-order model appear not only in various works on biological aggregations [MEK99, TBL06] but also arise in a number of other applications, such as the granular media [LT04, CMV06], the self-assembly of nanoparticles [HP06], the Ginzburg-Landau vortices [DZ03] and the molecular dynamics simulations of (soft) matter [Hai92].

The field of *crowd dynamics* must certainly be mentioned here too, since in that field for me the scientific path started, which has led to this thesis. Crowd dynamics is the research area that is concerned with modelling, explaining and predicting the motion of pedestrians. The idea of combining mechanics with human social behaviour dates back to at least [Har10, Por12]. The seminal work in this field is by Helbing [HM95] who proposed a *social force model*[5] by which individuals move according to a Newton-like law where the physical forces are replaced by social forces. Such forces model personal targets, interactions with others and geometrical restrictions. Both first- and second-order models are in use. The formation of certain (dynamic) patterns observed in real crowds have driven scientists to reproduce these with simple models. A benchmark example is the formation of lanes in a corridor in which two groups of people move in opposite directions (counterflow). In each such lane, pedestrians tend to align in such a way that they simply follow someone going in the same direction. This phenomenon is observed both in pedestrian walking experiments[6] and in simulation studies. See Figure 1.3 for simulation results obtained by means of a first-order model.

The validation of models with experimental or real-life data is very important and is an art in itself; see e.g. Section 1.3 of [CPT14] for a brief introduction. A frequently used

[5] The name given to this model inspired me, many years later, for the title of this thesis.

[6] A video of a bidirectional flow experiment is available at `www.youtube.com/watch?v=J4J__1OOV2E`. Lanes are formed without the participants being instructed to do so. See [ZKSS12] in which snapshots of the experiment are shown.

object is the so-called *fundamental diagram*: a constitutive relation between the density and the velocity or between the density and the flux, which is the product of the density and the velocity. The resemblance between the theoretically and experimentally obtained fundamental diagrams is studied e.g. in [ZKSS12]. This work uses experimental data from a counterflow experiment executed under 'laboratory conditions': the experiments involve volunteers and take place in set-ups (walls, corridors, doors) created for the occasion. Experiments of this *in vitro* type are also used in [HD07, DH13], which focus on a bottleneck scenario. From the data, maximum likelihood estimators are derived for the parameters of certain models. In particular, [HD07] compares and judges different models based on the quality of the parameter fit.
Real-life data is analyzed e.g. in [CBMT14, CMV15]. Their data was acquired at Eindhoven University of Technology. Higher-order statistics related to the probability density of the ensemble of all recorded trajectories are presented in [CBMT14]. The aforementioned fundamental diagram is one of these statistics. The approach in [CMV15] resembles [HD07] in the sense that maximum likelihood estimators for parameters are used to assess which variants of a model are better than others.
An interesting idea is presented in [GPF$^+$15], where data of sheep passing a bottleneck in a farm is studied. The authors explicitly point out the possible relevance of their work to pedestrian dynamics.
Processing experimental data is not one of the key topics of the present work. This aspect is not touched in the rest of this thesis, except for Section 7.2.

The study of colloidal particles is an area of research with similarities to our work. *Colloids* are particles floating in a solvent that are of such size that

1. they are small enough to undergo Brownian motion due to collisions with solvent molecules;
2. they are large enough to be considered discrete particles embedded in a continuum.

It should not be a surprise that the theory of colloids connects to the subject of this thesis. Smoluchowski [vS06, vS17] was one of the founding fathers of this theory, while his name was used here in the context of the Smoluchowski SDE. Indeed, the Smoluchowski SDE can be used to model the motion of a single colloidal particle. In the many-colloids limit, upscaling to a Fokker-Planck-like PDE would be a natural thing to do. What is interesting for us, is the fact that colloids have mutual interactions due to the attractive Van der Waals force, repulsive hard-core interaction and more subtle hydrodynamic interactions that are transmitted via the solvent; see [Dho96] Section 1.1.2 and Chapter 4. Pattern formation also occurs. A connection to Figure 1.3 is provided in [VWR$^+$11] and [Löw10], Figures 3 and 4, in which lane formation is observed (both experimentally and by simulations) in a system of oppositely charged colloids in an electric field. In Section 2 of [MCKB14] a model for colloids is explicitly applied to crowd dynamics and group formation. Also [FW14] is interesting in this respect. An experimental procedure for producing oblong colloids is considered. The creation of such particles is relevant, since these can be used to build systems that are governed by anisotropic interactions. Although the correspondence between this type of anisotropy and a field of vision (see Section 1.2 of this thesis) is not one-to-one, the resemblance between non-living and living 'particles' is still striking. An interesting idea is to test crowd dynamics models via traffic experiments involving colloidal particles.

A first-order equation is also used for modelling the motion of defects in crystallographic lattices (called *dislocations*, see [HB11]). The movement of these imperfections results on the macroscopic scale in plastic deformation of metals. Therefore the collective dynamics of these dislocations is a subject of scientific interest. A *linear drag law* is used, which relates the velocity directly to internal stresses; see (3.5) and (4.36) in [HB11]. A specific modelling assumption is that dislocations moving in two-dimensional space are arranged equidistantly along vertical lines (called *walls*). Summation of the interactions over the dislocations in a wall, yields a one-dimensional model for the positions of the walls. This model possesses a gradient flow structure, and the corresponding energy is a combination of (1.35) for interactions and (1.36) for an externally applied force; see (2.1) in [vMM14]. In [GPPS13, vMMP14, vMM14], Γ-convergence is used to perform the many-dislocation limit. An implication of Γ-convergence (under additional conditions) is that minimizers of the energy converge to minimizers of the limit energy. Another advantage is the fact that (un)boundedness of the interaction potential around the origin is not a problem. Steady states are the focus of [GPPS13, vMMP14] (note the importance of scaling in these works), while (upscaling of) the dynamics leading to such steady state is treated in [vMM14]. Their equation of motion is surprisingly similar to the transport equations that appear in this thesis.

1.7 Content of this thesis

This section contains an outline of the content of this thesis. In this overview we explain how the chapters of the thesis fit in the broader picture drawn in the previous sections of this introductory chapter.

1.7.1 Anisotropy

Our focus on systems of *social* individuals leads to the general question:

Can we include visual perception in our modelling procedure?

In Section 1.2 we already introduced part of the answer. In Chapter 2 we address this question for a model for the dynamics of N individuals with positions $x_i \in \mathbb{R}^d$, $i \in \{1, \dots, N\}$. The starting point is the system (1.29), with K a general (application-dependent) potential, which incorporates inter-individual social interactions such as long-range attraction and short-range repulsion.

In biological applications, (1.29) is used to model animal aggregations, such as insect swarms, fish schools, bird flocks, etc. [MEK99]. The interaction potential K in (1.29) is *isotropic*, as it depends only on the pairwise distances between individuals. As argued in Section 1.2, this assumption is often unrealistic, since individuals have a field of vision. However, despite the extensive literature on model (1.29), there has been no systematic study of its (more realistic) anisotropic extensions. The primary goal of Chapter 2 is to fill this gap. We note that anisotropy/non-symmetry of interactions was considered, both analytically and numerically, in works on *second-order* aggregation models

[CFTV10, Fro12, AP13], where the velocity is governed by a differential equation itself. However, adding anisotropy to *first-order* models, though similar conceptually, is very different at a mathematical and numerical level.

We introduce perception restrictions in (1.29) via weights in (1.29b) that limit the influence by individuals j on the reference individual i:

$$v_i = -\frac{1}{N}\sum_{j\neq i} \nabla_{x_i} K(|x_i - x_j|)\, w_{ij}. \tag{1.37}$$

The weights w_{ij} depend on the relative position $x_j - x_i$ of individual j with respect to the current direction of motion v_i of individual i and hence incorporate the angle under which individual i perceives individual j. Mathematically, we model w_{ij} as

$$w_{ij} = g\left(\frac{x_i - x_j}{|x_i - x_j|}\cdot\frac{v_i}{|v_i|}\right), \tag{1.38}$$

with a function g chosen such that w_{ij} is largest when j is right ahead of individual i ($x_j - x_i$ is in the same direction of v_i) and smallest when j is right behind individual i ($x_j - x_i$ in the opposite direction of v_i). The weights w_{ij} are *not* symmetric: in general, $w_{ij} \neq w_{ji}$.

At this point we raise the mathematical question:

How to guarantee existence and uniqueness of solutions to the first-order model with included field of vision?

By (1.37) and (1.38), the velocities v_i are no longer explicitly given in terms of the spatial configuration $\{x_1, x_2, \ldots, x_N\}$ as in (1.29), but are defined implicitly through (1.37)–(1.38), which, in general, may have multiple solutions. Hence, non-uniqueness of the velocity is a major issue immediately brought up by the anisotropic extension.

The second important issue is the loss of smoothness of the velocity as a function of time. The roots of (1.37)–(1.38) may disappear dynamically, as the spatial configuration $\{x_1, x_2, \ldots, x_N\}$ changes in time. Hence, velocities have to be allowed to be discontinuous at these jump times, and a selection criterion for the allowable/physical jumps should be defined and enforced. Finally, a third issue is that velocities in (1.37)–(1.38) can become zero (particles can stop) in finite time, and the model, at least as it appears in (1.37)–(1.38), is not even defined if some $v_i = 0$.

The main tool in dealing with the issues above is to introduce a relaxation term in the equation for the velocities v_i. More precisely, we consider the following regularized system

$$\begin{cases} \dfrac{dx_i}{dt} = v_i, \\[2ex] \varepsilon\dfrac{dv_i}{dt} = -v_i - \dfrac{1}{N}\displaystyle\sum_{j\neq i} \nabla_{x_i} K(|x_i - x_j|)\, g\left(\dfrac{x_i - x_j}{|x_i - x_j|}\cdot\dfrac{v_i}{|v_i|}\right). \end{cases} \tag{1.39}$$

The interpretation of (1.39) and its connection to the first-order model we started from, was discussed extensively in Section 1.3. This regularization turns out to be essential in dealing with the anisotropic interactions.

As already anticipated in Section 1.3, the limit $\varepsilon \to 0$ in (1.39) exists in the smooth regime (that is, away from jumps), under some stability condition. This is a result by Tikhonov [Tik52, Vas63], and relies on the notion of asymptotic stability; more details are given in Section 2.3.1. At the times of velocity jumps in the first-order model, we use the relaxation model (1.39) to enforce a 'physical' jump selection criterion. The main goal of Chapter 2 is to demonstrate how the regularization (1.39) can be used as an analytical, and a numerical tool to understand and simulate solutions to the first-order anisotropic model. We restrict ourselves to two-dimensional simulations, where we show how (1.39) can be used to deal with instantaneous root losses, as well as particle stopping.

1.7.2 Convergence of measure-valued evolutions

Chapter 3 is driven by the following general question:

How to use particles to approximate a continuum?

Our desire to approximate a continuum arises in this chapter primarily from computational considerations. The intrinsic discrete character of any numerical tool is compatible with the use of a finite number of particles. The chapter is inspired by the philosophy of continuum mechanics. We use a Lagrangian way of describing the motion of material points, which leads to a mesh-free numerical method. As opposed to e.g. the Finite Element Method (cf. Chapter XX of [DL00]) that does require a fixed mesh, mesh-free methods are beneficial for problems in which either there is a substantial amount of deformation or free boundaries are present. In Chapter 3 we answer the following two mathematical questions:

How can we derive particle schemes in a systematic way?

In what sense do these schemes converge in the many-particle limit to the continuum equations of motion?

The central object of interest in Chapter 3 is a system of the form

$$\begin{cases} \dfrac{\partial \rho}{\partial t} + \nabla \cdot (\rho\, v) = 0 \,, \\[2ex] \dfrac{\partial}{\partial t}(\rho\, v_k) + \nabla \cdot (\rho\, v\, v_k) = \rho \left(-\nabla P(\rho) - \eta\, v - \nabla V + \mathcal{K} * \rho \right)_k \,, \end{cases} \tag{1.40}$$

where the subscript k denotes the kth component of a vector in $\mathbb{R}^d$. Compare (1.20) and (1.23) in Section 1.4. We use the functions P, η, V and $\mathcal{K}$ for modelling pressure, friction, external conservative forces and interactions, respectively. The system (1.40) is a specific form of the Euler equations with an additional nonlocal term.

In view of the questions we ask, Chapter 3 consists of the following two parts:

- A systematic procedure for deriving a measure-valued formulation of (1.40) from the Lagrangian that builds on the principle of least action and leads ultimately to a particle system.
- A convergence result using the Wasserstein distance on the space of probability measures, that connects the particle system to the continuum limit.

The chapter is motivated in particular by the numerical method called Smoothed Particle Hydrodynamics (SPH). An overview of the applications of this method is given in [Mon12]. The term 'particle' should *not* be interpreted as a physical object of any scale (like an atom, molecule or grain) but rather as a numerical, artificial entity attributed with mass, position, velocity and other properties of the medium it represents.

We derive systematically the equation of motion for a measure from the Lagrangian and the principle of least action. To make the step from continuum mechanics to measures, a regularization of the density is required. We obtain eventually a second-order equation for a motion mapping Φ that dictates the evolution of the measure by means of push-forward, cf. (1.5)–(1.6). The exact form of the equation of motion for Φ depends on the order in which regularization and the principle of least action are applied. We obtain two different equations, whose discrete counterparts coincide with two different schemes: the one traditionally used in SPH, and the one treated in [LGP98], respectively. We also show how to incorporate nonconservative forces.

We prove that measure-valued solutions converge in the Wasserstein distance as the initial measure is approximated. The order of convergence is determined by the rate at which the initial (continuum) measure is approximated. A result similar in nature to ours is given in [CCR11]. Particularly relevant is Corollary 5.4, where convergence in the Wasserstein distance is proven locally in time. A difference with our work is that the intermediate level of the kinetic equation plays an important role; cf. Corollary 5.2 and Lemma 5.3 of [CCR11] and also Proposition 3.2 of [CDP09]. Moreover, they consider a different class of right-hand sides. Our line of arguments is mainly inspired by [LGP98], the first reference in which measures are employed in combination with the Wasserstein distance to prove the convergence of the SPH method. The earlier work [Oel91] uses a different technique and considers only mutual interactions between particles (see Section 1.4). In [Sch14], measure-valued solutions and the Wasserstein distance are used; this paper establishes Γ-convergence of the Lagrangian and convergence of the stationary points. Other approaches to obtain convergence are given e.g. by [Ben06, BSO12] using local maximum entropy estimates, [QBL06] employing estimates for the truncation error, and [Rav85, IK10].
It should be noted that the scheme treated in [LGP98] is not the aforementioned traditional scheme. Our proof applies both to traditional SPH and to the scheme covered by [LGP98]. Moreover, we allow for a much more general class of force fields, including external and internal conservative forces, as well as friction and nonlocal interactions. These interactions are of particular interest in the scope of this thesis.

Chapter 3 contains a general result (Theorem 3.3.10), in the sense that convergence holds for a general sequence of approximating measures, and is not restricted to particle

systems. Although SPH is used as a numerical tool, the underlying connection between discrete and continuum formulations is interesting in its own right. Note that only a few convergence proofs for SPH-like methods exist.

1.7.3 Boundary conditions

Often it is essential to model (measure-valued) evolutions on *bounded* domains. We treat this issue in Chapters 4 and 5. Inspired by applying our models to a pedestrian dynamics scenario, we ask the following two general questions:

Can we use our way of modelling also on bounded domains?

If yes, how should we incorporate impermeable walls, exits and entrances?

Typically, in the context of PDEs one answers these questions by introducing Neumann boundary conditions for the flux, where zero flux denotes a wall and nonzero flux denotes in- or outflow. We should realize however that for measures the concept of a normal derivative is not even defined. Our guiding mathematical question is therefore:

What is the correct way to define zero-flux or general flux boundary conditions in terms of measures?

In Chapter 4, we consider the flow induced by a bounded Lipschitz velocity field v, which is restricted to the interval $[0,1]$. The result is a *stopped flow* that allows for a description in terms of a semigroup. Flux boundary conditions are established by a combination of this stopped flow and a (local) source-sink term. That is, in the style of (1.1) and (1.8), we write the short-hand notation

$$\frac{\partial}{\partial t}\mu_t + \frac{\partial}{\partial x}(\mu_t v) = f \cdot \mu_t \qquad \text{on } [0,1], \tag{1.41}$$

where $f : [0,1] \to \mathbb{R}$ is a *piecewise bounded Lipschitz function* with finitely many discontinuities. The product $f \cdot \mu_t$ is a measure on $[0,1]$ with density f with respect to μ_t. The particular choice $f(x) = -a\,\mathbb{1}_{\{1\}}(x)$, where $\mathbb{1}_E$ is the indicator function of the set E and $a > 0$, reduces equation (1.41) to

$$\frac{\partial}{\partial t}\mu_t + \frac{\partial}{\partial x}(\mu_t\, v) = -a\mu_t(\{1\})\delta_1. \tag{1.42}$$

If $v(1) > 0$, then (1.42) represents a system with mass transport and sticking boundaries [Tai04] of which $x = 1$ is *partially absorbing*: mass arriving at $x = 1$ stays there, while it is removed at a constant rate a. This represents a *flux boundary condition*, or Robin-like boundary condition, in a measure-valued formulation. Note that in this formulation the flux condition appears as a discontinuous perturbation boundary term in the bulk equation. This way of introducing boundary conditions does not require a concept of normal derivative of measures on the boundary.

Finding the correct flux boundary conditions is a topic often addressed in the literature, but this has not yet been treated in the measure-theoretical framework. We refer

here for instance to [AJCRB08, FGHS07, JCRB11, MS08] (in the context of reaction and diffusion scenarios) and Gurtin [Gur93] (the shrinking pillbox principle in continuum mechanics).

In Chapter 4 we first prove existence and uniqueness of *measure-valued mild solutions* and continuous dependence of these solutions on initial data. The solution is a continuous map from $\mathbb{R}^+$ to the space $\mathcal{M}([0,1])$ of finite Borel measures that satisfies the variation of constants formula with linear, but discontinuous perturbation. The subsequent part of the chapter is on approximation by regularization (Section 4.4). We replace the piecewise bounded Lipschitz function f in (1.41) by a bounded Lipschitz function f_ε that differs from f on an ε-thin neighbourhood of each discontinuity. We show, that if we pick a sequence of such functions $f_n = f_{\varepsilon_n}$ with $\varepsilon_n \downarrow 0$, then the corresponding solutions $\mu_t^{(n)}$ converge to the solution μ_t of (1.41). Moreover, we compute the rate of convergence of the solution as $n \to \infty$. Such result shows on the one hand that (1.41) with instantaneous spatial change in f can be viewed as an idealization of a continuous (Lipschitzian), but very fast, change. On the other hand, it shows that (1.42) indeed represents a flux boundary condition, as it results from appropriate interaction with the boundary in a thin boundary layer, in the limit of vanishing thickness.

Formulation (1.41) unifies a continuum formulation in terms of density functions with respect to the Lebesgue measure and a particle description for this mass evolution problem within the framework of measure-valued differential equations. We investigate this resemblance numerically in Sections 4.5.1 and 4.5.2. The result on continuous dependence on initial data implies (as a special case) a discrete-to-continuum limit, provided that a discrete (continuum) initial condition yields a discrete (continuum) solution for all time. This is – at least in the interior of $[0,1]$ – the case. Hence, Chapter 4 contains the arrow from 'first-order ODE' to 'Fokker-Planck' in Figure 1.2.

Chapter 5 is an extension of Chapter 4, in the sense that we obtain the well-posedness of

$$\frac{\partial}{\partial t}\mu_t + \frac{\partial}{\partial x}(\mu_t v[\mu_t]) = f \cdot \mu_t \qquad \text{on } [0,1], \tag{1.43}$$

for velocity fields that are no longer fixed elements of $\mathrm{BL}([0,1])$. In (1.43), the velocity $v[\mu_t]$ depends functionally on the solution μ_t.

By the introduction of measure-dependent velocity fields the transport problem becomes nonlinear. The way the semigroup approach was presented in Section 1.1 is a one-directional approach where the ODE is solved and the time-evolution of the measure follows by push-forward. This approach works in Chapter 4, but does not readily extend to measure-dependent v. Inevitably, this forces us to look for alternative techniques to prove well-posedness. This is exactly what is presented in Chapter 5. We use a forward-Euler-like approach for a partition of the time interval $[0,T]$. On each subinterval, we fix the velocity and let our measure-valued solution evolve accordingly. Hence, restricted to a subinterval, the evolution satisfies the requirements of Chapter 4. We then refine the partitioning of $[0,T]$, estimate the difference between the subsequent Euler approximations and show that this procedure converges. Here, we rely on completeness of the encom-

passing space of measure-valued trajectories. We were inspired by [CG09] and [Hoo13], the latter of which was in turn inspired by [GLMC10].

1.7.4 Approximation of a finite-size object by a point source

In physics it is common practice to replace objects of negligible size by point masses. For instance, grains or colloids in a solution [JN82], electrostatic particles [Jac75] or defects in crystalline structures [CB13, vMMP14]. Of particular interest is the setting in which the exchange of mass, energy etc. between the interior and the exterior of the object takes place at its boundary. In this case the object is approximated not by a mere point mass, but by a point source. The question that we ask is:

What error do we make when approximating a small object by a point source?

We address this question in Chapter 6, focussing on a simple scenario.

In $\mathbb{R}^2$, we consider an object of fixed shape and position and of finite size that contains the origin. In the exterior of the object – called Ω – there is a concentration of mass u that evolves by diffusion:

$$\frac{\partial u}{\partial t} = D\Delta u,$$

where $D > 0$ denotes the constant diffusion coefficient. On the boundary Γ of the object there is prescribed mass flux in normal direction: $D\nabla u \cdot n = \phi$, with n the outward-pointing unit normal and ϕ the prescribed flux. This flux is a simplistic way of describing the result of processes that occur in the interior of the object. We wish to approximate this object by a point source. To this aim we replace the original diffusion equation on the exterior domain Ω by a diffusion equation on the whole of $\mathbb{R}^2$ with a Dirac measure included at its right-hand side:

$$\frac{\partial \hat{u}}{\partial t} = D\Delta \hat{u} + \bar{\phi}\,\delta_0,$$

where $\bar{\phi}$ represents the magnitude of the mass source. Of course this requires the extension of the initial conditions of the first problem to the whole space. The exact formulation of the equations will be made clear in Section 6.1.

This is a first step towards modelling and analyzing the mass distribution dynamics in realistic settings involving a large number of small objects moving around in a bounded domain while exchanging mass. Our motivation comes from the intracellular transport of chemical compounds in vesicles, like neurotransmitters in neurons (cf. [LE97]) or the hypothetical vesicular transport mechanism for the plant hormone auxin proposed in [BŠM03] as an alternative to the conventional auxin transport paradigm (in analogy to neurotransmitters). Auxin is a crucial molecule regulating growth and shape in plants. The vesicles are small membrane-bound balls covered by specific transmembrane transporter proteins that take up auxin from the surrounding cytoplasm. The vesicles are driven by molecular motors over a network of intracellular filaments [HNT10, Rav13], e.g. from one end of the cell to the other as in Polar Auxin Transport (PAT). Experimental investigations of

PAT in *Chara* species [BLH$^+$12] revealed that neither diffusion nor cytoplasmic streaming can be the driving mechanism of PAT in the long (3-8 cm) internodal *Chara* cells. See [BLH$^+$12, Rav13] for further discussion and an overview.

A substantial amount of mathematical modelling efforts on PAT have focussed on pattern formation in plant cell tissues (see [vBdBStT13, Kra08, MdPIB07] and the references cited therein). Upscaling to an effective macroscopic continuum description for transport at tissue level was considered in [CKP10]. All models are based however on the assumption of diffusion as intracellular transport mechanism for auxin. Ultimately, we aim at obtaining a convenient mathematical description of the vesicle-driven transport dynamics *within* a cell, in particular in terms of an effective continuum model, which is needed to replace diffusion in an upscaling argument similar to [CKP10]. In view of the absence of relevant mathematical literature, this perspective seems to be rather unexplored.

For the problem posed on Ω, we consider as solutions functions in a suitable Sobolev space. The well-posedness of the problem is guaranteed since we are in a special case covered by [DHP03, DHP07]. The measure-valued source makes that for the corresponding problem on $\mathbb{R}^2$ a different solution concept is needed. We consider mild solutions (cf. Chapters 4–5) that satisfy the variation of constants formula involving the diffusion semigroup with the source as a perturbation. We are interested in comparing the solutions on Ω, while Ω is assumed to be bounded away from the origin. Due to the regularizing effect of the diffusion semigroup and the fact that Ω is at positive distance from the origin, the mild solution is absolutely continuous with density $\hat{u}$ in a suitable Sobolev space. This density satisfies a weak formulation of the problem.

We posed the question what error we make when approximating a small object by a point source. In Chapter 6 we answer its mathematical counterpart:

Can we quantify the difference between the solutions u and $\hat{u}$ and their fluxes on Γ in a suitable Sobolev norm?

For all time t, we derive an $L^2([0,t];L^2(\Gamma))$-bound on the difference in flux on the boundary. Moreover, we derive for all $t>0$ an $L^2(\Omega)$-bound and an $L^2([0,t];H^1(\Omega))$-bound for the difference of the solutions to the two models u and $\hat{u}$. A conjecture is given about when we expect these bounds actually to go to zero.

Why do we introduce measures to this problem? This modelling strategy is especially useful once we wish to describe the interaction between multiple moving objects (vesicles). We expect the mathematical description to be much simpler in terms of discrete measures and the analysis and numerical approximation likewise (see, for instance, [RKM03, SGTK12] for a related case). Here, we emphasize that a model for moving full-size vesicles would lead to a moving-boundary problem (Stefan-like), with all its associated difficulties; see e.g. [MB09, AM13]. In view of the aforementioned discrete-to-continuum limits, one could coin the approximation of a vesicle by a point as a 'continuum-to-discrete limit'.

The concentration of auxin within a cell can be modelled as a multiscale measure (see

e.g. [CPT11, CPT14]) or a system of coupled measures, in which Dirac measures account for the auxin content of (now zero-size) vesicles and the absolutely continuous part represents the concentration in the cytoplasm. Mutual interactions *between* point masses determine the dynamics (cf. also the topic of colloidal particles described in Section 1.6), and hence the results of Chapter 6 are connected to the rest of this thesis. However, before we can go to this advanced setting, we first need to investigate the quality of the vesicle approximation for a simple reference scenario; this is the main concern of Chapter 6.

The main results of Chapter 6 are formulated in terms of Sobolev norms, while it is not directly clear that a semigroup approach was used to obtain solutions for the problem with measure-valued source. However, because of the use of semigroups, also from a purely technical and mathematical point of view Chapter 6 is in line with the other parts of the thesis.

Chapter 2

Anisotropy

In this chapter we start off from a first-order model with interactions, formulated at the level of ODEs and extend it by including a field of vision. This is one of the ingredients that makes systems of living individuals different from systems of nonliving particles. We model anisotropy by limited sensorial perception of individuals that depends on their current direction of motion. Consequently, the first-order model becomes *implicit*, which leads to new analytical issues, such as non-uniqueness and jump discontinuities in velocities. Our main concern in this chapter is to answer the question:

How to guarantee existence and uniqueness of solutions to the first-order model with included field of vision?

2.1 Introduction

Consider the following system of equations for the positions x_i of N particles in $\mathbb{R}^d$:

$$\begin{cases} \dfrac{dx_i}{dt} = v_i; & \text{(2.1a)} \\ v_i = -\dfrac{1}{N}\displaystyle\sum_{j\neq i} \nabla_{x_i} K(|x_i - x_j|). & \text{(2.1b)} \end{cases}$$

We introduce weights w_{ij} in (2.1b) to model the effect of perception on the influence that individual j has on the reference individual i:

$$v_i = -\frac{1}{N}\sum_{j\neq i} \nabla_{x_i} K(|x_i - x_j|)\, w_{ij}. \tag{2.2}$$

The choice of the weights w_{ij} depends on what limitations on the field of perception one wants to consider. We assume that the social perception is entirely *visual* and that

This chapter is based on joint work with Razvan Fetecau and Lenya Ryzhik, submitted for publication in Nonlinearity [EFR14]. A substantial part of this work was done during my visit to Simon Fraser University, Burnaby, Canada, in February-March 2014.

individuals have a limited field of vision centred around their direction of motion. We come back to this choice for the direction of the field of vision in the discussion of this chapter, Section 2.6. Given a reference individual located at x_i moving with velocity v_i, the weights w_{ij} depend on the angle under which individual i perceives individual j when looking in the direction of v_i. Mathematically, this is denoted by a dependence on the position of individual j relative to individual i, i.e. $x_j - x_i$, and on the current direction of motion v_i. Hence, we define w_{ij} as

$$w_{ij} := g\left(\frac{x_i - x_j}{|x_i - x_j|} \cdot \frac{v_i}{|v_i|}\right). \tag{2.3}$$

As explained in Section 1.7.1, the function $g : [-1, 1] \to [0, 1]$ is such that w_{ij} is largest when $x_j - x_i$ is in the same direction as v_i (j is right ahead of individual i) and smallest when $x_j - x_i$ and v_i point in opposite directions (j is behind i). In general, $w_{ij} \neq w_{ji}$.

The modifications introduced in (2.2) and (2.3), turn the original model (2.1) into

$$\begin{cases} \dfrac{dx_i}{dt} = v_i; & \text{(2.4a)} \\ v_i = -\dfrac{1}{N}\displaystyle\sum_{j\neq i} \nabla_{x_i} K(|x_i - x_j|)\, g\left(\dfrac{x_i - x_j}{|x_i - x_j|} \cdot \dfrac{v_i}{|v_i|}\right), & \text{(2.4b)} \end{cases}$$

which is the model that we study in this chapter; its main properties are discussed in Section 2.2. The *implicit* equation (2.4b) may, in general, have multiple solutions. Moreover, solutions of (2.4) may lack *smoothness*. Velocities have to be allowed to be discontinuous, as roots of (2.4b) may disappear in time due to changes in the spatial configuration $\{x_1, x_2, \ldots, x_N\}$. At these jump times, a selection criterion for the jumps is needed. Note moreover that particles can stop, as velocities in (2.4) can become zero in finite time. This is a degeneracy problem since (2.4) is not defined if $v_i = 0$ for some particle i.

In the spirit of Section 1.3, we associate to (2.4) the following second-order system:

$$\begin{cases} \dfrac{dx_i}{dt} = v_i; \\ \varepsilon\dfrac{dv_i}{dt} = -v_i - \dfrac{1}{N}\displaystyle\sum_{j\neq i} \nabla_{x_i} K(|x_i - x_j|)\, g\left(\dfrac{x_i - x_j}{|x_i - x_j|} \cdot \dfrac{v_i}{|v_i|}\right). \end{cases} \tag{2.5}$$

If $\nabla K(|\cdot|)$ and g are bounded and Lipschitz continuous (cf. the assumptions at the end of Section 2.2.1), solutions to the system (2.5) exist (locally in time) and are unique. The results by Tikhonov concerning the limit $\varepsilon \to 0$, which were mentioned in Section 1.7.1, are stated in Section 2.3. We use (2.5) with small or vanishing ε to serve as a jump criterion when the velocity in (2.4) becomes discontinuous. The relaxation term in (2.5) smoothes out the trajectories of (2.4), as is illustrated by Figures 2.1b–2.1c.

The modes of breakdown of (2.4) and the jump selection through the relaxation model (2.5) are presented in Section 2.4 of this chapter. We do not deal here with extensive

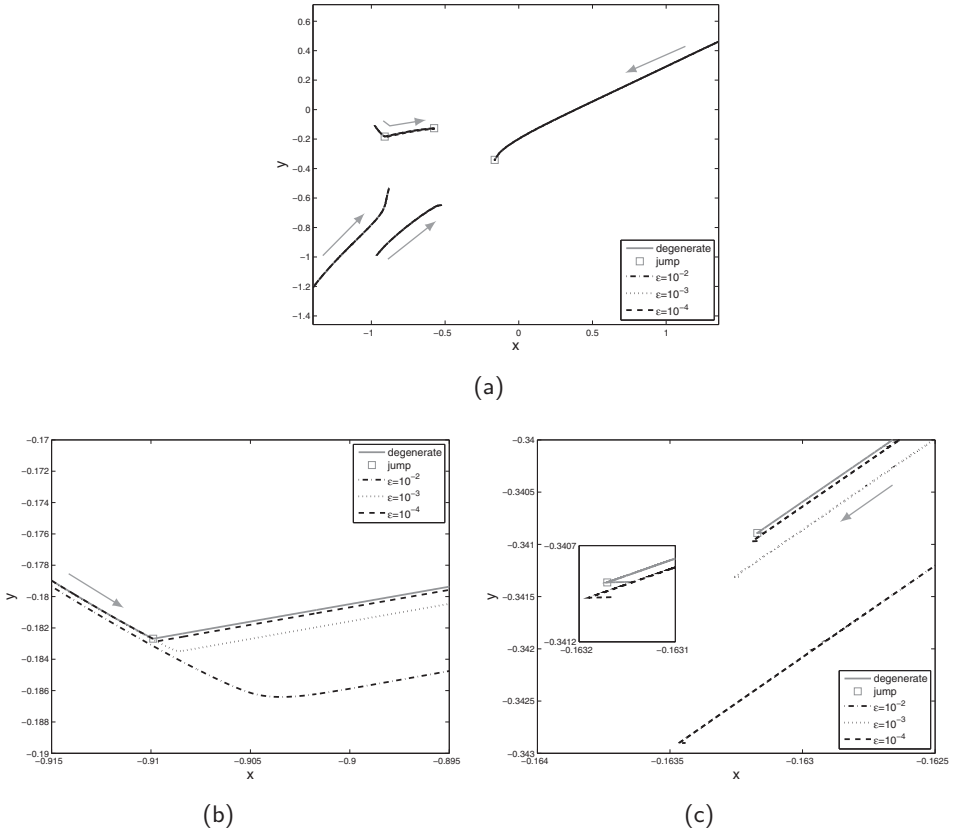

Figure 2.1: Time evolution of a random initial configuration of four particles. The arrows indicate the direction in which the particles move. (a): The solid line represents the solution of the anisotropic first-order model (2.4). The extension of the solution beyond breakdown times (indicated by squares) is explained in Section 2.4. On top of this plot we graph the solution of the relaxation model (2.5) for three values of ε: $\varepsilon = 10^{-2}, 10^{-3}$, and 10^{-4}. The plots are indistinguishable at the scale of the figure. (b) and (c): Zoomed images near two of the breakdown times of model (2.4). Note how the ε-model (2.5) captures the discontinuities in velocity, as well as approximates solutions of (2.4) away from the jumps.

numerical simulations and the complex issue of the long term behaviour of (2.4) is only briefly addressed in Section 2.5. We restrict ourselves to the two-dimensional simulations of (2.4), using (2.5) to deal with instantaneous root losses, as well as particle stopping.

2.2 The anisotropic model (2.4)

Given a fixed spatial configuration $\{x_i\}_{i=1}^N$, we study the existence of a velocity field that satisfies the fixed point equation (2.4b). Then we study the dynamic evolution of solutions to (2.4), initialized at some configuration $x_i(0) = x_i^0$.

2.2.1 The interaction kernel

The system (2.4) with $g \equiv 1$ is a well-established model, extensively studied in the last decade; see also Sections 1.3, 1.5 and 1.7.1. The properties of the interaction potential K are crucial for obtaining the well-posedness and the long-time behaviour of the solutions to (2.1) (or its continuum limit). We are interested in biologically relevant choices of K which incorporate short-range repulsive and long-range attractive interactions. One such choice is the Morse potential [LTB09, CDM$^+$07], which has the form

$$K(|x|) = -C_a e^{-|x|/l_a} + C_r e^{-|x|/l_r}, \tag{2.6}$$

with the constants C_a, C_r, l_a and l_r representing the strengths and ranges of the attractive and repulsive interactions, respectively. Our theoretical results apply both to the Morse potential, and to a large set of other choices of K (for example, power-laws with positive exponents and the antiderivative of the $\tanh$ function [KSUB11, vBUKB12]).

The function g that models the field of vision is the main new ingredient and its choice is far from unique. Denote by ϕ_{ij} the angle between $x_j - x_i$ and v_i. See Figure 2.2a for an illustration. Hence

$$\frac{x_i - x_j}{|x_i - x_j|} \cdot \frac{v_i}{|v_i|} = -\cos\phi_{ij}.$$

The weights $w_{ij} = g(-\cos\phi_{ij})$ should be the largest (value 1) for $\phi_{ij} = 0$ (when the vectors $x_j - x_i$ and v_i are parallel) and the smallest (possibly 0) for $\phi_{ij} = \pi$ (when $x_j - x_i$ and v_i anti-parallel). Two choices of g that capture this behaviour are

$$g(-\cos\phi) = [\tanh(a(\cos\phi + 1 - b/\pi)) + 1]/c, \tag{2.7}$$

with c a normalization constant such that $g(-1) = 1$, and

$$g(-\cos\phi) = [a\cos\phi + b]/(a + b). \tag{2.8}$$

The $\tanh$ function (2.7) is illustrated in Figure 2.2b. The function takes values close to 1 in the field of vision (around $\phi = 0$) and decays steeply toward the blind zone. These regions of high values, steep descent and low values are indicated in dark grey, light grey and white in Figure 2.2a. In (2.7) the parameter a controls the steepness of the graph and b controls its width (size of field of vision).

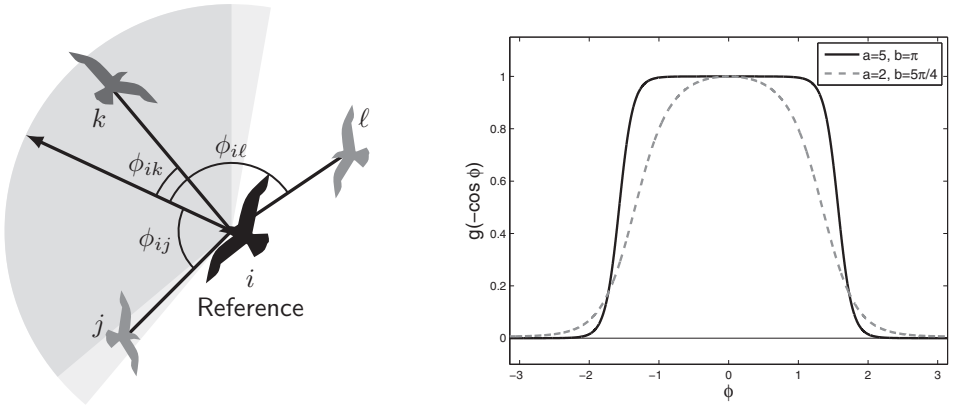

(a) (b)

Figure 2.2: (a): Illustration of the angle dependency in the visual perception of a reference individual i: the field of vision (dark grey), the peripheral vision (light grey) and the blind zone (white). Interactions are weighted: $w_{ik} > w_{ij} > w_{i\ell}$. (b): The weight function g given by (2.7). The following parameters are shown: $a = 5$ and $b = \pi$ (solid), $a = 2$ and $b = 5\pi/4$ (dashed) – a controls the steepness of the graph and b controls its width. The function takes values close to 1 in a region around $\phi = 0$ (field of vision), has a steep decay to nearly 0 in the peripheral vision, and takes negligible values near $\phi = \pm\pi$ (blind zone).

In this chapter we are not concerned with sharp analytical results and we assume that K and g satisfy enough properties for the analysis to be carried over simply and with the least technical difficulties. Some of the results can be obtained under weaker assumptions. In general, the following assumptions on K and g are needed:

$$K : \mathbb{R}_0^+ \to \mathbb{R} \quad \text{is } C^2\text{, with bounded derivatives,} \tag{2.9}$$

and

$$g : [-1, 1] \to [0, 1] \quad \text{is } C^1. \tag{2.10}$$

In particular, K' and g are bounded and Lipschitz continuous.

2.2.2 The implicit equation for v_i – existence and non-uniqueness

We investigate the existence and uniqueness of a fixed point of the implicit equation (2.4b) for v_i. Note that particle stopping ($v_i = 0$ for some i) is not well-defined for (2.4). The reason is that the field of vision of an individual is intrinsically defined in terms of its current direction of motion, along v_i. However, we observe in numerical simulations that particles do have a tendency to stop. Stopping may occur for instance when a particle loses sense of the others, brakes down and stops before making a sudden turn to redirect itself toward the rest of the group. Or, in an opposite situation, when a particle gets to a point where its repulsive interactions are dominant, and makes a turn to avoid getting too close to the rest. Such a sudden change in direction due to stopping is illustrated in Figure 2.1c.

To deal with the stopping, as is common in the ODE theory with discontinuous non-linearities [CL71, Fil88], we introduce a *generalized* definition of a fixed point of (2.4b). We will regard $\operatorname{sgn}(z)$ as a set-valued function given by the subdifferential of the Euclidean norm $|z|$:

$$\operatorname{sgn}(z) := \partial|z| = \begin{cases} \frac{z}{|z|} & z \neq 0, \\ \overline{B(0,1)} & z = 0. \end{cases}$$

Given a spatial configuration $\{x_i\}$, the resting scenario can now be considered as a solution of (2.4b) if the following generalization of a solution is taken[1].

Definition 2.2.1 (Generalized fixed point)**.** *We call $v \in \mathbb{R}^d$ a generalized solution of* (2.4b) *if there exists an $s \in \operatorname{sgn}(v)$ such that*

$$v = -\frac{1}{N} \sum_{j \neq i} \nabla_{x_i} K(|x_i - x_j|)\, g\left(\frac{(x_i - x_j)}{|x_i - x_j|} \cdot s \right). \tag{2.11}$$

We show in Theorem 2.2.2 that the implicit equation (2.4b) always has at least one generalized solution in the sense of Definition 2.2.1. However, in view of the next example, we do not expect such solutions to be unique.

[1] The idea for this approach arose during one of our CASA 'Wednesday morning sessions', for which I thank Giovanni Bonaschi, Manh Hong Duong, Patrick van Meurs, Georg Prokert and, in particular, Mark Peletier.

Non-uniqueness

To show that solutions of (2.4b) are generally non-unique, we look at a simple example in two dimensions ($d = 2$) with four particles ($N = 4$) situated at the four corners of a square, where *each* equation for v_i ($i = 1, \dots, 4$) has three solutions. Hence, there are $81 = 3^4$ different combinations of v_i that solve (2.4b) ($i = 1, \dots, 4$) for this particular example! To be more precise, we take the anisotropy function g to be linear, as in (2.8): $g(\omega) = (1 - \omega)/2$, and K to be the Morse potential (2.6). For such K, the derivative $K'(r)$ is negative (repulsive) at short distances and positive (attractive) at long ranges. It is easy to see that we can find $\beta > 0$ with $K'(\beta) < 0$ (β in the repulsive range) such that

$$K'(\beta) + \frac{1}{2}\sqrt{2}\, K'(\beta\sqrt{2}) = 0. \tag{2.12}$$

Let the four particles be located at the corners of a square of size β (see Figure 2.3):

$$x_1 = \frac{\beta}{2}\begin{bmatrix}1\\1\end{bmatrix},\ x_2 = \frac{\beta}{2}\begin{bmatrix}-1\\1\end{bmatrix},\ x_3 = \frac{\beta}{2}\begin{bmatrix}-1\\-1\end{bmatrix},\ x_4 = \frac{\beta}{2}\begin{bmatrix}1\\-1\end{bmatrix}.$$

Then, for each particle there are three admissible velocities in the sense of Definition 2.2.1, as illustrated in Figure 2.3. The first is the stopping/zero velocity indicated by a circle. The second is a velocity vector pointing inward (toward the centre) and the third solution is a velocity pointing outward, opposite in direction and equal in size to the previous.

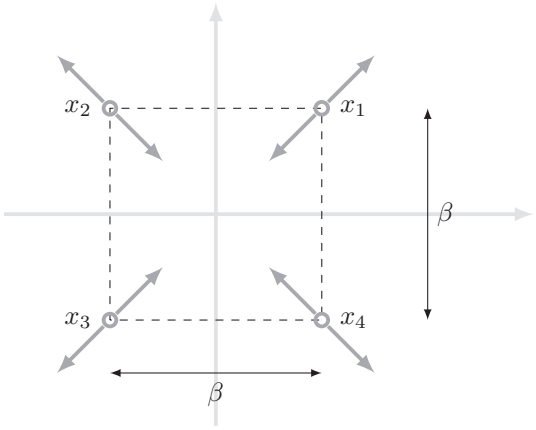

Figure 2.3: Four particles positioned on the corners of a square of size β. Each of them has three admissible velocities (generalized solutions of (2.4b)): one pointing inward, one pointing outward and $v = 0$ (indicated by a circle).

Indeed, consider, for instance, particle 1 in this square configuration and the velocity equation (2.4b) with $i = 1$. We have

$$x_1 - x_2 = \beta\begin{bmatrix}1\\0\end{bmatrix},\ x_1 - x_3 = \beta\begin{bmatrix}1\\1\end{bmatrix},\ x_1 - x_4 = \beta\begin{bmatrix}0\\1\end{bmatrix}, \tag{2.13}$$

and

$$|x_1 - x_2| = \beta,\ |x_1 - x_3| = \beta\sqrt{2},\ |x_1 - x_4| = \beta, \tag{2.14}$$

so that

$$\begin{aligned} -\frac{1}{4}\sum_{j\neq 1} \nabla_{x_1} K(|x_1 - x_j|)\, g\left(\frac{(x_1 - x_j)}{|x_1 - x_j|}\cdot s\right) \\ = -\underbrace{\frac{1}{8}\sum_{j\neq 1} K'(|x_1 - x_j|)\,\frac{x_1 - x_j}{|x_1 - x_j|}}_{=0} + \frac{1}{8}\sum_{j\neq 1} K'(|x_1 - x_j|)\,\frac{x_1 - x_j}{|x_1 - x_j|}\,\frac{(x_1 - x_j)}{|x_1 - x_j|}\cdot s, \end{aligned} \tag{2.15}$$

for any $s \in \overline{B(0,1)}$. The first term on the right-hand side vanishes due to (2.12), (2.13) and (2.14). This is equivalent to the fact that the square configuration with size β is an equilibrium of the isotropic model ($g \equiv 1$). For $v = 0$, $s = 0$ is an element of $\mathrm{sgn}(v)$ and

$$0 = \frac{1}{8}\sum_{j\neq 1} K'(|x_1 - x_j|)\,\frac{x_1 - x_j}{|x_1 - x_j|}\,\frac{(x_1 - x_j)}{|x_1 - x_j|}\cdot 0.$$

Hence, $v_1 = 0$ is a *generalized* fixed point of (2.4b).

We look now for a nonzero solution $v = (v^1, v^2)$ of (2.4b). Given (2.15), we have to solve for v in

$$\begin{aligned} v &= \frac{1}{8}\sum_{j\neq 1} K'(|x_1 - x_j|)\,\frac{x_1 - x_j}{|x_1 - x_j|}\,\frac{(x_1 - x_j)}{|x_1 - x_j|}\cdot\frac{v}{|v|} \\ &= \frac{1}{8|v|}\left(v^1 K'(\beta)\begin{bmatrix}1\\0\end{bmatrix} + \frac{1}{2}(v^1 + v^2)\,K'(\beta\sqrt{2})\begin{bmatrix}1\\1\end{bmatrix} + v^2 K'(\beta)\begin{bmatrix}0\\1\end{bmatrix}\right). \end{aligned}$$

Looking for a particular solution with $v^1 = v^2$, we find

$$v^1 = \frac{1}{8\sqrt{2}}\,\frac{v^1}{|v^1|}\left(K'(\beta) + K'(\beta\sqrt{2})\right),$$

or, in view of (2.12),

$$|v^1| = \frac{\sqrt{2}}{16}\left(1 - \frac{1}{2}\sqrt{2}\right)K'(\beta\sqrt{2}). \tag{2.16}$$

Note that since $K'(\beta\sqrt{2}) > 0$, the right-hand side of (2.16) is, indeed, positive. Hence, there are two (opposite in sign, but equal in magnitude) solutions for v^1. This yields two velocity vectors as illustrated in Figure 2.3. The same argument applies to the other particles due to the rotational symmetry.

Existence

We now prove the existence of a generalized solution of (2.4b). Let $\{x_j\}_{j=1}^N \subset \mathbb{R}^d$ be a *fixed* set of distinct positions and take a specific index $i \in \{1, \ldots, N\}$.

Theorem 2.2.2. *Assume that $K : \mathbb{R}^+ \to \mathbb{R}$ has a bounded derivative, and $g : [-1, 1] \to [0, 1]$ is continuous. Then there exists a generalized fixed point in the sense of Definition 2.2.1.*

Proof. To deal with the singularity of (2.4b) at $v = 0$, we use a regularization argument. For any $\alpha > 0$, define the mapping $\mathcal{F}^\alpha : \mathbb{R}^d \to \mathbb{R}^d$ by

$$\mathcal{F}^\alpha(v) := -\frac{1}{N} \sum_{j \neq i} \nabla_{x_i} K(|x_i - x_j|)\; g\left(\frac{(x_i - x_j)}{|x_i - x_j|} \cdot \frac{v}{\alpha + |v|} \right) \text{ for all } v \in \mathbb{R}^d. \quad (2.17)$$

The map $\mathcal{F}^\alpha$ is continuous and uniformly bounded on $\mathbb{R}^d$ with

$$|\mathcal{F}^\alpha(v)| \leqslant \|K'\|_\infty \, \|g\|_\infty \qquad \text{for all } v \in \mathbb{R}^d.$$

Brouwer's Fixed Point Theorem implies that $\mathcal{F}^\alpha$ has a fixed point (which depends on α) in the closed ball $\overline{B(0, \rho)}$ where $\rho := \|K'\|_\infty \, \|g\|_\infty$. We now show that a generalized fixed point satisfying (2.11) can be obtained by passing to the limit $\alpha \downarrow 0$. Assume that $\alpha_n \to 0$, with $\alpha_n > 0$, and let $\{v^{\alpha_n}\}$ be a corresponding set of fixed points of $\mathcal{F}^{\alpha_n}$:

$$v^{\alpha_n} = -\frac{1}{N} \sum_{j \neq i} \nabla_{x_i} K(|x_i - x_j|)\; g\left(\frac{(x_i - x_j)}{|x_i - x_j|} \cdot \frac{v^{\alpha_n}}{\alpha_n + |v^{\alpha_n}|} \right). \quad (2.18)$$

Since $|v^{\alpha_n}| \leqslant \rho$ is uniformly bounded, $\{v^{\alpha_n}\}$ converges along a subsequence. For convenience, relabel this subsequence as $\{v^{\alpha_n}\}$ and define its limit:

$$v = \lim_{n \to \infty} v^{\alpha_n}.$$

If $v \neq 0$, then, as

$$\lim_{n \to \infty} \frac{v^{\alpha_n}}{\alpha_n + |v^{\alpha_n}|} = \frac{v}{|v|},$$

we can simply pass to the limit $n \to \infty$ in the fixed point equation (2.18), and conclude that v is a fixed point.

On the other hand, if $v = 0$, we set

$$w_n = \frac{v^{\alpha_n}}{\alpha_n + |v^{\alpha_n}|},$$

and note that $|w_n| < 1$. Thus, up to extraction of a subsequence, w_n converges to a limit

$$s = \lim_{k \to \infty} w_{n_k},$$

with $|s| \leqslant 1$. Sending $k \to \infty$ in the fixed point equation (2.18) for $v^{\alpha_{n_k}}$ we find that $v = 0$ satisfies (2.11), with $s \in \overline{B(0, 1)} = \operatorname{sgn}(v)$. □

2.2.3 Local continuity of trajectories

Given that a velocity field always exists for a given configuration, we study now the local existence of continuous solutions to (2.4). We denote by bold characters $\mathbf{x}$ and $\mathbf{v}$ the concatenation of all particles' locations and velocities, respectively, i.e.,

$$\mathbf{x} = (x_1, \dots, x_N), \quad \mathbf{v} = (v_1, \dots, v_N).$$

To rule out issues such as collisions or particle stopping, we look for solutions $(\mathbf{x}(t), \mathbf{v}(t))$, in the set

$$\mathcal{R}_{\lambda,\mu} := \left\{(x_1, \dots, x_N, v_1, \dots, v_N) \in \mathbb{R}^{2Nd} : |x_i - x_j| > \lambda \text{ if } i \neq j, |v_i| > \mu\right\}, \quad (2.19)$$

for fixed $\lambda > 0$ and $\mu > 0$.

The implicit equation (2.4b) for v_i does not depend on the velocities v_j of the other particles $j \neq i$. This motivates the definition of

$$\mathcal{F}_i : \tilde{\mathcal{R}}_{\lambda,\mu} \to \mathbb{R}^d,$$

$$\mathcal{F}_i(\mathbf{x}, v) = \mathcal{F}_i(x_1, \dots, x_N, v) := -v - \frac{1}{N} \sum_{j \neq i} \nabla_{x_i} K(|x_i - x_j|)\, g\left(\frac{(x_i - x_j)}{|x_i - x_j|} \cdot \frac{v}{|v|}\right), \quad (2.20)$$

where

$$\tilde{\mathcal{R}}_{\lambda,\mu} := \left\{(x_1, \dots, x_N, v) \in \mathbb{R}^{Nd} \times \mathbb{R}^d : |x_i - x_j| > \lambda \text{ if } i \neq j, |v| > \mu\right\},$$

for any $\lambda, \mu > 0$. For a given configuration $\mathbf{x}$, the velocity v_i is among the zeros of $\mathcal{F}_i(\mathbf{x}, \cdot)$ regarded as a function of v. Let $J_v \mathcal{F}_i$ denote the Jacobian matrix of $\mathcal{F}_i$ with respect to its v-dependence. Hence, $J_v \mathcal{F}_i$ is a mapping into $\mathbb{R}^{d \times d}$. The Implicit Function Theorem – see [Eva10], Appendix C.7 – implies immediately the following:

Theorem 2.2.3 (Local continuity)**.** *Assume that at time τ the phase space configuration $(\mathbf{x}(\tau), \mathbf{v}(\tau)) \in \mathcal{R}_{\lambda,\mu}$, with $\mathcal{F}_i(\mathbf{x}(\tau), v_i(\tau)) = 0$ for all $i \in \{1, \dots, N\}$, satisfies*

$$\det J_v \mathcal{F}_i(\mathbf{x}(\tau), v_i(\tau)) \neq 0 \quad \text{for all } i \in \{1, \dots, N\}.$$

Then there is a $\Delta\tau > 0$ such that the system

$$\begin{cases} \dfrac{d\mathbf{x}}{dt} = \mathbf{v}, \\ \\ \mathcal{F}_i(\mathbf{x}, v_i) = 0, \ \text{for all } i \in \{1, \dots, N\}, \end{cases} \quad (2.21)$$

has a unique (local) solution $(\mathbf{x}, \mathbf{v}) : (\tau - \Delta\tau, \tau + \Delta\tau) \to \mathcal{R}_{\lambda,\mu}$ that is continuous and that passes through $(\mathbf{x}(\tau), \mathbf{v}(\tau))$ at time τ.

Proof. The proof is elementary. It follows from the Implicit Function Theorem that for each $i \in \{1, \dots, N\}$ there exists an open set W_i and a unique map $\gamma_i \in C^1(W_i; \mathbb{R}^d)$, such that $\mathbf{x}(\tau) \in W_i$, the image $\gamma_i(W_i)$ is an open set containing $v_i(\tau) = \gamma_i(\mathbf{x}(\tau))$,

and $\mathcal{F}_i(\mathbf{x}, \gamma_i(\mathbf{x})) = 0$ for all $\mathbf{x} \in W_i$. Define $\Gamma(\mathbf{x}) := (\gamma_1(\mathbf{x}), \dots, \gamma_N(\mathbf{x}))$ on a closed bounded subset of $\Omega := \bigcap_{i=1}^N W_i$. Since Γ is C^1, it is Lipschitz continuous, and the theorem follows from the Picard-Lindelöf Theorem (cf. [Tes12], Theorem 2.2) applied to the system

$$\frac{d\mathbf{x}}{dt} = \Gamma(\mathbf{x}).$$

□

Remark 2.2.4. Given $\mathbf{x}^*$ a space configuration and $\mathbf{v}^* = (v_1^*, \dots, v_N^*)$ a corresponding velocity, i.e. $\mathcal{F}_i(\mathbf{x}^*, v_i^*) = 0$ for all $i \in \{1, \dots, N\}$, the non-vanishing determinant condition

$$\det J_v \mathcal{F}_i(\mathbf{x}^*, v_i^*) \neq 0 \quad \text{ for all } i \in \{1, \dots, N\}$$

guarantees that the fixed point $\mathbf{v}^*$ is isolated, and Theorem 2.2.3 provides a unique solution of (2.4) starting at configuration $\mathbf{x}^*$ in the direction $\mathbf{v}^*$. There could be multiple velocities $\mathbf{v}^*$ corresponding to the same configuration $\mathbf{x}^*$ but as long as such a velocity vector is isolated, there exists a unique continuous trajectory through $\mathbf{x}^*$ in its direction. This will be revisited in Section 2.3 in connection with the $\varepsilon \to 0$ limit of the relaxation system (2.5).

Remark 2.2.5. The (local) continuous solutions provided by Theorem 2.2.3 can be extended in time for as long as we do not encounter collisions or particle stopping (see definition (2.19) of $\mathcal{R}_{\lambda,\mu}$) *and* the Jacobian matrices $J_v\mathcal{F}_i$ remain invertible along the trajectory. Ruling out collisions and stopping, we conclude that model (2.4) has a unique solution that is continuous in position and velocity *up to the moment* that $\det J_v \mathcal{F}_i = 0$ for some i. Numerical experiments in Section 2.4 show that, in the absence of collisions or stopping, discontinuities in velocities occur at such times. To deal with such velocity jumps both analytically and numerically, we use the relaxation model (2.5) (see Sections 2.3 and 2.4).

The two-dimensional case

We now apply the above considerations to two dimensions to show that the nonzero determinant condition can be reduced to a very simple scalar form.

Assume that the configuration $\{x_1, \dots, x_N\} \subset \mathbb{R}^2$ is given, and that we search for a nonzero solution of (2.4b). Using the polar coordinate representation $v_i = r_i[\cos\theta_i, \sin\theta_i]^T$, we write (2.4b) as

$$r_i \begin{bmatrix} \cos\theta_i \\ \sin\theta_i \end{bmatrix} = -\frac{1}{N} \sum_{j \neq i} \nabla_{x_i} K(|x_i - x_j|)\, g\left(\frac{x_i - x_j}{|x_i - x_j|} \cdot \begin{bmatrix} \cos\theta_i \\ \sin\theta_i \end{bmatrix} \right). \tag{2.22}$$

Taking the inner product with $[-\sin\theta_i, \cos\theta_i]^T$ and $[\cos\theta_i, \sin\theta_i]^T$, the vector equation (2.22) can be written as

$$\begin{cases} 0 = -\dfrac{1}{N} \displaystyle\sum_{j \neq i} \nabla_{x_i} K(|x_i - x_j|) \cdot \begin{bmatrix} -\sin\theta_i \\ \cos\theta_i \end{bmatrix} g\left(\dfrac{x_i - x_j}{|x_i - x_j|} \cdot \begin{bmatrix} \cos\theta_i \\ \sin\theta_i \end{bmatrix} \right), \\ r_i = -\dfrac{1}{N} \displaystyle\sum_{j \neq i} \nabla_{x_i} K(|x_i - x_j|) \cdot \begin{bmatrix} \cos\theta_i \\ \sin\theta_i \end{bmatrix} g\left(\dfrac{x_i - x_j}{|x_i - x_j|} \cdot \begin{bmatrix} \cos\theta_i \\ \sin\theta_i \end{bmatrix} \right). \end{cases} \tag{2.23}$$

The advantage of the polar coordinates is that the first equation in (2.23) is for θ_i *only*. Define the following functions ($i = 1, \dots, N$):

$$H_i(\theta) = -\frac{1}{N} \sum_{j \neq i} \nabla_{x_i} K(|x_i - x_j|) \cdot \begin{bmatrix} -\sin\theta \\ \cos\theta \end{bmatrix} g\left(\frac{x_i - x_j}{|x_i - x_j|} \cdot \begin{bmatrix} \cos\theta \\ \sin\theta \end{bmatrix} \right), \tag{2.24a}$$

$$R_i(\theta) = -\frac{1}{N} \sum_{j \neq i} \nabla_{x_i} K(|x_i - x_j|) \cdot \begin{bmatrix} \cos\theta \\ \sin\theta \end{bmatrix} g\left(\frac{x_i - x_j}{|x_i - x_j|} \cdot \begin{bmatrix} \cos\theta \\ \sin\theta \end{bmatrix} \right). \tag{2.24b}$$

Using (2.23) to solve for θ_i and r_i is equivalent to finding a root θ_i of H_i and subsequently expressing r_i explicitly:

$$H_i(\theta_i) = 0, \qquad r_i = R_i(\theta_i). \tag{2.25}$$

Note that a root θ_i of H_i generates a (nonzero) admissible velocity if $R_i(\theta_i) > 0$.

For a fixed choice of $\mathbf{x}$, we introduce the notation

$$\tilde{\mathcal{F}}_i(r, \theta) := \mathcal{F}_i\left(\mathbf{x}, r \begin{bmatrix} \cos\theta \\ \sin\theta \end{bmatrix} \right) = \begin{pmatrix} \cos\theta & -\sin\theta \\ \sin\theta & \cos\theta \end{pmatrix} \cdot \begin{bmatrix} -r + R_i(\theta) \\ H_i(\theta) \end{bmatrix}, \tag{2.26}$$

with $\mathcal{F}_i$ defined in (2.20). The chain rule of differentiation yields

$$J_{(r,\theta)} \tilde{\mathcal{F}}_i = J_v \mathcal{F}_i \cdot J_{(r,\theta)} v, \tag{2.27}$$

where $J_{(r,\theta)} v$ is the Jacobian matrix of the coordinate transform. Differentiating (2.26), we find that the second column of $J_{(r,\theta)} \tilde{\mathcal{F}}_i$ is

$$\frac{\partial \tilde{\mathcal{F}}_i}{\partial \theta} = \begin{pmatrix} \cos\theta & -\sin\theta \\ \sin\theta & \cos\theta \end{pmatrix} \cdot \begin{bmatrix} R_i'(\theta) \\ H_i'(\theta) \end{bmatrix} + \begin{pmatrix} -\sin\theta & -\cos\theta \\ \cos\theta & -\sin\theta \end{pmatrix} \cdot \begin{bmatrix} -r + R_i(\theta) \\ H_i(\theta) \end{bmatrix}. \tag{2.28}$$

Let $(\mathbf{x}^*, v^*) \in \tilde{\mathcal{R}}_{\lambda,\mu}$ satisfy $\mathcal{F}_i(\mathbf{x}^*, v^*) = 0$, so that $\tilde{\mathcal{F}}_i(r^*, \theta^*) = 0$, whence

$$\begin{bmatrix} -r^* + R_i(\theta^*) \\ H_i(\theta^*) \end{bmatrix} = 0. \tag{2.29}$$

Thus, we have

$$J_{(r,\theta)} \tilde{\mathcal{F}}_i = \begin{pmatrix} \cos\theta^* & -\sin\theta^* \\ \sin\theta^* & \cos\theta^* \end{pmatrix} \begin{pmatrix} -1 & R_i'(\theta^*) \\ 0 & H_i'(\theta^*) \end{pmatrix}. \tag{2.30}$$

Finally, taking the determinant on both sides of (2.27) and using (2.30), we obtain

$$|H_i'(\theta^*)| = r^* \, |\det J_v \mathcal{F}_i(\mathbf{x}^*, v^*)|.$$

The condition $\det J_v \mathcal{F}_i(\mathbf{x}^*, v^*) \neq 0$ is thus equivalent to $H_i'(\theta^*) \neq 0$. In other words, in two dimensions, the continuity issues are only to be expected either when H_i' becomes zero, or when trajectories reach the boundary of $\mathcal{R}_{\lambda,\mu}$ (particles collide or one of the velocities reaches zero).

2.3 Relaxation model (2.5): convergence for $\varepsilon \to 0$

In this section we investigate the relaxation system (2.5). This system is well-posed locally in time. We explain in what sense solutions of (2.5) converge to those of (2.4) as $\varepsilon \to 0$.

2.3.1 Convergence of solutions to (2.5) as $\varepsilon \to 0$

As opposed to (2.4), the regularized system (2.5) has *unique* local solutions, for each $\varepsilon > 0$, provided that $\nabla K(|\cdot|)$ and g are bounded and Lipschitz continuous.

We now apply the theory developed by Tikhonov [Tik52, Vas63] to study the limit $\varepsilon \to 0$ of solutions to (2.5). We start by paraphrasing some of the results presented in [Vas63]. Consider the system of equations

$$\begin{cases} \dfrac{d\mathbf{x}}{dt} = \mathbf{v}, \\ \varepsilon \dfrac{d\mathbf{v}}{dt} = \mathcal{F}(\mathbf{x}, \mathbf{v}), \end{cases} \tag{2.31}$$

where $\mathbf{x}, \mathbf{v} \in \mathbb{R}^{Nd}$ and $\varepsilon > 0$ is a small parameter. On a closed and bounded set $D \subset \mathbb{R}^{Nd}$, let $\Gamma : D \to \mathbb{R}^{Nd}$ be such that $\mathbf{v} = \Gamma(\mathbf{x})$ is a solution of the system of equations

$$\mathcal{F}(\mathbf{x}, \mathbf{v}) = 0. \tag{2.32}$$

The function Γ is called a *root* of (2.32). The system

$$\begin{cases} \dfrac{d\mathbf{x}}{dt} = \mathbf{v}, \\ \mathbf{v} = \Gamma(\mathbf{x}), \end{cases} \tag{2.33}$$

is called *the degenerate system of equations corresponding to the root* $\mathbf{v} = \Gamma(\mathbf{x})$.

Note that the systems of our interest (2.4) and (2.5) can be written in the short-hand notation (2.33) and (2.31), respectively. Indeed, define $\mathcal{F} : \mathcal{R}_{\lambda,\mu} \to \mathbb{R}^{Nd}$ using (2.20) as

$$\mathcal{F}(\mathbf{x}, \mathbf{v}) := \left(\mathcal{F}_1(\mathbf{x}, v_1), \ldots, \mathcal{F}_N(\mathbf{x}, v_N)\right), \tag{2.34}$$

for all $(\mathbf{x}, \mathbf{v}) \in \mathcal{R}_{\lambda,\mu}$. Then, locally in time, (2.5) can be written compactly as (2.31), and (2.4) is a *degenerate* system in the form (2.33), with function $\Gamma = (\gamma_1, \ldots, \gamma_N)$ provided by the Implicit Function Theorem (see Theorem 2.2.3 and its proof).

Definition 2.3.1 (Isolated root)**.** *The root Γ is called isolated if there is a $\delta > 0$ such that for all $\mathbf{x} \in D$ the only element in $B(\Gamma(\mathbf{x}), \delta)$ that satisfies $\mathcal{F}(\mathbf{x}, \mathbf{v}) = 0$ is $\mathbf{v} = \Gamma(\mathbf{x})$.*

Definition 2.3.2 (Adjoined system and positive stability)**.** *For fixed $\mathbf{x}^*$, the system*

$$\frac{d\mathbf{v}}{d\tau} = \mathcal{F}(\mathbf{x}^*, \mathbf{v}), \tag{2.35}$$

is called the adjoined system of equations. An isolated root Γ *is called positively stable in* D*, if* $\mathbf{v}^* = \Gamma(\mathbf{x}^*)$ *is an asymptotically stable stationary point of* (2.35) *as* $\tau \to \infty$*, for each* $\mathbf{x}^* \in D$*.*

Definition 2.3.3 (Domain of influence)**.** *The domain of influence of an isolated positively stable root* Γ *is the set of points* $(\mathbf{x}^*, \tilde{\mathbf{v}})$ *such that the solution of* (2.35) *satisfying* $\mathbf{v}|_{\tau=0} = \tilde{\mathbf{v}}$ *tends to* $\mathbf{v}^* = \Gamma(\mathbf{x}^*)$ *as* $\tau \to \infty$*.*

The following theorem, due to Tikhonov [Tik52], states under which conditions and in what sense solutions of (2.31) converge to solutions of the degenerate system (2.33).

Theorem 2.3.4 (cf. [Tik52] or [Vas63], Thm. 1.1)**.** *Assume that* Γ *is an isolated positively stable root of* (2.32) *in some bounded closed domain* D*. Consider a point* $(\mathbf{x}_0, \mathbf{v}_0)$ *in the domain of influence of this root, and assume that the degenerate system* (2.33) *has a solution* $\mathbf{x}(t)$ *initialized at* $\mathbf{x}(t_0) = \mathbf{x}_0$*, that lies in* D *for all* $t \in [t_0, T]$*. Then, as* $\varepsilon \to 0$*, the solution* $(\mathbf{x}^\varepsilon(t), \mathbf{v}^\varepsilon(t))$ *of* (2.31) *initialized at* $(\mathbf{x}_0, \mathbf{v}_0)$*, converges to* $(\mathbf{x}(t), \mathbf{v}(t)) := (\mathbf{x}(t), \Gamma(\mathbf{x}(t)))$ *in the following sense:*

(i) $\lim\limits_{\varepsilon \to 0} \mathbf{v}^\varepsilon(t) = \mathbf{v}(t)$ *for all* $t \in (t_0, T^*]$*, and*

(ii) $\lim\limits_{\varepsilon \to 0} \mathbf{x}^\varepsilon(t) = \mathbf{x}(t)$ *for all* $t \in [t_0, T^*]$*,*

for some $T^* < T$*.*

Remark 2.3.5. The degenerate system requires an initial condition $\mathbf{x}_0$ only for positions, while for the ε-system both $\mathbf{x}_0$ and $\mathbf{v}_0$ need to be provided. It is possible that $\mathbf{v}_0$ is *incompatible* in the sense that $\mathbf{v}_0 \neq \Gamma(\mathbf{x}_0)$. This is exactly why the convergence of $\mathbf{v}^\varepsilon(t)$ to $\mathbf{v}(t)$ only holds for $t > t_0$. In case of incompatible initial conditions an initial layer forms, which gets narrower as $\varepsilon \to 0$.

The following result is a direct consequence of Theorem 2.3.4; it shows convergence of solutions of (2.5) to solutions of (2.4).

Theorem 2.3.6 (Convergence of the relaxation model as $\varepsilon \to 0$)**.** *Assume that the isolated root* Γ *is* positively stable *in* D*, and take* $(\mathbf{x}_0, \mathbf{v}_0)$ *in the domain of influence of this root. Denote by* $\mathbf{x}(t)$ *the (local) solution in* D *of the degenerate system* (2.4) *with initial configuration* $\mathbf{x}_0$ *(the existence of this solution is provided by Theorem 2.2.3). Then, the solution* $(\mathbf{x}^\varepsilon(t), \mathbf{v}^\varepsilon(t))$ *of the regularized system* (2.5)*, initialized at* $(\mathbf{x}_0, \mathbf{v}_0)$*, converges as* $\varepsilon \to 0$ *to* $(\mathbf{x}(t), \mathbf{v}(t)) := (\mathbf{x}(t), \Gamma(\mathbf{x}(t)))$ *in the sense (i) and (ii) given in Theorem 2.3.4.*

Remark 2.3.7. Unless collisions or stopping occur, a C^1 solution $\mathbf{x}(t)$ of (2.4) exists as long as $\det J_v \mathcal{F}_i(\mathbf{x}(t), v_i(t)) \neq 0$ for all $i \in \{1, \dots, N\}$. Compare Remark 2.2.5. Positive stability of $\mathbf{v}(t) = \Gamma(\mathbf{x}(t))$ is guaranteed if the eigenvalues of $J_v \mathcal{F}_i(\mathbf{x}(t), v_i(t))$ are negative along the trajectory, for all $i \in \{1, \dots, N\}$. Moreover, once all these eigenvalues are negative at the initial time, they remain negative through the domain of existence of $\mathbf{x}(t)$, because none of these eigenvalues can change sign before $\det J_v \mathcal{F}_i(\mathbf{x}(t), v_i(t))$ touches 0 for some i. Hence, we infer that the convergence in Theorem 2.3.6 applies in all smooth regions of solutions $\mathbf{x}(t)$ of (2.4), before a breakdown of the solution occurs.

Remark 2.3.8. Theorem 2.3.6 (trivially) implies the convergence result for the isotropic case $g \equiv 1$ as $\varepsilon \to 0$. Note that the assumption (2.9) on K warrants a unique global-in-time solution of the isotropic model (2.1) – no collisions can occur – and hence, the convergence in Theorem 2.3.6 holds for all times $t > t_0$. Less regular potentials (e.g. $K(r) \sim r^{1+\alpha}$, $0 < \alpha < 1$; cf. [BCL09]) can lead to collisions in the isotropic model (2.1), in which case the convergence of the relaxation model is only local in time, as for the anisotropic case.

2.3.2 Positive stability of roots in two dimensions

Next, we elaborate the above convergence result with an example in dimension $d = 2$. In particular, we show that the stability of the fixed point Γ is essential, as otherwise the convergence fails. The notion of asymptotic stability in Definition 2.3.2 should be understood in the sense of Lyapunov. A stationary point $\mathbf{v}^* = \Gamma(\mathbf{x}^*)$ of (2.35) is asymptotically stable, if all eigenvalues of $J_{\mathbf{v}}\mathcal{F}(\mathbf{x}^*, \mathbf{v}^*)$ have strictly negative real part. Due to (2.34), the set of eigenvalues of $J_{\mathbf{v}}\mathcal{F}$ equals the union of the eigenvalues of all $J_v\mathcal{F}_i$, $i \in \{1, \dots, N\}$. Let $\mathbf{v}^* = (v_1^*, \dots, v_N^*)$ be a stationary point of (2.35), that is, $\mathcal{F}_i(\mathbf{x}^*, v_i^*) = 0$ for all $i \in \{1, \dots, N\}$. We write each velocity v_i^* in the polar coordinates, $v_i^* = r_i^*[\cos\theta_i^*, \sin\theta_i^*]^T$. To compute the eigenvalues of $J_v\mathcal{F}_i(\mathbf{x}^*, v_i^*)$, we use (2.27) and (2.30), to get

$$\underbrace{\begin{pmatrix} \cos\theta_i^* & -\sin\theta_i^* \\ \sin\theta_i^* & \cos\theta_i^* \end{pmatrix}}_{=:M} \begin{pmatrix} -1 & R_i'(\theta_i^*) \\ 0 & H_i'(\theta_i^*) \end{pmatrix} = J_v\mathcal{F}_i(\mathbf{x}^*, v_i^*) \underbrace{\begin{pmatrix} \cos\theta_i^* & -r_i^*\sin\theta_i^* \\ \sin\theta_i^* & r_i^*\cos\theta_i^* \end{pmatrix}}_{=:M_r}. \tag{2.36}$$

The functions H_i and R_i used here (see (2.24)) correspond to the fixed spatial configuration $\mathbf{x}^*$. The matrices $M_r^{-1}J_v\mathcal{F}_iM_r$ and $J_v\mathcal{F}_i$ have the same set of eigenvalues, and hence, we conclude from (2.36) that $J_v\mathcal{F}_i(\mathbf{x}^*, v_i^*)$ only has eigenvalues with negative real part, if and only if this is the case for

$$M_r^{-1}\, M \begin{pmatrix} -1 & R_i'(\theta_i^*) \\ 0 & H_i'(\theta_i^*) \end{pmatrix}.$$

We have

$$M_r^{-1}\, M = \begin{pmatrix} 1 & 0 \\ 0 & 1/r_i^* \end{pmatrix},$$

and the eigenvalues of

$$\begin{pmatrix} 1 & 0 \\ 0 & 1/r_i^* \end{pmatrix} \begin{pmatrix} -1 & R_i'(\theta_i^*) \\ 0 & H_i'(\theta_i^*) \end{pmatrix}$$

are

$$\lambda_1 = -1 \quad \text{and} \quad \lambda_2 = H_i'(\theta_i^*)/r_i^*. \tag{2.37}$$

Note that (within $\mathcal{R}_{\lambda,\mu}$) all eigenvalues are real-valued. Therefore, in view of (2.37), a sufficient condition for $\mathbf{v}^* = \Gamma(\mathbf{x}^*)$ to be asymptotically stable is

$$H_i'(\theta_i^*) < 0 \quad \text{for all} \quad i \in \{1, \dots, N\}. \tag{2.38}$$

Remark 2.3.9. An even more direct way of reaching (2.38) is to express the adjoined system (2.35) in terms of polar coordinates. Indeed, for each index i, (2.35) yields

$$\frac{dv_i}{d\tau} = \mathcal{F}_i(\mathbf{x}^*, v_i). \tag{2.39}$$

Let us write v_i in polar coordinates $v_i = r_i[\cos\theta_i, \sin\theta_i]^T$ and use (2.20) and notation (2.24) (with functions H_i and R_i corresponding to the spatial configuration $\mathbf{x}^* = (x_1^*, \dots, x_N^*)$), to derive from (2.39):

$$\frac{d\theta_i}{d\tau} = \frac{1}{r_i} H_i(\theta_i), \tag{2.40a}$$

$$\frac{dr_i}{d\tau} = -r_i + R_i(\theta_i). \tag{2.40b}$$

The condition (2.38) for the asymptotic stability can then be seen directly from (2.40). Indeed, the linearization of (2.40) around the stationary point (r_i^*, θ_i^*) yields the Jacobian matrix

$$\begin{pmatrix} H_i'(\theta_i^*)/r_i^* & 0 \\ R_i'(\theta_i^*) & -1 \end{pmatrix},$$

with the eigenvalues given by (2.37).

Remark 2.3.10. We note that using the polar coordinates in two dimensions reduces the problem to *scalar* expressions. For a better clarification of this point, let us summarize the findings so far. For convenience of notations, we drop the $*$ superscript.

Consider a given spatial configuration $\mathbf{x} = (x_1, \dots, x_N)$. Then the following statements hold:

- To find the velocities v_i corresponding to this configuration (solve $\mathcal{F}_i(\mathbf{x}, v_i) = 0$), it is more convenient to use polar coordinates $v_i = r_i[\cos\theta_i, \sin\theta_i]^T$. The problem reduces to finding the roots θ_i of $H_i(\theta) = 0$. Then take $r_i = R_i(\theta_i)$ for all $i \in \{1, \dots, N\}$. For a θ_i to be admissible, $R_i(\theta_i) > 0$ is required.
- The condition $\det J_v \mathcal{F}_i(\mathbf{x}, v_i) \neq 0$ for all $i = 1, \dots, N$ guarantees that the fixed point $\mathbf{v} = \Gamma(\mathbf{x})$ is isolated and that (2.4) has a unique continuous solution through $\mathbf{x}$ in the direction $\mathbf{v}$ (see Remark 2.2.4). In polar coordinates this condition is equivalent to $H_i'(\theta_i) \neq 0$, that is, θ_i is a *simple* root of H_i for all $i \in \{1, \dots, N\}$.
- The isolated root $\mathbf{v} = \Gamma(\mathbf{x})$ is positively stable, as required for the convergence of the ε-regularization (see Theorem 2.3.6), if $H_i'(\theta_i) < 0$ for all $i \in \{1, \dots, N\}$.

2.3.3 Numerical example

In *all* numerical experiments presented in this chapter we use the same choices of the potential K and field-of-vision function g. For the potential K we take the Morse potential (2.6) with $C_a = 3$, $C_r = 2$, $l_a = 2$, $l_r = 1$. The function g for the field of vision is taken as in (2.7) with parameters $a = 5$, $b = \pi$. This choice corresponds to the solid line

in Figure 2.2b. Note that the width of the field of vision is approximately 180° (frontal vision).

We present here a numerical example in two dimensions to illustrate the convergence of the ε system in Theorem 2.3.6. We consider a randomly-generated initial configuration of four particles – see Figure 2.4a. For the top left particle, labeled as particle 1, we plot the functions H_1 and R_1 defined by (2.24), and note that there are three admissible initial directions (see (2.25) and Figure 2.4b): $\theta_1 \approx -1.78$, $\theta_1 \approx -1.28$, $\theta_1 \approx -1.00$, and they are all simple roots since $H_1'(\theta_1) \neq 0$. Consequently, there are three isolated fixed points v_1 that represent the possible initial velocities for particle 1. The other three particles have unique velocities at this configuration; see Figure 2.4a where the admissible velocities are indicated by arrows.

Each such v_1 corresponds to a continuous trajectory of (2.4) starting from the initial configuration in Figure 2.4a. In the numerical implementation one has to *select* one of these admissible initial velocities and then evolve the system (2.4) in time. We use the 4th-order Runge-Kutta method for the numerical implementation. Figure 2.4c shows the trajectories of particle 1 that correspond to two of these admissible initial velocities: grey dashed (corresponding to root $\theta_1 \approx -1.28$) and grey solid (corresponding to $\theta_1 \approx -1.00$). Each trajectory in Figure 2.4c is the unique continuous solution given by Theorem 2.2.3 plotted on its *maximal* interval of existence – the possible modes of breakdown are discussed in detail in Section 2.4.

We turn now to the convergence of the ε regularization (2.5) and the role of the positive stability assumption in Theorem 2.3.6. Note that at the centre root $\theta_1 \approx -1.28$, H_1 has positive slope, while $H_1' < 0$ at the other two roots. It means that only the roots at $\theta_1 \approx -1.78$ and $\theta_1 \approx -1.00$ are positively stable, the centre one is not. The regularized system (2.5) is *not* expected to converge to the trajectory corresponding to the centre root and Figure 2.4c illustrates this fact. More specifically, the dash-dotted line shows the trajectory $x_1^\varepsilon(t)$ of particle 1, obtained by integrating numerically (2.5) starting from the configuration in Figure 2.4a and an initial velocity that corresponds to the root at $\theta_1 \approx -1.28$. Here, $\varepsilon = 10^{-4}$. Note that, due to the instability of this root, the trajectory of the ε-model does not follow the dashed trajectory of model (2.4). Instead, it approaches in a thin initial layer, the solid trajectory of (2.4) that corresponds to the stable root $\theta_1 \approx -1.00$.

Since identifying domains of influence of stable roots is a challenge in itself, we do not address here the question why the root at $\theta_1 \approx -1.00$ was 'chosen' instead of $\theta_1 \approx -1.78$. We simply note that the initial velocity we provided for the ε-system happened to be in the domain of influence of $\theta_1 \approx -1.00$. For an enhanced visualization, the stability/instability of the roots is also illustrated in Figure 2.4d. This figure shows the time evolution of the polar angle $\theta_1(t)$ of $v_1(t)$. The dashed grey and solid grey lines represent the evolution $\theta_1(t)$ corresponding to the like-marked trajectories in Figure 2.4c. These trajectories are continuous solutions of (2.4) that correspond to initial $\theta_1 \approx -1.28$ and $\theta_1 \approx -1.00$, respectively. The black dash-dotted line represents the evolution $\theta_1^\varepsilon(t)$ obtained from (2.5). Initialized at the unstable root, θ_1^ε undergoes a fast transition and approaches the solid

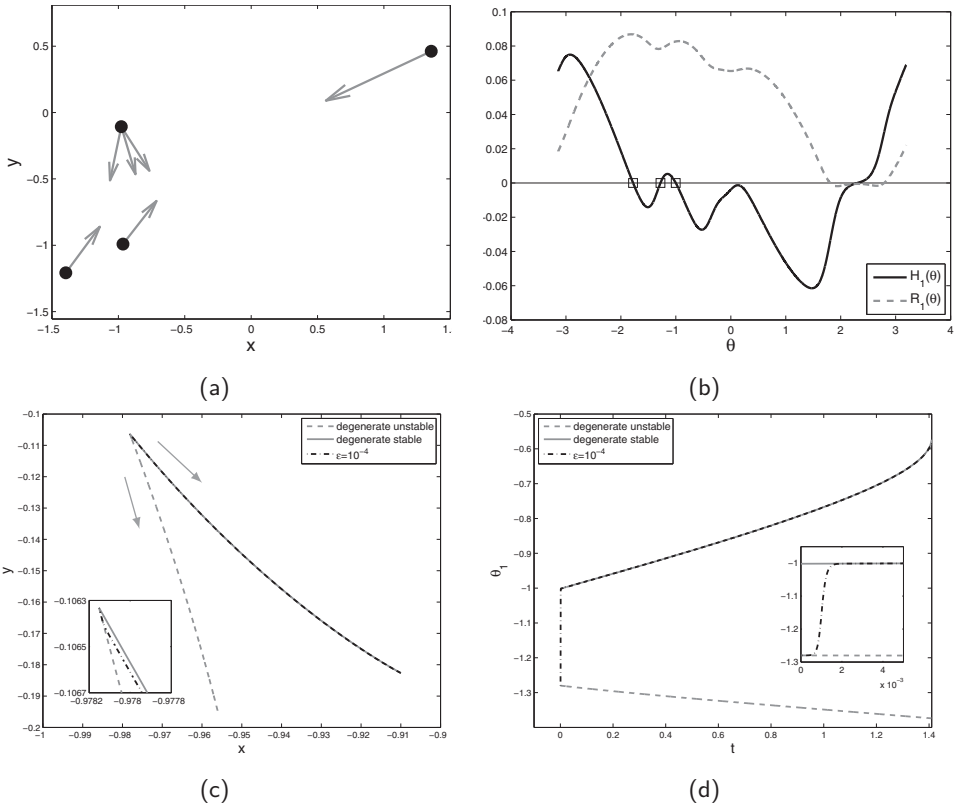

Figure 2.4: Illustration of the limit $\varepsilon \to 0$. (a): A randomly generated initial configuration of 4 particles, with indication of their admissible velocities. Only one of them (the top left particle, labeled as particle 1) allows for multiple initial velocities. (b): Plot of the functions H_1 and R_1 for particle 1. There are three admissible values of θ_1 for which $H_1(\theta_1) = 0$ and $R_1(\theta_1) > 0$, each indicated by a square. All the three roots are simple, resulting in the three *isolated* velocities shown on the left. The centre root is unstable, while the other two are stable. (c): Trajectories $x_1(t)$ of the anisotropic (degenerate) system (2.4) starting in the directions of the centre root $\theta_1 \approx -1.28$ and of the right-side root $\theta_1 \approx -1.00$, are shown in grey dashed and grey solid, respectively. The dash-dotted line represents the trajectory $x_1^\varepsilon(t)$ of the ε-system (2.5) with $\varepsilon = 10^{-4}$, initialized in the direction of the centre root. Since this root is unstable, x_1^ε leaves this direction and approaches in an initial layer (see the insert) the solution of the degenerate system that corresponds to a stable root (in this case, the right-side root). The arrows indicate the direction of motion along the trajectories. (d): The same numerical experiment as in (c), now showing the polar angle θ_1 of the velocity v_1 as a function of time. The ε-system starts at the unstable root $\theta_1 \approx -1.28$ and relaxes via an initial layer (see the insert) to the the solution of the degenerate system that starts at the stable root $\theta_1 \approx -1.00$.

grey line corresponding to the stable initial root $\theta_1 \approx -1.00$.

2.4 Breakdown and jump selection

Smooth solutions to (2.1) may cease to exist due to various factors. In this section, we investigate modes of breakdown and explain how jumps can be meaningfully enforced. We provide numerical illustrations in two dimensions.

2.4.1 Modes of breakdown: classification

A possible breakdown of C^1 solutions to (2.4) was already indicated in previous sections (see Remark 2.2.5). Namely, it may occur when one of the Jacobian matrices $J_v\mathcal{F}_i$ becomes singular for some particle i. At such time, the phase-space trajectory $(x_i(t), v_i(t))$ may cease to be continuous, provided that, for any continuous extension of $\{x_1, \dots, x_N\}$ in the direction of $\{v_1, \dots, v_N\}$, there is no zero of (2.20) in a (sufficiently small) neighbourhood of v_i. In other words, the *current* velocity v_i may cease to be a zero of (2.20) beyond this time and a jump in v_i has to be enforced. We call such a discontinuity in velocities, due to root losses of $\mathcal{F}_i$, a jump of Type I.

Other modes of breakdown are also possible: collision of particles and stopping. Collisions are a delicate matter, even in the context of isotropic models. Particle collisions have been discussed in [BCL09, CDF$^+$11, BCDP15] for instance, but the corresponding potentials are purely attractive. Using a measure-valued formulation, [CDF$^+$11] shows that if collisions happen in finite time, colliding particles merge into one particle and simultaneously move on. For general interaction potentials K, collisions and collapse do not occur – in finite or infinite time – if the repulsion component of K is strong enough to counteract the attraction. For our purpose, we sidestep this issue, and focus instead on particle stopping, that is, when one $v_i = 0$. In fact, this mode of breakdown is not present in the isotropic model (2.1), being entirely characteristic to the anisotropic model (2.4).

Note that, as given by (2.4), the anisotropic model is not even defined when one particle is at rest ($v_i = 0$). This is because the definition of the field of vision assumes the existence of a current direction of motion (an individual facing a certain direction). However, $v_i = 0$ can be considered as a solution of (2.4b) in the generalized interpretation of Definition 2.2.1. In our numerical computations, we observe that $v_i = 0$ does occur, in a sense that is consistent with this definition. More precisely, we observe numerically that a generic particle i brakes and then stops in a *continuous* fashion along its direction of motion. One-sided continuity of $v_i/|v_i|$ at the stopping time (called here t^*) is essential, as this enables us to pass to the limit $t \nearrow t^*$ in (2.4b) and find that $v_i = 0$ is a solution of (2.11), with $s = \lim_{t \nearrow t^*} v_i(t)/|v_i(t)|$.

To illustrate the stopping idea in two dimensions, take the polar coordinate representation $v_i(t) = r_i(t)[\cos\theta_i(t), \sin\theta_i(t)]^T$. Then, by braking continuously and stopping at time t^*, we mean that:

$$\lim_{t \nearrow t^*} r_i(t) = 0, \qquad \lim_{t \nearrow t^*} \theta_i(t) = \theta_i^*, \tag{2.41}$$

for some angle θ_i^*. Hence, since $v_i(t)/|v_i(t)| = [\cos\theta_i(t), \sin\theta_i(t)]^T$, equation (2.4b) has a well defined limit $t \nearrow t^*$. By passing to the limit we find

$$0 = -\frac{1}{N}\sum_{j\neq i} \nabla_{x_i} K(|x_i^* - x_j^*|)\, g\left(\frac{(x_i^* - x_j^*)}{|x_i^* - x_j^*|} \cdot \begin{bmatrix}\cos\theta_i^* \\ \sin\theta_i^*\end{bmatrix}\right),$$

where $\{x_j^*\}$ represent the spatial configuration at t^*. Hence, $v_i = 0$ solves (2.11) at $t = t^*$ with $s = [\cos\theta_i^*, \sin\theta_i^*]^T$.

In all numerical experiments we performed, we noticed that particles stop continuously in the sense of (2.41). However, the typical scenario is that there is no continuous phase-space trajectory $(x_i(t), v_i(t))$ for particle i beyond its stopping at time t^*. Similar to the root loss jump (Type I), $v_i = 0$ is a (generalized) solution of (2.20) at $t = t^*$, but to evolve the system further in time a jump in v_i has to be enforced. We call the jumps due to particle stopping, jumps of Type II.

We emphasize that throughout this section, by jump discontinuities for (2.4) we mean jumps in velocities v_i, and not in the actual trajectories x_i. The latter remain continuous through jumps.

2.4.2 Numerical illustrations in two dimensions

We illustrate the two modes of breakdown in two dimensions. A breakdown of Type I occurs when $H_i'(\theta_i) = 0$ for some i at $t = t^*$ (see Remark 2.3.10). Equivalently, θ_i is no longer a simple root of H_i. For a numerical illustration, we reconsider the run of (2.4) indicated by solid grey lines in Figures 2.4c and (d), that is, the solution that starts in the direction of the stable initial root $\theta_1 \approx -1.00$. At $t^* = 1.41$, the current direction $\theta_1 \approx -0.57$ becomes a *double* root of H_1, as illustrated in Figure 2.5. The empty circle represents the root θ_1 just before the jump at t^* occurs.

Moreover, there exists no *continuous* extension of the phase-space trajectory beyond $t = t^*$ (since the double root would disappear and would no longer be a root immediately after t^*!). The insert in Figure 2.5 illustrates this transition. The solid black line shows the graph of $H_1(\theta)$ before the jump, where the root $\theta_1 \approx -0.57$ is still present. By extending the dynamics in the direction of the current velocity, this root disappears (the dash-dotted line in the insert).

Assume for now that we have a criterion for setting a velocity jump at $t^* = 1.41$. Assume moreover that we reinitialize (2.4) at the current spatial configuration $\mathbf{x}(t^*)$, but in the direction of the new velocity, and that we can continue the time evolution of (2.4) until a new breakdown occurs. Anticipating the results, suppose that θ_1 takes after the jump the new value indicated by the filled circle in Figure 2.5 ($\theta_1 \approx 0.22$) and that the evolution of (2.4) continues in this new direction. The motivating Figure 2.1a corresponds in fact to the same run of (2.4) as that considered here, and shows this extended trajectory. More precisely, let us inspect the trajectory $x_1(t)$ of the top left particle (particle 1) indicated by a solid line in Figure 2.1a. The first segment of this trajectory (up to the first break-

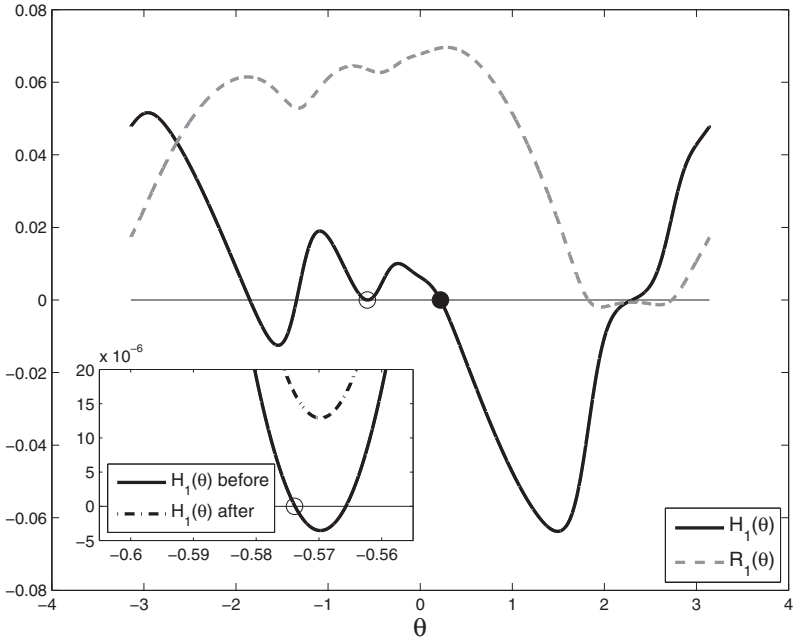

Figure 2.5: Functions H_1 and R_1 (see (2.24)) at breakdown $t^* = 1.41$ when root loss (jump of Type I) occurs for particle $i = 1$. The dynamics of (2.4) cannot continue in the direction of the current root $\theta_1 \approx -0.57$ (indicated by an empty circle), as this value would no longer be a root immediately after t^*. The zoomed-in insert illustrates this scenario: before jump (solid line), when the root indicated by an empty circle is still present, and an extension (dash-dotted line) in the direction of the current velocity, which leads to root loss. A jump in velocity has to be enforced in order to extend the dynamics of (2.4) beyond breakdown. The new value is indicated by a filled circle – see Section 2.4.3.

down time t^* indicated by a square) is the same as the solid grey line in Figure 2.4c. At $t^* = 1.41$ the trajectory $x_1(t)$ makes a sharp turn (θ_1 jumps from the empty-circle to the filled-circle value) and then continues until a second breakdown is encountered. This next breakdown, indicated by the second square along the trajectory of particle 1, is also a breakdown of Type I, and can be discussed using similar considerations as for the first jump. We do not treat this breakdown in detail, but enforce a jump (as discussed in Section 2.4.3), and continue the evolution.

We focus instead on the breakdown indicated by the square on the trajectory of the particle that starts from top right in Figure 2.1a; we label this particle as particle 2. This breakdown is of Type II. Particle 2 brakes continuously, as described in Section 2.4.1, and stops. Figure 2.6 shows the plots of H_2 and R_2 at this stopping time $t^* = 34.34$. The particle stops in the direction $\theta_2^* \approx -2.09$ indicated by the empty circle, which is simultaneously a root of H_2 and R_2. This is equivalent to the fixed point equation (2.22)

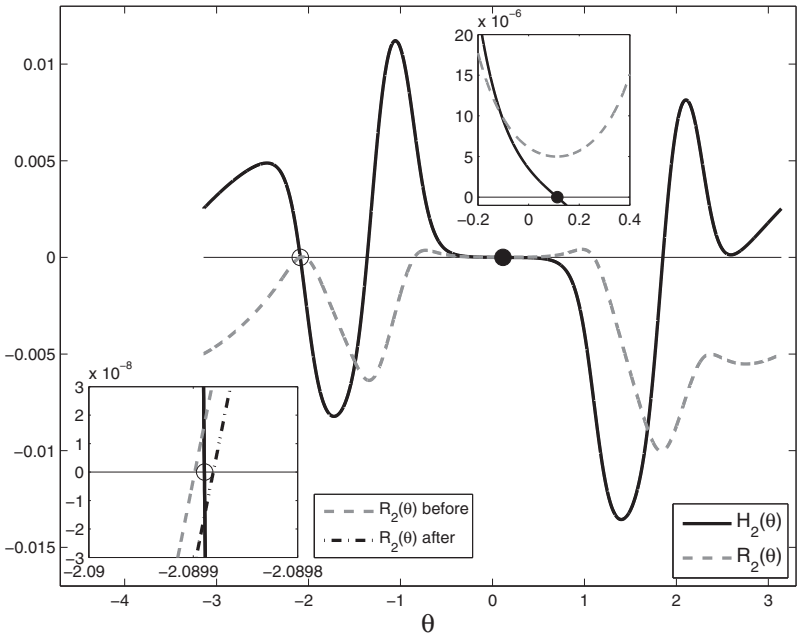

Figure 2.6: Functions H_2 and R_2 (see (2.24)) at breakdown $t^* = 34.34$ when particle $i = 2$ stops (jump of Type II). Particle 2 has stopped in the direction $\theta_2^* \approx -2.09$ (empty circle), which is simultaneously a root of H_2 and R_2 (see (2.25)). The bottom left insert shows zoomed-in plots of H_2 (solid black) and R_2 (dashed grey) near θ_2^*, shortly before the breakdown at $t = t^*$. Had the numerical integration continued in the current direction, $R_2(\theta)$ would become negative (dash-dotted black), and the root would no longer be admissible. A jump in velocity has to be enforced in order to extend the dynamics of (2.4) beyond the stopping breakdown. The post-jump direction is indicated by a filled circle – see Section 2.4.3. The top right insert shows that indeed, this new root is admissible, as R_2 is positive (but small) there.

(for $i = 2$) to have the solution $r_2 = 0$, $\theta_2 = \theta_2^*$ (see also (2.25)). In the bottom left insert of Figure 2.6 we show the functions H_2 (solid black) and R_2 (dashed grey) shortly before breakdown. Since R_2 is positive (but very small, note the scale of the vertical axis in the insert) at the root of H_2 indicated by the empty circle, the corresponding velocity is admissible. However, by evolving *numerically* (2.4) in the direction of the current root $\theta_2^* \approx -2.09$, $R_2(\theta)$ becomes negative (dash-dotted black line) and the root is no longer admissible. We conclude that beyond stopping time, phase-space trajectories cannot be extended continuously, and a jump in v_2 has to occur. We remark that the two graphs of H_2 (before breakdown and after extension) nearly coincide and the difference is not visible in the plot. The filled circle in Figure 2.6 indicates the value of θ_2 after the jump (see Section 2.4.3). We include the top right insert in Figure 2.6 to clarify that R_2 is indeed positive at the new θ_2.

2.4.3 Jump selection through the relaxation model

A central issue in this chapter is how to continue the solutions of (2.4) beyond a breakdown time, by enforcing a jump in velocity. Note that, having reached a breakdown time, there could be multiple options for a jump in velocity. For instance, at the breakdown time $t^* = 1.41$ in Figure 2.5, there are three simple roots of H_1 which are admissible (that is, $R_1 > 0$ at these roots). Enforcing a jump in θ_1 to any of these *isolated* roots would enable us to continue the dynamics of (2.4) beyond the breakdown.

The question is how to select which jump to perform. This is done using the relaxation system (2.5). Based on the interpretation of this model as including small but positive inertia or response time, we expect that *physically relevant* solutions of the anisotropic model (2.4) should be attained as limits $\varepsilon \to 0$ of solutions to (2.5). It would thus be meaningful to choose the jump that the ε-system selects in the $\varepsilon \to 0$ limit.

We perform runs of the relaxation model (2.5) using three values of ε: $\varepsilon = 10^{-2}, 10^{-3}$, and 10^{-4}. We initialize (2.5) with a phase-space configuration that corresponds to the numerical run presented in Section 2.3.2 and used in the considerations above: initial spatial configuration as in Figure 2.4a, and initial velocity as the fixed point of (2.4b) that corresponds to the stable root $\theta_1 \approx -1.00$ in Figure 2.4b. As discussed and illustrated in Section 2.3, starting from a stable root, we have convergence of the ε-model to solutions of (2.4), before a breakdown of (2.4) occurs. Figure 2.1a shows the trajectories of (2.5), though on the scale of the figure they are indistinguishable from the solution of (2.4).

Upon approaching the first breakdown time of (2.4), $t^* = 1.41$, solutions of (2.5) steepen and approach, via a fast dynamics, a different isolated stable root of (2.4). The zoomed plots in Figure 2.1b, as well as those in Figure 2.7, show this evolution of the ε-system near $t^* = 1.41$. Figure 2.1b shows the trajectory $x_1^\varepsilon(t)$, while Figures 2.7a and 2.7b plot $\theta_1^\varepsilon(t)$ and $|v_1^\varepsilon(t)|$, respectively. In each such figure, we observe the fast transition of solutions within an $\mathcal{O}(\varepsilon)$ time interval. Returning to Figure 2.5, and inspecting Figure 2.7a, we notice that indeed, the stable root $\theta_1 \approx 0.22$ (filled circle) of the degenerate system is being selected by the ε-model. Note again that this is not the only admissible stable root (with $H_1' < 0$, $R_1 > 0$) available at the jump (see Figure 2.5). But in light of the convergence result in Section 2.3.1, the selection of θ_1 at the filled circle was in fact expected, and the reason is discussed in the following paragraph.

Consider the adjoined system associated to the ε-model – see (2.39) and (2.40) for $i = 1$. At a fixed spatial configuration $\mathbf{x}^*$, evolving the *fictitious* time $\tau \to \infty$ yields indication on the asymptotic stability of a root. Hence, consider hypothetically the adjoined system (2.40) with $i = 1$ for a spatial configuration $\mathbf{x}_+^*$ consisting of an infinitesimal extension from $t = t^*$ to $t = t_+^*$ of the spatial configuration $\mathbf{x}^*$ at the jump of the degenerate system (2.4), extension taken in the current direction of motion of (2.4). The plots of H_1 and R_1 corresponding to such an extension to t_+^* would be infinitesimal perturbations of the plots in Figure 2.5, where most importantly, the double root indicated by an empty circle is no longer a root of H_1 at t_+^* (this "root loss" is the reason for the breakdown, cf. the insert in Figure 2.5). Evolving the adjoined system (2.40) with $i = 1$ at the frozen,

hypothetical, *post-jump* configuration $\mathbf{x}_+^*$ is expected to provide the new asymptotically stable root that the ε-system would converge to. The evolution of θ_1 is simply driven by the sign of the right-hand-side in (2.40a) ($i = 1$), and since $r_1 > 0$, this sign is given by H_1 at t_+^*. It is now clear from Figure 2.5 that initializing (2.40a) ($i = 1$) with θ_1 near the empty circle, which is the value it had before jump, would result in selecting the stable fixed point indicated by the filled circle. This observation serves as the starting point in designing the numerical method to simulate model (2.4) presented in Section 2.5.

Model (2.4) encounters a breakdown of Type II at $t^* = 34.34$, when particle 2 stops in the current direction $\theta^* \approx -2.09$ (the root of H_2 indicated by empty circle in Figure 2.6). On the contrary, solutions of the ε-model (2.5) continue through t^* and capture again a jump in a certain direction. Figure 2.1c plots the trajectory $x_2^\varepsilon(t)$ near the second jump $t^* = 34.34$, while Figures 2.8a and 2.8b show $\theta_2^\varepsilon(t)$ and $|v_2^\varepsilon(t)|$, respectively. Note indeed that Figure 2.8b captures the braking of particle 2 that occurs in the degenerate system ($|v_2|$ reaches order $\mathcal{O}(10^{-8})$). The difference though is that solutions of the ε-system do not actually stop, as particle 2 changes direction (see Figure 2.8a where θ_2 evolves fast from ≈ -2.09 to ≈ 0.11), picks up a higher velocity (of order $\mathcal{O}(10^{-5})$), and continues the motion. This fast transition results in a very sharp turn in the trajectory, as illustrated in the zoomed plot Figure 2.1c (see also the insert in the figure).

By inspecting Figure 2.6 one observes that the ε-system has selected the jump to root $\theta_2 \approx 0.11$ indicated by the filled circle. In this case this was in fact the only admissible root of H_2 at t^*, as the others have $R_2 < 0$. However, were there more admissible roots, it is not as clear as it was for the Type I jump in Figure 2.5, whether similar considerations regarding the adjoined system (2.40) can be used to predict the selection of the post-jump velocity. First, there is no natural extension (from t^* to t_+^*) of a configuration $\mathbf{x}^*$ at a breakdown that involves a *resting* particle. In a numerical simulation however, this point is less relevant, as the numerical value of a particle that attempts to stop becomes very small, but it does not actually reach zero. Hence, extending the numerics into a post-jump configuration is possible (this was done for instance to produce the insert in Figure 2.6). Second, from a theoretical point of view, the evolution $\tau \to \infty$ in (2.40a) with $i = 2$, at an infinitesimally extended spatial configuration $\mathbf{x}_+^*$, cannot be argued as for jump I, by invoking the sign of the right-hand-side (in this case, the sign of H_2 at t_+^*). The full two-dimensional evolution of the adjoined system (2.39) would have to be employed instead, and issues such as the domain of influence and getting attracted into a certain fixed point, are more subtle. We conclude by noting that in practice, for numerical simulations, the frozen/adjoined-system idea seems to work fine for jumps of Type II as well, it is just its theoretical foundation that is less solid than for jumps of Type I. Alternatively, one could use the *real* time evolution of the ε-system near the breakdown in order to select a jump (as discussed below in Section 2.5).

The numerical observations reported in this section have been confirmed with various other simulations, involving different initial conditions and larger number of particles. The two types of jumps discussed here and the shock-capturing of the ε-system are typical findings.

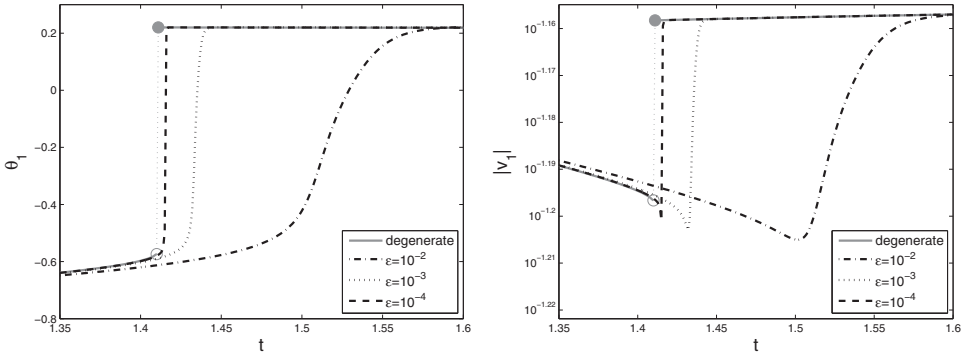

(a) (b)

Figure 2.7: Solution of the relaxation system (2.5) near the first breakdown time $t^* = 1.41$ of the anisotropic model (2.4), due to root loss. The plots show (a): $\theta_1^\varepsilon(t)$ and (b): $|v_1^\varepsilon(t)|$. Three values of ε are used to illustrate shock capturing: $10^{-2}, 10^{-3}$, and 10^{-4}. Near t^*, the direction changes from $\theta_1 \approx -0.57$ to $\theta_1 \approx 0.22$, values indicated, respectively, by the empty and filled circles in Figure 2.5. Complete trajectories for this run can be found in Figure 2.1a. The breakdown time $t^* = 1.41$ is indicated by the first square along the trajectory of the top-left particle (particle 1). A zoomed trajectory $x_1^\varepsilon(t)$ near t^* can be found in Figure 2.1b.

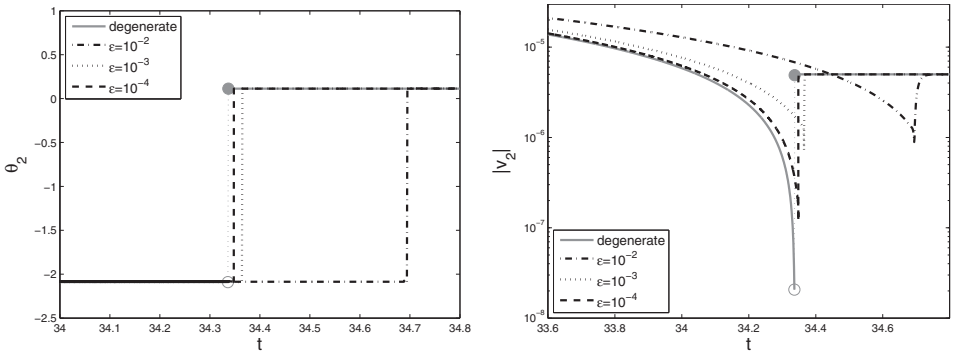

(a) (b)

Figure 2.8: Solution of the relaxation system (2.5) near the third breakdown time $t^* = 34.34$ of (2.4), due to stopping of particle 2. The plots show (a): $\theta_2^\varepsilon(t)$ and (b): $|v_2^\varepsilon(t)|$. Three values of ε are used to illustrate shock capturing: $10^{-2}, 10^{-3}$, and 10^{-4}. The direction changes from $\theta_2 \approx -2.09$ to $\theta_2 \approx 0.11$, values indicated, respectively, by the empty and filled circles in Figure 2.6. The complete trajectories can be found in Figure 2.1a, where the breakdown time $t^* = 34.34$ is indicated by the square along the trajectory of particle 2 (top right). A zoomed trajectory $x_2^\varepsilon(t)$ near breakdown can be found in Figure 2.1c.

2.5 Implementation and long-time evolution

2.5.1 Numerical implementation of (2.4) in two dimensions

Evolving the relaxation system (2.5) with small ε for large times is not practically feasible. The numerical strategy for the long-time evolution of (2.4) is to run the anisotropic model through its intervals of continuity and use the ε-model only to capture the jumps. For jumps of Type I, this procedure is rather easy to implement in two dimensions, as illustrated in Section 2.4.3. Indeed, suppose that in a numerical simulation of (2.4) a root loss has been identified in the discrete time step from t_{n-1} to t_n. That is, for some particle i, the numerical velocity v_i^n at time t_n is no longer a fixed point of $\mathcal{F}_i$. Then, by "freezing" the *post-jump* spatial configuration $\mathbf{x}^n$ at the time t_n, one can run the adjoined system (2.39) with the fictitious time $\tau \to \infty$, in order to select the new, asymptotically stable root. Rename this root v_i^n and then continue the evolution of (2.4). This procedure is the time-discrete version of the considerations from Section 2.4.3 on the selection of a jump by an infinitesimal extension of the spatial configuration at the breakdown time.

Jumps of Type II can be similarly recovered, by freezing the post-jump spatial configuration. As explained in Section 2.4.3, this procedure is less theoretically grounded for jumps of Type II, but we found that it works well in practice and captures the correct jumps. We confirmed this with full, *real*-time evolutions of the relaxation model through Type II discontinuities. That is, after detecting a jump in the discrete time interval from t_{n-1} to t_n, return to the *pre-jump* phase-space configuration $(\mathbf{x}^{n-1}, \mathbf{v}^{n-1})$ at time t_{n-1}, initialize (2.5) with this data, and run the relaxation system with a fine time resolution to capture the steep solution that selects the post-jump root $\mathbf{v}^n$.

2.5.2 Long-time behaviour

An extensive numerical study of the long-time behaviour of solutions to (2.4) is beyond the scope of this chapter. We only report our preliminary observations. The main feature is that the dynamics slows down significantly after a relatively short initial interval. For instance, particles in the numerical simulation considered above (referred to as IC 1 here) reach velocities of order $\mathcal{O}(10^{-4})$ by the stopping breakdown time $t^* = 34.34$, and continue to decrease steadily after the jump. In Figure 2.9b we plot the maximum speed $\max_i |v_i|$ over time, to $t = 5,000$. We also considered the long time run corresponding to the same initial spatial configuration from Figure 2.4a, but with an initial velocity v_1 pointing in the other stable direction, $\theta_1 \approx -1.78$; we refer to this initial condition as IC 2. The evolution of $\max_i |v_i|$ is also shown in Figure 2.9b, with similar qualitative behaviour as for IC 1.

The full evolution of the trajectories for IC 2 is shown in Figure 2.9a, with the final configuration at $t = 5,000$ indicated by filled diamonds. The empty diamonds in the figure represent the state at $t = 5,000$ of the run with IC 1. We do not plot the full evolution of the trajectories corresponding to IC 1, since at the scale of the figure these would be indistinguishable from the solutions shown in Figure 2.1a. Note that the two sets of configurations have different centres of mass. The centre of mass is not being

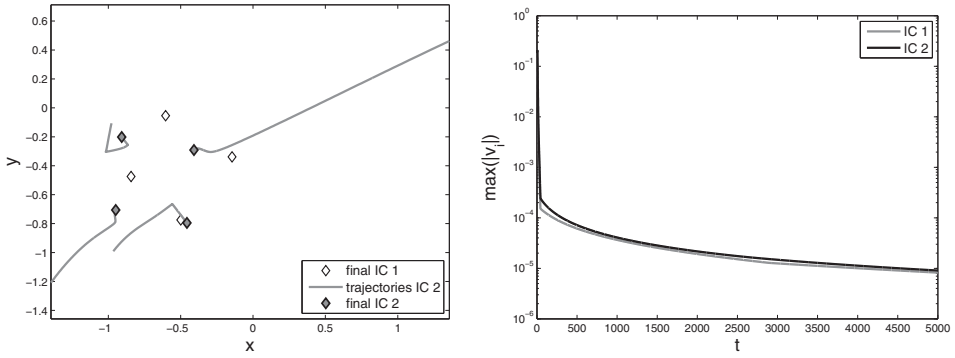

(a) (b)

Figure 2.9: Long-time behaviour of (2.4). (a): The solid grey lines represent the evolution of (2.4) starting from the initial configuration in Figure 2.4a, in the direction of the stable root $\theta_1 \approx -1.78$ – we refer to this initial condition as IC 2. The initialization in the direction of the other stable root, $\theta_1 \approx -1.00$, is referred to as IC 1. The filled and empty diamonds indicate the configurations of the two runs at $t = 5,000$. (b): Plot of $\max_i |v_i|$ over time, for the two sets of initial conditions. Particles reduce their speed and seem to approach a quasi-equilibrium.

conserved by the anisotropic model (2.4), as it is for the isotropic model (2.1).

Figure 2.9 shows that both runs feature a fast initial dynamics (involving several jumps of both types), followed by slow motion. The numerical results suggest that velocities continue to decrease indefinitely, and the system reaches a quasi-steady state. Stopping jumps become more typical at low speeds, as particles make small jiggles, turning toward and from the others, trying to reach an equilibrium. This jiggling aspect is not present in the isotropic model, as there, the unobstructed sensing of the others drives the particles quickly into an equilibrium configuration.

2.6 Discussion

In this chapter we proposed a procedure for obtaining a unique solution to the first-order model in which the field of vision is taken into account. We provided a selection criterion for jumps in velocity and illustrated this criterion numerically.

There are some subtleties in the numerical procedure described in Section 2.5. Often it is clear from a figure like Figure 2.7 what the new velocity should be – the limit $\tau \to \infty$ in (2.40a) – but it is not sufficient if we can only manually determine what the jump should be. Hence we need to be able to rely on our numerical implementation in the sense that it always makes the proper selection. In case of a jump, the configuration *after* root loss is

required to obtain the new velocity: the root needs to be actually lost, otherwise the jump criterion will select the original root. The question is however *how far* to extrapolate into the post-jump time. This question is a consequence of the intrinsic discreteness of any numerical approach. In fact we *approximate* the post-jump configuration $\mathbf{x}_+^*$ by $\mathbf{x}^* + \delta \cdot \tilde{\mathbf{v}}$, where $\mathbf{x}^*$ is the pre-jump configuration, $\tilde{\mathbf{v}}$ is the pre-jump velocity and $\delta > 0$ is fixed. Consider the adjoined system (2.35) with $\mathbf{x}^*$ replaced by $\mathbf{x}^* + \delta \cdot \tilde{\mathbf{v}}$. Assume that for each $\delta > 0$ its limit as $\tau \to \infty$ is given by $\mathbf{v}_\delta^*$. Hence, what we really want to find is $\lim_{\delta \downarrow 0} \mathbf{v}_\delta^*$ as our post-jump velocity. This idea was described in words in Section 2.4.3. Numerically, finding a sufficiently small δ such that the proper post-jump velocity is found, is often a matter of trial-and-error. Here, *proper* means that this post-jump velocity coincides with the one predicted by the full ε-system. The rigorous investigation of the limit $\delta \downarrow 0$ is a direction for future research.

We have seen in Sections 2.2.3 (the second half) and 2.3.2 how polar coordinates help us to get intuition and they essentially reduce the problem to a scalar one. However, if we perform the limit $\tau \to \infty$ in (2.40), rather than in (2.39), this induces extra issues in some cases and is therefore not recommended to obtain a robust implementation. We illustrate such cases in which problems arise, using Figure 2.5. Assume that the function H_1 is as in the figure, but that R_1 is instead positive near the open circle but negative near the closed circle. Consequently, the closed circle is not an admissible root. From the figure we deduce that there is only one other admissible root: the one to the left of the open circle where H_1' is negative. This root is admissible under the assumption that R_1 is positive there. Now, 'simply' performing the limit $\tau \to \infty$ in (2.40) is impossible. Due to (2.40a) θ_1 converges to the filled circle at $\theta_1 \approx 0.22$, but hence R_1 becomes negative at some point and due to (2.40b), r_1 decreases until it becomes zero. Once r_1 reaches zero, with $R_1 < 0$ (2.40b) has the tendency to decrease r_1 even further and hence the original definition of the polar coordinates is no longer valid. This example shows that the implementation of (2.39) is preferred.

The considerations in the previous two paragraphs mainly concern jumps of Type I. In Section 2.5, we stated that for jumps of Type II, often the adjoined system can be used, although there is no theoretical basis for its effectiveness. Our implementation is such that if the approach using the adjoined system does not work, then the full ε-system is used. An additional difficulty is the choice of ε. Figures 2.7 and 2.8 show that even $\varepsilon = 10^{-2}$ (which is not extremely small) is sufficient to predict the correct jump. However, this is not guaranteed *a priori*.

In view of existing literature, a valid question to ask is whether the field of vision should or should not be centred around the direction of the actual velocity. A so-called *desired velocity* can be easily incorporated in our definition of the velocity. This is an extra contribution, independent of the other particles' positions, that models the velocity that an individual would have if no others were around. In principle this desired velocity field is given, and can be considered as being part of the model data. It is common practice in literature to define the field of vision with respect to the direction of the desired velocity; see e.g. Section 5.2.2 of [CPT14], or Equation (7) in [HM95]. The (implicitly stated) motivation for this modelling choice is that individuals look in the direction of their desired

motion – that is, towards their goal – and *not* in the direction of their actual velocity. My preliminary work [GEML13] and [EMvdV13] follows this approach. On the other hand, on p. 321 of [CFTV10] the cone of vision *is* directed along the actual velocity. Note that in first-order models the latter choice causes the difficulties described in this chapter. In second-order models, this choice has less drastic effects and only makes the model slightly more involved; cf. [BHW13], Section 2.

There is a resemblance between the approach taken in this chapter, and the method of *vanishing viscosity* in hyperbolic PDEs. In the latter method, a diffusion term (Laplacian) multiplied by a small parameter is included in the original equation. The effect is that solutions are regularized. In the limit for vanishing parameter, weak solutions (shocks) are obtained. For more details about the vanishing viscosity method the reader is referred e.g. to Section 7.3 of [Eva10]. In this chapter, the small parameter also corresponds to a term with higher derivatives than the other terms in the equation. The similarity between the vanishing viscosity approach and the approach in this chapter concerns mainly their philosophy. There is no direct analogy.

As the number of particles becomes large, accounting for all jumps that take place in the dynamics of (2.4) becomes quite challenging. Formally, the continuum limit (see Section 1.4) of (2.4) consists of the continuity equation for the density ρ:

$$\frac{\partial \rho}{\partial t} + \nabla \cdot (\rho\, v) = 0, \tag{2.42}$$

completed with the following implicit expression for v:

$$v(x) = -\int_{\mathbb{R}^d} \nabla K(|x-y|) g\left(\frac{x-y}{|x-y|} \cdot \frac{v(x)}{|v(x)|}\right) \rho(y)\, dy \quad \text{for all } x \in \mathbb{R}^d. \tag{2.43}$$

Here K and g have the same meaning as throughout the chapter. We refer for the limit procedure and properties of the limit equation for the system without anisotropy, to [BV05, BV06, CCH14, FS14]. A direction for future research is to investigate whether similar results can be derived for the anisotropic model. Rather than just a goal in its own right, the PDE can be a tool. Our analytical considerations for the limit $\varepsilon \to 0$ in the ODE are not yet completely satisfactory. On the PDE level we would have the momentum equation with a parameter ε and the use of PDE techniques might be a better way to go when letting ε vanish. This limit $\varepsilon \to 0$ is indicated by the arrow (labelled also 'Chapter 2') from the hydrodynamic equation to the Fokker-Planck equation in Figure 1.2.

Chapter 3

Convergence of measure-valued evolutions in the Wasserstein distance

In this chapter we derive the equation of motion for a system, starting from its action. The equation of motion we obtain is the Lagrangian formulation of (a regularized version of) the PDE (1.40) given in Section 1.7.2, which is formulated in a Eulerian way. We use the solution of this equation of motion in Lagrangian form as a motion mapping that dictates the evolution of a particle approximation. Our question in this approach is:

How can we derive particle-based schemes in a systematic way?

Our systematic procedure consists of three steps: application of the principle of least action; formulation of the problem in terms of measures (which requires a regularization of the density); and substitution of a discrete measure. The obtained equation of motion depends on the order in which regularization and the principle of least action are applied. We also show how to generalize this procedure to systems involving nonconservative forces.

The second question that we ask, concerns the quality of our particle approximation:

In what sense do these schemes converge in the many-particle limit to the continuum equations of motion?

In this chapter, we prove the convergence in the Wasserstein distance of the corresponding measure-valued evolutions, to the solution of the *regularized* limit equation. Moreover, we provide the order of convergence of the SPH method.

This chapter is based on joint work with Iason Zisis, Bas van der Linden and Manh Hong Duong, submitted for publication in Archive for Rational Mechanics and Analysis [EZvdLD15].

3.1 Introduction

The numerical method called Smoothed Particle Hydrodynamics (SPH) was initially introduced to solve the equations governing the motion of astrophysical flows. In the course of time, SPH found application to equations for a great variety of physical processes (cf. [Mon12]). The main idea of the method is to approximate a continuum by a collection of particles. One expects that the approximation improves when the number of particles increases.

It is well-established that the classical scheme in SPH can be derived formally by applying the *principle of least action* to the particle system, where the specific way in which the density is approximated in SPH acts as a constraint; see e.g. [Mon05, Pri12, ZvdLGK14]. The importance of the particle system's Lagrangian function was already recognized in the first articles describing SPH; cf. [GM78]. A subtlety lies in the fact that in the derivation of the SPH equations, the action of the particle system is minimized rather than the action of the continuum. The minimization of the action at the continuum level and the subsequent discretization of the motion equation in terms of particles does not necessarily yield the same equation.

The two main achievements of this chapter are:

- We introduce a systematic procedure for deriving measure-valued and particle formulations of continuum mechanics equations. We obtain two different schemes depending on the stage at which a regularization of the density is introduced. See Section 3.2.
- We prove the convergence of both schemes using the Wasserstein distance defined on the space of probability measures; cf. Section 3.3.

In the first part (Section 3.2), we aim at clarifying the exact difference in outcome between minimizing the action of the particle system and minimizing the action at the continuum level. To achieve this, we introduce a systematic procedure consisting of the following three steps:

A formulation in terms of measures and, simultaneously, the regularization of the density;

B introduction of a particle formulation;

C application of the principle of least action.

These three steps are introduced in more detail in Section 3.2.2. It turns out that the order in which these steps are executed, determines the structure of the resulting equation. To be more precise, the classical SPH scheme (as described e.g. in [Mon05]) is obtained, whenever the regularization of the density takes place before applying the principle of least action. That is, whenever the steps are executed in the order **A**-**B**-**C** or **A**-**C**-**B**. Both procedures are presented here; see Sections 3.2.3 and 3.2.4. If we apply the principle of least action (to the action at the continuum mechanics level) before regularizing the density then we obtain a scheme that appears in [LGP98] and [CGP14]. However, this

variant of the scheme is studied far less in literature. The procedure to derive this scheme follows the order **C**-**A**-**B**; see Section 3.2.5. We underline that although both schemes originate from the principle of least action, the latter can also be obtained directly by taking Newton's Second Law and replacing the density by the regularized density.

In Section 3.2.7, we show that this three-step strategy can be generalized to include nonconservative forces.

Regularization of the density practically means that the original problem is deliberately turned into a regularized one, which is afterwards solved by means of some variant of an SPH scheme. Hence, by choosing SPH as solution method one is automatically bound to studying a different problem than the original one at the continuum level. Thus, regarding the convergence of our particle approximation, two questions naturally rise:

- Does the solution of the regularized problem converge (in a certain sense) to the solution of the original problem?
- Does the particle solution corresponding to the regularized problem converge (in a certain sense) to the solution of the regularized continuum problem?

The former is out of the scope of this chapter (it was treated in [LGP97]), while the latter is the topic of Section 3.3 and further.

Inspired by the approach in [LGP98], we use in this chapter the Wasserstein distance on the space of probability measures. For an overview of related literature and alternative approaches to prove convergence, the reader is referred to Section 1.7.2. The Wasserstein distance has the advantage that it can be formulated as the *infimum* over a set of joint representations (more details follow in Definitions 3.3.2 and 3.3.3). This is convenient, since one can thus obtain an upper bound (needed to prove convergence) by choosing any admissible joint representation. We refer the reader also to [Vil09], Chapter 6, for further discussion on the Wasserstein distance.

The theoretical result of this chapter is supported by a numerical investigation of the order of convergence in Section 3.6 for one- and two-dimensional examples involving different force fields.

3.2 Systematic derivation of the equations of motion

In this section we derive equations of motion from Hamilton's principle of least action, which involves the Lagrangian function posed in a continuum mechanics setting. We describe an explicit 'recipe', hence avoiding the need to introduce approximations in an *ad hoc* manner. This recipe consists of three building blocks (coined **A**, **B** and **C**; see Section 3.2.2). The order in which these blocks are executed, determines the final outcome. As such, the systematic procedure we describe here also shows exactly how different schemes arise from the same basic principles.

Ultimately, we show how to generalize this recipe to systems in which nonconservative forces are present; see Section 3.2.7.

3.2.1 Derivation of the action in a continuous setting

Assume that for fixed time t a mass density ρ_t on a spatial domain Ω_t is given. We define the *Lagrangian density* of our system as

$$\mathcal{L}(\rho_t, y, u) := \left(\frac{1}{2}|u|^2 - e(\rho_t(y), y)\right)\rho_t(y),$$

where y and u are independent Eulerian position and velocity coordinates, and e denotes the internal energy density. To obtain the *Lagrangian* L, we integrate $\mathcal{L}$ over the spatial domain Ω_t:

$$L(t) := \int_{\Omega_t} \mathcal{L}(\rho_t, y, u)\, dy. \tag{3.1}$$

For this integration to make sense, we assume that u is actually a function of t and y: $u := u(t, y)$. Furthermore, we assume that there is a motion mapping Φ_t that governs the transition of the system at time 0 to the system at time t. Then in particular, $\Omega_t = \Phi_t(\Omega_0)$ holds for some initial domain Ω_0. We transform the integral (3.1) according to $y = \Phi_t(x)$ with $x \in \Omega_0$ and obtain

$$L[\Phi](t) = \int_{\Omega_0} \left(\frac{1}{2}|u(t, \Phi_t(x))|^2 - e\Big(\rho_t(\Phi_t(x)), \Phi_t(x)\Big)\right)\rho_t(\Phi_t(x))\ |J\Phi_t(x)|\ dx. \tag{3.2}$$

The *functional dependence* of L on the motion mapping is indicated by explicitly including Φ in square brackets. The expression $|J\Phi_t(x)|$ denotes the determinant of the Jacobian matrix of the transformation, consisting of the derivatives of the components of Φ_t with respect to the components of x. Because we assumed that Φ_t governs the evolution, the density ρ_t relates to the initial density ρ_0 in the following way (see e.g. [Cha76], p. 90):

$$\rho_0(x) = \rho_t(\Phi_t(x))\ |J\Phi_t(x)|\,. \tag{3.3}$$

Combined, (3.2) and (3.3) yield

$$L[\Phi](t) = \int_{\Omega_0} \left(\frac{1}{2}|u(t, \Phi_t(x))|^2 - e\Big(\rho_t(\Phi_t(x)), \Phi_t(x)\Big)\right)\rho_0(x)\, dx.$$

In the above we fixed t, but all arguments can be repeated for every t in some interval $[0, T]$. We are interested in those motion mappings that are continuous and differentiable in time, and we wish to obtain the corresponding equation of motion. The introduction of the motion mapping $(\Phi_t)_{t\in[0,T]}$ has taken us from Eulerian coordinates in (3.1) towards Lagrangian (material) coordinates in (3.2). The crucial and final step to complete this procedure is to specify the velocity field u. To remain consistent with the motion mapping we introduced, we identify u with the time derivative of Φ_t. More precisely, we postulate the relation:

$$u(t, \Phi_t(x)) = \dot{\Phi}_t(x) \ \text{ for all } x \in \Omega_0. \tag{3.4}$$

The velocity u at time t and position $\Phi_t(x)$ is the velocity at time t of a material point that started in x at time 0, and – in words – (3.4) means that this velocity is equal to the time derivative at time t of the position of that particular material point. By connecting the Eulerian velocity u to the Lagrangian velocity $\dot{\Phi}_t$, we obtain the Lagrangian functional

$$L[\Phi](t) = \int_{\Omega_0} \left(\frac{1}{2} |\dot{\Phi}_t(x))|^2 - e\Big(\rho_t(\Phi_t(x)), \Phi_t(x)\Big) \right) \rho_0(x)\, dx. \tag{3.5}$$

We define the *action* of our system by

$$S[\Phi] := \int_0^T L[\Phi](t)\, dt. \tag{3.6}$$

3.2.2 Three derivation procedures

Our aim is to derive equations of motion from the action (3.6), by means of the Euler-Lagrange equations. These will appear in different forms. Moreover, we wish to derive these equations of motion for a particle system (which naturally induces a numerical scheme). A methodological way to go from the continuum (Section 3.2.1) to a particle system, is via a measure-valued formulation. Our motivation to do so is the fact that we need a framework that incorporates the 'real physics', i.e. the density ρ_t, and an approximating particle system to establish the convergence of the particle scheme to the continuum.

To obtain the transition from the continuous action (3.6) to equations of motion for the particle positions, three steps are necessary:

- **A** introduction of measures: replace $\rho_t(x)dx$ by $d\mu_t(x)$ and where needed approximate ρ_t by some $\tilde{\rho}_t$ that depends on μ_t;
- **B** substituting for μ_t a discrete measure $\bar{\mu}_t^N = \sum m_i \delta_{x_i(t)}$;
- **C** deriving the Euler-Lagrange equations (either classically or in variational sense).

The steps are described here in a simplified way; their true meaning becomes clear in Sections 3.2.3, 3.2.4 and 3.2.5. Step **A** introduces a regularized version of the problem, which is a problem different from the original one. Step **B** cannot happen before **A**, but we have the freedom to choose the further ordering. This gives rise to three different derivations:

ABC this procedure discretizes the Lagrangian and derives the corresponding equations of motion afterwards; see Section 3.2.3.

ACB this procedure derives the equations of motion from the measure-valued Lagrangian and discretizes these equations afterwards; see Section 3.2.4.

CAB this procedure derives the equations of motion from the continuum Lagrangian, writes them in measure-valued form and discretizes afterwards; see Section 3.2.5.

Procedures **ABC** and **ACB** eventually yield the same particle scheme. This is the scheme traditionally used in the SPH community (cf. [Mon05]). Procedure **CAB** is the one that yields the equations used in [LGP98] and [CGP14].

3.2.3 Equations of motion via the route ABC

Step A

In Section 3.2.1 we introduced (for each t) the density ρ_t as the image of the initial density ρ_0 under the mapping Φ_t. In this section, we lift the evolution of ρ_t to the space of (time-dependent) measures. Let μ_0 and μ_t be measures with densities ρ_0 and ρ_t, respectively. These measures relate via $\mu_t = \Phi_t \# \mu_0$. We substitute $\rho_0(x)dx$ by $d\mu_0(x)$ in (3.5)–(3.6). Afterwards, there is one more aspect that we need to 'repair' before obtaining a measure-formulation. The internal energy density e depends on ρ_t itself, via pointwise evaluation. An approximation of ρ_t is needed to obtain a general expression that is even well-defined for measures that do not have a density (with respect to the Lebesgue measure). We propose to introduce a regularization – cf. [Fri44] – via convolution with a smoothing function:

$$\tilde{\rho}_t(\xi) := (\gamma * \mu_t)(\xi) = \int_{\Omega_t} \gamma(\xi - y)\, d\mu_t(y), \tag{3.7}$$

for all $\xi \in \operatorname{supp} \mu_t$. The smoothing function γ is nonnegative and even. The convolution regularizes the solution, introducing an artificial 'density' $\tilde{\rho}_t$, such that pointwise evaluation and its gradient are defined even if ρ_t does not exist pointwise or is not differentiable.

Remark 3.2.1. In the literature on SPH, the notation W_h is used for the smoothing function γ entering (3.7). Here, $h > 0$ is a small parameter, and W_h is such that $W_h \rightharpoonup \delta_0$ in the narrow topology as $h \to 0$ (i.e. tested against bounded continuous functions). A typical example is the Gaussian with zero mean and variance $h^2/2$. If μ_t has a density ρ_t then the convergence of $\tilde{\rho}_t = W_h * \mu_t$ to ρ_t holds pointwise for every t for instance if ρ_t is continuous and bounded (by definition of $W_h \rightharpoonup \delta_0$). In this chapter we do not consider varying h or the limit $h \to 0$, hence we use the notation γ for a *fixed* smoothing function. This avoids confusion with the Wasserstein distance of order p (introduced in Definition 3.3.3) which is denoted by W_p.

Note that $\tilde{\rho}_t$ can also be written as

$$\tilde{\rho}_t(\xi) = \int_{\Omega_0} \gamma(\xi - \Phi_t(x))\, d\mu_0(x),$$

by definition of the push-forward; see (1.4). Hence, we ought to keep in mind that $\tilde{\rho}_t$ has either a functional dependence on μ_t, or an extra dependence on $\Phi_t(\cdot)$ (depending on the formulation we choose), but we do not write this dependence explicitly.

We substitute $\tilde{\rho}_t$ for ρ_t in e and redefine the Lagrangian (in a measure-formulation) such that the action becomes

$$S[\Phi] = \int_0^T L[\Phi](t)\, dt = \int_0^T \int_{\Omega_0} \left(\frac{1}{2} |\dot{\Phi}_t(x)|^2 - e\Big(\tilde{\rho}_t(\Phi_t(x)), \Phi_t(x)\Big) \right) d\mu_0(x)\, dt. \tag{3.8}$$

This new, generalized formulation in terms of measures makes it possible to consider more types of solutions, simply by allowing more general initial conditions. This is exactly what we exploit in the following step, substituting a particle approximation.

Step B

In this step, we substitute for μ_0 a discrete measure of the form $\bar{\mu}_0^N = \sum_{i=1}^N m_i \delta_{x_{i,0}}$. Under push-forward, the measure remains a discrete measure with positions of the Diracs $\{x_i(t)\}$ evolving under the motion mapping: $x_i(t) = \Phi_t(x_{i,0})$. We emphasize that the equation for Φ_t is yet unknown and is to be derived in the next step.

The Lagrangian takes the form

$$L[\Phi](t) = \sum_{i=1}^N m_i \left(\frac{1}{2}|\dot{x}_i(t)|^2 - e\Big(\tilde{\rho}_t(x_i(t)), x_i(t)\Big)\right), \tag{3.9}$$

with

$$\tilde{\rho}_t(x_i(t)) = \sum_{j=1}^N m_j \, \gamma\Big(x_i(t) - x_j(t)\Big),$$

for all $t \geqslant 0$.

Step C

The equations of motion are obtained via the 'classical' Euler-Lagrange equations, applied to the Lagrangian

$$L[\Phi](t) = \sum_{i=1}^N m_i \left(\frac{1}{2}|u_i|^2 - e\left(\sum_{j=1}^N m_j \, \gamma(y_i - y_j) \, , \, y_i \right) \right),$$

cf. (3.9). The corresponding Euler-Lagrange equations – cf. (1.57) in [GPS01] – are

$$\frac{d}{dt}\left(\nabla_{u_k} L \Big|_{(y_i,u_i)=(\Phi_t(x_{i,0}),\dot{\Phi}_t(x_{i,0}))} \right) - \nabla_{y_k} L \Big|_{(y_i,u_i)=(\Phi_t(x_{i,0}),\dot{\Phi}_t(x_{i,0}))} = 0, \tag{3.10}$$

for each $k \in \{1, \dots, N\}$. The subscript "$(y_i, u_i) = (\Phi_t(x_{i,0}), \dot{\Phi}_t(x_{i,0}))$" denotes a substitution for all $i \in \{1, \dots, N\}$.

After calculating the derivatives ∇_{u_k} and ∇_{y_k} in (3.10), we obtain

$$\begin{aligned} m_k \frac{d}{dt}\dot{\Phi}_t(x_{k,0}) = &- m_k \, \frac{\partial e}{\partial \rho}\Big(\tilde{\rho}_t(\Phi_t(x_{k,0})), \Phi_t(x_{k,0})\Big) \, \nabla \tilde{\rho}_t(\Phi_t(x_{k,0})) \\ &+ \sum_{i=1}^N m_i \, \frac{\partial e}{\partial \rho}\Big(\tilde{\rho}_t(\Phi_t(x_{i,0})), \Phi_t(x_{i,0})\Big) \, m_k \, \nabla \gamma\Big(\Phi_t(x_{i,0}) - \Phi_t(x_{k,0})\Big) \\ &- m_k \, \nabla_y e \left(\tilde{\rho}_t(\Phi_t(x_{k,0})), \Phi_t(x_{k,0})\right), \end{aligned} \tag{3.11}$$

with

$$\tilde{\rho}_t(\Phi_t(x_{\ell,0})) = \sum_{j=1}^N m_j \, \gamma\Big(\Phi_t(x_{\ell,0}) - \Phi_t(x_{j,0})\Big) \quad \text{for all } \ell \in \{1, \dots, N\}.$$

We denote by $\nabla_y e$ the gradient of e only in the explicit spatial coordinate; that is, the second variable of e. We divide all terms by m_k (which is nonzero without loss of generality). If we take $\partial e/\partial\rho$ in the first line inside the sum and we use in the second line that $\nabla\gamma$ is an odd function, then the corresponding terms in (3.11) can be combined, and we obtain

$$\begin{aligned}\ddot{\Phi}_t(x_{k,0}) = -\sum_{i=1}^{N} m_i\,\nabla\gamma\Big(\Phi_t(x_{k,0})-\Phi_t(x_{i,0})\Big)\Bigg[\frac{\partial e}{\partial\rho}\Big(\tilde{\rho}_t(\Phi_t(x_{k,0})),\Phi_t(x_{k,0})\Big)\\ +\frac{\partial e}{\partial\rho}\Big(\tilde{\rho}_t(\Phi_t(x_{i,0})),\Phi_t(x_{i,0})\Big)\Bigg]\\ -\nabla_y e\Big(\tilde{\rho}_t(\Phi_t(x_{k,0})),\Phi_t(x_{k,0})\Big),\end{aligned} \tag{3.12}$$

for each $k\in\{1,\dots,N\}$.

3.2.4 Equations of motion via the route ACB

Step A

This step is exactly the same as in Section 3.2.3.

Step C

We start off from the action given in (3.8). Instead of using the classical Euler-Lagrange equations directly, we employ here the principle of least action as described e.g. on p. 127 of [Ber09]. This principle states that the evolution of the system is described by Φ_t such that the action is stationary. That is,

$$S'[\Phi](\Psi)=0, \tag{3.13}$$

for all test functions $\Psi\in C_c^\infty((0,T);C_c^\infty(\Omega_0;\mathbb{R}^d))$, where $S'[\Phi](\Psi)$ denotes the variation of S in the direction of Ψ. We have:

$$S'[\Phi](\Psi) := \frac{d}{d\varepsilon}S[\Phi+\varepsilon\Psi]\bigg|_{\varepsilon=0}. \tag{3.14}$$

Note that

$$\frac{d}{d\varepsilon}\left[e\left(\int_{\Omega_0}\gamma\Big(\Phi_t(x)+\varepsilon\Psi_t(x)-\Phi_t(y)-\varepsilon\Psi_t(y)\Big)\,\mu_0(dy)\,,\,\Phi_t(x)+\varepsilon\Psi_t(x)\right)\right]_{\varepsilon=0}$$

$$=\frac{\partial e}{\partial\rho}\left(\int_{\Omega_0}\gamma\Big(\Phi_t(x)-\Phi_t(y)\Big)\,d\mu_0(y)\,,\,\Phi_t(x)\right)\cdot$$

$$\cdot\int_{\Omega_0}\nabla\gamma\Big(\Phi_t(x)-\Phi_t(y)\Big)\cdot(\Psi_t(x)-\Psi_t(y))\,d\mu_0(y)$$

$$+\nabla_y e\left(\int_{\Omega_0}\gamma\Big(\Phi_t(x)-\Phi_t(y)\Big)\,d\mu_0(y)\,,\,\Phi_t(x)\right)\cdot\Psi_t(x). \tag{3.15}$$

To avoid lengthy notation, we denote by $e'[\Phi](\Psi)(x)$ the whole expression in (3.15). The variation of S can then be expressed as

$$\begin{aligned}S'[\Phi](\Psi)&=\int_0^T\int_{\Omega_0}\Big(\dot\Phi_t(x)\cdot\dot\Psi_t(x)-e'[\Phi](\Psi)(x)\Big)\,d\mu_0(x)\,dt\\&=\int_0^T\int_{\Omega_0}\Big(-\ddot\Phi_t(x)\cdot\Psi_t(x)-e'[\Phi](\Psi)(x)\Big)\,d\mu_0(x)\,dt,\end{aligned}\tag{3.16}$$

where the last step follows from integration by parts. The boundary terms disappear because Ψ has compact support within $(0,T)$.

We rewrite the part involving $\Psi_t(y)$ in (3.15) as follows:

$$\int_0^T\int_{\Omega_0}-\frac{\partial e}{\partial\rho}\Big(\tilde\rho_t(\Phi_t(x)),\Phi_t(x)\Big)\int_{\Omega_0}\nabla\gamma\Big(\Phi_t(x)-\Phi_t(y)\Big)\cdot\Psi_t(y)\,d\mu_0(y)\,d\mu_0(x)\,dt$$

$$=\int_0^T\int_{\Omega_0}\int_{\Omega_0}\frac{\partial e}{\partial\rho}\Big(\tilde\rho_t(\Phi_t(y)),\Phi_t(y)\Big)\,\nabla\gamma\Big(\Phi_t(x)-\Phi_t(y)\Big)\,d\mu_0(y)\cdot\Psi_t(x)\,d\mu_0(x)\,dt, \tag{3.17}$$

by subsequently interchanging the order of integration, using that the function $\nabla\gamma$ is odd, and replacing x by y and *vice versa*. A combination of (3.13), (3.15), (3.16) and (3.17) yields for $S'[\Phi](\Psi)$ an integral of the form

$$\int_0^T\int_{\Omega_0}[\ldots]\cdot\Psi_t(x)\,d\mu_0(x)\,dt, \tag{3.18}$$

where we deliberately do not write the integrand in square brackets explicitly. Since this integral vanishes for all $\Psi\in C_c^\infty((0,T);C_c^\infty(\Omega_0;\mathbb{R}^d))$ – cf. (3.13) – the part of the

integrand in square brackets vanishes for almost all $t \in [0,T]$ and for μ_0-almost every x. Hence, we obtain

$$\ddot{\Phi}_t(x) = -\int_{\Omega_0} \nabla\gamma\Big(\Phi_t(x)-\Phi_t(y)\Big)\left[\frac{\partial e}{\partial \rho}\Big(\tilde{\rho}_t(\Phi_t(x)),\Phi_t(x)\Big) + \frac{\partial e}{\partial \rho}\Big(\tilde{\rho}_t(\Phi_t(y)),\Phi_t(y)\Big)\right] d\mu_0(y) - \nabla_y e\Big(\tilde{\rho}_t(\Phi_t(x)),\Phi_t(x)\Big). \tag{3.19}$$

Step B

The transition to a particle system takes place by substitution of $\bar{\mu}_0^N = \sum_{i=1}^N m_i\,\delta_{x_{i,0}}$ for μ_0 in (3.19). Moreover, in $\tilde{\rho}_t$ we replace μ_t by $\bar{\mu}_t^N := \Phi_t \# \bar{\mu}_0^N$. Note that, after substitution, (3.19) holds $\bar{\mu}_0^N$-a.e. and should therefore (only) be evaluated at $x = x_{k,0}$ for all $k \in \{1,\dots,N\}$. In this way, we obtain (3.12).

3.2.5 Equations of motion via the route CAB

Step C

At the continuum level, deriving the Euler-Lagrange equations resembles considerably what we did in Section 3.2.4 starting from (3.13). Here, the action is used as defined in (3.5)–(3.6). In (3.5), the explicit dependence of $\rho_t(\Phi_t(x))$ on $\Phi_t(x)$ corresponds to the position at which ρ_t is evaluated. However, if *the mapping* Φ_t is varied, also the *function* ρ_t itself changes. This is an implicit, 'hidden' dependence of ρ_t on the motion mapping Φ_t. The exact relation is given by (3.3), which we therefore substitute in (3.5). The variation becomes

$$S'[\Phi](\Psi) = \frac{d}{d\varepsilon}\left(\int_0^T\int_{\Omega_0}\left[\frac{1}{2}|\dot{\Phi}_t(x)+\varepsilon\,\dot{\Psi}_t(x)|^2 - e\left(\frac{\rho_0(x)}{|J(\Phi_t+\varepsilon\,\Psi_t)(x)|}\,,\,\Phi_t(x)+\varepsilon\,\Psi_t(x)\right)\right]\rho_0(x)\,dx\,dt\right)\Bigg|_{\varepsilon=0},$$

cf. (3.14). Regarding the ε-dependence of the Jacobian matrix, we refer to Section 2 of [SW68], where the equation of motion is derived from the action for the case where e has no explicit dependence on the spatial coordinate; i.e. $e = e(\rho)$. The determinant of the Jacobian matrix is a polynomial in the entries of that matrix. The basic idea in [SW68] is to apply the chain rule with respect to every element of the Jacobian matrix. To avoid extra notation, we only state the result of [SW68], *viz.*

$$\ddot{\Phi}_t(x) = -\frac{1}{\rho_t}\nabla\left(\rho_t^2\,\frac{\partial e}{\partial\rho}\right)\Bigg|_{\Phi_t(x)} = -\left(2\frac{\partial e}{\partial\rho}\Big(\rho_t(\Phi_t(x))\Big) + \rho_t(\Phi_t(x))\frac{\partial^2 e}{\partial\rho^2}\Big(\rho_t(\Phi_t(x))\Big)\right)\nabla\rho_t(\Phi_t(x)). \tag{3.20}$$

On the right-hand side of (3.20) the gradient of the pressure P appears, essentially due to the thermodynamic relation $\partial e/\partial\rho = P/\rho^2$; cf. (9) in [SW68] in the absence of the entropy term $T\,dS$. The notation used in [SW68] differs substantially from ours, but the philosophy of deriving the equations of motion is the same.

If $e = e(\rho, y)$, then instead of (3.20) we have

$$\ddot{\Phi}_t(x) = -\left(2\frac{\partial e}{\partial \rho}\Big(\rho_t(\Phi_t(x)), \Phi_t(x)\Big) + \rho_t(\Phi_t(x))\frac{\partial^2 e}{\partial \rho^2}\Big(\rho_t(\Phi_t(x)), \Phi_t(x)\Big)\right)\nabla\rho_t(\Phi_t(x)) - \nabla_y e\Big(\rho_t(\Phi_t(x)), \Phi_t(x)\Big), \tag{3.21}$$

due to similar steps as the ones leading to (3.19). We omit further details here.

Step A

In this step, we formulate (3.21) in terms of measures. We approximate ρ_t in (3.21) by $\tilde{\rho}_t$ as defined in (3.7) and obtain

$$\ddot{\Phi}_t(x) = -\left(2\frac{\partial e}{\partial \rho}\Big(\tilde{\rho}_t(\Phi_t(x)), \Phi_t(x)\Big) + \tilde{\rho}_t(\Phi_t(x))\frac{\partial^2 e}{\partial \rho^2}\Big(\tilde{\rho}_t(\Phi_t(x)), \Phi_t(x)\Big)\right)\nabla\tilde{\rho}_t(\Phi_t(x)) - \nabla_y e\Big(\tilde{\rho}_t(\Phi_t(x)), \Phi_t(x)\Big). \tag{3.22}$$

Step B

We take $\bar{\mu}_0^N := \sum_{i=1}^N m_i\,\delta_{x_{i,0}}$ and replace μ_t by $\bar{\mu}_t^N := \Phi_t \# \bar{\mu}_0^N$ in $\tilde{\rho}_t$ that appears in (3.22). We evaluate the resulting equation at $x = x_{k,0}$ for all $k \in \{1, \dots, N\}$ to obtain

$$\ddot{\Phi}_t(x_{k,0}) = -\left(2\frac{\partial e}{\partial \rho}\Big(\tilde{\rho}_t(\Phi_t(x_{k,0})), \Phi_t(x_{k,0})\Big) + \tilde{\rho}_t(\Phi_t(x_{k,0}))\frac{\partial^2 e}{\partial \rho^2}\Big(\tilde{\rho}_t(\Phi_t(x_{k,0})), \Phi_t(x_{k,0})\Big)\right)\nabla\tilde{\rho}_t(\Phi_t(x_{k,0})) - \nabla_y e\Big(\tilde{\rho}_t(\Phi_t(x_{k,0})), \Phi_t(x_{k,0})\Big), \tag{3.23}$$

where each appearance of $\tilde{\rho}_t$ denotes a sum over all particle positions. Namely,

$$\tilde{\rho}_t(\Phi_t(x_{k,0})) = \sum_{j=1}^N m_j\,\gamma\Big(\Phi_t(x_{k,0}) - \Phi_t(x_{j,0})\Big), \quad \text{and} \tag{3.24}$$

$$\nabla\tilde{\rho}_t(\Phi_t(x_{k,0})) = \sum_{j=1}^N m_j\,\nabla\gamma\Big(\Phi_t(x_{k,0}) - \Phi_t(x_{j,0})\Big). \tag{3.25}$$

3.2.6 Comparison of the resulting equations (3.12) and (3.23)

Procedures **ABC** and **ACB** yield the same equations of motion, namely (3.12). As announced already in Section 3.2.2, the equation resulting from Procedure **CAB** is different; see (3.23). This difference between the two resulting equations arose because we

introduced the regularization via $\tilde{\rho}$ at different stages. In fact, (3.12) contains an extra regularization in space, as we will show now.

Only the term involving $\partial e/\partial\rho$ and $\partial^2 e/\partial\rho^2$ is different. In (3.12), we have

$$-\sum_{i=1}^{N} m_i \nabla\gamma\Big(\Phi_t(x_{k,0}) - \Phi_t(x_{i,0})\Big)\cdot \\ \cdot\left[\frac{\partial e}{\partial\rho}\Big(\tilde{\rho}_t(\Phi_t(x_{k,0})),\Phi_t(x_{k,0})\Big) + \frac{\partial e}{\partial\rho}\Big(\tilde{\rho}_t(\Phi_t(x_{i,0})),\Phi_t(x_{i,0})\Big)\right],$$

while the corresponding part in (3.23) is

$$-\left(2\frac{\partial e}{\partial\rho}\Big(\tilde{\rho}_t(\Phi_t(x_{k,0})),\Phi_t(x_{k,0})\Big) \right. \\ \left. + \tilde{\rho}_t(\Phi_t(x_{k,0}))\frac{\partial^2 e}{\partial\rho^2}\Big(\tilde{\rho}_t(\Phi_t(x_{k,0})),\Phi_t(x_{k,0})\Big)\right)\nabla\tilde{\rho}_t(\Phi_t(x_{k,0})).$$

Note that both of them contain a part

$$-\frac{\partial e}{\partial\rho}\Big(\tilde{\rho}_t(\Phi_t(x_{k,0})),\Phi_t(x_{k,0})\Big)\,\nabla\tilde{\rho}_t(\Phi_t(x_{k,0})).$$

Hence, let us consider in (3.23) only

$$-\left(\frac{\partial e}{\partial\rho}\Big(\tilde{\rho}_t(\Phi_t(x_{k,0})),\Phi_t(x_{k,0})\Big) \right. \\ \left. + \tilde{\rho}_t(\Phi_t(x_{k,0}))\frac{\partial^2 e}{\partial\rho^2}\Big(\tilde{\rho}_t(\Phi_t(x_{k,0})),\Phi_t(x_{k,0})\Big)\right)\nabla\tilde{\rho}_t(\Phi_t(x_{k,0})) \\ = -\nabla\left(\tilde{\rho}_t(\Phi_t(x_{k,0}))\frac{\partial e}{\partial\rho}\Big(\tilde{\rho}_t(\Phi_t(x_{k,0})),\Phi_t(x_{k,0})\Big)\right). \tag{3.26}$$

To obtain (3.26), we have assumed that $\nabla_y \partial e/\partial\rho \equiv 0$; this assumption anticipates the choice we make in (3.35). Let us go back one more step and consider this term before the introduction of $\tilde{\rho}$, i.e. as in (3.21). To see how this term relates to the corresponding one in (3.12), we take the convolution with γ, and proceed as follows:

$$\begin{aligned} &-\int_{\Omega_t}\gamma(\xi-y)\nabla_y\left(\rho_t(y)\frac{\partial e}{\partial\rho}(\rho_t(y),y)\right)\,dy \\ &=\int_{\Omega_t}\nabla_y\gamma(\xi-y)\,\rho_t(y)\,\frac{\partial e}{\partial\rho}(\rho_t(y),y)\,dy \\ &=-\int_{\Omega_0}\nabla\gamma\Big(\xi-\Phi_t(y)\Big)\,\frac{\partial e}{\partial\rho}\Big(\rho_t(\Phi_t(y)),\Phi_t(y)\Big)\,\rho_t(\Phi_t(y))|J\Phi_t(y)|\,dy \\ &=-\int_{\Omega_0}\nabla\gamma\Big(\xi-\Phi_t(y)\Big)\,\frac{\partial e}{\partial\rho}\Big(\rho_t(\Phi_t(y)),\Phi_t(y)\Big)\,\rho_0(y)\,dy. \end{aligned} \tag{3.27}$$

In the first step, we performed an integration by parts, with vanishing boundary terms on $\partial\Omega_t$. This is because $\Omega_t = \operatorname{supp}\rho_t$ and hence ρ_t vanishes on its boundary. Now, we replace $\rho_0(y)dy$ by $d\mu_0(y)$ and approximate ρ_t by $\tilde{\rho}_t$. Take $\mu_0 := \sum_{i=1}^N m_i\,\delta_{x_{i,0}}$ and evaluate at $\xi = \Phi_t(x_{k,0})$ to obtain

$$-\sum_{i=1}^{N} m_i\,\nabla\gamma\Big(\Phi_t(x_{k,0}) - \Phi_t(x_{i,0})\Big)\,\frac{\partial e}{\partial\rho}\Big(\tilde{\rho}_t(\Phi_t(x_{i,0})), \Phi_t(x_{i,0})\Big).$$

This expression appears in (3.12). To summarize: the connection between (3.12) and (3.23) is that in the former during the derivation procedure an extra regularization in space was introduced for *a part of* the right-hand side.

If we only consider the part involving $\partial e/\partial\rho$, then (3.12) is the same as Equation (3.8) in [Mon05]. The notation used in (3.8) of [Mon05] shows the direct dependence on the pressure. In Equation (3.5) of [Mon05], the equivalent of (3.23) is given. The reason why (3.12) is traditionally used in the SPH community is given in [Mon05]: it does conserve linear and angular momentum exactly, as opposed to (3.23). Moreover, the first part on the right-hand side of (3.23) is of the form

$$-\frac{1}{\tilde{\rho}}\,P'(\tilde{\rho})\,\nabla\tilde{\rho},$$

due to the relation $\partial e/\partial\rho = P/\rho^2$ that was mentioned in Section 3.2.5. Hence, an analytical expression for $dP/d\rho$ is needed.

3.2.7 Nonconservative forces

In the previous sections, we assumed implicitly that there were no nonconservative forces. If these are present, it is still possible to use to action as an ingredient to derive the equations of motion. Instead of a *variational principle* (3.13), which characterizes a stationary point of the action, we formulate a *variational equation* in which the variation of the action is not zero but equal to another functional; cf. e.g. [Ber09], Section 4.4.

In this section we discuss how to generalize the results of Sections 3.2.3, 3.2.4 and 3.2.5 in this respect.

Route ABC

In Section 3.2.3, only Step **C** needs to be reconsidered. The required generalization of (3.10) is given on p. 23 of [GPS01]:

$$\frac{d}{dt}\left(\nabla_{u_k} L\Big|_{(y_i,u_i)=(\Phi_t(x_{i,0}),\dot{\Phi}_t(x_{i,0}))}\right) - \nabla_{y_k} L\Big|_{(y_i,u_i)=(\Phi_t(x_{i,0}),\dot{\Phi}_t(x_{i,0}))}$$

$$= m_k\,q[\bar{\mu}_t^N](\Phi_t(x_{k,0}), \dot{\Phi}_t(x_{k,0})), \quad (3.28)$$

for each $k \in \{1, \dots, N\}$, where q is the force density (per unit mass) of the nonconservative forces. The functional dependence in square brackets denotes that q incorporates a nonlocal interaction term. More details are given in (3.37). The resulting equations of motion are obtained in the same way as (3.12). They are

$$\begin{aligned}\ddot{\Phi}_t(x_{k,0}) = -\sum_{i=1}^{N} m_i \, \nabla\gamma\Big(\Phi_t(x_{k,0}) - \Phi_t(x_{i,0})\Big) \Bigg[\frac{\partial e}{\partial \rho}\Big(\tilde{\rho}_t(\Phi_t(x_{k,0})), \Phi_t(x_{k,0})\Big) \\ + \frac{\partial e}{\partial \rho}\Big(\tilde{\rho}_t(\Phi_t(x_{i,0})), \Phi_t(x_{i,0})\Big)\Bigg] \\ - \nabla_y e\Big(\tilde{\rho}_t(\Phi_t(x_{k,0})), \Phi_t(x_{k,0})\Big) + q[\bar{\mu}_t^N](\Phi_t(x_{k,0}), \dot{\Phi}_t(x_{k,0})),\end{aligned} \tag{3.29}$$

for each $k \in \{1, \dots, N\}$.

Route ACB

Equation (4.49) in [Ber09] provides the main idea of how to generalize (3.13) to a variational equation including nonconservative forces. The specific right-hand side 'δA' that leads to (4.50) in [Ber09] indicates how to remain consistent with the way in which we included nonconservative forces in (3.28). Following the idea of [Ber09], we use the variational equation

$$S'[\Phi](\Psi) = -Q[\Phi](\Psi), \tag{3.30}$$

for all test functions $\Psi \in C_c^\infty((0,T); C_c^\infty(\Omega_0; \mathbb{R}^d))$, with a functional $Q[\Phi](\Psi)$ of the form

$$Q[\Phi](\Psi) := \int_0^T \int_{\Omega_0} q[\mu_t](\Phi_t(x), \dot{\Phi}_t(x)) \cdot \Psi_t(x) \, d\mu_0(x) \, dt \tag{3.31}$$

to generalize Step **C** of Section 3.2.4. Here, q is the same force density as in (3.28). By the same idea as in Section 3.2.4, we obtain an equation of the form (3.18). It follows directly from the structure of (3.31) that an extra term $q[\mu_t](\Phi_t(x), \dot{\Phi}_t(x))$ is present within the square brackets of this modified equation. This is the only difference with the former (3.18). Consequently, in the presence of nonconservative forces, we obtain instead of (3.19) the following equation:

$$\begin{aligned}\ddot{\Phi}_t(x) = -\int_{\Omega_0} \nabla\gamma\Big(\Phi_t(x) - \Phi_t(y)\Big) \Bigg[\frac{\partial e}{\partial \rho}\Big(\tilde{\rho}_t(\Phi_t(x)), \Phi_t(x)\Big) \\ + \frac{\partial e}{\partial \rho}\Big(\tilde{\rho}_t(\Phi_t(y)), \Phi_t(y)\Big)\Bigg] d\mu_0(y) \\ - \nabla_y e\Big(\tilde{\rho}_t(\Phi_t(x)), \Phi_t(x)\Big) + q[\mu_t](\Phi_t(x), \dot{\Phi}_t(x)).\end{aligned} \tag{3.32}$$

To perform Step **B**, we substitute $\bar{\mu}_0^N$ and $\bar{\mu}_t^N := \Phi_t \# \bar{\mu}_0^N$ for μ_0 and μ_t, respectively, and evaluate the equation at $x = x_{k,0}$ for all $k \in \{1, \dots, N\}$. The resulting equation of motion is the same as (3.29).

Route CAB

To generalize Step **C** of Section 3.2.5, we use (3.30) and

$$Q[\Phi](\Psi) := \int_0^T \int_{\Omega_0} q[\rho_t](\Phi_t(x), \dot{\Phi}_t(x)) \cdot \Psi_t(x)\, \rho_0(x)\, dx\, dt. \tag{3.33}$$

Note that, in correspondence with q as it was introduced underneath (3.28), the dependence on ρ_t (in square brackets) indicates the presence of a nonlocal term; cf. (3.37). When we generalize Step **A** of Section 3.2.5, this becomes a dependence on the measure μ_t like before. The measure-valued equation obtained is

$$\begin{aligned}\ddot{\Phi}_t(x) = &- \left(2\frac{\partial e}{\partial \rho}\Big(\tilde{\rho}_t(\Phi_t(x)), \Phi_t(x)\Big) + \tilde{\rho}_t(\Phi_t(x))\frac{\partial^2 e}{\partial \rho^2}\Big(\tilde{\rho}_t(\Phi_t(x)), \Phi_t(x)\Big)\right) \nabla \tilde{\rho}_t(\Phi_t(x)) \\ &- \nabla_y e\Big(\tilde{\rho}_t(\Phi_t(x)), \Phi_t(x)\Big) + q[\mu_t](\Phi_t(x), \dot{\Phi}_t(x)).\end{aligned} \tag{3.34}$$

Finally, performing the transition to discrete measures as in Step **A** of Section 3.2.5, we obtain an equation like (3.23) with an additional term $q[\bar{\mu}_t^N](\Phi_t(x_{k,0}), \dot{\Phi}_t(x_{k,0}))$ on the right-hand side.

Remark 3.2.2. The contributions of the nonconservative forces to (3.32) and (3.34) are the same. The discussion about the difference between the two schemes in Section 3.2.6 is therefore analogous if we include nonconservative forces.

3.2.8 Measure-valued formulation

In Sections 3.2.3, 3.2.4 and 3.2.5 we derived particle-based approximation schemes and we incorporated nonconservative forces in Section 3.2.7. To establish the convergence of these schemes as $N \to \infty$ we use a measure-valued framework. Hence, we focus on the measure-formulations (3.32) and (3.34), without the specific choice $\mu_0 = \bar{\mu}_0^N$.

Although (3.32) and (3.34) are different (cf. Section 3.2.6), we wish to establish the convergence proof for both formulations simultaneously. Hence, we introduce a switching parameter $\theta \in \{0, 1\}$ to unify both variants in a single equation of motion. First, we assume that e is of the form

$$e(\rho, y) := V(y) + \bar{F}(\rho), \tag{3.35}$$

in agreement with the remark we already made underneath (3.26). Here, $V \in C_b^2(\mathbb{R}^d; \mathbb{R})$ and $\bar{F} \in C^2(\mathbb{R}^+; \mathbb{R})$, where $\mathbb{R}^+ := (0, \infty)$. Note that $\partial e/\partial \rho = \bar{F}'$ and $\nabla_y e = \nabla V$. We introduce an auxiliary function F_θ, with $\theta \in \{0, 1\}$, that is defined by

$$F_0(\rho) := \frac{1}{\rho}\frac{d}{d\rho}\left(\rho^2 \bar{F}'(\rho)\right), \quad \text{and} \quad F_1(\rho) := \bar{F}'(\rho). \tag{3.36}$$

We choose q to be of the form

$$q[\mu](y, u) := -\eta(y)\, u + (\mathcal{K} * \mu)(y), \tag{3.37}$$

with $\eta \in C_b^1(\mathbb{R}^d;\mathbb{R}^+)$ and $\mathcal{K} \in C_b^1(\mathbb{R}^d;\mathbb{R}^d)$.

We assign the value $\theta = 0$ to the formulation in (3.34), and $\theta = 1$ to (3.32). Both equations are now simultaneously written as

$$\ddot{\Phi}_t(x) = -F_\theta\left(\tilde{\rho}_t(\Phi_t(x))\right)\nabla\tilde{\rho}_t(\Phi_t(x)) - \theta\left(\nabla\gamma * [(F_\theta\circ\tilde{\rho}_t)\,\mu_t]\right)(\Phi_t(x)) \\ - \nabla V\left(\Phi_t(x)\right) - \eta(\Phi_t(x))\,\dot{\Phi}_t(x) + (\mathcal{K}*\mu_t)(\Phi_t(x)). \quad (3.38)$$

Here we use the shorthand notation

$$\left(\nabla\gamma * [(F_\theta\circ\tilde{\rho}_t)\,\mu_t]\right)(\xi) = \int_{\Omega_t} \nabla\gamma(\xi-y)F_\theta(\tilde{\rho}_t(y))\,d\mu_t(y).$$

In (3.38) we slightly abuse notation. The equation should be read as follows: whenever $\theta = 0$ we disregard the term $\theta\left(\nabla\gamma * [(F_\theta\circ\tilde{\rho}_t)\,\mu_t]\right)(\Phi_t(x))$ completely, irrespective of whether the convolution term is well-defined, bounded etc.

Remark 3.2.3. We emphasize that F_0 and F_1 are physically different objects in the sense that F_0 contains all contributions of $\bar{F}$ to the flow, while F_1 only contains part of that influence. Hence, although the notation might suggest so, by setting $\theta = 1$ we are not *adding* terms. However, F_0 and F_1 do have the same physical dimension and if, for instance, $\bar{F}$ is given by $\bar{F}(\rho) \sim \rho^\kappa$ for some $\kappa \in \mathbb{R}\setminus\{0\}$, then both $F_0, F_1 \sim \rho^{\kappa-1}$. We use one function F_θ for the ease of presentation in the sequel.

Now, we arrive at the evolution problem that is central to the rest of this chapter. Fix a final time $T > 0$. Recall from Chapter 1 that $\mathcal{P}(\mathbb{R}^d)$ is the space of probability measures on $\mathbb{R}^d$. Assume that $\mu_0 \in \mathcal{P}(\mathbb{R}^d)$ and that there is an $r_0 > 0$ such that

$$\operatorname{supp}\mu_0 \subset \overline{B(r_0)}. \quad (3.39)$$

Let $v_0 \in C_b^1(\mathbb{R}^d;\mathbb{R}^d)$ and $\theta \in \{0,1\}$ be fixed. We consider the system

$$\begin{cases} \ddot{\Phi}_t(x) = -F_\theta\left(\tilde{\rho}_t(\Phi_t(x))\right)\nabla\tilde{\rho}_t(\Phi_t(x)) - \theta\left(\nabla\gamma * [(F_\theta\circ\tilde{\rho}_t)\mu_t]\right)(\Phi_t(x)) \\ \qquad\qquad -\nabla V\left(\Phi_t(x)\right) - \eta(\Phi_t(x))\,\dot{\Phi}_t(x) + (\mathcal{K}*\mu_t)(\Phi_t(x)); \\ \tilde{\rho}_t := \gamma * \mu_t; \\ \mu_t = \Phi_t\#\mu_0; \\ \Phi_0(x) = x,\ \dot{\Phi}_0(x) = v_0(x), \end{cases} \quad (3.40)$$

for all $x \in \operatorname{supp}\mu_0$ and all $t \in (0,T]$.

Remark 3.2.4. We could have taken $\bar{\mathcal{K}} * (\gamma * \mu_t)$ for some $\bar{\mathcal{K}}$, instead of $\mathcal{K} * \mu_t$, to comply with the pressure term (i.e. the one involving F_θ) that only depends on the *regularized* density $\tilde{\rho}_t$. We prefer the shorter form $\mathcal{K} * \mu_t$. This choice can be made without loss of generality if we take $\mathcal{K} = \bar{\mathcal{K}} * \gamma$.

Remark 3.2.5. It is not *a priori* clear whether the term $\mathcal{K} * \mu_t$ is a conservative or a nonconservative force density, hence it is not clear whether it should be part of q or be related to e. Assume there is a K such that $\mathcal{K}(\xi) = -K'(|\xi|)\xi/|\xi|$. Then either way yields the same equation of motion. Indeed, if we include the energy density $\frac{1}{2}K * \mu_t$ in e instead of including $\mathcal{K} * \mu_t$ in q, we also obtain (3.38).

3.3 Main convergence result

In this section we first introduce some preliminary notions. Afterwards, we summarize the assumptions required to derive the main convergence result (Theorem 3.3.10). This theorem is a general result, of which the convergence of SPH schemes is a special case; see Corollary 3.3.11. The proof of Theorem 3.3.10 is given in Section 3.4.

3.3.1 Preliminaries

We recall the concept of push-forward which was already introduced in (1.4). The following is a more precise definition:

Definition 3.3.1 (Push-forward). *The push-forward of a probability measure $\mu \in \mathcal{P}(\mathbb{R}^d)$ by a Borel measurable mapping $\Phi : \mathbb{R}^d \to \mathbb{R}^d$, notation $\Phi\#\mu$, is defined by*

$$(\Phi\#\mu)(B) := \mu(\Phi^{-1}(B))$$

for all sets B in the Borel σ-algebra of $\mathbb{R}^d$. Equivalently, we can define $\Phi\#\mu$ as the push-forward of μ by Φ if

$$\int_{\mathbb{R}^d} f(x)\, d(\Phi\#\mu)(x) = \int_{\mathbb{R}^d} f(\Phi(x))\, d\mu(x) \tag{3.41}$$

for all measurable, bounded functions f on $\mathbb{R}^d$.

Definition 3.3.2 (Joint representation). *A joint representation of two measures $\mu_1, \mu_2 \in \mathcal{P}(\mathbb{R}^d)$ is a measure π on $\mathbb{R}^d \times \mathbb{R}^d$ such that*

$$\pi(A \times \mathbb{R}^d) = \mu_1(A), \quad \text{and} \quad \pi(\mathbb{R}^d \times B) = \mu_2(B),$$

for all sets A and B taken from the Borel σ-algebra of $\mathbb{R}^d$. We denote by $\Pi(\mu_1, \mu_2)$ the set of all joint representations of μ_1 and μ_2.

Joint representations are also called *couplings*. The measures μ_1 and μ_2 are called *marginals* of π. A useful property of any joint representation $\pi \in \Pi(\mu_1, \mu_2)$ is that for each $i \in \{1, 2\}$ one has the identity

$$\int_{\mathbb{R}^d \times \mathbb{R}^d} f(x_i)\, d\pi(x_1, x_2) = \int_{\mathbb{R}^d} f(x)\, d\mu_i(x)$$

for all measurable, bounded functions f on $\mathbb{R}^d$. In fact, this can be seen as an alternative definition.

Definition 3.3.3 (Wasserstein distance). *For any $p \in [1, \infty)$, the Wasserstein distance of order p, or p-Wasserstein distance, between two probability measures $\mu_1, \mu_2 \in \mathcal{P}(\mathbb{R}^d)$ is defined as*

$$W_p(\mu_1, \mu_2) := \left(\inf_{\pi \in \Pi(\mu_1, \mu_2)} \int_{\mathbb{R}^d \times \mathbb{R}^d} |x - y|^p \, d\pi(x, y) \right)^{1/p}. \tag{3.42}$$

In this chapter, we use the 1-Wasserstein distance; that is, (3.42) for $p = 1$. The particular choice $p = 1$ is compatible with the Lipschitz properties of the functions and the kind of motion mapping that we use. For more details on the Wasserstein distance and the related concept of *optimal transport*, we refer to [Vil03, Vil09] and the references cited therein.

3.3.2 Assumptions

We assume the following:

Assumption 3.3.4. *The functions V, η and $\mathcal{K}$ satisfy the following regularity constraints: $V \in C_b^2(\mathbb{R}^d;\mathbb{R})$, $\eta \in C_b^1(\mathbb{R}^d;\mathbb{R}^+)$ and $\mathcal{K} \in C_b^1(\mathbb{R}^d;\mathbb{R}^d)$.*

Remark 3.3.5. Assumption 3.3.4 implies in particular that ∇V and $\mathcal{K}$ are Lipschitz continuous. We denote their Lipschitz constants by $|\nabla V|_{\mathrm{L}}$ and $|\mathcal{K}|_{\mathrm{L}}$, respectively. In general, the Lipschitz constant of any Lipschitz continuous $\phi : \mathbb{R}^d \to \mathbb{R}^k$, $k \in \mathbb{N}^+$, is defined by

$$|\phi|_{\mathrm{L}} := \sup\left\{ \frac{|\phi(x) - \phi(y)|}{|x-y|} \;\middle|\; x, y \in \mathbb{R}^d,\ x \neq y \right\}. \tag{3.43}$$

The conditions on F_θ and γ depend on the value of θ. Recall that $\mathbb{R}^+ := (0,\infty)$ and define $\mathbb{R}_0^+ := [0,\infty)$.

Assumption 3.3.6. *The function $\gamma \in C_b^2(\mathbb{R}^d;\mathbb{R}_0^+)$ is even and satisfies $\int_{\mathbb{R}^d} \gamma(x)\,dx = 1$.*

Assumption 3.3.7 (The case $\theta = 0$)**.** *We require that $F_0 \in C^1(\mathbb{R}^+;\mathbb{R})$. Moreover, we assume that there is an $M_1 > 0$ such that for all $\mu \in \mathcal{P}(\mathbb{R}^d)$*

$$\sup_{x \in \operatorname{supp}\mu} |F_0\left((\gamma * \mu)(x)\right) \nabla(\gamma * \mu)(x)| \leqslant M_1, \tag{3.44}$$

and we assume there are constants $M_2, M_3 > 0$ such that

$$\sup_{u \in U_{T,\gamma}} |F_0(u)| \leqslant M_2, \quad \textit{and}$$
$$\sup_{u \in U_{T,\gamma}} |F_0'(u)| \leqslant M_3,$$

where

$$U_{T,\gamma} := \left\{ u \in \mathbb{R}_0^+ : \left(\inf_{\overline{B}(2r(T))} \gamma \right) \leqslant u \leqslant \|\gamma\|_\infty \right\}, \quad \textit{and}$$
$$r(T) := r_0 + T\,\|v_0\|_\infty + \frac{1}{2}\,T^2\,(\|\nabla V\|_\infty + M_1 + \|\mathcal{K}\|_\infty).$$

The value of $r(T)$ follows from Lemma 3.4.1 and Corollary 3.4.2. Under these assumptions, F_0 may have singularities at the origin, but *only* if γ is strictly positive everywhere in $\overline{B}(2r(T))$. Such choices of F_0 and γ are used in [LGP98]; see also Section 3.5.

If $\theta = 1$ we need the following assumption:

Assumption 3.3.8 (The case $\theta = 1$)**.** *We require that* $F_1 \in C^1(\mathbb{R}_0^+;\mathbb{R})$. *Moreover, let* $M_2, M_3 > 0$ *be such that*

$$\sup_{u\in[0,\|\gamma\|_\infty]} |F_1(u)| \leqslant M_2, \text{ and}$$
$$\sup_{u\in[0,\|\gamma\|_\infty]} |F_1'(u)| \leqslant M_3.$$

Take $M_1 := 2\, M_2\, \|\nabla\gamma\|_\infty$.

To simplify the notation, we use the same letters for the constants.

Remark 3.3.9. Condition (3.44) in Assumption 3.3.7 is needed to get an *a priori* bound on the propagation speed in Lemma 3.4.1. Hence, we can restrict ourselves to measures with bounded support afterwards; cf. Corollary 3.4.2. To achieve the result of Lemma 3.4.1 for $\theta = 1$, we need Assumption 3.3.8. This assumption does not allow for singularities in F_1 around zero.
We indicate now why a weaker assumption for F_1, resembling (3.44) is not feasible. Assume that $F_1(\rho) := \rho^\alpha$ with $\alpha \in (-1, 0)$. This is the case also considered in [LGP98]. To bound the first term on the right-hand side of (3.38), [LGP98] assumes that

$$|\nabla\gamma(\xi)| \leqslant c|\gamma(\xi)|^{-\alpha}$$

for some $c > 0$ and for all $\xi \in \mathbb{R}^d$. In our case, an estimate on

$$\sup_{x\in\operatorname{supp}\mu} |(\nabla\gamma * [(F_1 \circ (\gamma * \mu))\,\mu])(x)| \tag{3.45}$$

is needed. Let γ be strictly positive everywhere. Since $\gamma \in L^1(\mathbb{R}^d)$, we have that $\lim_{\xi\to\infty}\gamma(\xi) = 0$. Let γ satisfy the aforementioned condition $|\nabla\gamma(\xi)| \leqslant c|\gamma(\xi)|^{-\alpha}$. Then also $\lim_{\xi\to\infty}|\nabla\gamma(\xi)| = 0$. Under these (not very strict) conditions one can show that (3.45) is unbounded. We use e.g. the sequence of measures $(\mu^k)_{k\in\mathbb{N}^+}$ defined by

$$\mu^k := (\delta_{-k\underline{e}_1} + \delta_{k\underline{e}_1} + \delta_{(k+1)\underline{e}_1})/3 \quad \text{for each } k \in \mathbb{N}^+,$$

where $\underline{e}_1$ is the first unit vector in $\mathbb{R}^d$. Note in particular that (3.45) is unbounded if γ is a Gaussian. However, we want the Gaussian to be admissible, since it is one of the standard choices for γ.

3.3.3 Convergence result

Let $\{\mu_0^N\}_{N\in\mathbb{N}} \subset \mathcal{P}(\mathbb{R}^d)$, and assume that

$$\operatorname{supp}\mu_0^N \subset \overline{B(r_0)} \quad \text{for all } N \in \mathbb{N},$$

where $r_0 > 0$ is the same constant as in (3.39). For each $N \in \mathbb{N}$ we associate to the measure μ_0^N a system of equations analogous to (3.40):

$$\begin{cases} \ddot{\Phi}_t^N(x) = -F_\theta\left(\tilde{\rho}_t^N(\Phi_t^N(x))\right)\nabla\tilde{\rho}_t^N(\Phi_t^N(x)) - \theta\,(\nabla\gamma * [(F_\theta \circ \tilde{\rho}_t^N)\,\mu_t^N])(\Phi_t^N(x)) \\ \qquad\qquad -\nabla V\left(\Phi_t^N(x)\right) - \eta(\Phi_t^N(x))\,\dot{\Phi}_t^N(x) + (\mathcal{K} * \mu_t^N)(\Phi_t^N(x)); \\ \tilde{\rho}_t^N := \gamma * \mu_t^N; \\ \mu_t^N = \Phi_t^N \# \mu_0^N; \\ \Phi_0^N(x) = x,\ \dot{\Phi}_0^N(x) = v_0(x), \end{cases} \tag{3.46}$$

for all $x \in \operatorname{supp}\mu_0^N$ and all $t \in [0,T]$. Note that the only difference with (3.40) lies in the initial distribution μ_0^N versus μ_0; the initial velocity v_0 is the same.

For any $r>0$, define $\mathcal{P}_r(\mathbb{R}^d) := \left\{\mu \in \mathcal{P}(\mathbb{R}^d) : \operatorname{supp}\mu \subset \overline{B(r)}\right\}$.

The main result of this chapter is the following theorem:

Theorem 3.3.10. *Fix $\theta \in \{0,1\}$. Assume that $v_0 \in C_b^1(\mathbb{R}^d;\mathbb{R}^d)$, and that Assumptions 3.3.4 and 3.3.6 hold. Let moreover (depending on the value of θ) Assumption 3.3.7 or 3.3.8 be satisfied, and take the sequence $\{\mu_0^N\} \subset \mathcal{P}_{r_0}(\mathbb{R}^d)$ such that*

$$W_1(\mu_0^N,\mu_0) \overset{N\to\infty}{\longrightarrow} 0, \tag{3.47}$$

for some $\mu_0 \in \mathcal{P}_{r_0}(\mathbb{R}^d)$. Then:

1. *there is a unique pair*

$$(\mu,\Phi) \in C([0,T];\mathcal{P}_{r(T)}(\mathbb{R}^d)) \times C^2([0,T];\{\phi : \operatorname{supp}\mu_0 \to \mathbb{R}^d\})$$

that satisfies (3.40)*;*

2. *if, for all $N \in \mathbb{N}$, the pair*

$$(\mu^N,\Phi^N) \in C([0,T];\mathcal{P}_{r(T)}(\mathbb{R}^d)) \times C^2([0,T];\{\phi : \operatorname{supp}\mu_0 \to \mathbb{R}^d\})$$

is a solution of (3.46)*, then*

$$\sup_{t\in[0,T]} W_1(\mu_t^N,\mu_t) \overset{N\to\infty}{\longrightarrow} 0.$$

The proof of Theorem 3.3.10 is given in Section 3.4. As a direct consequence, we obtain the convergence of the SPH scheme in the many-particle limit $N \to \infty$.

Corollary 3.3.11. *Fix $\theta \in \{0,1\}$. For each $N \in \mathbb{N}^+$, let*

$$\bar{\mu}_0^N := \sum_{j=1}^N m_j \delta_{x_{j,0}} \in \mathcal{P}_{r_0}(\mathbb{R}^d)$$

for some $\{m_j\}_{j=1}^N \subset \mathbb{R}^+$ such that $\sum_{j=1}^N m_j = 1$, and for some $\{x_{j,0}\}_{j=1}^N \subset \overline{B(r_0)}$.
Assume that $W_1(\bar{\mu}_0^N,\mu_0) \overset{N\to\infty}{\longrightarrow} 0$ for some $\mu_0 \in \mathcal{P}_{r_0}(\mathbb{R}^d)$.
Then the discrete measure $\bar{\mu}_t^N = \sum_{k=1}^N m_k \delta_{\Phi_t(x_{k,0})}$ associated to the particle scheme defined for each $k \in \{1,\dots,N\}$ by:

$$\begin{aligned}\ddot{\Phi}_t(x_{k,0}) = &-\sum_{i=1}^N m_i\, \nabla\gamma(\Phi_t(x_{k,0}) - \Phi_t(x_{i,0}))\, \left[F_\theta\left(\tilde{\rho}_t(\Phi_t(x_{k,0}))\right) + \theta F_\theta\left(\tilde{\rho}_t(\Phi_t(x_{i,0}))\right)\right] \\ &- \nabla V\left(\Phi_t(x_{k,0})\right) - \eta(\Phi_t(x_{k,0}))\,\dot{\Phi}_t(x_{k,0}) + (\mathcal{K} * \bar{\mu}_t^N)(\Phi_t(x_{k,0})),\end{aligned} \tag{3.48}$$

converges to the solution μ_t of (3.40) *in the following sense:*

$$\sup_{t\in[0,T]} W_1(\bar{\mu}_t^N,\mu_t) \overset{N\to\infty}{\longrightarrow} 0. \tag{3.49}$$

3.4 Proof of Theorem 3.3.10 – Convergence

Before proving the main result, Theorem 3.3.10, we provide two lemmas concerning basic properties of the motion mapping Φ_t. The first lemma is an upper estimate for Φ_t.

Lemma 3.4.1. *Let Assumptions 3.3.4, 3.3.6 and 3.3.7 or 3.3.8 (depending on the value of θ) be satisfied. Then for any* given $\mu \in C([0,T];\mathcal{P}(\mathbb{R}^d))$ *the mapping Φ_t in* (3.38), *completed with $\tilde{\rho}_t := \gamma * \mu_t$, $\Phi_0(x) = x$ and $\dot{\Phi}_0(x) = v_0(x)$, satisfies*

$$|\Phi_t(x)| \leqslant |x| + t\|v_0\|_\infty + \frac{1}{2}\, t^2\, (M_1 + \|\nabla V\|_\infty + \|\mathcal{K}\|_\infty), \tag{3.50}$$

for all $x \in \operatorname{supp} \mu_{t=0}$ and all $t \in [0,T]$.

Proof. For μ fixed, and for each $x \in \operatorname{supp} \mu_{t=0}$, the ODE (3.38) is well-posed on $[0,T]$, given the assumptions on V, η, F_θ, γ and $\mathcal{K}$, and the fact that μ is continuous in time. The well-posedness follows from the Picard-Lindelöf Theorem; further details on the proof are omitted.
Using an integrating factor $H(t) := \exp\left(\int_0^t \eta(\Phi_r(x))\, dr\right)$, we deduce from (3.38) that

$$\begin{aligned}
|\Phi_t(x)| \leqslant & |\Phi_0(x)| + |v_0(x)\, t| + \left| \int_0^t \frac{1}{H(s)} \int_0^s H(r) \Big(\ddot{\Phi}_r(x) + \eta(\Phi_r(x))\, \dot{\Phi}_r(x) \Big)\, dr\, ds \right| \\
\leqslant & |x| + t\, \|v_0\|_\infty + \int_0^t \int_0^s \frac{H(r)}{H(s)} \left| \ddot{\Phi}_r(x) + \eta(\Phi_r(x))\, \dot{\Phi}_r(x) \right|\, dr\, ds.
\end{aligned}$$

Since η is a positive function and hence $0 \leqslant H(r)/H(s) \leqslant 1$ in the inner integral, it follows that

$$\begin{aligned}
|\Phi_t(x)| \leqslant |x| + t\, \|v_0\|_\infty + \int_0^t \int_0^s \Big| & - \nabla V(\Phi_r(x)) + (\mathcal{K} * \mu_r)(\Phi_r(x)) \\
& - F_\theta\left((\gamma * \mu_r)(\Phi_r(x))\right) \nabla(\gamma * \mu_r)(\Phi_r(x)) \\
& - \theta\left(\nabla\gamma * [(F_\theta \circ (\gamma * \mu_r))\mu_r]\right)(\Phi_r(x))\Big)\Big|\, dr\, ds.
\end{aligned} \tag{3.51}$$

In the case $\theta = 0$, the following estimate holds due to Assumption 3.3.7:

$$\begin{aligned}
\Big| & F_\theta\left((\gamma * \mu_r)(\Phi_r(x))\right) \nabla(\gamma * \mu_r)(\Phi_r(x)) \\
& + \theta\left(\nabla\gamma * [(F_\theta \circ (\gamma * \mu_r))\mu_r]\right)(\Phi_r(x))\Big| = \left|F_0\left((\gamma * \mu_r)(\Phi_r(x))\right) \nabla(\gamma * \mu_r)(\Phi_r(x))\right| \\
& \leqslant M_1.
\end{aligned} \tag{3.52}$$

Note that for any $\mu \in \mathcal{P}(\mathbb{R}^d)$ the estimate $\|\gamma * \mu\|_\infty \leqslant \|\gamma\|_\infty$ holds. Hence, for $\theta = 1$ we obtain:

$$\begin{aligned}
\Big| & F_\theta\left((\gamma * \mu_r)(\Phi_r(x))\right) \nabla(\gamma * \mu_r)(\Phi_r(x)) \\
& + \theta\left(\nabla\gamma * [(F_\theta \circ (\gamma * \mu_r))\mu_r]\right)(\Phi_r(x))\Big| \leqslant M_2\, \|\nabla\gamma\|_\infty + \|\nabla\gamma\|_\infty\, M_2 \\
& = M_1,
\end{aligned} \tag{3.53}$$

where the bounds from Assumption 3.3.8 are used.

A suitable combination of (3.51), (3.52) and (3.53) yields that for each $\theta \in \{0,1\}$

$$|\Phi_t(x)| \leqslant |x| + t\,\|v_0\|_\infty + \int_0^t \int_0^s \left(\|\nabla V\|_\infty + \|\mathcal{K}\|_\infty + M_1\right) dr\,ds$$

holds for all $x \in \operatorname{supp}\mu_{t=0}$ and $t \in [0,T]$, from which the statement of the lemma follows. □

Corollary 3.4.2. *Let $\mu_0 \in \mathcal{P}_{r_0}(\mathbb{R}^d)$, and let Assumptions 3.3.4, 3.3.6 and 3.3.7 or 3.3.8 (depending on the value of θ) be satisfied. Then any solution of* (3.40) *must satisfy*

$$\operatorname{supp}\mu_t \subset \overline{B(r(t))},$$

for each $t \in [0,T]$, where

$$r(t) := r_0 + t\|v_0\|_\infty + \frac{1}{2}\,t^2\,(M_1 + \|\nabla V\|_\infty + \|\mathcal{K}\|_\infty). \tag{3.54}$$

The next lemma provides a Lipschitz-like estimate on Φ_t.

Lemma 3.4.3. *Let $\nu^1, \nu^2 \in C([0,T]; \mathcal{P}_{r(T)}(\mathbb{R}^d))$ be given. Consider the motion mappings corresponding to ν^i ($i \in \{1,2\}$) defined by*

$$\begin{aligned}\ddot{\Phi}_t^{\nu^i}(\xi) = &- F_\theta\left((\gamma * \nu_t^i)(\Phi_t^{\nu^i}(\xi))\right)\nabla(\gamma * \nu_t^i)(\Phi_t^{\nu^i}(\xi)) \\ &- \theta\,(\nabla\gamma * [(F_\theta \circ (\gamma * \nu_t^i))\,\nu_t^i])(\Phi_t^{\nu^i}(\xi)) \\ &- \nabla V(\Phi_t^{\nu^i}(\xi)) - \eta(\Phi_t^{\nu^i}(\xi))\dot{\Phi}_t^{\nu^i}(\xi) + (\mathcal{K} * \nu_t^i)(\Phi_t^{\nu^i}(\xi))\end{aligned} \tag{3.55}$$

for all $\xi \in \operatorname{supp}\nu_0^i$ and all $t \in [0,T]$, completed with initial conditions $\Phi_0^{\nu^i}(\xi) = \xi$ and $\dot{\Phi}_0^{\nu^i}(\xi) = v_0(\xi)$. Then, for all $t \in [0,T]$, $x \in \operatorname{supp}\nu_0^1$ and $y \in \operatorname{supp}\nu_0^2$, it holds that

$$\begin{aligned}|\Phi_t^{\nu^1}(x) - \Phi_t^{\nu^2}(y)| \leqslant\; &(1 + t\,\|\eta\|_\infty)\,|x-y| + t\,|v_0(x) - v_0(y)| \\ &+ \int_0^t (M_4\,(t-s) + \|\eta\|_\infty)\,\left|\Phi_s^{\nu^1}(x) - \Phi_s^{\nu^2}(y)\right| ds \\ &+ M_5 \int_0^t (t-s) \int |z-w|\; d\tilde{\pi}_s(z,w)\,ds,\end{aligned} \tag{3.56}$$

where

$$\begin{aligned}M_4 &:= |\nabla V|_{\mathrm{L}} + (1+\theta)M_2\,\|\operatorname{Hess}\gamma\|_\infty + M_3\,\|\nabla\gamma\|_\infty^2 + |\mathcal{K}|_{\mathrm{L}}, \\ M_5 &:= (1+\theta)M_2\,\|\operatorname{Hess}\gamma\|_\infty + (1+\theta)M_3\,\|\nabla\gamma\|_\infty^2 + |\mathcal{K}|_{\mathrm{L}},\end{aligned}$$

and $\tilde{\pi}_s$ is an arbitrary element of $\Pi(\nu_s^1, \nu_s^2)$ for all $s \in [0,t]$.

Proof. Note that, by the Fubini's Theorem, for any integrable function f, we have

$$\int_0^t \int_0^r f(s)\,ds\,dr = \int_0^t \int_s^t f(s)\,dr\,ds = \int_0^t (t-s) f(s)\,ds. \tag{3.57}$$

Integration of (3.55) in time together with (3.57) yields that

$$\begin{aligned}
|\Phi_t^{\nu^1}(x) - \Phi_t^{\nu^2}(y)| \leqslant\, & |x-y| + t\,|v_0(x) - v_0(y)| \\
& + \int_0^t (t-s) |\nabla V(\Phi_s^{\nu^1}(x)) - \nabla V(\Phi_s^{\nu^2}(y))|\,ds \\
& + \left| \int_0^t \int_0^r \eta(\Phi_s^{\nu^1}(x)) \dot{\Phi}_s^{\nu^1}(x) - \eta(\Phi_s^{\nu^2}(y)) \dot{\Phi}_s^{\nu^2}(y)\,ds\,dr \right| \\
& + \int_0^t (t-s) \Big| F_\theta \left((\gamma * \nu_s^1)(\Phi_s^{\nu^1}(x)) \right) \nabla (\gamma * \nu_s^1)(\Phi_s^{\nu^1}(x)) \\
& \qquad - F_\theta \left((\gamma * \nu_s^2)(\Phi_s^{\nu^2}(y)) \right) \nabla (\gamma * \nu_s^2)(\Phi_s^{\nu^2}(y)) \Big|\,ds \\
& + \theta \int_0^t (t-s) \Big| (\nabla \gamma * [(F_\theta \circ (\gamma * \nu_s^1)) \nu_s^1])(\Phi_s^{\nu^1}(x)) \\
& \qquad - (\nabla \gamma * [(F_\theta \circ (\gamma * \nu_s^2)) \nu_s^2])(\Phi_s^{\nu^2}(y)) \Big|\,ds \\
& + \int_0^t (t-s) \left| (\mathcal{K} * \nu_s^1)(\Phi_s^{\nu^1}(x)) - (\mathcal{K} * \nu_s^2)(\Phi_s^{\nu^2}(y)) \right|\,ds.
\end{aligned} \tag{3.58}$$

Furthermore, we have

$$\int_0^t (t-s) |\nabla V(\Phi_s^{\nu^1}(x)) - \nabla V(\Phi_s^{\nu^2}(y))|\,ds \leqslant |\nabla V|_{\mathrm{L}} \int_0^t (t-s) |\Phi_s^{\nu^1}(x) - \Phi_s^{\nu^2}(y)|\,ds, \tag{3.59}$$

and

$$\begin{aligned}
\left| \int_0^t \int_0^r \eta(\Phi_s^{\nu^1}(x)) \dot{\Phi}_s^{\nu^1}(x) - \eta(\Phi_s^{\nu^2}(y)) \dot{\Phi}_s^{\nu^2}(y)\,ds\,dr \right| &= \left| \int_0^t \int_0^r \frac{d}{ds} \left(\int_{\Phi_s^{\nu^2}(y)}^{\Phi_s^{\nu^1}(x)} \eta(z)\,dz \right) ds\,dr \right| \\
= \left| \int_0^t \left(\int_{\Phi_r^{\nu^2}(y)}^{\Phi_r^{\nu^1}(x)} \eta(z)\,dz - \int_y^x \eta(z)\,dz \right) dr \right| &\leqslant \|\eta\|_\infty \int_0^t |\Phi_r^{\nu^1}(x) - \Phi_r^{\nu^2}(y)|\,dr + \|\eta\|_\infty\, t\,|x-y|.
\end{aligned} \tag{3.60}$$

Regarding the term involving F_θ on the fourth and fifth line of (3.58), we proceed as follows: we have

$$\begin{aligned}
&\left|F_\theta\left((\gamma*\nu_s^1)(\xi_1)\right)\nabla(\gamma*\nu_s^1)(\xi_1) - F_\theta\left((\gamma*\nu_s^2)(\xi_2)\right)\nabla(\gamma*\nu_s^2)(\xi_2)\right| \\
&\leqslant \left|F_\theta\left((\gamma*\nu_s^1)(\xi_1)\right)\right|\left|\nabla(\gamma*\nu_s^1)(\xi_1) - \nabla(\gamma*\nu_s^1)(\xi_2)\right| \\
&\quad + \left|F_\theta\left((\gamma*\nu_s^1)(\xi_1)\right)\right|\left|\nabla(\gamma*\nu_s^1)(\xi_2) - \nabla(\gamma*\nu_s^2)(\xi_2)\right| \\
&\quad + \left|F_\theta\left((\gamma*\nu_s^1)(\xi_1)\right) - F_\theta\left((\gamma*\nu_s^1)(\xi_2)\right)\right|\left|\nabla(\gamma*\nu_s^2)(\xi_2)\right| \\
&\quad + \left|F_\theta\left((\gamma*\nu_s^1)(\xi_2)\right) - F_\theta\left((\gamma*\nu_s^2)(\xi_2)\right)\right|\left|\nabla(\gamma*\nu_s^2)(\xi_2)\right|. \qquad (3.61)
\end{aligned}$$

We only consider $\xi_1 \in \operatorname{supp}\nu_s^1$ and $\xi_2 \in \operatorname{supp}\nu_s^2$. This actually implies that $\xi_1, \xi_2 \in \overline{B(r(T))}$. For each $i, j \in \{1,2\}$, we have the following estimates:

$$(\gamma*\nu_s^i)(\xi_j) \leqslant \|\gamma\|_\infty,$$

and

$$(\gamma*\nu_s^i)(\xi_j) \geqslant \inf_{\xi_j, z \in \overline{B}(r(T))} \gamma(\xi_j - z) = \inf_{\overline{B}(2r(T))} \gamma.$$

Thus we get $(\gamma*\nu_s^i)(\xi_j) \in U_{T,\gamma}$. We continue the estimation of (3.61) with

$$\begin{aligned}
&\left|F_\theta\left((\gamma*\nu_s^1)(\xi_1)\right)\nabla(\gamma*\nu_s^1)(\xi_1) - F_\theta\left((\gamma*\nu_s^2)(\xi_2)\right)\nabla(\gamma*\nu_s^2)(\xi_2)\right| \\
&\quad\leqslant M_2\,\|\operatorname{Hess}\gamma\|_\infty\,|\xi_1-\xi_2| + M_2\left|\nabla(\gamma*\nu_s^1)(\xi_2) - \nabla(\gamma*\nu_s^2)(\xi_2)\right| \\
&\qquad + M_3\,\|\nabla\gamma\|_\infty^2\,|\xi_1-\xi_2| + M_3\,\|\nabla\gamma\|_\infty\left|(\gamma*\nu_s^1)(\xi_2) - (\gamma*\nu_s^2)(\xi_2)\right|, \qquad (3.62)
\end{aligned}$$

where $\operatorname{Hess}\gamma$ denotes the Hessian matrix containing the second derivatives of γ. We used here that $\|\nabla(\gamma*\nu_s^2)\|_\infty \leqslant \|\nabla\gamma\|_\infty$, $\|\operatorname{Hess}(\gamma*\nu_s^2)\|_\infty \leqslant \|\operatorname{Hess}\gamma\|_\infty$ and the fact that $|\psi|_{\mathrm{L}} = \|\nabla\psi\|_\infty$ and $|\nabla\psi|_{\mathrm{L}} = \|\operatorname{Hess}\psi\|_\infty$ for any differentiable function ψ. Note that:

$$\begin{aligned}
\left|(\gamma*\nu_s^1)(\xi_2) - (\gamma*\nu_s^2)(\xi_2)\right| &= \left|\int\gamma(\xi_2 - z)\,d\nu_s^1(z) - \int\gamma(\xi_2 - w)\,d\nu_s^2(w)\right| \\
&\leqslant \int|\gamma(\xi_2 - z) - \gamma(\xi_2 - w)|\;d\tilde{\pi}_s(z,w) \\
&\leqslant \|\nabla\gamma\|_\infty\int|z-w|\;d\tilde{\pi}_s(z,w), \qquad (3.63)
\end{aligned}$$

where $\tilde{\pi}_s \in \Pi(\nu_s^1, \nu_s^2)$ is arbitrary. We emphasize that the bound (3.63) is independent of the choice of ξ_1, ξ_2. Analogously, we have

$$\left|\nabla(\gamma*\nu_s^1)(\xi_2) - \nabla(\gamma*\nu_s^2)(\xi_2)\right| \leqslant \|\operatorname{Hess}\gamma\|_\infty\int|z-w|\;d\tilde{\pi}_s(z,w), \qquad (3.64)$$

for an arbitrary $\tilde{\tilde{\pi}}_s \in \Pi(\nu_s^1, \nu_s^2)$. We choose $\tilde{\tilde{\pi}}_s = \tilde{\pi}_s$. It follows that

$$\begin{aligned}
&\left|F_\theta\left((\gamma * \nu_s^1)(\xi_1)\right) \nabla(\gamma * \nu_s^1)(\xi_1) - F_\theta\left((\gamma * \nu_s^2)(\xi_2)\right) \nabla(\gamma * \nu_s^2)(\xi_2)\right| \\
&\leqslant \left(M_2 \left\| \operatorname{Hess} \gamma \right\|_\infty + M_3 \left\| \nabla \gamma \right\|_\infty^2 \right) \left(|\xi_1 - \xi_2| + \int |z - w| \, d\tilde{\pi}_s(z, w) \right). \qquad (3.65)
\end{aligned}$$

If $\theta = 1$, then similar estimates as in the first term on the right-hand side of (3.62), and as in (3.63) and (3.64) yield

$$\begin{aligned}
&\Big|(\nabla\gamma * [(F_\theta \circ (\gamma * \nu_s^1))\nu_s^1])(\xi_1) \\
&\quad -(\nabla\gamma * [(F_\theta \circ (\gamma * \nu_s^2))\nu_s^2])(\xi_2)\Big| \leqslant M_2 \left\| \operatorname{Hess} \gamma \right\|_\infty |\xi_1 - \xi_2| \\
&\qquad\qquad + M_3 \left\| \nabla \gamma \right\|_\infty^2 \int |z - w| \, d\tilde{\pi}_s(z, w) \\
&\qquad\qquad + M_2 \left\| \operatorname{Hess} \gamma \right\|_\infty \int |z - w| \, d\tilde{\pi}_s(z, w), \qquad (3.66)
\end{aligned}$$

where the same $\tilde{\pi}_s \in \Pi(\nu_s^1, \nu_s^2)$ as in (3.63) is chosen.

We treat the last term in (3.58) as follows:

$$\begin{aligned}
\left|(\mathcal{K} * \nu_s^1)(\xi_1) - (\mathcal{K} * \nu_s^2)(\xi_2)\right| &\leqslant \left|(\mathcal{K} * \nu_s^1)(\xi_1) - (\mathcal{K} * \nu_s^1)(\xi_2)\right| \\
&\quad + \left|(\mathcal{K} * \nu_s^1)(\xi_2) - (\mathcal{K} * \nu_s^2)(\xi_2)\right| \\
&\leqslant |\mathcal{K}|_{\mathrm{L}} \left(|\xi_1 - \xi_2| + \int |z - w| \, d\tilde{\pi}_s(z, w) \right). \qquad (3.67)
\end{aligned}$$

The bound on the second term is obtained like in (3.63).

We combine (3.58), (3.59), (3.60), (3.65), (3.66) and (3.67) to get

$$\begin{aligned}
|\Phi_t^{\nu^1}(x) - \Phi_t^{\nu^2}(y)| &\leqslant (1 + t \left\| \eta \right\|_\infty) |x - y| + t \, |v_0(x) - v_0(y)| \\
&\quad + \int_0^t (M_4 (t - s) + \left\| \eta \right\|_\infty) \, |\Phi_s^{\nu^1}(x) - \Phi_s^{\nu^2}(y)| \, ds \\
&\quad + M_5 \int_0^t (t - s) \int |z - w| \, d\tilde{\pi}_s(z, w) \, ds,
\end{aligned}$$

with M_4 and M_5 as defined in the statement of the lemma. □

We now have all ingredients to prove Theorem 3.3.10.

Proof of Part 1 of Theorem 3.3.10.

Proof. (Existence and uniqueness of solutions). If $M_5 = 0$, then the well-posedness of (3.40) is straightforward. In that case, $F_\theta \circ (\gamma * \mu_t) = 0$ on $\operatorname{supp}\mu_t$ for all t and moreover $\mathcal{K}$ must be constant, so the first equation in (3.40) is independent of μ_t. For each $x \in \operatorname{supp}\mu_0$, the Picard-Lindelöf Theorem guarantees the existence and uniqueness of the motion mapping (as mentioned before). The solution $(\mu_t)_{0\leqslant t\leqslant T}$ is therefore uniquely defined by the push-forward $\mu_t = \Phi_t \# \mu_0$.

If $M_5 \neq 0$, then the well-posedness proof is based on Banach's Fixed Point Theorem. Let $T > 0$ be fixed. Choose $\mathcal{N} \in \mathbb{N}^+$ large enough, such that $T^* := T/\mathcal{N}$ satisfies

$$\kappa_{T^*} := \frac{1}{2}\,(T^*)^2\, M_5\, \exp\left(\|\eta\|_\infty\, T^* + \frac{1}{2}\, M_4\, (T^*)^2\right) < 1. \tag{3.68}$$

Let $j \in \{1, \dots, \mathcal{N}\}$ be fixed. Suppose that $\mu_0^{(j)} \in \mathcal{P}(\mathbb{R}^d)$ and $v_0^{(j)} \in C_b^1(\mathbb{R}^d; \mathbb{R}^d)$ are given. Consider a mapping $\mathcal{F}^{(j)} \colon \nu \mapsto \mu := \mathcal{F}^{(j)}(\nu)$ from the space

$$\mathcal{C}_j := \left\{ \nu \in C([0, T^*]; \mathcal{P}_{r(jT^*)}(\mathbb{R}^d)) : \nu|_{t=0} = \mu_0^{(j)} \right\} \tag{3.69}$$

to itself, where, given ν, the image $\mu_t = (\mathcal{F}^{(j)}\nu)_t$ is defined for all $t \in [0, T^*]$ by

$$\mu_t = [\Phi_t^{(j)}]^\nu \# \mu_0^{(j)}.$$

The motion mapping $[\Phi^{(j)}]^\nu : \mathbb{R}^+ \times \mathbb{R}^d \to \mathbb{R}^d$ solves the following ODE

$$\begin{cases} [\ddot{\Phi}_t^{(j)}]^\nu(x) = -F_\theta\left(\tilde{\rho}_t([\Phi_t^{(j)}]^\nu(x))\right) \nabla\tilde{\rho}_t([\Phi^{(j)}]_t^\nu(x)) \\ \qquad\qquad\qquad -\theta\,(\nabla\gamma * [(F_\theta \circ \tilde{\rho}_t)\nu_t])([\Phi_t^{(j)}]^\nu(x)) \\ \qquad\qquad\qquad -\nabla V\left([\Phi_t^{(j)}]^\nu(x)\right) - \eta\left([\Phi_t^{(j)}]^\nu(x)\right)\, [\dot{\Phi}_t^{(j)}]^\nu(x) \\ \qquad\qquad\qquad +(\mathcal{K} * \nu_t)([\Phi_t^{(j)}]^\nu(x)); \\ \tilde{\rho}_t := \gamma * \nu_t; \\ \Phi_0^\nu(x) = x,\ \dot{\Phi}_0^\nu(x) = v_0^{(j)}(x), \end{cases} \tag{3.70}$$

for all $x \in \operatorname{supp}\mu_0^{(j)}$ and all $t \in (0, T^*]$.

The space $\mathcal{C}_j$ is complete for arbitrary $j \in \{1, \dots, \mathcal{N}\}$ due to Corollary A.4 in Appendix A. Note that a fixed point $\mu^{(j)}$ of this mapping together with the corresponding motion mapping $\Phi^{(j)}$ is a solution of (3.40) on $[0, T^*]$ with initial data $\mu_0^{(j)}$ and $v_0^{(j)}$.
We create a hierarchy of the mappings $\mathcal{F}^{(j)}$ for $j \in \{1, \dots, \mathcal{N}\}$ by defining the initial conditions for $\mathcal{F}^{(j+1)}$ based on the fixed point of $\mathcal{F}^{(j)}$:

$$\begin{aligned} \mu_0^{(j+1)} &:= \mu_{T^*}^{(j)} \\ v_0^{(j+1)} &:= \dot{\Phi}_{T^*}^{(j)} \end{aligned}$$

completed with $\mu_0^{(1)} := \mu_0$ and $v_0^{(1)} := v_0$. We now prove that the mapping $\mathcal{F}^{(j)}$ has a unique fixed point and thus $\mu_{T^*}^{(j)}$ and $\dot{\Phi}_{T^*}^{(j)}$ are well-defined.

For any $\nu \in \mathcal{C}_j$ the image $\mu = \mathcal{F}^{(j)}(\nu)$ exists and is an element of $\mathcal{C}_j$, as we show now. Well-posedness of the motion mapping (for given ν and for each $x \in \operatorname{supp}\mu_0^{(j)}$) follows from the Picard-Lindelöf Theorem (see before), and hence the existence and uniqueness of μ is guaranteed.
The support of the image measure, $\operatorname{supp}\mu_t$, is contained in a ball of radius

$$r(jT^*) = r_0 + jT^*\,\|v_0\|_\infty + \frac{1}{2}(jT^*)^2\,(M_1 + \|\nabla V\|_\infty + \|\mathcal{K}\|_\infty).$$

This is easily checked by use of (3.50) and a recursive relation involving $\|[\dot{\Phi}_{T^*}^{(k)}]^\nu\|_\infty = \|v_0^{(k+1)}\|_\infty$ for each $k \in \{1,\dots,\mathcal{N}-1\}$. Thus, the image μ of our mapping $\mathcal{F}^{(j)}$ is an element of $\mathcal{C}_j$.

Consider two measures $\nu^1, \nu^2 \in \mathcal{C}_j$ and their corresponding images $\mu^1 := \mathcal{F}^{(j)}(\nu^1)$ and $\mu^2 := \mathcal{F}^{(j)}(\nu^2)$. Let $\pi_0 \in \Pi(\mu_0^{(j)}, \mu_0^{(j)})$ be arbitrary. For an arbitrary fixed $t \in [0, T^*]$, define $\pi_t \in \Pi(\mu_t^1, \mu_t^2)$ by

$$\pi_t := \left([\Phi_t^{(j)}]^{\nu^1}, [\Phi_t^{(j)}]^{\nu^2}\right)\#\pi_0.$$

Note that this π_t is a joint representation of μ_t^1 and μ_t^2 for each t. We do not indicate explicitly the dependence on j of π_0, μ^1, μ^2 and π_t since no ambiguity appears. By definition of the push-forward operator and of the Wasserstein distance (see Definitions 3.3.1 and 3.3.3), we have that

$$W_1(\mu_t^1, \mu_t^2) \leqslant \int |z-w|\,d\pi_t(z,w) = \int \left|[\Phi_t^{(j)}]^{\nu^1}(x) - [\Phi_t^{(j)}]^{\nu^2}(y)\right|\,d\pi_0(x,y) \tag{3.71}$$

holds for each $t \in [0, T^*]$. Applied to (3.56), Gronwall's Lemma yields that for each $x, y \in \operatorname{supp}\mu_0^{(j)}$ it holds that

$$\begin{aligned}\left|[\Phi_t^{(j)}]^{\nu^1}(x) - [\Phi_t^{(j)}]^{\nu^2}(y)\right| \leqslant \Bigg[&(1 + t\,\|\eta\|_\infty)\,|x-y| + t\,|v_0^{(j)}(x) - v_0^{(j)}(y)| \\ &+ M_5 \int_0^t (t-s) \int |z-w|\;\tilde{\pi}_s(dz,dw)\,ds\Bigg]\,\exp\left(\|\eta\|_\infty\,t + \frac{1}{2}\,M_4\,t^2\right).\end{aligned} \tag{3.72}$$

We remark that Gronwall's Lemma may be applied, mainly because the term $|v_0^{(j)}(x) - v_0^{(j)}(y)|$ is bounded. One can show this fact using estimates similar to those in the proof of Lemma 3.4.1. Now, we combine (3.71) and (3.72) and obtain

$$\begin{aligned}W_1(\mu_t^1, \mu_t^2) \leqslant \Bigg[&(1 + t\,\|\eta\|_\infty) \int |x-y|\,d\pi_0(x,y) + t \int |v_0^{(j)}(x) - v_0^{(j)}(y)|\,d\pi_0(x,y) \\ &+ M_5 \int_0^t (t-s) \int |z-w|\;d\tilde{\pi}_s(z,w)\,ds\Bigg]\,\exp\left(\|\eta\|_\infty\,t + \frac{1}{2}\,M_4\,t^2\right).\end{aligned} \tag{3.73}$$

The integration with respect to $d\pi_0(x,y)$ disappeared from the third term inside the square brackets, since this term is independent of x and y, and moreover $\int d\pi_0(x,y) = 1$. Recall furthermore that $\tilde{\pi}_s \in \Pi(\nu_s^1, \nu_s^2)$ is arbitrary (and in particular independent of π_0). Thus, choosing a specific π_0 on the right-hand side does not affect the third term. We take

$$\pi_0 := (I \otimes I)\#\mu_0^{(j)},$$

which is the measure concentrated on the diagonal $x = y$ with both marginals equal to $\mu_0^{(j)}$. With some abuse of notation this particular π_0 can also be written as

$$d\pi_0(x,y) := \delta(x-y)d\mu_0^{(j)}(y).$$

For this choice of π_0, we have that

$$\int |x-y|\, d\pi_0(x,y) = 0,$$

and

$$\int |v_0^{(j)}(x) - v_0^{(j)}(y)|\, d\pi_0(x,y) = 0.$$

Only the third term in the square brackets on the right-hand side of (3.73) remains. Within the integral we take the infimum over $\tilde{\pi}_s \in \Pi(\nu_s^1, \nu_s^2)$ for each s independently (which is allowed by Lebesgue's Dominated Convergence Theorem, [Bog07a], Theorem 2.8.1) and continue to estimate:

$$W_1(\mu_t^1, \mu_t^2) \leqslant \frac{1}{2}\, t^2\, M_5\, \exp\left(\|\eta\|_\infty\, t + \frac{1}{2}\, M_4\, t^2\right) \sup_{s\in[0,t]} W_1(\nu_s^1, \nu_s^2).$$

Finally, we take the supremum over $t \in [0, T^*]$:

$$\sup_{t\in[0,T^*]} W_1(\mu_t^1, \mu_t^2) \leqslant \frac{1}{2}\, (T^*)^2\, M_5\, \exp\left(\|\eta\|_\infty\, T^* + \frac{1}{2}\, M_4\, (T^*)^2\right) \sup_{t\in[0,T^*]} W_1(\nu_t^1, \nu_t^2).$$

By the specific choice of T^*, $\mathcal{F}^{(j)}$ is a contraction mapping for each j, since

$$\sup_{t\in[0,T^*]} W_1(\mu_t^1, \mu_t^2) \leqslant \kappa_{T^*} \sup_{t\in[0,T^*]} W_1(\nu_t^1, \nu_t^2),$$

where $\kappa_{T^*} < 1$ by assumption; cf. (3.68). As mentioned underneath (3.70), the space $\mathcal{C}_j$ is a complete metric space for each j due to Corollary A.4 in Appendix A. Banach's Fixed Point Theorem guarantees the existence of a unique fixed point of $\mathcal{F}^{(j)}$ for each j.

Using the construction of $(\mu^{(j)}, \Phi^{(j)})$ on $[0, T^*]$ for $j \in \{1, \ldots, \mathcal{N}\}$, we define a couple (μ, Φ) of a measure and a motion mapping on the interval $[0, T]$ as follows

$$(\mu_t, \Phi_t) := \left(\mu^{(j)}_{t-(j-1)T^*}, \Phi^{(j)}_{t-(j-1)T^*}\right) \qquad \text{if } t \in ((j-1)T^*, jT^*],$$

for each $j \in \{1, \dots, \mathcal{N}\}$.

By construction, we have that

$$(\mu, \Phi) \in C([0,T]; \mathcal{P}_{r(T)}(\mathbb{R}^d)) \times C^2([0,T]; \{\phi : \operatorname{supp}\mu_0 \to \mathbb{R}^d\})$$

and (μ, Φ) uniquely satisfies (3.40) with initial data μ_0 and v_0. □

Proof of Part 2 of Theorem 3.3.10.

Proof. (Convergence of approximate solutions). Note that Part 1 of the proof implies that for all initial measures μ_0 and μ_0^N (for any $N \in \mathbb{N}$) there are corresponding unique solutions (μ, Φ) and (μ^N, Φ^N), respectively. Fix $N \in \mathbb{N}$ and $\pi_0 \in \Pi(\mu_0^N, \mu_0)$ arbitrarily. We use (3.56) with $\nu^1 = \mu^N$ and $\nu^2 = \mu$. Thus $\Phi^{\nu^1} = \Phi^N$ and $\Phi^{\nu^2} = \Phi$. First of all, we observe that

$$|v_0(x) - v_0(y)| \leqslant \|\nabla v_0\|_\infty |x - y|, \tag{3.74}$$

for all $x \in \operatorname{supp}\mu_0^N$ and all $y \in \operatorname{supp}\mu_0$. This estimate holds, since $v_0 \in C_b^1(\mathbb{R}^d; \mathbb{R}^d)$ is given, is defined on the whole of $\mathbb{R}^d$ and has bounded derivative. It is not possible to use a similar estimate in (3.72), because $v_0^{(j)}$ is part of the solution and only defined on $\operatorname{supp}\mu_0^{(j)}$. In general, $\nabla v_0^{(j)}$ might not even be defined. Using the Lipschitz estimate (3.74) and integrating (3.56) against $d\pi_0(x,y)$, we obtain

$$\begin{aligned}\int |\Phi_t^N(x) - \Phi_t(y)|\, d\pi_0(x,y) \leqslant & (1 + t\,(\|\nabla v_0\|_\infty + \|\eta\|_\infty)) \int |x-y|\, d\pi_0(x,y) \\ & + \int_0^t (M_4(t-s) + \|\eta\|_\infty) \int |\Phi_s^N(x) - \Phi_s(y)|\, d\pi_0(x,y)\, ds \\ & + M_5 \int_0^t (t-s) \int |z-w|\; d\tilde{\pi}_s(z,w)\, ds, \end{aligned} \tag{3.75}$$

where we use that the last term is independent of x and y, and the fact that π_0 is a probability measure on $\mathbb{R}^d \times \mathbb{R}^d$. Recall that $\tilde{\pi}_s \in \Pi(\nu_s^1, \nu_s^2) = \Pi(\mu_s^N, \mu_s)$ is arbitrary and in general does not depend on π_0. We now *introduce* an explicit relation between $\tilde{\pi}_s$ and π_0 by choosing

$$\tilde{\pi}_s := (\Phi_s^N, \Phi_s)\#\pi_0 \tag{3.76}$$

for each $s \in [0,T]$. We substitute (3.76) in (3.75) and apply Gronwall's Lemma to obtain

$$\begin{aligned}\int |\Phi_t^N(x) - \Phi_t(y)|\, d\pi_0(x,y) \leqslant & (1 + t\,(\|\nabla v_0\|_\infty + \|\eta\|_\infty)) \int |x-y|\, d\pi_0(x,y) \cdot \\ & \cdot \exp\left(\|\eta\|_\infty t + \frac{1}{2}(M_4 + M_5)\, t^2\right). \end{aligned} \tag{3.77}$$

Using the already defined joint representation $\tilde{\pi}_t = (\Phi_t^N, \Phi_t)\#\pi_0 \in \Pi(\mu_t^N, \mu_t)$, we obtain an estimate like in (3.71). Together with (3.77) this estimate yields the bound

$$W_1(\mu_t^N, \mu_t) \leqslant$$
$$\left((1 + t\,(\|\nabla v_0\|_\infty + \|\eta\|_\infty)) \int |x-y|\, d\pi_0(x,y)\right) \exp\left(\|\eta\|_\infty\, t + \frac{1}{2}\,(M_4 + M_5)\, t^2\right).$$

We take the infimum over $\pi_0 \in \Pi(\mu_0^N, \mu_0)$ on the right-hand side:

$$W_1(\mu_t^N, \mu_t) \leqslant (1+t\,(\|\nabla v_0\|_\infty + \|\eta\|_\infty)) \exp\left(\|\eta\|_\infty\, t + \frac{1}{2}\,(M_4 + M_5)\, t^2\right) W_1(\mu_0^N, \mu_0).$$

Finally, we take the supremum over $t \in [0,T]$ on both sides of the inequality and obtain

$$\sup_{t\in[0,T]} W_1(\mu_t^N, \mu_t) \leqslant$$
$$(1 + T\,(\|\nabla v_0\|_\infty + \|\eta\|_\infty)) \exp\left(\|\eta\|_\infty\, T + \frac{1}{2}\,(M_4 + M_5)\, T^2\right) W_1(\mu_0^N, \mu_0).$$

Hence $W_1(\mu_0^N, \mu_0) \overset{N\to\infty}{\longrightarrow} 0$ implies

$$\sup_{t\in[0,T]} W_1(\mu_t^N, \mu_t) \overset{N\to\infty}{\longrightarrow} 0.$$

The proof is now complete. □

3.5 Comments on Assumptions 3.3.7 and 3.3.8, and the condition (3.47)

In this section, we comment on the assumptions needed for Theorem 3.3.10.

Assumptions on F_θ and γ: We observe that in [LGP98] only $\theta = 0$ is used, and furthermore $\nabla V \equiv 0$, $\eta \equiv 0$ and $\mathcal{K} \equiv 0$. All possible choices of F_0 and γ treated in [LGP98] satisfy Assumption 3.3.7:

1. $F_0(u) = u^\alpha$, for $\alpha \geqslant 0$, satisfies the assumptions for all choices of $\gamma \in C_b^2(\mathbb{R}^d; \mathbb{R}_0^+)$;
2. $F_0(u) = u^\alpha$, for $-1 < \alpha < 0$, satisfies the assumptions if γ is an element of $C_b^2(\mathbb{R}^d; \mathbb{R}^+)$ and satisfies the extra condition $|\nabla\gamma(x)| \leqslant c\,|\gamma(x)|^{-\alpha}$ for all x, for some constant $c > 0$.

The class of admissible pairs (F_0, γ) covered by Assumption 3.3.7 is more general than the class of admissible pairs in [LGP98], where only F_0 of the form $F_0(u) = u^\alpha$ is treated. For instance, in our case any $F_0 \in C_b^1(\mathbb{R}_0^+; \mathbb{R}_0^+)$ (bounded and with bounded derivative) is allowed in combination with an arbitrary $\gamma \in C_b^2(\mathbb{R}^d; \mathbb{R}_0^+)$.

Assumption (3.47) **on convergence of initial data:** Given the initial probability measure μ_0 supported in the closed ball $\overline{B(r_0)}$, we demonstrate here two ways of constructing an approximating sequence of measures $(\mu_0^N)_{N\in\mathbb{N}^+}$.

The first way of constructing μ_0^N is deterministic and has been used in [Bol08]. For simplicity of presentation, we assume $d = 1$ and $\operatorname{supp}\mu_0 \subset [0,1]$. For each $N \in \mathbb{N}^+$, define

$$\mu_0^N := \sum_{i=1}^{N} m_i\, \delta_{\frac{i}{N}-\frac{1}{2N}}, \tag{3.78}$$

where $m_i := \int_{[\frac{i-1}{N},\frac{i}{N})} d\mu_0(x)$, for each $i = 1,\dots,N-1$, and $m_N := \int_{[1-\frac{1}{N},1]} d\mu_0(x)$. It follows that $\sum_i m_i = \int d\mu_0(x) = 1$ and $\mu_0^N \in \mathcal{P}(\mathbb{R})$. Define a map

$$\Psi : [0,1] \to \left\{ \frac{i}{N} - \frac{1}{2N} : 1 \le i \le N \right\}$$

by $\Psi(x) := \frac{i}{N} - \frac{1}{2N}$ if $\frac{i-1}{N} \le x < \frac{i}{N}$ and $\Psi(1) := 1 - \frac{1}{2N}$. For every measurable and bounded function f defined on $[0,1]$, we have that

$$\int\limits_{[0,1]} f(x) d\mu_0^N(x) = \int\limits_{[0,1]} f(\Psi(x))\, d\mu_0(x).$$

Hence, $\mu_0^N = \Psi\#\mu_0$. Note that $|x - \Psi(x)| \leqslant \frac{1}{2N}$ for every $x \in [0,1]$. Therefore,

$$W_1(\mu_0^N,\mu_0) \le \int\limits_{[0,1]} |x-\Psi(x)|\, d\mu_0(x) \le \frac{1}{2N} \int\limits_{[0,1]} d\mu_0(x) = \frac{1}{2N}, \tag{3.79}$$

where we obtain the first inequality by defining $\pi \in \Pi(\mu_0^N,\mu_0)$ as $\pi := (I\times\Psi)\#\mu_0$. This implies that $W_1(\mu_0^N,\mu_0) \overset{N\to\infty}{\longrightarrow} 0$.

This procedure can be generalized to the case $d > 1$ (but with more involved notation). Let $\operatorname{supp}\mu_0 \subset [0,1]^d$ and let $N \in \{k^d : k \in \mathbb{N}^+\}$. Dividing the hypercube $[0,1]^d$ into N equal subcubes, we obtain, similarly as in (3.79), that the convergence rate is $\mathcal{O}(1/\sqrt[d]{N})$.

A second way of constructing μ_0^N is probabilistic and is based on the law of large numbers as was already pointed out in [LGP98]. Suppose that the points X_i, with indices $i \in \{1,\dots,N\}$, are independent identically distributed random variables with the same distribution $\mu_0 \in \mathcal{P}\big(\overline{B(r_0)}\big)$. Let μ_0^N be the empirical measure, defined by

$$\mu_0^N := \frac{1}{N}\sum_{i=1}^{N} \delta_{X_i}.$$

According to [Dud04], Theorem 11.4.1, the sequence (μ_0^N) converges *almost surely* to μ_0. This implies that for *almost every* realization $\bar{X}_1, \bar{X}_2, \dots$ the corresponding sequence

of measures $(\bar{\mu}_0^N) \subset \mathcal{P}(\overline{B(r_0)})$ given by $\bar{\mu}_0^N := 1/N \sum_i \delta_{\bar{X}_i}$, converges in the narrow topology to μ_0. That is,

$$\int_{\overline{B}(r_0)} f(x) d\mu_0^N(x) \to \int_{\overline{B}(r_0)} f(x) d\mu_0(x) \text{ for all } f \in C_b(\overline{B(r_0)}).$$

In fact there is an underlying probability space Ω and $X_i : \Omega \to \overline{B(r_0)}$. Hence μ_0^N is, strictly speaking, a mapping from Ω to $\mathcal{P}(\overline{B(r_0)})$; i.e. $\mu_0^N : \Omega \to \mathcal{P}(\overline{B(r_0)})$. The term 'almost every realization' refers to the fact that the set (in Ω) on which the narrow convergence does *not* hold, has zero probability (with respect to the probability distribution on Ω). In layman's terms, this means that if we draw a random sample $\bar{X}_1, \bar{X}_2, \ldots$, it is 'unlikely' that the corresponding sequence $(\bar{\mu}_0^N)$ does not converge narrowly.

Assume that our random sample did yield such narrowly converging sequence $(\bar{\mu}_0^N)$. Since all $\bar{\mu}_0^N$ are probability measures on a bounded domain $\overline{B(r_0)}$, their first moments are uniformly integrable (i.e. uniformly in N). Consequently, Theorem 7.1.5 in [AGS08] implies that

$$W_1(\bar{\mu}_0^N, \mu_0) \overset{N\to\infty}{\longrightarrow} 0.$$

3.6 Numerical illustration

We illustrate the theoretical convergence result of Theorem 3.3.10 by two simple numerical examples. The first one involves only the first term on the right-hand side of (3.48). We consider both schemes ($\theta = 0$ and $\theta = 1$), in dimension $d = 1$ and $d = 2$. In the second example only the nonlocal interaction term and a drag force in (3.48) are present and we take $d = 2$. We use a leapfrog algorithm – cf. [LRS96] – with a constant timestep. This algorithm is a second-order symplectic integrator, thus the momentum of the system is preserved, when conservative processes are studied.

We assume that the initial measure μ_0 has a density ρ_0 such that $\rho_0(x) = 1$ for all $x \in [0,1]^d$ and $\rho_0(x) = 0$ otherwise. We construct the measure μ_0^N, corresponding to the N-particle approximation, according to (3.78) or its d-dimensional counterpart. Hence, the initial particle configuration is realized for $d = 1$ by equipartitioning the initial domain $[0,1]$ into N intervals. For the two-dimensional examples, the initial domain is the square $[0,1]^2 \subset \mathbb{R}^2$, which we subdivide in N square subcells. Particles are placed initially in the center of each subcell. For both $d = 1$ and $d = 2$, masses are assigned as $m_i = \rho_0(x_i)/N$ for each $i \in \{1, \ldots, N\}$, the factor $1/N$ denoting the length (if $d = 1$) or area (if $d = 2$) of each subcell.
As argued underneath (3.78), the sequence $(\mu_0^N)_{N\in\mathbb{N}^+}$ constructed in this way converges to μ_0 and the convergence rate is $\mathcal{O}(1/\sqrt[d]{N})$. Hence, the corresponding solutions $(\mu^N)_{N\in\mathbb{N}^+}$ converge at the same rate; see the last lines of the proof of Part 2 of Theorem 3.3.10.

The problem involving only the pressure-related force, considers the spontaneous expansion of a gas cloud (initially at rest, $v_0 \equiv 0$) until time $T = 1$, governed by the equation

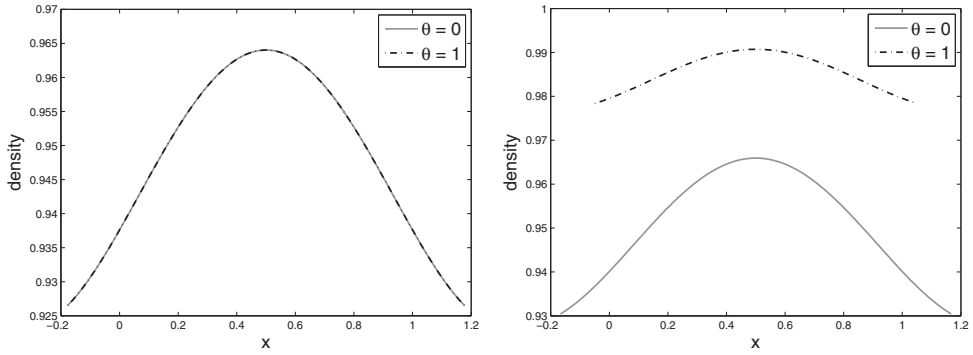

(a) (b)

Figure 3.1: The density $\tilde{\rho}$ at final time $T = 1$ for $N = 2^9$ particles in the system with a pressure term only. Solid grey and dashed black plots refer to the schemes for $\theta = 0$ and $\theta = 1$, respectively. (a): For the exponent $\kappa = 2$ the two schemes coincide. (b): For the exponent $\kappa = 7$ the two schemes give different results.

of state $P(\rho) = c\rho^\kappa$, where c is a parameter and κ is the so-called *polytropic exponent*. We recall that P relates to e via $\partial e/\partial\rho = P/\rho^2$. In dimension $d = 1$, we use a Gaussian regularization function, defined by

$$\gamma(x) := \frac{1}{\sqrt{\pi}} e^{-|x|^2}, \tag{3.80}$$

for all $x \in \mathbb{R}$. We take $c = 1$. In Figure 3.1, results are shown for $\kappa = 2$ and $\kappa = 7$, respectively. Solid grey graphs correspond to the scheme for $\theta = 0$ and dashed black graphs to the scheme $\theta = 1$. The plots show the result for the density $\tilde{\rho}$ at $T = 1$, as obtained for $N = 2^9$ particles.

For $d = 1$, we perform calculations subsequently for $N = 2^k$ particles, where $k \in \{1, \dots, 9\}$, and compute the supremum over time of the Wasserstein distance between subsequent solutions; cf. (3.49). We compute the Wasserstein distance by solving a linear programming problem based on a formulation in terms of optimal transportation. Due to the high computational cost (for large k), we use the following approximation to reduce the number of evaluations of W_1:

$$\sup_{t\in[0,T]} W_1(\mu_t^{2^k}, \mu_t^{2^{k+1}}) \approx \max_{\tau\in I} W_1(\mu_\tau^{2^k}, \mu_\tau^{2^{k+1}}) =: A_{k,k+1}^{(1)}. \tag{3.81}$$

Here,

$$I := \left\{ \frac{jT}{N_W - 1} \,:\, j = 0, \dots, (N_W - 1) \right\} \tag{3.82}$$

and we take $N_W = 10$. For the majority of the computations however, the maximum distance is observed at the final time T.

We estimate numerically the order of convergence q, that is the value of q such that

$$\sup_{t\in[0,T]} W_1(\mu_t^{2^k}, \mu_t) = \mathcal{O}\left(\left(\frac{1}{2^k}\right)^q\right),$$

as $k \to \infty$, where μ_t denotes the limit measure. As mentioned before, $q = 1$ should hold in the one-dimensional case; cf. (3.79). We use the quantity

$$\log_2\left(\frac{A^{(1)}_{k,k+1}}{A^{(1)}_{k+1,k+2}}\right) \tag{3.83}$$

to approximate the value of q. The results (for $\kappa = 2$ and $\kappa = 7$) are given in Table 3.1 and support our theoretical claim.

		$\theta = 0$	$\theta = 1$
k	$\kappa = 2$	$\kappa = 7$	$\kappa = 7$
1	1.0144	1.0119	1.0048
2	1.0035	1.0029	1.0012
3	1.0009	1.0009	1.0001
4	1.0005	0.9999	1.0005
5	0.9998	1.0001	0.9997
6	1.0000	1.0003	0.9991
7	0.9992	1.0008	1.0004

Table 3.1: Estimation of the order of convergence q for the system with only a pressure term, where $d = 1$. The table shows the quantity $\log_2(A^{(1)}_{k,k+1}/A^{(1)}_{k+1,k+2})$, see (3.83), where k refers to the number $N = 2^k$ of particles involved. Note that for $\kappa = 7$ the order of convergence is demonstrated both for $\theta = 0$ and for $\theta = 1$, while for $\kappa = 2$ these two schemes coincide. The values in the table confirm the theoretical result from Theorem 3.3.10 combined with (3.79) stating that the order of convergence is $\mathcal{O}(1/N)$.

There are several points to be mentioned about Figure 3.1 and Table 3.1. First, note that for $\kappa = 2$ the schemes corresponding to $\theta = 0$ and $\theta = 1$ are identical. This is because in this case $\partial e/\partial\rho = \bar{F}' \equiv c$; cf. (3.36). Both for $\theta = 0$ and for $\theta = 1$ the pressure-related force (i.e. the first line of the right-hand side) in (3.38) is $-2c\,\nabla\tilde{\rho}_t$. Table 3.1 implies that in all three cases presented the solution converges in the many-particle limit. However, for $\kappa = 7$ the two schemes do not converge to the *same* limit, as Figure 3.1b shows. As argued in Section 3.2.6, compared to the scheme for $\theta = 0$, the scheme for $\theta = 1$ contains an extra regularization. We only expect the effect of this regularization to vanish (and hence the schemes to coincide) when "$\gamma \to \delta_0$". In this chapter we only treat fixed γ – cf. Remark 3.2.1 – but we will comment on vanishing regularization in the discussion section, Section 3.7.

In two spatial dimensions, the corresponding problem is the expansion of an initially square gas cloud, until time $T = 1$. We include a nonzero velocity field $(v_{0,x}, v_{0,y}) = (-y, x)$.

The same equation of state as in the one-dimensional computation is used, with $\kappa \in \{2, 7\}$. For $d = 2$, the cubic Wendland function – cf. (2.16) in [MR13] – is used, whence for all $x \in \mathbb{R}^2$:

$$\gamma(x) := \begin{cases} \frac{1}{8}(1 + 3|x|/2)(2 - |x|)^3, & |x| \leq 2, \\ 0, & |x| > 2. \end{cases}$$

This choice deviates from (3.80) to illustrate that we can handle γ both with bounded and with unbounded support.

To be able to construct initially a square arrangement of particles, we consider for $d = 2$ a sequence of approximations of the form $N = (2^k)^2$ for $k \in \{1, \dots, 6\}$. Analogous to the case $d = 1$ we approximate the supremum of the wasserstein distance by

$$\sup_{t\in[0,T]} W_1(\mu_t^{4^k}, \mu_t^{4^{k+1}}) \approx \max_{\tau\in I} W_1(\mu_\tau^{4^k}, \mu_\tau^{4^{k+1}}) =: A^{(2)}_{k,k+1}, \tag{3.84}$$

with I given by (3.82). The order of convergence is in this case the value q such that

$$\sup_{t\in[0,T]} W_1(\mu_t^{4^k}, \mu_t) = \mathcal{O}\left(\left(\frac{1}{4^k}\right)^q\right),$$

as $k \to \infty$, where μ_t denotes the limit measure. We estimate q by

$$\frac{1}{2}\log_2\left(\frac{A^{(2)}_{k,k+1}}{A^{(2)}_{k+1,k+2}}\right). \tag{3.85}$$

The d-dimensional counterpart of (3.79) suggests that $q = 1/d$, hence we expect to find $q = 1/2$ here. This claim is supported by Table 3.2. The computational effort for the calculation of the Wasserstein distance makes the investigation of larger k not feasible.

		$\theta = 0$	$\theta = 1$
k	$\kappa = 2$	$\kappa = 7$	$\kappa = 7$
1	0.5078	0.5063	0.5022
2	0.5018	0.5016	0.5005
3	0.5005	0.5003	0.5001
4	0.4988	0.4981	0.5023

Table 3.2: Estimation of the order of convergence q for the system with only a pressure term, where $d = 2$. The table shows the quantity $1/2 \cdot \log_2(A^{(2)}_{k,k+1}/A^{(2)}_{k+1,k+2})$, see (3.85), where k refers to the number $N = 4^k$ of particles involved. As in Table 3.1, there is only one column for $\kappa = 2$ since the schemes for $\theta = 0$ and $\theta = 1$ coincide. The values in the table confirm the theoretical result that the order of convergence is $\mathcal{O}(1/\sqrt{N})$.

The second numerical example considers the nonlocal force and the drag term corresponding to $\mathcal{K}$ and η, respectively. There are no contributions from the pressure and the external potential V. Therefore the problem does not depend on θ nor on γ. We take

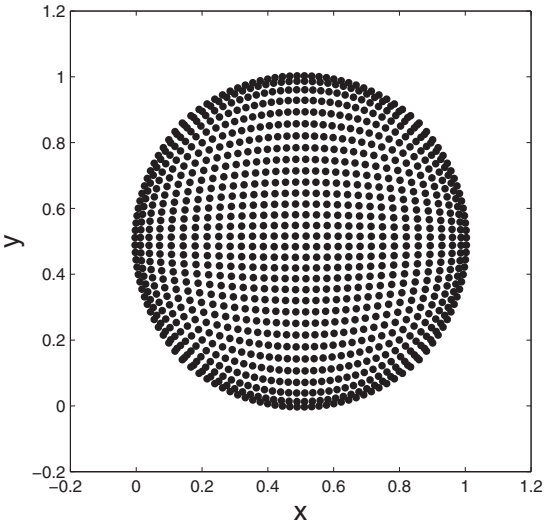

Figure 3.2: Configuration of $N = 4^5 = 1024$ particles at final time $T = 100$ corresponding to the nonlocal force and drag term. The drag coefficient is $\eta \equiv 10$.

$\mathcal{K}$ such that it is the gradient of the Morse potential (2.6) with parameters $C_a = 2.0$, $C_r = 1.5$, $l_a = 1.0$ and $l_r = 2.0$. To enforce the required C_b^1-regularity of $\mathcal{K}$, we included a short-range regularization around the origin to the potential K. A side-effect is that automatically self-interactions are no longer present.
We take a constant drag coefficient $\eta \equiv 10$. Initially the particles are at rest. Figure 3.2 shows the configuration at final time $T = 100$. We verified numerically that at that time an equilibrium has been reached. Due to the relatively large drag coefficient, one still recognizes the square grid of the original configuration in the equilibrium state. Compare the plot for $\eta \equiv 0.1$ in [EZvdLD15], which exhibits a different pattern.

We use (3.85) to estimate the order of convergence. The theoretical prediction $q = 1/2$ is supported by the results in Table 3.3. The deviation from the predicted value is small compared to Tables 3.1 and 3.2, whence the values in Table 3.3 are given with higher precision.

3.7 Discussion

In this chapter we answered the question how to derive particle schemes in a systematic way, by proposing a three-step procedure. These three steps are: the formulation of the equations in terms of measures (including a regularization of the density); substitution of a discrete measure; and the application of the principle of least action. We have seen that the equation of motion we obtain for the particle system depends on the order in which regularization and the principle of least action are applied. We also showed how this procedure works if there are nonconservative forces.

k	$1/2 \cdot \log_2(A^{(2)}_{k,k+1}/A^{(2)}_{k+1,k+2})$
1	0.5000000074
2	0.5000000017
3	0.4999999994
4	0.4999999967

Table 3.3: Estimation of the order of convergence q for the system with a nonlocal force term, where $d = 2$. The table shows the quantity $1/2 \cdot \log_2(A^{(2)}_{k,k+1}/A^{(2)}_{k+1,k+2})$, see (3.85), where k refers to the number $N = 4^k$ of particles involved. The values in the table confirm the theoretical prediction that the order of convergence is $\mathcal{O}(1/\sqrt{N})$.

The second question that we asked concerns the convergence of the particle schemes in the limit $N \to \infty$.
The proof in Section 3.4 for the existence and uniqueness of a solution to the scheme required a fixed-point argument (on a concatenation of sufficiently small time-intervals). The argument relies on the completeness of the space of measure-valued trajectories that we use. In the introduction of this thesis (see Section 1.1), we presented a semigroup approach for finding a solution. This is a one-directional approach where the equation of motion is solved for the motion mapping and the solution measure follows by push-forward. This approach does not readily extend to the situation in which the right-hand side is measure-dependent. Therefore, in this chapter an alternative method was required.

In this chapter we provided a proof for the convergence of the particle solutions to the solution of the *regularized* continuum equation. The convergence result (in the 1-Wasserstein distance) is not restricted to particle approximations. The theorem provides convergence of solutions given a general sequence of corresponding initial measures approximating the initial condition of the limit problem.

The result of Theorem 3.3.10 however does not state:

- whether the approximations corresponding to $\theta = 0$ and $\theta = 1$, respectively, actually converge to the same limit solution. Our computations show (see Figure 3.1) that this is certainly not the case for fixed γ, except for the trivial case $\kappa = 2$ in which the schemes coincide.

- whether the limit $N \to \infty$ in any of the two cases $\theta = 0$ or $\theta = 1$ is actually like the 'real physics'. To investigate this, in principle one would need to consider the limit $\gamma \rightharpoonup \delta_0$ and prove in which sense the solutions of the regularized equation converge to the solutions of the original Euler-like equation, e.g. (1.40). As said before, this is beyond the scope of this chapter.

The latter point refers to a situation in which first the limit $N \to \infty$ is taken and afterwards the limit $\gamma \rightharpoonup \delta_0$. A more favourable approach (also from a numerical point of view) would be to have the convergence $N \to \infty$ and $\gamma \rightharpoonup \delta_0$ simultaneously. This is an issue only if the pressure-related term is present. This is the only part where regularization is needed.

In the SPH literature, the smoothing function γ is typically written as W_h, where the subscript h denotes explicitly the dependence on the parameter h called *smoothing length*; see Remark 3.2.1. The convergence $\gamma \rightharpoonup \delta_0$ should now be read as $W_h \rightharpoonup \delta_0$ as $h \to 0$. Let V_0 denote a representative volume assigned initially to each particle based on the initial configuration. In Section 3.6, V_0 corresponded to either a subinterval of $[0,1]$ with length $1/N$ (for $d=1$), or a square subcell of $[0,1]^d$ with area $1/N$ (for $d=2$). In a general bounded domain, V_0 typically scales as $V_0 \sim 1/N$. It is common practice to achieve $h \to 0$ simultaneously with $N \to \infty$ by taking $h = \sigma \sqrt[d]{V_0}$, with parameter $1.2 \leqslant \sigma \leqslant 1.5$, cf. (4.2) in [Mon05].

In [EZvdLD15] we illustrate the use of h variable (that is, variable with N, but not in time). The numerical investigations presented there show that convergence of solutions as $N \to \infty$ may be expected also if $h \sim 1/\sqrt[d]{N}$. Moreover, the difference between the schemes for $\theta = 0$ and $\theta = 1$ is shown to be smaller. A suggestion for further research is to investigate theoretically the convergence of solutions as $N \to \infty$ for N-dependent h.

This chapter connects to the rest of this thesis in the following way:

- This chapter proposes a particle-based numerical scheme for a measure-valued evolution equation and proves convergence of the scheme. The same principle is applicable to more general problems. Both second-order and first-order (see below) equations of motion can be dealt with. In Section 4.5 of Chapter 4 we use a similar particle-based method.

- The pressure-related term does not appear in the rest of the thesis. Moreover, we mostly deal with a first-order equation of motion. If we assume the pressure-related force to be absent, the first-order equation can be obtained, at least formally, by taking $\eta \equiv 1/\varepsilon$, and replacing V and $\mathcal{K}$ by V/ε and $\mathcal{K}/\varepsilon$, respectively. If now $\varepsilon \to 0$, an equation of the form

$$\dot{\Phi}_t(x) = -\nabla V(\Phi_t(x)) + (\mathcal{K} * \mu_t)(\Phi_t(x)),$$

  is obtained. The convolution term appears throughout this thesis. The term involving ∇V is relevant in the sense that it can be used to incorporate μ-independent parts in the velocity. The limit $\varepsilon \to 0$ is like the overdamped limit introduced in Section 1.3. In this case this limit corresponds to the arrow leading from 'hydrodynamic' to 'Fokker-Planck' in Figure 1.2.

- The crucial estimates in this chapter are given in Lemmas 3.4.1 and 3.4.3. Similar expression can be obtained analogously for the first-order equation of motion (see

previous point); in fact the calculations are much simpler. The final estimates are:

$$|\Phi_t(x)| \leqslant |x| + t\,(\|\nabla V\|_\infty + \|\mathcal{K}\|_\infty), \text{ and}$$

$$|\Phi_t^{\nu^1}(x) - \Phi_t^{\nu^2}(y)| \leqslant |x-y| + (|\nabla V|_{\mathrm{L}} + |\mathcal{K}|_{\mathrm{L}}) \int_0^t |\Phi_s^{\nu^1}(x) - \Phi_s^{\nu^2}(y)|\, ds$$

$$+ |\mathcal{K}|_{\mathrm{L}} \int_0^t \int |z-w|\, d\tilde{\pi}(z,w)\, ds,$$

where $\tilde{\pi}_s \in \Pi(\nu_s^1, \nu_s^2)$ for each $s \in [0,t]$. The latter estimate uses (3.59) – without the factor $(t-s)$ in the integral – and (3.67). *Mutatis mutandis*, the rest of the convergence proof in this chapter still holds for a first-order equation of motion.

Chapter 4

Flux boundary conditions: prescribed velocity

As was formulated Section 1.7.3, our guiding mathematical question in this chapter is:

What is the correct way to define zero-flux or general flux boundary conditions in terms of measures?

We investigate the well-posedness and approximation of mild solutions to a class of linear transport equations on the unit interval $[0,1]$ endowed with a linear discontinuous production term, formulated in the space $\mathcal{M}([0,1])$ of finite Borel measures. A particular choice for this production term describes the process of gating away mass at a certain rate from a zone close to the boundary. We demonstrate a detailed boundary layer analysis by which we are able to pass to the singular limit where thickness of the layer vanishes. We obtain not only a suitable concept of solutions to the chosen measure-valued evolution problem, but also derive convergence rates for the approximation procedure and get insight in the structure of flux boundary conditions for the limit problem.

4.1 Introduction

Consider the measure-valued equation

$$\frac{\partial}{\partial t}\mu_t + \frac{\partial}{\partial x}(v\mu_t) = f \cdot \mu_t, \qquad \text{on } [0,1], \tag{4.1}$$

where $f : [0,1] \to \mathbb{R}$ is a *piecewise bounded Lipschitz function* with finitely many discontinuities. That is, f has finitely many points of discontinuity and the restriction of f to each of the intervals of continuity is bounded Lipschitz. We assume that the velocity field $v : [0,1] \to \mathbb{R}$ is bounded Lipschitz and interpret a v that points outwards at either one of the boundary points $x = 0$ or $x = 1$ (i.e. $v(0) < 0$ or $v(1) > 0$) as describing the presence

This chapter is based on joint work with Sander Hille and Adrian Muntean, published in Comptes Rendus Mathématique [EHM14] and in revised form in Journal of Differential Equations [EHM15a].

of a 'sticking boundary' (cf. [Tai04]) at that point. Alternatively, other researchers (e.g. [GJMC12]) have replaced v by a discontinuous $\hat{v}$ that equals v on $(0,1)$, but is set to zero at boundary points where v points outwards.

If f in (4.1) were bounded Lipschitz, then the proof of well-posedness would follow standard arguments for semilinear equations (e.g. see [Paz83, Lun95, CH99]), except for the technical point that $\mathcal{M}([0,1])$ is not complete for the natural norms used in measure-valued equations (see also [CCC13]). These are the equivalent Fortet-Mourier norm $\|\cdot\|^*_{\mathrm{FM}}$ and dual bounded Lipschitz norm $\|\cdot\|^*_{\mathrm{BL}}$. More details on these norms follow in Section 4.1.1. In our setting, with piecewise bounded Lipschitz f, the perturbation map

$$F_f : \mathcal{M}([0,1]) \to \mathcal{M}([0,1]) : \mu \mapsto f \cdot \mu$$

is not Lipschitz, but (mildly) discontinuous. Nevertheless, continuous dependence on initial conditions still holds, which is shown using a different approach.

In Section 1.7.3 we already introduced the particular choice $f(x) = -a\mathbb{1}_{\{1\}}(x)$, with $a > 0$, by which (4.1) simplifies to

$$\frac{\partial}{\partial t}\mu_t + \frac{\partial}{\partial x}(v\mu_t) = -a\mu_t(\{1\})\delta_1. \tag{4.2}$$

On the right-hand side, δ_1 denotes the Dirac measure at 1.

Our approach to equation (4.1) differs from [AI05, GLMC10, CCGU12, GJMC12] that use appropriate weak solution concepts. The notion of solution to (4.1) introduced here is that of *measure-valued mild solution*. We interpret equation (4.1) as expressing formally that the semigroup $(P_t)_{t\geqslant 0}$ of operators on $\mathcal{M}([0,1])$ associated to mass transport along characteristics defined by the velocity field v is perturbed by F_f. A mild solution is then a continuous map $t \mapsto \mu_t$ from an interval $[0,T]$ into $\overline{\mathcal{M}}([0,1])_{\mathrm{BL}}$, which is the completion of $\mathcal{M}([0,1])]$ equipped with $\|\cdot\|^*_{\mathrm{BL}}$, that satisfies the variation of constants formula

$$\mu_t = P_t\mu_0 + \int_0^t P_{t-s}F_f(\mu_s)\,ds, \qquad 0 \leqslant t \leqslant T. \tag{4.3}$$

Although F_f is discontinuous, the map $s \mapsto F_f(\mu_s)$ is Bochner measurable if the map $s \mapsto \mu_s$ is Bochner measurable. Thus, integral equation (4.3) is well-defined. In our solution concept we need to include the technical condition that the total variation function $t \mapsto \|\mu_t\|_{\mathrm{TV}}$ of the solution must be bounded on $[0,T]$. The solution concept is introduced in more detail in Section 4.2.2.

There are several reasons *why* we consider mild solutions rather than weak solutions. First of all, the mild formulation in terms of the variation of constants formula (4.3) follows directly from a probabilistic interpretation, as we will see in Section 4.6. Therefore the choice for mild solutions is justified by a modelling argument. Secondly, usually uniqueness of weak solutions cannot be expected to hold, while mild solutions are unique when the perturbation is Lipschitz. Even in our particular setting, where the perturbation

has discontinuities, we obtain uniqueness of the mild solution. This is one of the main results of this chapter. In the works [AI05, GLMC10, CCGU12, GJMC12] a specific weak solution is constructed that is precisely the mild solution that we obtain by different means. Finally, there is a technical advantage of using mild solutions. Most of our estimates are in terms of $\|\cdot\|^*_{\mathrm{BL}}$. Our calculations are therefore often simpler, because the test functions do not appear explicitly. Moreover, our estimates are in fact uniform over test functions in a bounded set.

Some preliminaries on measure theory are introduced in Section 4.1.1. Afterwards, Section 4.2.1 derives fundamental estimates for the movement of single individuals in the domain, i.e. the *individualistic flow*, where there is no absorption yet, but sticking boundaries only. After recalling basic semigroup estimates, we state and prove a technical lemma concerning regularization by averaging over orbits (see Lemma 4.2.3) that will play a crucial role in obtaining the main results. The concept of mild solution formulated in the space $\mathcal{M}([0,1])$ of finite Borel measures is introduced in Section 4.2.2. In Section 4.3, we prove the well-posedness of our problem and we address the approximation of the mild solution in Section 4.4. There, the piecewise bounded Lipschitz function f in (4.1) is replaced by a bounded Lipschitz function f_ε that differs from f on an ε-thin neighbourhood of each discontinuity.

Well-posedness together with Lyapunov stability of measure-valued solutions (for suitable metrics) imply that particle dynamics and continuum solutions stay close once initial conditions are sufficiently close. We investigate this resemblance and the order of convergence numerically in Section 4.5. Note that we do not prove Lyapunov stability in this chapter; the result on continuous dependence on initial data given in Proposition 4.3.8 only holds on compact time intervals $[0,T]$. This result does not generalize from $[0,T]$ to $[0,\infty)$, because the involved proportionality constant grows exponentially in T. A different technique, not involving Gronwall's Lemma, would be needed to obtain Lyapunov stability.

The chapter closes with a section that provides a probabilistic underpinning of our solution concept (Section 4.6) and the proof of the central lemma, Lemma 4.2.3 (Section 4.7).

4.1.1 Preliminaries on measures

If S is a topological space, we denote by $\mathcal{M}(S)$ the space of finite Borel measures on S and $\mathcal{M}^+(S)$ the convex cone of positive measures included in it. For $x \in S$, δ_x denotes the Dirac measure at x. Let

$$\langle \mu, \phi \rangle := \int_S \phi \, d\mu \tag{4.4}$$

denote the natural pairing between measures $\mu \in \mathcal{M}(S)$ and bounded measurable functions ϕ. Recall Definition 3.3.1, that generalizes trivially from $\mathcal{P}(\mathbb{R}^d)$ to $\mathcal{M}(S)$ in the following way: the *push-forward* or *image measure* of μ under Borel measurable $\Phi : S \to S$ is the measure $\Phi\#\mu$ defined on Borel sets $E \subset S$ by

$$(\Phi\#\mu)(E) := \mu\big(\Phi^{-1}(E)\big). \tag{4.5}$$

It is easily verified that $\langle \Phi \# \mu, \phi \rangle = \langle \mu, \phi \circ \Phi \rangle$; cf. (3.41).

We denote by $C_b(S)$ the Banach space of real-valued bounded continuous functions on S equipped with the supremum norm $\|\cdot\|_\infty$. The *total variation norm* $\|\cdot\|_{\mathrm{TV}}$ on $\mathcal{M}(S)$ is given by

$$\|\mu\|_{\mathrm{TV}} := \sup\left\{ \langle \mu, \phi \rangle \;\middle|\; \phi \in C_b(S),\ \|\phi\|_\infty \leqslant 1 \right\}.$$

It follows immediately that for $\Phi : S \to S$ continuous, $\|\Phi \# \mu\|_{\mathrm{TV}} \leqslant \|\mu\|_{\mathrm{TV}}$.
The total variation norm is too strong for our application, since $\|\delta_x - \delta_y\|_{\mathrm{TV}} = 2$ if $x \neq y$. The natural topology to consider is the weak topology induced by $C_b(S)$ through the pairing (4.4). In this topology $x \mapsto \delta_x : S \to \mathcal{M}^+(S)$ is continuous.

In our setting, S is a Polish space (separable, completely metrizable topological space; cf. [Dud04], p. 344). It is well-established (cf. [Dud66, Dud74]) that in this case the weak topology *on the positive cone* $\mathcal{M}^+(S)$ is metrizable by a metric derived from a norm, e.g. the Fortet-Mourier norm or the Dudley norm. The latter is also called the *dual bounded Lipschitz norm*, that we shall introduce now. To that end, let d be a metric on S that metrizes the topology, such that (S, d) is separable and complete. Let $\mathrm{BL}(S, d) = \mathrm{BL}(S)$ be the vector space of real-valued bounded Lipschitz functions on (S, d). For $\phi \in \mathrm{BL}(S)$, let

$$|\phi|_{\mathrm{L}} := \sup\left\{ \frac{|\phi(x) - \phi(y)|}{d(x, y)} \;\middle|\; x, y \in S,\ x \neq y \right\}$$

be its Lipschitz constant. This is a generalization of the Euclidean case defined in (3.43). Now

$$\|\phi\|_{\mathrm{BL}} := \|\phi\|_\infty + |\phi|_{\mathrm{L}} \tag{4.6}$$

defines a norm on $\mathrm{BL}(S)$ for which it is a Banach space [FM53, Dud66]. In fact it makes $\mathrm{BL}(S)$ a Banach algebra for pointwise product of functions:

$$\|\phi \cdot \psi\|_{\mathrm{BL}} \leq \|\phi\|_{\mathrm{BL}}\, \|\psi\|_{\mathrm{BL}}. \tag{4.7}$$

Alternatively, one may define on $\mathrm{BL}(S)$ the equivalent norm[1]

$$\|\phi\|_{\mathrm{FM}} := \max\bigl(\|\phi\|_\infty, |\phi|_{\mathrm{L}}\bigr).$$

Let $\|\cdot\|^*_{\mathrm{BL}}$ be the dual norm of $\|\cdot\|_{\mathrm{BL}}$ on the dual space $\mathrm{BL}(S)^*$, i.e. for any $x^* \in \mathrm{BL}(S)^*$:

$$\|x^*\|^*_{\mathrm{BL}} := \sup\{ |\langle x^*, \phi \rangle| \mid \phi \in \mathrm{BL}(S),\ \|\phi\|_{\mathrm{BL}} \leqslant 1 \}.$$

The map $\mu \mapsto I_\mu$ with $I_\mu(\phi) := \langle \mu, \phi \rangle$ defines a linear *embedding* of $\mathcal{M}(S)$ into $\mathrm{BL}(S)^*$ ([Dud66], Lemma 6). Thus $\|\cdot\|^*_{\mathrm{BL}}$ induces a norm on $\mathcal{M}(S)$, which is denoted by the same symbols. It is called the dual bounded Lipschitz norm or Dudley norm. Generally, $\|\mu\|^*_{\mathrm{BL}} \leqslant \|\mu\|_{\mathrm{TV}}$. For positive measures the norms coincide:

$$\|\mu\|^*_{\mathrm{BL}} = \mu(S) = \|\mu\|_{\mathrm{TV}} \qquad \text{for all } \mu \in \mathcal{M}^+(S). \tag{4.8}$$

[1] See Lemma C.1 in Appendix C.

One may also consider the restriction to $\mathcal{M}(S)$ of the dual norm $\|\cdot\|^*_{\mathrm{FM}}$ of $\|\cdot\|_{\mathrm{FM}}$ on $\mathrm{BL}(S)^*$. This yields an equivalent norm[2] on $\mathcal{M}(S)$ that is called the Fortet-Mourier norm (see e.g. [LMS02, Zah00]):

$$\|\mu\|^*_{\mathrm{BL}} \leqslant \|\mu\|^*_{\mathrm{FM}} \leqslant 2\|\mu\|^*_{\mathrm{BL}}. \tag{4.9}$$

It also satisfies $\|\mu\|^*_{\mathrm{FM}} \leqslant \|\mu\|_{\mathrm{TV}}$, so (4.8) holds for $\|\cdot\|^*_{\mathrm{FM}}$ too. Moreover (cf. [HW09a], Lemma 3.5), for any $x, y \in S$,

$$\|\delta_x - \delta_y\|^*_{\mathrm{BL}} = \frac{2d(x,y)}{2+d(x,y)} \leqslant \min(2, d(x,y)) = \|\delta_x - \delta_y\|^*_{\mathrm{FM}}. \tag{4.10}$$

The space $\mathcal{M}(S)$ is not complete for $\|\cdot\|^*_{\mathrm{BL}}$ generally. We denote by $\overline{\mathcal{M}}(S)_{\mathrm{BL}}$ its completion, viewed as closure of $\mathcal{M}(S)$ within $\mathrm{BL}(S)^*$. The following lemma shows that $\mathcal{M}^+(S)$ is closed.

Lemma 4.1.1. *If S is a Polish space, then $\mathcal{M}^+(S)$ is closed for $\|\cdot\|^*_{\mathrm{BL}}$.*

Proof. Since S is complete, Theorem 3.8 of [HW09b] implies that $\mathcal{M}^+_s(S)$ is closed in $\|\cdot\|^*_{\mathrm{BL}}$. This is the space of positive, finite and *separable* Borel measures. Because S is separable, $\mathcal{M}^+_s(S) = \mathcal{M}^+(S)$ holds trivially (see p. 23 in [Wor10]). □

As a consequence (see Lemma A.2 in Appendix A), $\mathcal{M}^+(S)$ is complete for $\|\cdot\|^*_{\mathrm{BL}}$.

The $\|\cdot\|^*_{\mathrm{BL}}$-norm topology on $\mathcal{M}^+(S)$ coincides with the restriction of the weak topology $\sigma(\mathcal{M}(S), C_b(S))$; see [Dud66], Theorem 12. In Section 4.2 and further, we choose for S the unit interval $[0,1]$. In this case $\mathcal{M}(S) = C_b^*(S)$ by the Riesz Representation Theorem; cf. [Tay06], Theorem 13.7, where it should be noted that on any Polish space finite Borel measures are Radon measures, due to [Bog07b], Theorem 7.1.7. Hence, the restriction of the $\|\cdot\|^*_{\mathrm{BL}}$-norm topology to $\mathcal{M}^+(S)$ coincides with the weak-$*$ topology.

Note that $\mathrm{BL}(S,d)$ varies with the metric d, hence $\|\cdot\|^*_{\mathrm{BL}}$ on $\mathcal{M}(S)$ also depends on d and so does $\overline{\mathcal{M}}(S)_{\mathrm{BL}}$.

The $\|\cdot\|^*_{\mathrm{BL}}$-norm is convenient also for integration. In Appendix B some technical results that are used in this chapter have been collected. The continuity of the map $x \mapsto \delta_x : S \to \mathcal{M}^+(S)_{\mathrm{BL}}$ together with (B.2) yields the identity

$$\mu = \int_S \delta_x \, d\mu(x) \tag{4.11}$$

as Bochner integral in $\mathcal{M}(S)_{\mathrm{BL}}$. This observation will essentially link 'continuum' ('μ') and particle description ('δ_x') for our linear equation on $[0,1]$; cf. also (4.24) and Proposition 4.3.6.

[2] See Lemma C.2 in Appendix C.

4.2 Model formulation and solution concept

Throughout the remainder of the chapter, we take $S = [0,1]$ and $f : [0,1] \to \mathbb{R}$ is a piecewise bounded Lipschitz function as defined in Section 4.1. The velocity field $v : [0,1] \to \mathbb{R}$ is bounded Lipschitz.

4.2.1 Mass transport and averaging along characteristics

We assume that a single particle ('individual') is moving in the domain $[0,1]$ deterministically, described by the differential equation for its position $x(t)$ at time t:

$$\begin{cases} \dot{x}(t) = v(x(t)), \\ x(0) = x_0. \end{cases} \tag{4.12}$$

A solution to (4.12) is unique, it exists for time up to reaching the boundary 0 or 1 and depends continuously on initial conditions. Let $x(\,\cdot\,; x_0)$ be this solution and I_{x_0} be its maximal interval of existence. Define

$$\tau_\partial(x_0) := \sup I_{x_0} \in [0, \infty],$$

i.e. $\tau_\partial(x_0)$ is the time at which the solution starting at x_0 reaches the boundary (if it happens) when x_0 is an interior point. Note that $\tau_\partial(x_0) = 0$ when x_0 is a boundary point where v points outwards, while $\tau_\partial(x_0) > 0$ when x_0 is a boundary point where v vanishes or points inwards.

The *individualistic stopped flow* on $[0,1]$ associated to v is the family of maps $\Phi_t : [0,1] \to [0,1]$, $t \geqslant 0$, defined by

$$\Phi_t(x_0) := \begin{cases} x(t; x_0), & \text{if } t \in I_{x_0}, \\ x(\tau_\partial(x_0); x_0), & \text{otherwise.} \end{cases} \tag{4.13}$$

Below we collect important properties of the family of maps $(\Phi_t)_{t \geqslant 0}$ in a series of lemmas.

Lemma 4.2.1. *$(\Phi_t)_{t \geq 0}$ is a semigroup of Lipschitz transformations of $[0,1]$. Moreover,*

(i) $|\Phi_t|_{\mathrm{L}} \leqslant e^{|v|_{\mathrm{L}} t}$ for $t \geqslant 0$.

(ii) For any $t, s \in \mathbb{R}_0^+$,

$$\sup_{x \in [0,1]} |\Phi_t(x) - \Phi_s(x)| \leqslant \|v\|_\infty \, |t - s|. \tag{4.14}$$

Proof. (i): A quick approach to the stated result is the following: extend $v : [0,1] \to \mathbb{R}$ to $\bar{v} : \mathbb{R} \to \mathbb{R}$ by putting $\bar{v}(x) := v(0)$ if $x \leqslant 0$ and $\bar{v}(x) := v(1)$ if $x \geqslant 1$. Then $\bar{v}$ is a bounded Lipschitz extension of v such that $\|\bar{v}\|_\infty = \|v\|_\infty$ and $|\bar{v}|_{\mathrm{L}} = |v|_{\mathrm{L}}$. Let $\bar{x}(t; x_0)$ be the unique (global) solution to (4.12) with v replaced by $\bar{v}$ with initial condition $x_0 \in \mathbb{R}$ and $\bar{\Phi}_t : \mathbb{R} \to \mathbb{R}$ the associated solution semigroup. That is, $\bar{\Phi}_t(x_0) := \bar{x}(t; x_0)$. A classical argument involving Gronwall's Lemma yields (i) for $\bar{\Phi}_t$ instead of Φ_t. Now, for $x_0 \in [0,1]$,

$$\Phi_t(x_0) = \min\big(\max(\bar{\Phi}_t, 0), 1\big).$$

Thus $|\Phi_t|_{\mathrm{L}} \leqslant |\bar{\Phi}_t|_{\mathrm{L}}$, using e.g. [Dud66], Lemma 4.
(ii): Let $t, s \in I_{x_0}$. Without loss of generality, assume that $t > s$.

$$|x(t) - x(s)| = |\int_0^t v(x(\sigma))\,d\sigma - \int_0^s v(x(\sigma))\,d\sigma| \leqslant \int_s^t |v(x(\sigma))|\,d\sigma$$
$$\leqslant \|v\|_\infty\,(t-s). \tag{4.15}$$

If both $t, s \in \mathbb{R}_0^+$ are not in I_{x_0}, then inequality (4.15) is trivially satisfied. Suppose now that $s \in I_{x_0}$, while t is not. Then $t > \tau_\partial(x_0)$, $\tau_\partial(x_0) \in I_{x_0}$ and

$$|x(t) - x(s)| = |x(\tau_\partial(x_0)) - x(s)| \leqslant \|v\|_\infty\,(\tau_\partial(x_0) - s),$$

according to (4.15). Clearly $\tau_\partial(x_0) - s \leqslant t - s$. The estimates are independent of $x_0 \in [0,1]$. Thus we obtain (4.14). □

We define $P_t : \mathcal{M}([0,1]) \to \mathcal{M}([0,1])$ by means of the push-forward under Φ_t: for all $\mu \in \mathcal{M}([0,1])$,

$$P_t\mu := \Phi_t \# \mu = \mu \circ \Phi_t^{-1}; \tag{4.16}$$

cf. (4.5) and (1.5). Clearly, P_t maps positive measures to positive measures and P_t is mass preserving on positive measures. Since the maps Φ_t, $t \geqslant 0$, form a semigroup, so do the maps P_t in the space $\mathcal{M}([0,1])$. That is, $(P_t)_{t\geqslant 0}$ is a *Markov semigroup* on $\mathcal{M}[0,1]$ (cf. [LMS02]). One has

$$\|P_t\mu\|_{\mathrm{TV}} \leqslant \|\mu\|_{\mathrm{TV}} \tag{4.17}$$

for general $\mu \in \mathcal{M}([0,1])$.

Lemma 4.2.2. *Let $\mu \in \mathcal{M}([0,1])$ and $t, s \in \mathbb{R}^+$. Then*

(i) $\|P_t\mu - P_s\mu\|_{\mathrm{BL}}^* \leqslant \|v\|_\infty\,\|\mu\|_{\mathrm{TV}}\,|t-s|$.

(ii) $\|P_t\mu\|_{\mathrm{BL}}^* \leqslant \max(1, |\Phi_t|_{\mathrm{L}})\,\|\mu\|_{\mathrm{BL}}^* \leqslant e^{|v|_{\mathrm{L}}t}\|\mu\|_{\mathrm{BL}}^*$.

Proof. For all $\phi \in \mathrm{BL}([0,1])$,

$$|\,\langle P_t\mu - P_s\mu, \phi\rangle\,| = |\,\langle \mu, \phi\circ\Phi_t - \phi\circ\Phi_s\rangle\,| \leqslant \|\mu\|_{\mathrm{TV}}\,\|\phi\circ\Phi_t - \phi\circ\Phi_s\|_\infty$$
$$\leqslant \|\mu\|_{\mathrm{TV}}\,|\phi|_{\mathrm{L}} \sup_{x\in[0,1]} |\Phi_t(x) - \Phi_s(x)| \leqslant \|\mu\|_{\mathrm{TV}}\,|\phi|_{\mathrm{L}}\,\|v\|_\infty\,|t-s|,$$

where we used Lemma 4.2.1(ii) in the last inequality. For the operator norm of P_t on $\mathcal{M}([0,1])_{\mathrm{BL}}$, use that for any $\phi \in \mathrm{BL}([0,1])$,

$$|\langle P_t\mu, \phi\rangle| = |\langle \mu, \phi\circ\Phi_t\rangle| \leqslant \|\mu\|_{\mathrm{BL}}^*\,\|\phi\circ\Phi_t\|_{\mathrm{BL}} \leqslant \|\mu\|_{\mathrm{BL}}^*\,\big(\|\phi\|_\infty + |\phi|_{\mathrm{L}}|\Phi_t|_{\mathrm{L}}\big).$$

The statement of the lemma follows, due to Lemma 4.2.1(i). □

For any bounded measurable function g on $[0,1]$ and $t \geqslant 0$, define the average over partial orbits under the flow Φ_t as the function $g_t^\Phi : [0,1] \to \mathbb{R}$ given by

$$g_t^\Phi(x) := \int_0^t g(\Phi_s(x))\, ds. \tag{4.18}$$

Clearly,

$$|g_t^\Phi(x) - g_{t'}^\Phi(x)| \leqslant \|g\|_\infty \cdot |t - t'|, \tag{4.19}$$

so $t \mapsto g_t^\Phi(x)$ is Lipschitz for any $x \in [0,1]$.

The following lemma is crucial for establishing the continuous dependence on initial conditions as stated in Proposition 4.3.8.

Lemma 4.2.3 (Regularization by averaging over orbits)**.** *Let $(\Phi_t)_{t\geqslant 0}$ be the individualistic stopped flow associated to the velocity field v. Let g be a piecewise bounded Lipschitz function on $[0,1]$ such that $v(x) \neq 0$ at any point of discontinuity of g. Then g_t^Φ is a bounded Lipschitz function on $[0,1]$ for any $t \geqslant 0$. Moreover,*

$$\sup_{0\leqslant s\leqslant t} |g_s^\Phi|_{\mathrm{L}} < \infty. \tag{4.20}$$

The proof is given in a separate section, Section 4.7, towards the end of this chapter.

Recall that we assume that v is bounded Lipschitz, hence continuous, on the *entire* interval $[0,1]$. We do not replace v by a function that is zero at boundary points where v points outwards. So, the conditions of Lemma 4.2.3 allow for the situation that g has a discontinuity at the boundary. This is a case of particular interest in view of a 'flux' boundary condition in a measure-valued formulation. See Section 4.4, Example 4.4.3, for further discussion of this point.

4.2.2 Mild solutions

Measure-valued equations on $\mathbb{R}^+$ or $\mathbb{R}^d$ of the form (4.1), among others, have been studied in e.g. [CCC13, GLMC10], where a concept of *weak solution* to the associated Cauchy problem was introduced and subsequently existence of such weak solution and continuous dependence on initial data was proven. [GJMC12] considers (in Section 3.1) a situation that is similar to ours by considering a measure-valued transport equation on a finite interval $[0, x^*]$ as in (4.1) with $f = 0$ in which the velocity field v is piecewise bounded Lipschitz, continuous at 0 with $v(0) > 0$ and $v(x) = 0$ at any point of discontinuity, including the other boundary point x^*. There, again the weak solution concept is employed (cf. [GJMC12], Definition 3.4, and references provided).

In this chapter and the next (Chapter 5), we use the concept of *measure-valued mild solution* to the Cauchy problem associated to equation (4.1) in the spirit of the semigroup approach to semilinear evolution equations (e.g. [Paz83, Lun95, CH99]). That is, we interpret the operator $\mu \mapsto -\frac{\partial}{\partial x}(v\mu)$ as generator of a strongly continuous semigroup in

$\overline{\mathcal{M}}([0,1])_{\mathrm{BL}}$: the semigroup $(P_t)_{t\geqslant 0}$ of mass transport along characteristics associated to the velocity field v that we defined in Section 4.2.1. Equation (4.1) is then viewed as perturbation of this semigroup by means of $F_f : \mu \mapsto f \cdot \mu$, which is defined on the dense subspace $\mathcal{M}([0,1])$ of $\overline{\mathcal{M}}([0,1])_{\mathrm{BL}}$ only. Generally, F_f is not $\|\cdot\|^*_{\mathrm{BL}}$-continuous, unless $f \in \mathrm{BL}([0,1])$. It is unclear whether F_f is a densely-defined closed linear map. So 'standard' perturbation results cannot be readily applied.

Moreover, we have to adapt slightly the classical concept of mild solution, since we are interested in measure-valued solutions while the Banach space $\overline{\mathcal{M}}([0,1])_{\mathrm{BL}}$ also contains points that are not measures, as closure of $\mathcal{M}([0,1])$ in $\mathrm{BL}([0,1])^*$.

Definition 4.2.4. *A* measure-valued mild solution *to the Cauchy-problem associated to* (4.1) *on* $[0,T]$ *with initial value* $\nu \in \mathcal{M}([0,1])$ *is a continuous map* $\mu : [0,T] \to \mathcal{M}([0,1])_{\mathrm{BL}}$ *that is* $\|\cdot\|_{\mathrm{TV}}$*-bounded and that satisfies the variation of constants formula*

$$\mu_t = P_t\,\nu \;+\; \int_0^t P_{t-s} F_f(\mu_s)\,ds \qquad \text{for all } t \in [0,T]. \tag{4.21}$$

Remark 4.2.5. The map $s \mapsto F_f(\mu_s)$ is typically not continuous. It is Bochner measurable though: there exist $f_n \in \mathrm{BL}([0,1])$ such that $f_n \to f$ pointwise while $\sup_n \|f_n\|_\infty < \infty$. Each map $s \mapsto F_{f_n}(\mu_s)$ is continuous, hence Bochner measurable, and $s \mapsto F_f(\mu_s)$ is the pointwise limit of $s \mapsto F_{f_n}(\mu_s)$. Consequently, $s \mapsto P_{t-s}F_f(\mu_s)$ is Bochner measurable and the integral in (4.21) is well-defined as Bochner integral in $\overline{\mathcal{M}}([0,1])_{\mathrm{BL}}$.

Remark 4.2.6. The condition of $\|\cdot\|_{\mathrm{TV}}$-boundedness also appears in [CCC13]. It cannot be deduced generally from the assumed continuity of μ. Although $C := \{\mu_t \mid t \in [0,T]\} \subset \mathcal{M}([0,1])_{\mathrm{BL}}$ is compact, this does not imply that $\sup_{0\leqslant t\leqslant T} \|\mu_t\|_{\mathrm{TV}} < \infty$, unless $C \subset \mathcal{M}^+([0,1])$. One can prove (for a Polish state space S), that if for every $K \subset \mathcal{M}(S)_{\mathrm{BL}}$ compact, $\sup_{\mu\in K} \|\mu\|_{\mathrm{TV}} < \infty$, then $(\mathcal{M}(S), \|\cdot\|_{\mathrm{TV}})$ is linearly isomorphic to $\overline{\mathcal{M}}(S)_{\mathrm{BL}}$, using [Hil05], Proposition 3.2. This is 'rarely' the case, see [HW09b], Theorem 3.11.

Remark 4.2.7. As was already mentioned in Section 4.1, integral equation (4.21) arises naturally from a probabilistic description of the system; see Section 4.6.

4.3 Well-posedness for a discontinuous perturbation

In this section we consider the problem of existence, uniqueness and continuous dependence on initial conditions for measure-valued mild solutions to (4.1). Due to failure of (Lipschitz) continuity of F_f the standard arguments using Picard iterations and Gronwall's Lemma cannot be used. In Chapter 5 we will revert to these standard arguments, though; cf. the results in Section 5.2.2 and Remark 5.4.4.

Lemma 4.3.1. *For each* $\nu \in \mathcal{M}([0,1])$ *and piecewise bounded Lipschitz* $f : [0,1] \to \mathbb{R}$ *the following estimate holds:*

$$\|F_f(\nu)\|_{\mathrm{TV}} \leqslant \|f\|_\infty \,\|\nu\|_{\mathrm{TV}}.$$

Proof. Define a sequence $(f_n)_{n\in\mathbb{N}} \subset C_b([0,1])$ such that f_n converges pointwise to f and $\|f_n\|_\infty \to \|f\|_\infty$ as $n \to \infty$. For any $\phi \in C_b([0,1])$ we have that

$$|\langle F_{f_n}(\nu), \phi\rangle| = |\langle \nu, f_n \cdot \phi\rangle| \leqslant \|f_n\|_\infty \|\phi\|_\infty \|\nu\|_{\mathrm{TV}},$$

hence

$$\|F_{f_n}(\nu)\|_{\mathrm{TV}} \leqslant \|f_n\|_\infty \|\nu\|_{\mathrm{TV}}$$

holds for all $n \in \mathbb{N}$. A uniform bound on $\|f_n\|_\infty$ exists, since $\|f_n\|_\infty \to \|f\|_\infty$. Moreover, f_n converges to f pointwise, so we can apply Lebesgue's Dominated Convergence Theorem (see [Bog07a], Theorem 2.8.1 and Remark 3.1.5 about signed measures) to obtain

$$\langle F_f(\nu), \phi\rangle = \lim_{n\to\infty} \langle F_{f_n}(\nu), \phi\rangle$$

for all $\phi \in C_b([0,1])$. Therefore

$$|\langle F_f(\nu), \phi\rangle| = \lim_{n\to\infty} |\langle F_{f_n}(\nu), \phi\rangle| \leqslant \lim_{n\to\infty} \|f_n\|_\infty \|\phi\|_\infty \|\nu\|_{\mathrm{TV}} = \|f\|_\infty \|\phi\|_\infty \|\nu\|_{\mathrm{TV}},$$

from which the statement of the lemma follows. □

Proposition 4.3.2 (Uniqueness)**.** *Equation* (4.1) *has at most one measure-valued mild solution.*

Proof. Let μ and $\hat{\mu} \in C([0,T], \mathcal{M}([0,1])_{\mathrm{BL}})$ be measure-valued mild solutions to (4.1). Then $\|\mu_t\|_{\mathrm{TV}}$ and $\|\hat{\mu}_t\|_{\mathrm{TV}}$ are bounded on $[0,T]$. According to Proposition B.2, the function $s \mapsto \|\mu_s - \hat{\mu}_s\|_{\mathrm{TV}}$ is measurable. Moreover, it is bounded on $[0,T]$ by assumption, hence L^1. Then again by Proposition B.2,

$$\|\mu_t - \hat{\mu}_t\|_{\mathrm{TV}} \leqslant \int_0^t \big\|P_{t-s}[F_f(\mu_s) - F_f(\hat{\mu}_s)]\big\|_{\mathrm{TV}}\, ds \leqslant \int_0^t \big\|F_f(\mu_s) - F_f(\hat{\mu}_s)\big\|_{\mathrm{TV}}\, ds, \quad (4.22)$$

where the second inequality follows from (4.17). We substitute the result of Lemma 4.3.1 with $\nu = \mu_s - \hat{\mu}_s$ in the integrand of (4.22) and obtain

$$\|\mu_t - \hat{\mu}_t\|_{\mathrm{TV}} \leqslant \|f\|_\infty \cdot \int_0^t \|\mu_s - \hat{\mu}_s\|_{\mathrm{TV}}\, ds. \quad (4.23)$$

Grownwall's Lemma yields $\|\mu_t - \hat{\mu}_t\|_{\mathrm{TV}} = 0$ for all $0 \leqslant t \leqslant T$. □

Corollary 4.3.3. *There exists at most one measure-valued mild solution to* (4.1) *in* $C([0,T], \mathcal{M}^+([0,1])_{\mathrm{BL}})$.

Remark 4.3.4. In many applications (e.g. crowd or population dynamics) only positive solutions are interpretable, hence of major interest.

Remark 4.3.5. Technically, for the application of Proposition B.2 in the proof of Proposition 4.3.2 it is only required that $t \mapsto \|\mu_t\|_{\mathrm{TV}}$ is an L^1-function. However, if this seemingly weaker condition than $\|\cdot\|_{\mathrm{TV}}$-boundedness holds, then an argument similar to (4.22)–(4.23) and application of Gronwall's Lemma yields that $t \mapsto \|\mu_t\|_{\mathrm{TV}}$ must be bounded on $[0,T]$.

Since we deal with a transport problem without diffusion, there is no 'smoothing effect' in the dynamics in the interior of the interval $[0,1]$. Therefore we expect Dirac masses to stay Dirac masses. These move according to P_t. The latter acts simply on Dirac masses: $P_t\delta_x = \delta_{\Phi_t(x)}$. Therefore one may try as particular solution to (4.21) with $\mu_0 = \varepsilon_x(0)\delta_x$:

$$\mu_t = \varepsilon_x(t)\delta_{\Phi_t(x)}. \tag{4.24}$$

Substitution of (4.24) into (4.21) yields, after evaluation of the measures on the Borel set $\{\Phi_t(x)\}$ and by use of (B.2):

$$\varepsilon_x(t) = \varepsilon_x(0) + \int_0^t \varepsilon_x(s) f(\Phi_s(x))\, ds. \tag{4.25}$$

Equation (4.25) is solved by the continuous (Lipschitz) function

$$\varepsilon_x(t) = \varepsilon_x(0)\exp\Big(\int_0^t f(\Phi_s(x))\, ds\Big) = \varepsilon_x(0)\exp(f_t^\Phi(x)).$$

See Lemma 4.2.3 for the notation used.
Any initial measure μ_0 is a superposition of Dirac masses, according to (4.11). Therefore we obtain the following existence result and integral representation for the unique globally existing mild solution to (4.1):

Proposition 4.3.6 (Existence)**.** *Let $f : [0,1] \to \mathbb{R}$ be a piecewise bounded Lipschitz function such that $v(x) \neq 0$ at any point x of discontinuity of f. Then for each $\mu_0 \in \mathcal{M}([0,1])$ there exists a continuous and locally $\|\cdot\|_{\mathrm{TV}}$-bounded solution $\mu : \mathbb{R}^+ \to \mathcal{M}([0,1])_{\mathrm{BL}}$ to* (4.21) *defined by*

$$\mu_t := \int_{[0,1]} \exp\Big(\int_0^t f(\Phi_s(x))\, ds\Big)\cdot \delta_{\Phi_t(x)}\, d\mu_0(x) = \int_{[0,1]} \exp(f_t^\Phi(x))\cdot\delta_{\Phi_t(x)}\, d\mu_0(x) \tag{4.26}$$

as Bochner integral in $\overline{\mathcal{M}}([0,1])_{\mathrm{BL}}$. It satisfies $\|\mu_t\|_{\mathrm{TV}} \leqslant e^{\|f\|_\infty t}\|\mu_0\|_{\mathrm{TV}}$. Moreover, μ is locally Lipschitz:

$$\|\mu_t - \mu_{t'}\|^*_{\mathrm{BL}} \leqslant \|\mu_0\|_{\mathrm{TV}}\cdot\big(\|f\|_\infty + \|v\|_\infty\big)\cdot e^{\|f\|_\infty \max(t,t')}\cdot|t-t'|. \tag{4.27}$$

Proof. Due to Lemma 4.2.3, the integrand in (4.26) is a bounded continuous function from $[0,1]$ into $\mathcal{M}^+([0,1])_{\mathrm{BL}}$. Thus for $\mu_0 \in \mathcal{M}^+([0,1])$ the Bochner integral exists, with value in $\mathcal{M}^+([0,1])$, because this cone is closed (cf. Corollary 8 in [DU77]). For $\mu_0 \in \mathcal{M}([0,1])$ the integral yields a *measure* in $\mathcal{M}([0,1]) \subset \overline{\mathcal{M}}([0,1])_{\mathrm{BL}}$, by using the Jordan decomposition $\mu_0 = \mu_0^+ - \mu_0^-$ (see [Hal59], p. 123 for more details on this decomposition). So $\mu_t \in \mathcal{M}([0,1])$ for all t.
Next we prove that μ_t defined by (4.26) satisfies (4.27). So let $t, t' \in \mathbb{R}^+$. We may

assume $t > t'$. Then

$$\begin{aligned}\|\mu_t - \mu_{t'}\|_{\mathrm{BL}}^* &\leqslant \int_{[0,1]} \big\|\exp(f_t^\Phi(x)) \cdot \delta_{\Phi_t(x)} - \exp(f_{t'}^\Phi(x)) \cdot \delta_{\Phi_{t'}(x)}\big\|_{\mathrm{BL}}^* \, d|\mu_0|(x) \\ &\leqslant \int_{[0,1]} \exp(f_t^\Phi(x)) \big\|\delta_{\Phi_t(x)} - \delta_{\Phi_{t'}(x)}\big\|_{\mathrm{BL}}^* \, d|\mu_0|(x) \\ &\quad + \int_{[0,1]} \big|\exp(f_t^\Phi(x)) - \exp(f_{t'}^\Phi(x))\big| \, d|\mu_0|(x).\end{aligned}$$

According to (4.19),

$$\big|\exp(f_t^\Phi(x)) - \exp(f_{t'}^\Phi(x))\big| \leqslant \|f\|_\infty e^{\|f\|_\infty \max(t,t')} \cdot |t - t'|.$$

Using (4.10) and Lemma 4.2.1(ii), we obtain

$$\big\|\delta_{\Phi_t(x)} - \delta_{\Phi_{t'}(x)}\big\|_{\mathrm{BL}}^* \leqslant |\Phi_t(x) - \Phi_{t'}(x)| \leqslant \|v\|_\infty \cdot |t - t'|.$$

Now (4.27) simply follows. □

Corollary 4.3.7. *For every $\mu_0 \in \mathcal{M}^+([0,1])$ there exists a unique mild solution to* (4.1) *that is in $\mathcal{M}^+([0,1])$ for all time.*

Proof. The statement of this corollary follows from the observation (cf. the proof of Proposition 4.3.6) that if $\mu_0 \in \mathcal{M}^+([0,1])$ then the right-hand side of (4.26) is in $\mathcal{M}^+([0,1])$ for all $t \geqslant 0$. □

The classical argument with Gronwall's Inequality to obtain continuous dependence on initial conditions (cf. Corollary 5.2.5) fails in this setting, because the perturbation is not Lipschitz continuous. Instead we use the crucial observation made in Lemma 4.2.3.

Proposition 4.3.8 (Continuous dependence on initial conditions)**.** *Assume that $f : [0,1] \to \mathbb{R}$ is a piecewise bounded Lipschitz function such that $v(x) \neq 0$ at any point x of discontinuity of f. Then for each $T \geqslant 0$, there exists $C_T > 0$ such that for all initial values $\mu_0, \mu_0' \in \mathcal{M}([0,1])$ the corresponding $\|\cdot\|_{\mathrm{TV}}$-bounded mild solutions μ and μ' to* (4.21) *satisfy*

$$\|\mu_t - \mu_t'\|_{\mathrm{BL}}^* \leqslant C_T \|\mu_0 - \mu_0'\|_{\mathrm{BL}}^* \tag{4.28}$$

for all $t \in [0,T]$.

Proof. Let $\phi \in \mathrm{BL}([0,1])$ and $t \geqslant 0$. According to Lemma 4.2.3, f_t^Φ is a bounded Lipschitz function on $[0,1]$. Hence so is $x \mapsto \exp(f_t^\Phi(x))$. According to the representation (4.26), we have

$$|\,\langle \mu_t - \mu_t', \phi\rangle\,| = |\,\big\langle \mu_0 - \mu_0', (\phi \circ \Phi_t) \cdot (\exp \circ f_t^\Phi)\big\rangle\,|.$$

Because $(\mathrm{BL}([0,1]), \|\cdot\|_{\mathrm{BL}})$ is a Banach algebra for pointwise multiplication of functions, cf. (4.7),

$$\begin{aligned}|\,\langle \mu_t - \mu_t', \phi\rangle\,| &\leqslant \|\mu_0 - \mu_0'\|_{\mathrm{BL}}^* \cdot \|\phi \circ \Phi_t\|_{\mathrm{BL}} \|\exp \circ f_t^\Phi\|_{\mathrm{BL}} \\ &\leqslant \|\mu_0 - \mu_0'\|_{\mathrm{BL}}^* \cdot \max(1, |\Phi_t|_{\mathrm{L}}) \|\phi\|_{\mathrm{BL}} \cdot e^{\|f\|_\infty t}(1 + |f_t^\Phi|_{\mathrm{L}}).\end{aligned}$$

We take the supremum over ϕ in the unit bal of $\mathrm{BL}([0,1])$ and use Lemma 4.2.1(i) and (4.20) to conclude that there exists $C_T < \infty$ such that (4.28) holds for all $0 \leqslant t \leqslant T$. □

4.4 Approximation by regularization

Equation (4.21) involving the piecewise bounded Lipschitz function f can be considered (formally) as a limit of a sequence of equations with f replaced by $f_n \in \mathrm{BL}([0,1])$, a 'regularization' of f, such that $f_n \to f$ as $n \to \infty$ in suitable sense, e.g. pointwise. Here, we investigate how mild solutions $\mu^{(n)}$ to (4.1) for f_n relate to the solution μ associated to the limiting piecewise bounded Lipschitz f discussed in the previous section.

Throughout this section, fix the bounded Lipschitz velocity field v on $[0,1]$ and let f be a piecewise bounded Lipschitz function on $[0,1]$ such that the set of discontinuities of f is disjoint from the set of zeros of v. Let $f_n \in \mathrm{BL}([0,1])$ such that $f_n \to f$ pointwise on $[0,1]$. Let $\mu_0 \in \mathcal{M}([0,1])$ and let $\mu^{(n)}$ be the unique mild solution to (4.1) associated to f_n and μ the solution associated to f, both with initial value μ_0. These unique solutions exist due to the results presented in Section 4.3.

Lemma 4.4.1. *Suppose there exists an $M \geqslant 0$ such that $\|f_n\|_\infty \leqslant M$ for all n. Then*

$$\|\mu_t^{(n)} - \mu_t\|_{\mathrm{BL}}^* \leqslant e^{Mt} \int_{[0,1]} \int_0^t \big|f_n(\Phi_s(x)) - f(\Phi_s(x))\big| \, ds \, d|\mu_0|(x). \tag{4.29}$$

In particular, $\mu_t^{(n)}$ converges to μ_t in $\mathcal{M}([0,1])_{\mathrm{BL}}$ as $n \to \infty$ for every $t \geqslant 0$.

Proof. First observe that $\|f\|_\infty \leqslant M$. Let $\phi \in \mathrm{BL}([0,1])$. Using the representation (4.26) for the mild solutions $\mu^{(n)}$ and μ, we obtain

$$\begin{aligned}\left|\left\langle \mu_t^{(n)} - \mu_t, \phi \right\rangle\right| &\leqslant \int_{[0,1]} \left|\exp\big((f_n)_t^\Phi(x)\big) - \exp\big(f_t^\Phi(x)\big)\right| \cdot |\phi(\Phi_t(x))| \, d|\mu_0|(x) \\ &\leqslant \|\phi\|_\infty e^{Mt} \int_{[0,1]} \big|(f_n)_t^\Phi(x) - f_t^\Phi(x)\big| d|\mu_0|(x).\end{aligned}$$

We obtain (4.29) by taking the supremum over ϕ in the unit ball. Lebesgue's Dominated Convergence Theorem then yields the latter statement, because of the pointwise convergence of f_n to f and the assumed uniform upper bound on all f_n. □

Lemma 4.4.1 and inspection of the double integral in equation (4.26) in particular, indicate that further properties of the convergence of $\mu^{(n)}$ to μ depend in a delicate way on the interplay between the way the approximating sequence (f_n) relates to f, the initial condition and properties of the flow $(\Phi_t)_{t \geqslant 0}$, such as uniformity of convergence on compact time intervals or the rate of convergence. We show now that a particular type of regularization of f provides approximating sequences $(f_n) \subset \mathrm{BL}([0,1])$ that yield uniform convergence on compact intervals together with an upper bound for the rate of convergence that holds for any initial condition in $\mathcal{M}([0,1])$.

Observe that there exist $f_n \in \mathrm{BL}([0,1])$ such that $f_n \to f$ pointwise and the sets

$$\Delta_n := \{x \in [0,1] \ : \ f_n(x) \neq f(x)\}$$

are such that $|\Delta_n| \to 0$ as $n \to \infty$, where $|\cdot|$ denotes Lebesgue measure of the set. Because the set of discontinuities of f is disjoint from the set of zeros for v, there exists such approximating sequences such that each difference set Δ_n is a union of finitely many open intervals where each interval contains precisely one point of discontinuity of f and the velocity field v is bounded away from zero on this interval, uniformly in n. Moreover, if $\sup_n \|f_n\|_\infty < \infty$, then we call such a sequence (f_n) a *regularly approximating sequence*.

Proposition 4.4.2. *Let (f_n) be a regularly approximating sequence for f, with difference sets Δ_n and uniform upper bound $M := \sup_n \|f_n\|_\infty$. Then there exists $C > 0$ such that*

$$\|\mu_t^{(n)} - \mu_t\|_{\mathrm{BL}}^* \leqslant 2CMe^{Mt} \cdot |\Delta_n|.$$

In particular, $\mu_t^{(n)}$ converges to μ_t uniformly on compact time intervals, at the same rate as $|\Delta_n| \to 0$ when $n \to \infty$.

Proof. Starting from (4.29) we obtain

$$\begin{aligned}\|\mu_t^{(n)} - \mu_t\|_{\mathrm{BL}}^* &\leqslant e^{Mt} \int_{[0,1]} \int_0^t \big|f_n(\Phi_s(x)) - f(\Phi_s(x))\big| \cdot \mathbb{1}_{\Delta_n}(\Phi_s(x))\, ds\, d|\mu_0|(x) \\ &\leqslant e^{Mt} \cdot 2M \int_{[0,1]} \int_0^t \mathbb{1}_{\Delta_n}(\Phi_s(x))\, ds\, d|\mu_0|(x). \end{aligned} \tag{4.30}$$

The inner integral in (4.30) is the time that the orbit under the flow $(\Phi_t)_{t\geqslant 0}$ starting at x spends in Δ_n. It is bounded from above by $(\inf_{x\in\Delta_n} |v(x)|)^{-1}|\Delta_n|$. Since (f_n) is a regularly approximating sequence, there exists $C > 0$ such that

$$\sup_n \big(\inf_{x\in\Delta_n} |v(x)|\big)^{-1} \leqslant C.$$

Thus,

$$\|\mu_t^{(n)} - \mu_t\|_{\mathrm{BL}}^* \leqslant 2Me^{Mt} \cdot \|\mu_0\|_{\mathrm{TV}} \cdot C|\Delta_n|.$$

The statement on uniform convergence and rate of convergence immediately follows. □

Example 4.4.3. Consider the situation where the velocity field $v \in \mathrm{BL}([0,1])$ satisfies $v(1) > 0$ and $f(x) = -a\,\mathbb{1}_{\{1\}}$, with $a > 0$. That is, in the interior of the unit interval no mass is removed or added, while mass that has accumulated at the boundary point 1 is removed at a rate a. The function f is discontinuous, but piecewise bounded Lipschitz, clearly. A sequence of regularizers for f may be defined by the sequence $(f_n) \subset \mathrm{BL}([0,1])$ given by $f_n(x) := -a[n(x - (1 - \frac{1}{n}))]^+$, where $[\,\cdot\,]^+$ denotes the positive part of the argument. That is,

$$f_n(x) := \begin{cases} 0, & \text{for } x \in [0, 1 - \frac{1}{n}); \\ -an(x - (1 - \frac{1}{n})), & \text{for } x \in [1 - \frac{1}{n}, 1]. \end{cases} \tag{4.31}$$

It is easy to see that $-a \leqslant f_n(x) \leqslant 0$, so $\|f_n\|_\infty \leqslant a$ and

$$\|f_n\|_{\mathrm{BL}} = \|f_n\|_\infty + |f_n|_{\mathrm{L}} = a(1+n). \tag{4.32}$$

Moreover, $\Delta_n = (1-1/n, 1]$ and $|\Delta_n| = 1/n$. Note that $(1-1/n, 1]$ is *open* in $[0,1]$. When n is taken sufficiently large, v is bounded away from zero on Δ_n, so (f_n) as defined above is a regularly approximating sequence for f. In effect, it realizes a family of systems in which there is a small boundary layer near 1, of thickness $1/n$, in which already mass is removed at rate a.
Proposition 4.4.2 predicts that the solutions $\mu^{(n)}$ corresponding to the regularized perturbation $f_n \in \mathrm{BL}([0,1])$ converge to the solution μ corresponding to the discontinuous perturbation f at rate $\mathcal{O}(1/n)$ for the norm $\|\cdot\|^*_{\mathrm{BL}}$.

In the next section we provide numerical support for the convergence rate given in Example 4.4.3.

4.5 Numerical approximations

We consider absolutely continuous and discrete initial data, leading *grosso modo* to an evolution in terms of a PDE and a system of ODEs, respectively. For the absorption of mass we consider both the regularization (boundary layer) and the limit process. We use the corresponding solutions to verify the order of convergence stated in Proposition 4.4.2 (in general) and Example 4.4.3 (specifically for the setting of this example).
Absorption is prescribed by f_n as defined in (4.31). For brevity and convenience, in the sequel we assume the limit case to be incorporated in this notation, i.e. we allow for $n = \infty$ and define then $f_\infty := f = -a\,\mathbb{1}_{\{1\}}$. As before v is bounded Lipschitz and for simplicity we let it satisfy $v(0) > 0$ and $v(1) > 0$. In fact, we take $v > 0$ everywhere in this section.

4.5.1 Two models

Let $\rho_0 : [0,1] \to \mathbb{R}^+$ be such that $\int_0^1 \rho_0(x)\,dx = 1$ and define the associated measure $\bar{\mu}_0$ by $d\bar{\mu}_0 := \rho_0 d\lambda$. Note that $\bar{\mu}_0$ is a probability measure on $[0,1]$, by definition of ρ_0.

Model 1 We consider our model equation (4.21) completed with initial data $\mu_0 = \bar{\mu}_0$. Because of the choice of ρ_0, the model simplifies to a linear transport equation for the density ρ. Due to the definition of the individualistic flow (4.13), mass accumulates at $x = 1$, as v points outward there. We keep track of the mass at $x = 1$, a quantity called $\nu = \nu(t)$, the time-derivative of which is related to the flux of ρ at $x = 1$. For some $n \in \mathbb{N}^+ \cup \{\infty\}$ we solve

$$\begin{cases} \dfrac{\partial \rho}{\partial t} + \dfrac{\partial}{\partial x}(\rho v) = f_n \rho, & \text{on } (0,1), \\ \rho(0,\cdot) = \rho_0, \\ \dfrac{d\nu}{dt} = \rho(t,1)\, v(1) - a\nu(t). \end{cases} \tag{4.33}$$

Since $v > 0$ on $[0,1]$, we use an upwind scheme – cf. e.g. Chapter 13 of [MRtT05]. At $x = 0$, we need to provide a boundary condition. The definition (4.16) of $(P_t)_{t\geqslant 0}$ by means of a push-forward mapping suggests that there should be no influx of mass at $x = 0$, because initially there is no mass located outside $[0,1]$. The boundary condition is therefore $\rho(t,0)v(0) \leqslant 0$ which simplifies, for strictly positive v, to $\rho(t,0) = 0$ for all times $t \geqslant 0$.

Model 2 We consider a particle system that is the discrete counterpart of (4.33). Note that both models are instances of the general measure-valued model (4.21) in their own right. Given a discrete initial measure, we know that the solution is a discrete measure for all time (see Section 4.3, Proposition 4.3.6 in particular). Once we have provided an initial measure $\mu_0 = \sum_{i=1}^N \alpha_i(0)\delta_{x_i(0)}$ (for some fixed N), we search for solutions $\mu = \sum_{i=1}^N \alpha_i(t)\delta_{x_i(t)}$. Particularly, we take $\alpha_i(0) = 1/N$ for all $i = 1,\dots,N$, while $\{x_i(0)\}_{i=1}^N$ consists of N independent random positions, distributed according to $\bar{\mu}_0$. The evolution of the positions $\{x_i(t)\}_{i=1}^N$ is deterministic, dictated by Φ_t in (4.13). The masses α_i satisfy

$$\frac{d\alpha_i}{dt} = f_n(x_i)\,\alpha_i, \tag{4.34}$$

for all $i \in \{1,\dots,N\}$, where $n \in \mathbb{N}^+ \cup \{\infty\}$.

The particles move without interactions, which implies that the numerics are relatively 'cheap'. To trace the evolution of the particles, we use a forward Euler scheme.

4.5.2 Evolution of mass within $[0,1)$ and at 1

We specify

$$\rho_0(x) := \begin{cases} 4x, & 0 \leqslant x \leqslant \dfrac{1}{2}, \\ 4-4x, & \dfrac{1}{2} < x \leqslant 1, \end{cases}$$

and

$$v(x) := \frac{3}{4} + 2(x-\frac{1}{2})^2 \qquad \text{for all } x \in [0,1].$$

Moreover, we take $a = 1/2$, and $N = 25000$ particles.

We first compare the solutions for the absolutely continuous and discrete initial measures described in Section 4.5.1. For the discrete measure, we derive an approximate density by splitting $[0,1)$ (excluding 1) in 100 intervals, and dividing the total mass in any interval by its length. In our graphs this associated density is indicated by 'av.', since mass is averaged over space.

See Figure 4.1 for the time evolution of the limit case (in which the boundary layer has vanished, "$n = \infty$"). Some features must be noted. First of all, we observe a deformation of the initial density profile as time proceeds, due to the fact that v is not

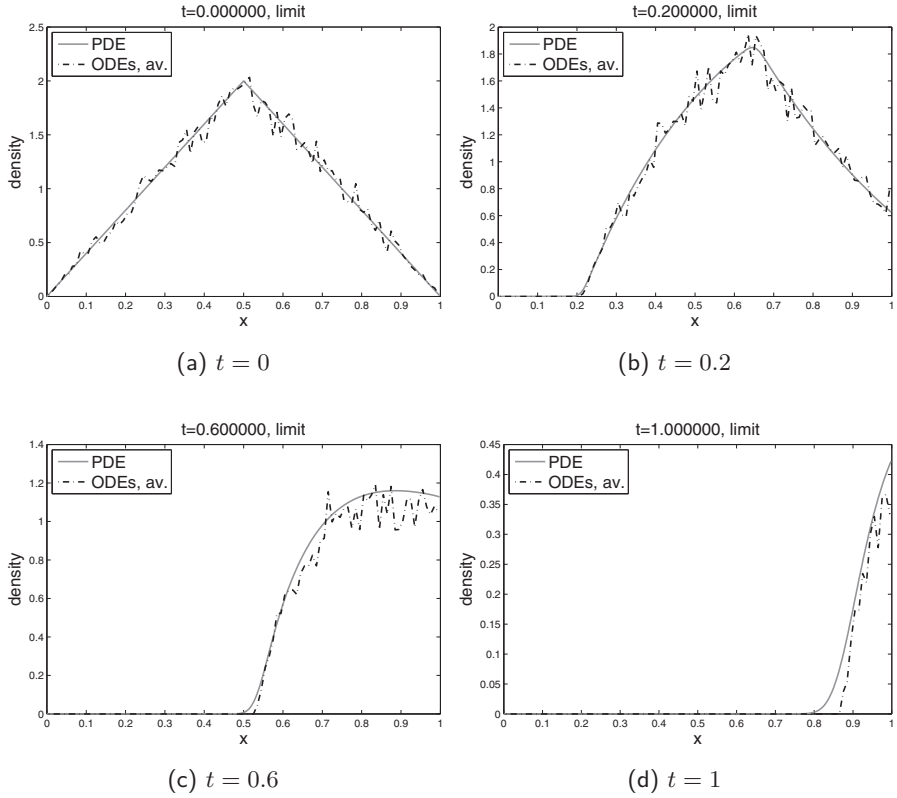

(a) $t = 0$ (b) $t = 0.2$

(c) $t = 0.6$ (d) $t = 1$

Figure 4.1: The limit case ("$n = \infty$"): Comparison of absolutely continuous ('PDE') and discrete ('ODEs, av.') solutions in the interior of the domain.

constant. Stretching and compression is a direct consequence of the change in monotonicity of v. The two solutions depict approximately the same behaviour. Oscillations are inherent to the nature of a particle system. As time proceeds, the discrete model deviates more from the PDE. The reason is that particles have accumulated in 1, leaving fewer particles in the interior, and thus leading to a coarser approximation.

In Figure 4.2 we show the results corresponding to the regularized system for $n = 2$. We observe the same behaviour as in Figure 4.1. Note that the densities in Figure 4.2 are slightly smaller than in Figure 4.1; in the regularized system mass already decays in the interior of the domain. The differences between the regularized and limit systems being small, reflect the fact that, apparently, the magnitude of v is large compared to the rate at which mass decays. Mass arrives at 1 due to v relatively fast, without having too much chance to decay.

In Figure 4.3 we compare the evolution of mass accumulation and decay at $x = 1$. Both for the limit case and the case $n = 2$ the solutions for absolutely continuous and discrete

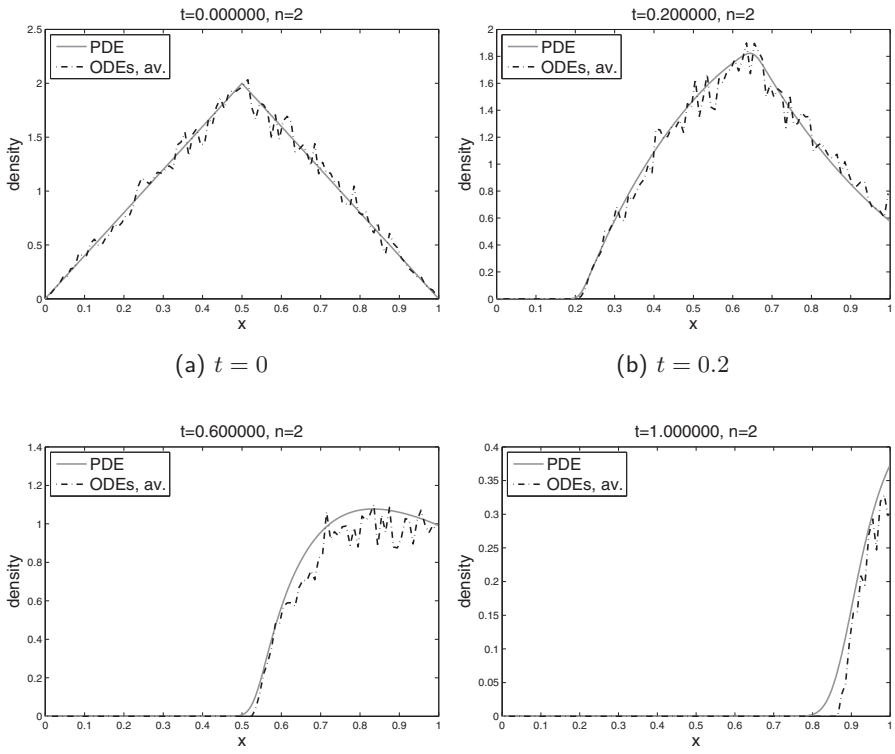

(a) $t = 0$ (b) $t = 0.2$

(c) $t = 0.6$ (d) $t = 1$

Figure 4.2: The regularized case ($n = 2$): Comparison of absolutely continuous ('PDE') and discrete ('ODEs, av.') solutions in the interior of the domain.

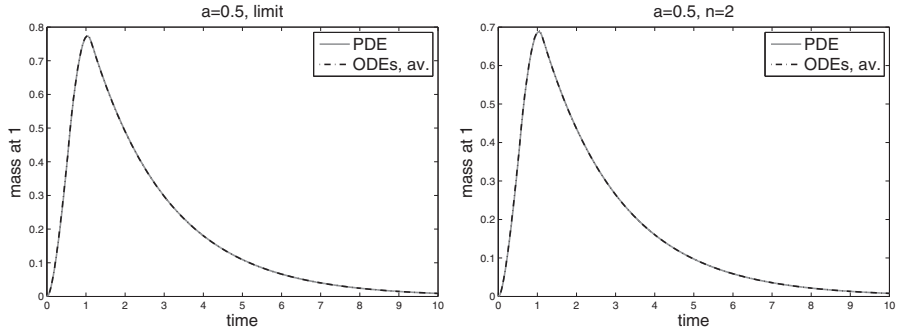

(a) Limit (b) Regularized, $n = 2$

Figure 4.3: Comparison of the mass at $x = 1$ for the absolutely continuous ('PDE') and discrete ('ODEs, av.') solutions.

initial data are nearly indistinguishable. It is worth noting that in the regularized case the peak value is smaller than in the limit case. This is in agreement with our observations above about mass distribution in the interior of the domain. Some mass is taken away in the boundary layer before arriving at $x = 1$.

For n larger than 2, we observe similar behaviour as in the case $n = 2$, be it that the solution of the limit problem is approximated even better. We omit to show the corresponding graphs.

4.5.3 Order of convergence

Proposition 4.4.2 (and Example 4.4.3) state that $\|\mu_t^{(n)} - \mu_t\|_{\mathrm{BL}}^* = \mathcal{O}(1/n)$, uniformly on compact time intervals. In this section, we confirm this statement numerically. We follow the idea of [JMC13] for calculating the flat metric. They choose to use the Fortet-Mourier norm $\|\cdot\|_{\mathrm{FM}} := \max\{\|\cdot\|_\infty, |\cdot|_{\mathrm{L}}\}$ on the space of bounded Lipschitz functions, rather than the BL norm, or Dudley norm $\|\cdot\|_{\mathrm{BL}} := \|\cdot\|_\infty + |\cdot|_{\mathrm{L}}$ used in this chapter. Consequently, the corresponding dual norm is different; $\|\cdot\|_{\mathrm{FM}}^*$ instead of $\|\cdot\|_{\mathrm{BL}}^*$. However, these norms are equivalent (see (4.9) and Lemma C.2 in Appendix C). So either one of them can be used for estimating the order of convergence.

The algorithm in [JMC13] can only be applied to (signed) discrete measures. In the sequel we thus focus on discrete measures only and fix the number of particles at $N = 25000$ like in Section 4.5.2. We have seen before that any discrete measure stays discrete as time evolves, which allows for the use of the algorithm in [JMC13]. For a comparison between the solutions for absolutely continuous and discrete initial data, we refer the reader back to Section 4.5.2. The algorithm is explained in detail in Appendix E.

k	$\log_2(A_k/A_{k+1})$
1	1.0531
2	1.0717
3	1.0446
4	1.0238
5	1.0123
6	1.0065
7	1.0024
8	1.0000

Table 4.1: Estimation of the order of convergence q, as used in (4.36), for $n = 2^k$, $k \in \mathbb{N}^+$. The numerical order of convergence is $\mathcal{O}(1/n)$, confirming the theoretical result from Proposition 4.4.2.

We take $n = 2^k$ for $k = 1, 2, \ldots$ and define

$$A_k := \sup_{t\in[0,T]} \|\mu_t^{(2^k)} - \mu_t\|^*_{\mathrm{FM}}. \tag{4.35}$$

In (4.35), T denotes the final time of the computation. We estimate the order of convergence q, that is the value of q such that

$$A_k = \mathcal{O}\left(\left(\frac{1}{2^k}\right)^q\right), \tag{4.36}$$

as $k \to \infty$. As mentioned before, $q = 1$ should hold. We approximate the value of q by $\log_2(A_k/A_{k+1})$. The results are in Table 4.1 and support our theoretical claim.

4.6 A probabilistic interpretation of the integral equation

The measure-valued variation of constants formula (4.3) follows naturally from a probabilistic view on the system, as we shall now describe.

Take N individuals in a confined space, with position $X_t^i \in [0,1]$ at time t say ($i = 1, \ldots, N$). We assume that the boundary at 1 is sticking. By this we mean that at the absorbing boundary we have a 'gate' that absorbs an individual present there a time T_i *after* arrival, which is an exponentially distributed random variable with (constant) rate a. We assume that the individuals are indistinguishable and the absorption of individuals (gating) occurs independently. We denote by $\pi_t^{(i)}$ the law of X_t^i when X_0^i is distributed according to the probability measure π_0.

Since individuals are independent, the expected number of individuals in a Borel set $E \subset [0,1]$ is given by the measure $\mu_t(E)$, where μ_t satisfies

$$\mu_t(E) = \mathbb{E}\left[\sum_{i=1}^N \mathbb{1}_{X_t^i}(E)\right] \;=\; \sum_{i=1}^N \pi_t^{(i)}(E). \tag{4.37}$$

The measures $\pi_t^{(i)}$ satisfy

$$\pi_t(E) = P_t\pi_0(E) - \delta_1(E)\int_0^t a\pi_s\left(\{1\}\right)ds, \tag{4.38}$$

such that (4.37) together with (4.38) yields (4.3) with the particular choice $f = -a\,\mathbb{1}_{\{1\}}$ as in Section 4.4, Example 4.4.3. To see that (4.38) holds, let us introduce the conditional probability

$$\begin{aligned} p(t,\Delta t) &:= \mathrm{Prob}\big(\text{Individual is gated in } [t,t+\Delta t] \mid X_t = 1\big) \\ &= 1 - e^{-a\Delta t}. \end{aligned}$$

Discretize the time interval $[0,t]$ into κ steps of length Δs and let s_j be the left point of the jth subinterval. Then the probability that the individual has been gated in $[0,t]$ is approximately

$$\begin{aligned} \sum_{j=1}^{\kappa} p(s_j,\Delta s)\pi_{s_j}\left(\{1\}\right) &= \sum_{j=1}^{\kappa} \frac{p(s_j,\Delta s)}{\Delta s}\pi_{s_j}\left(\{1\}\right)\Delta s \\ &\to \int_0^t a\pi_s\left(\{1\}\right)ds \end{aligned}$$

as $\kappa \to \infty$. Formulating now (4.38) in terms of measures in $\mathcal{M}^+([0,1])_{\mathrm{BL}}$, we obtain

$$\pi_t = P_t\pi_0 - \int_0^t a\pi_s\left(\{1\}\right)ds\,\delta_1.$$

To conclude this section, we compare the numerics of Section 4.5 to a numerical approximation of its probabilistic counterpart presented in this section. We only consider those results of Section 4.5 corresponding to the limit problem; cf. the dashed curves in Figure 4.1 and Figure 4.3a. For the deterministic and stochastic models, the same discrete initial measure is used with positions drawn randomly from the distribution $\bar{\mu}_0$. Recall that we use $N = 25000$ Diracs of initial mass $1/N$.

Differences between the solutions with random and continuous decay, respectively, can only occur at $x = 1$. In the interior there is no absorption of mass, while we use the same initial data and the evolution of positions is dictated by the same velocity field. Therefore we only show the mass at $x = 1$ as a function of time; see Figure 4.4. In the graph hardly any difference is observed between the two systems.

4.7 Proof of central Lemma 4.2.3 – Averaging over orbits

In this section we prove Lemma 4.2.3, which in turn builds on a number of other lemmas. Let $g : [0,1] \to \mathbb{R}$ be a piecewise bounded Lipschitz function, with finite set of

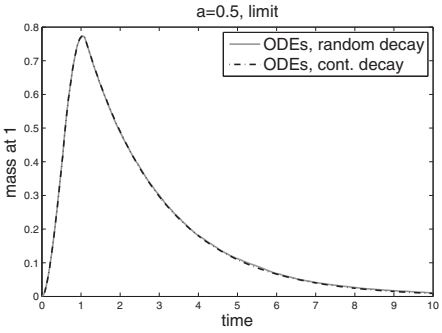

Figure 4.4: Mass at $x = 1$ for the system with discrete initial measure in the limit of vanishing boundary layer. Comparison between taking away all mass of a particle at a random time after arrival, and continuous decay at rate a.

discontinuities S_g. Number the points of $S_g \cup \{0, 1\}$ in increasing order:

$$x_0 := 0 < x_1 < x_2 < \cdots < x_{n-1} < 1 =: x_n.$$

For ease of exposition of the technical arguments, if $n = 1$ we include an 'artificial' point of discontinuity for g in $(0, 1)$ at position x where $v(x) \neq 0$, such that we can assume $n \geqslant 2$. The resulting partitioning of $[0, 1]$ has mesh size $m_g := \min_{1 \leqslant i \leqslant n}(x_i - x_{i-1})$. The restriction of g to the subinterval (x_{i-1}, x_i) has a unique Lipschitz extension to $[x_{i-1}, x_i]$ that we denote by g_i. Note that in general $g_i(x_i) \neq g(x_i) \neq g_{i+1}(x_i)$ may hold. By assumption v is a bounded Lipschitz velocity field on $[0, 1]$ such that $v(x) \neq 0$ for $x \in S_g$. Let (Φ_s) be the individualistic stopped flow associated to v (see Section 4.2.1).

The Lipschitz property of g_t^Φ is less straightforward to establish than it might seem at first sight, whence the technical proof that is presented in this section is required. One might think of starting from the observation that

$$g_t^\Phi(x) = \int_0^t g(\Phi_s(x))\, ds = \int_0^t \frac{g(\Phi_s(x))}{v(\Phi_s(x))} \frac{d\Phi_s(x)}{ds}\, ds = \int_x^{\Phi_t(x)} \frac{g(x')}{v(x')}\, dx'. \tag{4.39}$$

However, (4.39) holds for only for x that are not a sticking boundary point nor an interior steady state, and holds for $t \leqslant \tau_\partial(x)$ only. Moreover, when there is an internal steady state, then (4.39) does not give an easy Lipschitz estimate for $|g_t^\Phi(x) - g_t^\Phi(y)|$ when x and y lie on different sides of this steady state. This strongly limits the applicability of (4.39).

In our approach consider the *product flow* $(\Phi_s^\times)$ on $[0, 1] \times [0, 1]$ given by

$$\Phi_s^\times(x, y) := (\Phi_s(x), \Phi_s(y)) \qquad \text{for } s \geqslant 0$$

and define for $1 \leqslant i, j \leqslant n$ and $t \geqslant 0$:

$$\begin{aligned}
\overline{B}_{i,j} &:= \big\{(x,y) \in [0,1] \times [0,1] \mid x_{i-1} \leqslant x \leqslant x_i,\ x_{j-1} \leqslant y \leqslant x_j\big\},\\
I^t_{i,j}(x,y) &:= \big\{s \in [0,t] \mid \Phi^\times_s(x,y) \in \overline{B}_{i,j}\big\},\\
I^{t,\partial}_{i,j}(x,y) &:= \big\{s \in [0,t] \mid \Phi^\times_s(x,y) \in \partial\overline{B}_{i,j} \setminus \Delta_{[0,1]}\big\}.
\end{aligned}$$

Here, $\partial\overline{B}_{i,j}$ denotes the boundary of $\overline{B}_{i,j}$ and $\Delta_{[0,1]} := \{(x,y) \in [0,1] \times [0,1] \mid x = y\}$ is the diagonal in $[0,1] \times [0,1]$. Then one has for any $x, y \in [0,1]$,

$$\big|g^\Phi_t(x) - g^\Phi_t(y)\big| \leqslant \sum_{1 \leqslant i,j \leqslant n} \int\limits_{I^t_{i,j}(x,y)} \big|g(\Phi_s(x)) - g(\Phi_s(y))\big|\, ds. \tag{4.40}$$

The terms in (4.40) with $|i-j| \geqslant 2$, $|i-j| = 1$, and $i = j$ are estimated separately, since each requires a different approach. The last two cases are the most delicate. The estimates are as follows:

Case $|i-j| \geqslant 2$

For $s \in I^t_{i,j}(x,y)$, $\Phi_s(x)$ and $\Phi_s(y)$ are in intervals of the partitioning of $[0,1]$ that are not neighbours. So $|\Phi_s(x) - \Phi_s(y)| \geqslant m_g$. This implies that in this case

$$\begin{aligned}
\int\limits_{I^t_{i,j}(x,y)} |g(\Phi_s(x)) - g(\Phi_s(y))|\, ds &\leqslant \frac{2}{m_g}\|g\|_\infty \int\limits_{I^t_{i,j}(x,y)} |\Phi_s(x) - \Phi_s(y)|\, ds\\
&\leqslant \frac{2}{m_g}\|g\|_\infty\, e^{|v|_{\mathrm{L}} t} \cdot |I^t_{i,j}(x,y)| \cdot |x-y|,
\end{aligned}$$

according to Lemma 4.2.1. Here, $|A|$ denotes the Lebesgue measure of the (measurable) set A.

Case $|i-j| = 1$

The following lemma provides the crucial observation for this case:

Lemma 4.7.1. *Assume $n \geqslant 2$. Then for all $t \geqslant 0$ and $1 \leqslant i, j \leqslant n$ such that $|i-j| = 1$, there exist $L^t_{i,j} \geqslant 0$ such that*

$$|I^t_{i,j}(x,y)| \leqslant L^t_{i,j}\, |x-y| \tag{4.41}$$

for all $x, y \in [0,1]$. The functions $t \mapsto L^t_{i,j}$ are non-decreasing and locally bounded.

The terms in (4.40) with $|i-j| = 1$ can then be estimated as follows, where we limit our exposition to the case $j = i-1$:

$$\int\limits_{I^t_{i,i-1}(x,y)} |g(\Phi_s(x)) - g(\Phi_s(y))|\, ds \leqslant 2\|g\|_\infty \cdot |I^t_{i,i-1}(x,y)| \leqslant\ 2\|g\|_\infty L^t_{i,i-1} \cdot |x-y|.$$

Case $i = j$

Since g is possibly discontinuous at the points x_{i-1} and x_i we have, using Lemma 4.2.1,

$$\begin{aligned}\int\limits_{I^t_{i,i}(x,y)} \left|g(\Phi_s(x)) - g(\Phi_s(y))\right| ds \leqslant &\int\limits_{I^t_{i,i}(x,y)} |g_i(\Phi_s(x)) - g_i(\Phi_s(y))|\, ds \\ &+ \int\limits_{I^{t,\partial}_{i,i}(x,y)} |g(\Phi_s(x)) - g(\Phi_s(y))|\, ds \qquad (4.42)\\ \leqslant &|g_i|_{\mathrm{L}} e^{|v|_{\mathrm{L}} t} \cdot |I^t_{i,i}(x,y)| \cdot |x-y| + 2\|g\|_\infty |I^{t,\partial}_{i,i}(x,y)|. \qquad (4.43)\end{aligned}$$

Note that $I^{t,\partial}_{i,i}(x,y)$ does not contain times $s \in [0,t]$ at which $\Phi^\times_s(x,y) \in \Delta_{[0,1]}$. For these times the integrand is zero, however. The following lemma provides the Lipschitz estimate for the second term in (4.43), similar to Lemma 4.7.1:

Lemma 4.7.2. *If $2 \leqslant i \leqslant n-1$, then $|I^{t,\partial}_{i,i}(x,y)| = 0$ for all $x, y \in [0,1]$. If $i = 1$ and $v(0) \neq 0$, or $i = n$ and $v(1) \neq 0$, then for all $t \geqslant 0$ there exist $L^t_i \geqslant 0$ such that for all $x, y \in [0,1]$*

$$|I^{t,\partial}_{i,i}(x,y)| \leqslant L^t_i\, |x-y|. \qquad (4.44)$$

The function $t \mapsto L^t_i$ is non-decreasing and locally bounded.

The estimates for the various cases can now be put together when $v(x) \neq 0$ for $x \in \{0,1\}$, yielding

$$\begin{aligned}\left|g^\Phi_t(x) - g^\Phi_t(y)\right| \leqslant\ & \frac{2}{m_g}\|g\|_\infty \cdot e^{|v|_{\mathrm{L}} t} \left(\sum_{|i-j|\geqslant 2} |I^t_{i,j}(x,y)|\right) \cdot |x-y| \\ &+ 2\|g\|_\infty \left(\sum_{|i-j|=1} L^t_{i,j}\right) \cdot |x-y| \\ &+ \max_{1\leqslant i\leqslant n} |g_i|_{\mathrm{L}} \cdot e^{|v|_{\mathrm{L}} t} \left(\sum_{i=1}^n |I^t_{i,i}(x,y)|\right) \cdot |x-y| \\ &+ 2\|g\|_\infty (L^t_1 + L^t_n) \cdot |x-y| \\ \leqslant\ & |x-y| \cdot G \cdot \left(\frac{2n^2}{m_g} \cdot t e^{|v|_{\mathrm{L}} t} + 2 \sum_{|i-j|=1} L^t_{i,j} + 2(L^t_1 + L^t_n)\right),\end{aligned}$$

with $G := \max(\|g\|_\infty, |g_1|_{\mathrm{L}}, \ldots, |g_n|_{\mathrm{L}})$. Here we used that $\sum_{i,j} |I^t_{i,j}(x,y)| \leqslant n^2 t$. The functions $t \mapsto L^t_{i,j}$ are non-decreasing and locally bounded when $|i-j| = 1$, according to Lemma 4.7.1, while $t \mapsto L^t_1$ and $t \mapsto L^t_n$ are non-decreasing and locally bounded, due to Lemma 4.7.2. So for every $t \geqslant 0$, $\sup_{0\leqslant s\leqslant t} |g^\Phi_s|_{\mathrm{L}} < \infty$.

If $v(0) = 0$ or $v(1) = 0$, then g is continuous at the boundary points where v vanishes, by the assumptions imposed on v. Consider the case $v(0) = 0$. Then the domain of integration in the integral in (4.42) for $i = 1$ can be replaced by

$$\tilde{I}^{t,\partial}_{1,1}(x,y) := I^{t,\partial}_{1,1}(x,y) \setminus \{(x,y) \in [0,1] \times [0,1] \mid x = 0 \text{ or } y = 0\},$$

because of the continuity of g at 0. Since $v(x_1) \neq 0$, we obtain $|\tilde{I}^{t,\partial}_{1,1}(x,y)| = 0$ and the last term in (4.43) can be omitted in this case. A similar argument applies to the case $v(1) = 0$ and $i = n$. Again, for every $t \geqslant 0$, $\sup_{0 \leqslant s \leqslant t} |g^{\Phi}_s|_{\mathrm{L}} < \infty$. The proof of Lemma 4.2.3 is now complete.

Proofs of Lemma 4.7.1 and Lemma 4.7.2

First define for any $x, y \in [0,1]$:

$$\tau_y(x) := \inf\{s \geqslant 0 \ : \ y = \Phi_s(x)\},$$

with the convention that $\inf \emptyset = \infty$. If it is finite, then $\tau_y(x)$ is the arrival time at y of the solution starting at x. In that case,

$$\tau_y(x) = \int_0^{\tau_y(x)} \frac{1}{v(\Phi_s(x))} \cdot \frac{d\Phi_s(x)}{ds}\, ds = \int_x^y \frac{1}{v(x')}\, dx', \tag{4.45}$$

because $v(\Phi_s(x)) \neq 0$ for any $0 \leqslant s \leqslant \tau_y(x)$, otherwise y is not reachable (note that v Lipschitz implies that a steady state cannot be reached in finite time). For $t \geqslant 0$ define the truncation

$$t \wedge \tau_y(x) := \min(t, \tau_y(x)) \tag{4.46}$$

Lemma 4.7.3. *Let $n \geqslant 2$ and $t > 0$.*

(a) If $1 \leqslant i \leqslant n-1$, then $x \mapsto t \wedge \tau_{x_i}(x)$ is continuous on $[x_{i-1}, x_{i+1}]$ except at x_i. Moreover,

(i) If $v(x_i) > 0$, then $t \wedge \tau_{x_i}$ is Lipschitz continuous on $[x_{i-1}, x_i]$.

(ii) If $v(x_i) < 0$, then $t \wedge \tau_{x_i}$ is Lipschitz continuous on $[x_i, x_{i+1}]$.

In either of the cases, $t \wedge \tau_{x_i}(x) = t$ on the remaining part of $[x_{i-1}, x_{i+1}]$.

(b) If $v(0) < 0$, then $x \mapsto t \wedge \tau_{x_0}(x)$ is Lipschitz continuous on $[x_0, x_1]$.

(c) If $v(1) > 0$, then $x \mapsto t \wedge \tau_{x_n}(x)$ is Lipschitz continuous on $[x_{n-1}, x_n]$.

In all cases the corresponding Lipschitz constant of $t \wedge \tau_{x_i}$ on the stated interval is a non-decreasing function of t.

Proof. (a): First assume that $v(x_i) > 0$. Then τ_{x_i} is finite on the connected component of the set $S_i := \{x \in [x_{i-i}, x_i] \mid v(x) > 0\}$ that contains x_i. According to (4.45), $x \mapsto \tau_{x_i}(x)$ is strictly decreasing and continuously differentiable function on $S_i \setminus \{x_i\}$.

Hence, $t \wedge \tau_{x_i}$ is a Lipschitz function on $[x_{i-i}, x_i]$, with Lipschitz constant on this interval given by

$$|t \wedge \tau_{x_i}|_{\mathrm{L}}^{(i)} = \sup\left\{ \frac{1}{v(x')} \mid x' \in [x_{i-1}, x_i],\ \tau_{x_i}(x') \leqslant t \right\},$$

because of (4.45). So $t \mapsto |t \wedge \tau_{x_i}|_{\mathrm{L}}^{(i)}$ is a non-decreasing (and locally bounded) function. Note that $t \wedge \tau_{x_i}(x_i) = 0$, while $t \wedge \tau_{x_i}(x) = t$ for $x \in (x_i, x_{i+1}]$.

A similar argument applies to the case $v(x_i) < 0$. Now $x \mapsto \tau_{x_i}(x)$ is strictly increasing on the connected component of $S_i' := \{x \in [x_i, x_{i+1}] \mid v(x) < 0\}$ that contains x_i. Further details are left to the reader.

(b) and (c): The arguments are similar to the Lipschitz part of (a). □

Remark 4.7.4. If $v(x_i)$ were 0, then $t \wedge \tau_{x_i}$ is constant t on $[x_{i-1}, x_{i+1}] \setminus \{x_i\}$, but discontinuous for $t > 0$ at $x = x_i$, since $t \wedge \tau_{x_i}(x_i) = 0$. Hence, it is neither Lipschitz on $[x_{i-1}, x_i]$, nor on $[x_i, x_{i+1}]$.

Proof of Lemma 4.7.1

Proof. (Lemma 4.7.1). Because $I_{i,j}^t(x,y) = I_{j,i}^t(y,x)$, it suffices to consider the case $j = i-1$, $i \geqslant 2$. Fix $x, y \in [0,1]$. We can assume that $I_{i,j}^t(x,y) \neq \emptyset$. First suppose that $(x,y) \notin \overline{B}_{i,i-1}$. Then $t_0 := \inf(I_{i,j}^t(x,y))$ is the time of arrival of the product flow at $\partial\overline{B}_{i,i-1}$ before time t, when the flow starts at (x,y). Consequently,

$$|I_{i,i-1}^t(x,y)| = |I_{i,i-1}^{t-t_0}(\Phi_{t_0}^{\times}(x,y))|. \tag{4.47}$$

Since

$$|\Phi_{t_0}(x) - \Phi_{t_0}(y)| \leqslant e^{|v|_{\mathrm{L}} t_0} \cdot |x-y| \leqslant e^{|v|_{\mathrm{L}} t} \cdot |x-y|, \tag{4.48}$$

(cf. Lemma 4.2.1) it suffices to prove (4.41) for $(x,y) \in \overline{B}_{i,i-1}$.

We now estimate $|I_{i,i-1}^t(x,y)|$ for $(x,y) \in \overline{B}_{i,i-1}$ under the assumption that $v(x_{i-1}) > 0$, by distinguishing three cases:

Case $x_{i-1} \leqslant x < x_i$ and $x_{i-2} < y < x_{i-1}$. Using the continuity of v and $v(x_{i-1}) > 0$ and taking into account that the individualistic stopped flow will stay at the boundary points $x_0 = 0$ and $x_n = 1$ of $[0,1]$ once the solution arrives at these points (when $v(0) < 0$ and $v(1) > 0$), one gets by careful consideration that

$$|I_{i,i-1}^t(x,y)| = \begin{cases} \min\big(t \wedge \tau_{x_i}(x), t \wedge \tau_{x_{i-1}}(y)\big), & i = 2,\ n > 2; \\ \min\big(t \wedge \tau_{x_{i-2}}(y), t \wedge \tau_{x_{i-1}}(y)\big), & i = n,\ n > 2; \\ t \wedge \tau_{x_{i-1}}(y), & i = n = 2; \\ \min\big(t \wedge \tau_{x_i}(x), t \wedge \tau_{x_{i-2}}(y), t \wedge \tau_{x_{i-1}}(y)\big), & \text{otherwise.} \end{cases} \tag{4.49}$$

Here we used that $v(x_{i-1}) > 0$. Hence,

$$|I^t_{i,i-1}(x,y)| \leqslant t \wedge \tau_{x_{i-1}}(y) = t \wedge \tau_{x_{i-1}}(y) - \underbrace{t \wedge \tau_{x_{i-1}}(x_{i-1})}_{=0} \tag{4.50}$$

$$\leqslant |t \wedge \tau_{x_{i-1}}|^{(i-1)}_{\mathrm{L}} \, |x_{i-1} - y| \tag{4.51}$$

$$\leqslant |t \wedge \tau_{x_{i-1}}|^{(i-1)}_{\mathrm{L}} \, |x - y|. \tag{4.52}$$

Note that in (4.50) – (4.52) the assumption $j = i - 1$ is essential. To get (4.51) we applied Lemma 4.7.3(i).

Case $x_{i-1} \leqslant x \leqslant x_i$ and $y = x_{i-1}$. In this case $|I^t_{i,i-1}(x,y)| = 0$ due to the sign of v at x_{i-1}.

Case $x = x_i$ or $y = x_{i-2}$ (or both). Note that $|x - y| \geqslant m_g$. Hence,

$$|I^t_{i,i-1}(x,y)| = \frac{|I^t_{i,i-1}(x,y)|}{|x-y|} \cdot |x-y| \leqslant \frac{t}{m_g} \, |x-y|.$$

From the above cases we deduce that if $v(x_{i-1}) > 0$, then

$$|I^t_{i,i-1}(x,y)| \leqslant \max\Big(\frac{t}{m_g}, |t \wedge \tau_{x_{i-1}}|^{(i-1)}_{\mathrm{L}}\Big) \cdot |x-y|, \tag{4.53}$$

holds for all $(x,y) \in \overline{B}_{i,i-1}$. The prefactor on the right-hand side in (4.53) is non-decreasing and locally bounded in t.

If $v(x_{i-1}) < 0$, then $t \wedge \tau_{x_{i-1}}$ is not Lipschitz on $[x_{i-2}, x_{i-1}]$, but on $[x_{i-1}, x_i]$ instead (Lemma 4.7.3). We denote its Lipschitz constant on the latter interval by $|t \wedge \tau_{x_{i-1}}|^{(i)}_{\mathrm{L}}$, which is a non-decreasing function of t. The estimates for $|I^t_{i,i-1}(x,y)|$ follow from distinguishing between similar cases as for $v(x_{i-1}) > 0$. We obtain

$$|I^t_{i,i-1}(x,y)| \leqslant \max\Big(\frac{t}{m_g}, |t \wedge \tau_{x_{i-1}}|^{(i)}_{\mathrm{L}}\Big) \, |x-y|, \tag{4.54}$$

for all $(x,y) \in \overline{B}_{i,i-1}$, where $\max\big(\frac{t}{m_g}, |t \wedge \tau_{x_{i-1}}|^{(i)}_{\mathrm{L}}\big)$ is non-decreasing and locally bounded in t.

Since $v(x_{i-1}) \neq 0$ by assumption on the velocity field, the combination of (4.53) and (4.54) yields the result stated in the lemma. □

Proof of Lemma 4.7.2

Proof. (Lemma 4.7.2). Fix $x, y \in [0,1]$ such that $x \neq y$. Since $I^{t,\partial}_{i,i}(x,y) = I^{t,\partial}_{i,i}(y,x)$ we can assume $x < y$. Moreover, we can assume $I^{t,\partial}_{i,i}(x,y) \neq \emptyset$. Furthermore, it suffices to prove Lemma 4.7.2 for $(x,y) \in \overline{B}_{i,i}$ due to similar arguments as in (4.47)–(4.48).

If $n \geqslant 3$ and $2 \leqslant i \leqslant n-1$, then $v(x') \neq 0$ and $v(y') \neq 0$ for any $(x', y') \in \partial\overline{B}_{i,i}$ by assumption. Consequently, $|I^{t,\partial}_{i,i}(x,y)| = 0$ in this case.

Consider now $i = 1$. Recall that we have $n \geqslant 2$, $x_1 \in (0,1)$ and $v(x_1) \neq 0$. If $v(0) > 0$, i.e. 0 is non-sticking, then $|I^{t,\partial}_{1,1}(x,y)| = 0$ for all $x, y \in [0,1]$ with $x < y$. If $v(0) < 0$, then for $x, y \in [0,1]$ with $x < y$,

$$I^{t,\partial}_{1,1}(x,y) = \begin{cases} \{t \wedge \tau_{x_1}(y)\}, & \text{if } \tau_{x_1}(y) \leqslant t \wedge \tau_{x_0}(x), \\ \big[t \wedge \tau_{x_0}(x), \min(t \wedge \tau_{x_0}(y), t \wedge \tau_{x_1}(y))\big], & \text{if } \tau_{x_0}(x) \leqslant t \wedge \tau_{x_1}(y), \\ \emptyset, & \text{otherwise.} \end{cases} \tag{4.55}$$

Here we used that the flow does not stop at $x_1 \neq 1$. Moreover, in the second case in (4.55) we use that $\Delta_{[0,1]}$ is excluded in the definition of $I^{t,\partial}_{1,1}(x,y)$. Thus

$$|I^{t,\partial}_{1,1}(x,y)| = \begin{cases} \min(t \wedge \tau_{x_0}(y), t \wedge \tau_{x_1}(y)) - t \wedge \tau_{x_0}(x), & \text{if } \tau_{x_0}(x) \leqslant t \wedge \tau_{x_1}(y), \\ 0, & \text{otherwise.} \end{cases}$$

Hence, if $v(0) < 0$, then

$$|I^{t,\partial}_{1,1}(x,y)| \leqslant |t \wedge \tau_{x_0}(y) - t \wedge \tau_{x_0}(x)| \leqslant |t \wedge \tau_{x_0}|^{(1)}_{\mathrm{L}} \cdot |x - y|.$$

As argued in the proof of Lemma 4.7.1, $t \mapsto |t \wedge \tau_{x_0}|^{(1)}_{\mathrm{L}}$ is non-decreasing, locally bounded.

Consider $i = n$. If $v(1) < 0$, then $|I^{t,\partial}_{n,n}(x,y)| = 0$ for all $x, y \in [0,1]$ with $x < y$. If $v(1) > 0$, then

$$I^{t,\partial}_{n,n}(x,y) = \begin{cases} \{t \wedge \tau_{x_{n-1}}(x)\}, & \text{if } \tau_{x_{n-1}}(x) \leqslant t \wedge \tau_{x_n}(y), \\ \big[t \wedge \tau_{x_n}(y), \min(t \wedge \tau_{x_{n-1}}(x), t \wedge \tau_{x_n}(x))\big], & \text{if } \tau_{x_n}(y) \leqslant t \wedge \tau_{x_{n-1}}(x), \\ \emptyset, & \text{otherwise.} \end{cases} \tag{4.56}$$

Consequently, with similar argument as above, if $v(1) > 0$, then

$$|I^{t,\partial}_{n,n}(x,y)| \leqslant |t \wedge \tau_{x_n}(y) - t \wedge \tau_{x_n}(x)| \leqslant |t \wedge \tau_{x_n}|^{(n)}_{\mathrm{L}} \cdot |x - y|.$$

As argued before, each Lipschitz constant is non-decreasing and locally bounded in time. This completes the proof. □

4.8 Discussion

In this chapter, we have dealt with a one-dimensional evolution problem for a measure on the unit interval under a prescribed velocity field. A combination of the stopped flow and a source-sink right-hand side are used to model flux boundary conditions. We introduced an approximation procedure involving an absorptive boundary layer from which, in the limit of vanishing layer, a sink localized on the boundary is obtained. In the limit mass is

gated away from the system via the boundary at a certain rate. To a certain extent, this can be interpreted as a 'door' with finite capacity. Compare the question that we posed in Section 1.7.3 on how to incorporate exits and entrances. We note that the results of this chapter are not restricted to absorptive zones near the boundary; internal sources and sinks are also incorporated.

An important generalization is the extension to velocity fields that depend on the measure-valued solution itself. Those velocity fields are particularly interesting in view of mutual interactions. This step is taken in Chapter 5.

The current problem is posed on the unit interval. To be done is the (highly nontrivial) generalization to two or higher dimensions. As we have seen in this chapter (see Section 4.6), our model can be interpreted as a particle system with particles being gated away randomly at a certain rate from an absorption zone. We derived the limit as the width of this absorption zone goes to zero. In two (or more) dimensions, designing such limit procedure is more involved. The shape and regularity of the boundary influence the amount of mathematical difficulties that we will encounter. In the higher-dimensional variant of our model, we expect an additional contribution to the solution measure to be present, which accounts for the mass accumulated on the curves that bound the domain. Such parts of a measure, concentrating on a lower-dimensional manifold, are called *singular continuous*; see e.g. [KS07], p. 45.

The continuous dependence of solutions on the initial data was proved in Proposition 4.3.8. In Section 4.5 we demonstrated this property by means of a continuum and particle version of the model. Discrete initial measures yield a discrete solution measure for all time, since the positions of the Dirac masses are simply transported. A absolutely continuous initial measure yields *in the interior* an absolutely continuous solution. The latter is true, because v is Lipschitz continuous, and hence mass cannot accumulate into a point in finite time.
As is illustrated by Section 4.5, Proposition 4.3.8 contains a discrete-to-continuum limit as a special case. This is a side result while this chapter treats the problem at a more general level. However, the discrete-to-continuum limit of this chapter is indicated in Figure 1.2.

In Chapter 6 of [Ren13] a similar problem is treated. The dynamics in the interior domain are driven by diffusion there, which instantaneously regularizes the solution. This justifies the description of the solution in terms of a density on the open interval $(0, 1)$ and two Dirac masses at the boundaries 0 and 1 that account for the mass that has left the interior; see p. 91 of [Ren13]. The explicit splitting of the solution in these parts requires extra bookkeeping to match the interior dynamics with the time-evolution of the Dirac masses. Compare what we did in (4.33).
The mass at 0 and 1 is kept track of, because as a result the total mass is constant (density $+$ Diracs). This is important, because [Ren13] uses the Wasserstein distance, that is defined on probability measures. Note that no distinction can be made between mass that accumulates at the boundary, and mass that has actually been gated away. We do not have these problems, because we use a distance on general finite Borel measures

that does not require conservation of total mass. In our setting, the interior and boundary measures are combined into one solution measure. Moreover, mass that is concentrated on the boundary is interpreted as being physically present in the problem, while mass that was gated away is no longer visible. Also, our setting allows for net *influx* of mass.

Chapter 5

Flux boundary conditions: measure-dependent velocity

In the previous chapter, Chapter 4, we derived boundary conditions for a measure-valued evolution equation with prescribed velocity field. We now propose and investigate a procedure to generalize the results of Chapter 4 to velocity fields that depend on the solution itself. Such generalization makes it possible to model the dynamics on a bounded domain governed by interactions between the 'particles'. In Chapters 2 and 3 interaction terms of convolution type have already been used.

We are motivated in this chapter by the same mathematical question as in Chapter 4:

What is the correct way to define zero-flux or general flux boundary conditions in terms of measures?

The results in this chapter only hold for a source-sink right-hand side that is based on a function $f \in \mathrm{BL}([0,1])$. In view of Chapter 4, we are hence able to describe absorption in a boundary layer, but not yet absorption on the boundary alone. In the discussion section of this chapter we comment on the possibilities to extend our results to f that is piecewise bounded Lipschitz.

5.1 Introduction

As said before, in this chapter we consider (4.1) for velocity fields that are no longer *fixed* elements of $\mathrm{BL}([0,1))$. Instead of v, we write $v[\mu]$ for the velocity field that depends functionally on the solution. The transport equation on $[0,1]$ – cf. (1.43) – becomes

$$\frac{\partial}{\partial t}\mu_t + \frac{\partial}{\partial x}(\mu_t v[\mu_t]) = f \cdot \mu_t. \tag{5.1}$$

This chapter is based on work in progress with Sander Hille and Adrian Muntean. It builds both on Chapter 4 of this thesis and on Ron Hoogwater's master's thesis [Hoo13].

Due to the measure-dependency of the velocity, Equation (5.1) is nonlinear. To establish well-posedness despite the nonlinearity, we use a *forward-Euler-like approach* that builds on the fundamentals constructed in Chapter 4. We partition the time interval $[0,T]$ and fix, on each subinterval, the velocity. That is, restricted to a subinterval, the velocity depends only on the spatial variable and not on the solution measure. Within each subinterval the measure-valued solution evolves according to this fixed velocity and the evolution satisfies the requirements of Chapter 4. A more detailed description is given in Section 5.3. We refine the partitioning of $[0,T]$ and estimate the difference between the subsequent Euler approximations. The main result of this chapter is our proof of the fact that this procedure converges.

A forward-Euler scheme similar to ours is also used in [PR13] for absolutely continuous measures. Their results are extended to general measures in Chapter 7 of [CPT14]. The difference between their and our work is that they use the Wasserstein distance and that their domain is $\mathbb{R}^d$.
As mentioned in Section 1.7.3 of Chapter 1, the references that directly inspired us are [CG09, Hoo13, GLMC10]. The approach presented in this chapter deviates from [Hoo13], since we restrict ourselves to evolution on the interval $[0,1]$, while [Hoo13] considers $[0,\infty)$. Furthermore, our regularity conditions on the velocity – given in Assumption 5.3.1 – are weaker than in [Hoo13]; cf. Remark 5.3.3. Moreover, [Hoo13] restricts to velocity fields that point inwards at 0. In this way, no mass is allowed to flow out of the domain $[0,\infty)$. In our approach, the fact that the flow is stopped at the boundary is encoded in the semigroup $(P_t)_{t\geqslant 0}$, irrespective of the sign of the velocity there; cf. Section 4.2.1. Bearing in mind that the velocity $v[\mu]$ depends on the solution (see e.g. Example 5.3.2), we think it is too restrictive to have a condition on the sign of the velocity at 0 or 1.

This chapter is organized as follows. In Section 5.2 we collect a number of properties of the semigroup $(P_t)_{t\geqslant 0}$ and of the solution operator, called $(Q_t)_{t\geqslant 0}$, associated to Chapter 4. The forward-Euler-like approach to construct solutions is introduced in Section 5.3, in which we also state the main results of this chapter: existence and uniqueness of mild solutions to the nonlinear problem, and their continuous dependence on initial conditions. We prove these results in Section 5.4 using estimates between subsequent Euler approximations. In Section 5.5 we reflect on the achievements and open issues of this chapter and provide directions for further research.

5.2 Summary of technical preliminaries

5.2.1 Properties of the stopped flow

In this section we summarize results on the properties of $(P_t)_{t\geqslant 0}$: the semigroup corresponding to the stopped flow associated to $v \in \mathrm{BL}([0,1])$. We first recall Lemma 4.2.2:

Lemma 4.2.2. *Let $\mu \in \mathcal{M}([0,1])$ and $t,s \in \mathbb{R}^+$. Then*

(i) $\|P_t\mu - P_s\mu\|^*_{\mathrm{BL}} \leqslant \|v\|_\infty \|\mu\|_{\mathrm{TV}} |t-s|$.

(ii) $\|P_t\mu\|^*_{\mathrm{BL}} \leqslant \max(1, |\Phi_t|_{\mathrm{L}})\, \|\mu\|^*_{\mathrm{BL}} \leqslant e^{|v|_{\mathrm{L}} t} \|\mu\|^*_{\mathrm{BL}}$.

To distinguish between the semigroups on $\mathcal{M}([0,1])$ associated to $v, v' \in \mathrm{BL}([0,1])$, we write P^v and $P^{v'}$, respectively. Likewise notations we introduce for the semigroups $(\Phi^v_t)_{t\geqslant 0}$ and $(\Phi^{v'}_t)_{t\geqslant 0}$ on $[0,1]$ and for the intervals of existence $I^v_{x_0}$ and $I^{v'}_{x_0}$ associated to (4.12).

Lemma 5.2.1. *For all $\mu \in \mathcal{M}([0,1])$, $v, v' \in \mathrm{BL}([0,1])$ and $t \in \mathbb{R}^+_0$*

$$\|P^v_t\mu - P^{v'}_t\mu\|^*_{\mathrm{BL}} \leqslant \|v - v'\|_\infty\, t\, \|\mu\|_{\mathrm{TV}}\, e^{L\,t},$$

where $L := \min(|v|_{\mathrm{L}}\,, |v'|_{\mathrm{L}})$.

Proof. For any $\phi \in \mathrm{BL}([0,1])$

$$|\left\langle \phi, P^v_t\mu - P^{v'}_t\mu \right\rangle| = |\left\langle \phi\circ\Phi^v_t - \phi\circ\Phi^{v'}_t, \mu \right\rangle| \leqslant |\phi|_{\mathrm{L}}\, \|\Phi^v_t - \Phi^{v'}_t\|_\infty\, \|\mu\|_{\mathrm{TV}}, \tag{5.2}$$

hence

$$\|P^v_t\mu - P^{v'}_t\mu\|^*_{\mathrm{BL}} \leqslant \|\Phi^v_t - \Phi^{v'}_t\|_\infty\, \|\mu\|_{\mathrm{TV}}. \tag{5.3}$$

Case 1: $t \in I^v_x$ **and** $t \in I^{v'}_x$**.** For each $x \in [0,1]$

$$\begin{aligned} |\Phi^v_t(x) - \Phi^{v'}_t(x)| &= \left| \int_0^t v(\Phi^v_s(x)) - v'(\Phi^{v'}_s(x))\, ds \right| \\ &\leqslant |v|_{\mathrm{L}} \int_0^t |\Phi^v_s(x) - \Phi^{v'}_s(x)|\, ds + \|v - v'\|_\infty\, t. \end{aligned}$$

Gronwall's Lemma yields

$$|\Phi^v_t(x) - \Phi^{v'}_t(x)| \leqslant \|v - v'\|_\infty\, t\, e^{|v|_{\mathrm{L}}\, t}, \tag{5.4}$$

for all $x \in [0,1]$. Due to the symmetry of (5.4) in v and v', the same estimate can be obtained with $|v'|_{\mathrm{L}}$ instead of $|v|_{\mathrm{L}}$, and hence, we can write $\min(|v|_{\mathrm{L}}\,, |v'|_{\mathrm{L}})$ in the exponent. This observation yields, together with (5.3), the statement of the lemma.

Case 2: $t \notin I^v_x$**.** Extend $v : [0,1] \to \mathbb{R}$ to $\bar v : \mathbb{R} \to \mathbb{R}$ by defining $\bar v(x) := v(0)$ if $x < 0$ and $\bar v(x) := v(1)$ if $x > 1$. Then $\bar v$ is a bounded Lipschitz extension of v such that $\|\bar v\|_\infty = \|v\|_\infty$ and $|\bar v|_{\mathrm{L}} = |v|_{\mathrm{L}}$. Let $\Phi^{\bar v}_t : \mathbb{R} \to \mathbb{R}$ be the solution semigroup associated to the unique (global) solution to (4.12) with v replaced by $\bar v$ and with initial condition to be taken from the whole of $\mathbb{R}$. Extend v' analogously to $\bar v'$.
Irrespective of whether $t \in I^{v'}_x$ or $t \notin I^{v'}_x$, and whether in the latter case $\Phi^v_t(x) = \Phi^{v'}_t(x)$ or $\Phi^v_t(x) \neq \Phi^{v'}_t(x)$, the following estimate holds

$$|\Phi^v_t(x) - \Phi^{v'}_t(x)| \leqslant |\Phi^{\bar v}_t(x) - \Phi^{\bar v'}_t(x)| \tag{5.5}$$

for all $x \in [0,1]$. estimate $|\Phi_t^{\bar{v}}(x) - \Phi_t^{\bar{v}'}(x)|$ using the same ideas as in (5.3) and (5.4) and obtain

$$\|P_t^{\bar{v}}\mu - P_t^{\bar{v}'}\mu\|_{\mathrm{BL}}^* \leqslant \|\bar{v} - \bar{v}'\|_\infty \, t \, \|\mu\|_{\mathrm{TV}} \, \exp(\min(|\bar{v}|_{\mathrm{L}}, |\bar{v}'|_{\mathrm{L}})\, t).$$

The statement of the lemma follows from the equalities $|\bar{v}|_{\mathrm{L}} = |v|_{\mathrm{L}}$, $|\bar{v}'|_{\mathrm{L}} = |v'|_{\mathrm{L}}$, $\|\bar{v} - \bar{v}'\|_\infty = \|v - v'\|_\infty$ and Equation (5.5). The case $t \notin I_x^{v'}$ is analogous. □

5.2.2 Properties of the solution for prescribed velocity

In this section we give an overview of the properties of the solution treated in Chapter 4. We restrict ourselves to f that is bounded Lipschitz on $[0,1]$; cf. Section 5.5 for further discussion on this restriction. Let $v \in \mathrm{BL}([0,1])$ and $f \in \mathrm{BL}([0,1])$ be arbitrary. For all $t \geqslant 0$, we define $Q_t : \mathcal{M}([0,1]) \to \mathcal{M}([0,1])$ to be the operator that maps the initial condition to the solution – in the sense of Definition 4.2.4 – at time t. It follows from Propositions 4.3.2 and 4.3.6 that this operator is well-defined. Moreover, Q preserves positivity, due to Corollary 4.3.7.

Lemma 5.2.2 (Semigroup property)**.** *The set of operators $(Q_t)_{t\geqslant 0}$ satisfies the semigroup property. That is,*

$$Q_t \, Q_s \, \mu = Q_{t+s} \, \mu$$

for all $s, t \geqslant 0$ and for all $\mu \in \mathcal{M}([0,1])$.

Proof. The proof follows the lines of argument of [Š94], p. 283. We consider

$$\begin{aligned} Q_{t+s}\mu - Q_t \, Q_s \, \mu = P_{t+s}\mu + \int_0^{t+s} P_{t+s-\sigma} \, F_f(Q_\sigma \, \mu) \, d\sigma \\ - P_t \, Q_s \, \mu - \int_0^t P_{t-\sigma} \, F_f(Q_\sigma \, Q_s \, \mu) \, d\sigma, \end{aligned} \tag{5.6}$$

and observe that

$$\begin{aligned} P_t \, Q_s \, \mu &= P_t \, P_s \, \mu + P_t \int_0^s P_{s-\sigma} \, F_f(Q_\sigma \, \mu) \, d\sigma \\ &= P_{t+s} \, \mu + \int_0^s P_{t+s-\sigma} \, F_f(Q_\sigma \, \mu) \, d\sigma. \end{aligned} \tag{5.7}$$

Because $f \in \mathrm{BL}([0,1])$, the map $\sigma \mapsto P_{s-\sigma} \, F_f(Q_\sigma \, \mu)$ is continuous and hence it is measurable. Therefore, the second equality in (5.7) holds due to (B.3). Together, (5.6)

and (5.7) yield that

$$Q_{t+s}\mu - Q_t\, Q_s\, \mu = \int_s^{t+s} P_{t+s-\sigma}\, F_f(Q_\sigma\, \mu)\, d\sigma - \int_0^t P_{t-\sigma}\, F_f(Q_\sigma\, Q_s\, \mu)\, d\sigma$$
$$= \int_0^t P_{t-\sigma}\, \left(F_f(Q_{\sigma+s}\, \mu) - F_f(Q_\sigma\, Q_s\, \mu)\right)\, d\sigma. \tag{5.8}$$

To obtain the last step, we used the coordinate transformation $\tau = \sigma - s$ in the first integral and subsequently renamed the new variable τ as σ. We estimate the total variation norm of (5.8) in the following way:

$$\|Q_{t+s}\mu - Q_t\, Q_s\, \mu\|_{\mathrm{TV}} \leqslant \int_0^t \|P_{t-\sigma}\, \left(F_f(Q_{\sigma+s}\, \mu) - F_f(Q_\sigma\, Q_s\, \mu)\right)\|_{\mathrm{TV}}\, d\sigma$$
$$\leqslant \int_0^t \|F_f(Q_{\sigma+s}\, \mu) - F_f(Q_\sigma\, Q_s\, \mu)\|_{\mathrm{TV}}\, d\sigma$$
$$\leqslant \|f\|_\infty \int_0^t \|Q_{\sigma+s}\, \mu - Q_\sigma\, Q_s\, \mu\|_{\mathrm{TV}}\, d\sigma.$$

Here, we used Part (iii) of Proposition B.2 (noting that the integrands are continuous in σ) in the first line, (4.17) in the second line and the fact that $f \in \mathrm{BL}([0,1]) \subset C_b([0,1])$ in the last line. Gronwall's Lemma now implies that $\|Q_{t+s}\mu - Q_t\, Q_s\, \mu\|_{\mathrm{TV}} = 0$ for all $s, t \geqslant 0$. □

Lemma 5.2.3. *For all $\mu \in \mathcal{M}([0,1])$ and $s, t \geqslant 0$, we have that*

$$\|Q_t\mu - Q_s\mu\|^*_{\mathrm{BL}} \leqslant \|\mu\|_{\mathrm{TV}} \cdot \left(\|f\|_\infty + \|v\|_\infty\right) \cdot e^{\|f\|_\infty \max(t,s)} \cdot |t-s|.$$

Proof. The statement of this lemma is part of the result of Proposition 4.3.6. □

Lemma 5.2.4. *For all $\mu \in \mathcal{M}([0,1])$ and $t \geqslant 0$, we have that*

(i) $\|Q_t\mu\|_{\mathrm{TV}} \leqslant \|\mu\|_{\mathrm{TV}}\, \exp(\|f\|_\infty\, t)$, *and*

(ii) $\|Q_t\mu\|^*_{\mathrm{BL}} \leqslant \|\mu\|^*_{\mathrm{BL}}\, \exp(|v|_{\mathrm{L}}\, t + \|f\|_{\mathrm{BL}}\, t\, e^{|v|_{\mathrm{L}}\, t})$.

Proof. (i): This estimate is given in Proposition 4.3.6.
(ii): By applying (B.1) and Lemma 4.2.2(ii) we obtain from (4.21) the estimate

$$\|Q_t\, \mu\|^*_{\mathrm{BL}} \leqslant \exp(|v|_{\mathrm{L}}\, t)\, \|\mu\|^*_{\mathrm{BL}} + \int_0^t \exp(|v|_{\mathrm{L}}\, (t-s))\|f\|_{\mathrm{BL}}\, \|Q_s\mu\|^*_{\mathrm{BL}}\, ds.$$

Gronwall's Lemma now yields the statement of Part (ii) of the lemma. □

Corollary 5.2.5. *For all $\mu, \nu \in \mathcal{M}([0,1])$ and $t \geqslant 0$, we have that*

$$\|Q_t\,\mu - Q_t\,\nu\|^*_{\mathrm{BL}} \leqslant \|\mu - \nu\|^*_{\mathrm{BL}}\, \exp(|v|_{\mathrm{L}}\, t + \|f\|_{\mathrm{BL}}\, t\, e^{|v|_{\mathrm{L}}\, t}).$$

Proof. Apply Part (ii) of Lemma 5.2.4 to the measure $\mu - \nu \in \mathcal{M}([0,1])$. □

We write Q^v and $Q^{v'}$ to distinguish between the semigroups Q on $\mathcal{M}([0,1])$ associated to $v \in \mathrm{BL}([0,1])$ and $v' \in \mathrm{BL}([0,1])$, respectively.

Lemma 5.2.6. *For all $v, v' \in \mathrm{BL}([0,1])$, $\mu \in \mathcal{M}([0,1])$ and $t \geqslant 0$, the following estimate holds:*

$$\|Q^v_t\mu - Q^{v'}_t\mu\|^*_{\mathrm{BL}} \leqslant \|v - v'\|_\infty\, \|\mu\|_{\mathrm{TV}}\, \exp(L\, t + \|f\|_{\mathrm{BL}}\, t\, e^{L\, t}) \cdot [t + t^2 \|f\|_\infty\, e^{\|f\|_\infty\, t}],$$

where $L := \min(|v|_{\mathrm{L}}\,, |v'|_{\mathrm{L}})$.

Proof. We have

$$\|Q^v_t\mu - Q^{v'}_t\mu\|^*_{\mathrm{BL}} \leqslant \|P^v_t\mu - P^{v'}_t\mu\|^*_{\mathrm{BL}} + \int_0^t \|P^v_{t-s} F_f(Q^v_s\mu) - P^{v'}_{t-s} F_f(Q^{v'}_s\mu)\|^*_{\mathrm{BL}}\, ds. \quad (5.9)$$

Lemma 5.2.1 provides an appropriate estimate of the first term on the right-hand side. For the integrand in the second term, we have

$$\begin{aligned}\|P^v_{t-s} F_f(Q^v_s\mu) - P^{v'}_{t-s} F_f(Q^{v'}_s\mu)\|^*_{\mathrm{BL}} &\leqslant \|P^v_{t-s} F_f(Q^v_s\mu) - P^{v'}_{t-s} F_f(Q^v_s\mu)\|^*_{\mathrm{BL}} \\ &\quad + \|P^{v'}_{t-s} F_f(Q^v_s\mu) - P^{v'}_{t-s} F_f(Q^{v'}_s\mu)\|^*_{\mathrm{BL}} \\ &\leqslant \|v - v'\|_\infty\, (t-s)\, \|F_f(Q^v_s\mu)\|_{\mathrm{TV}}\, e^{L(t-s)} \\ &\quad + e^{|v'|_{\mathrm{L}}\,(t-s)}\, \|F_f(Q^v_s\mu) - F_f(Q^{v'}_s\mu)\|^*_{\mathrm{BL}}, \quad (5.10)\end{aligned}$$

due to Lemma 5.2.1 and Lemma 4.2.2(ii). We proceed by estimating the right-hand side of (5.10) and obtain

$$\begin{aligned}\|P^v_{t-s} F_f(Q^v_s\mu) - P^{v'}_{t-s} F_f(Q^{v'}_s\mu)\|^*_{\mathrm{BL}} &\leqslant \|v - v'\|_\infty\, (t-s)\, \|f\|_\infty\, \|\mu\|_{\mathrm{TV}}\, e^{\|f\|_\infty\, s}\, e^{L(t-s)} \\ &\quad + e^{|v'|_{\mathrm{L}}\,(t-s)}\, \|f\|_{\mathrm{BL}}\, \|Q^v_s\mu - Q^{v'}_s\mu\|^*_{\mathrm{BL}}, \quad (5.11)\end{aligned}$$

where we use Part (i) of Lemma 5.2.4 in the first term on the right-hand side. Since the estimate in (5.11) is symmetric in v and v', we can replace $|v'|_{\mathrm{L}}$ by L.
Substitution of the result of Lemma 5.2.1 and (5.11) in (5.9) yields

$$\begin{aligned}\|Q^v_t\mu - Q^{v'}_t\mu\|^*_{\mathrm{BL}} &\leqslant \|v - v'\|_\infty\, t\, \|\mu\|_{\mathrm{TV}}\, e^{Lt}\, (1 + t\, \|f\|_\infty\, e^{\|f\|_\infty\, t}) \\ &\quad + e^{Lt}\, \|f\|_{\mathrm{BL}} \int_0^t \|Q^v_s\mu - Q^{v'}_s\mu\|^*_{\mathrm{BL}}\, ds.\end{aligned}$$

The statement of the lemma follows from Gronwall's Lemma. □

5.3 Measure-dependent velocity fields: main results

In this section, we generalize the assumptions on v from Chapter 4 in the following way to measure-dependent velocity fields:

Assumption 5.3.1 (Assumptions on the measure-dependent velocity field)**.** *Assume that $v : \mathcal{M}([0,1]) \times [0,1] \to \mathbb{R}$ is a mapping such that:*

(i) $v[\mu] \in \mathrm{BL}([0,1])$*, for each* $\mu \in \mathcal{M}([0,1])$.

Furthermore, assume that for any $R > 0$ there are constants K_R, L_R, M_R such that for all $\mu, \nu \in \mathcal{M}([0,1])$ satisfying $\|\mu\|_{\mathrm{TV}} \leqslant R$ and $\|\nu\|_{\mathrm{TV}} \leqslant R$, the following estimates hold:

(ii) $\|v[\mu]\|_\infty \leqslant K_R$,

(iii) $|\, v[\mu]\,|_{\mathrm{L}} \leqslant L_R$, *and*

(iv) $\|v[\mu] - v[\nu]\|_\infty \leqslant M_R \, \|\mu - \nu\|^*_{\mathrm{BL}}$.

Example 5.3.2. An example of a function v satisfying Assumption 5.3.1 is:

$$v[\mu](x) := \int_{[0,1]} \mathcal{K}(x-y)\, d\mu(y) = (\mathcal{K} * \mu)(x), \tag{5.12}$$

for each $\mu \in \mathcal{M}([0,1])$ and $x \in [0,1]$, with $\mathcal{K} \in \mathrm{BL}([-1,1])$. This is a relevant choice, because it models interactions; see Section 1.2. In Chapters 2 and 3 interaction terms of the same type were used.

Remark 5.3.3. Parts (ii) and (iii) of Assumption 5.3.1 are an improvement compared to [Hoo13]. There, the infinity norm and Lipschitz constant are assumed to hold uniformly for all $\mu \in \mathcal{M}([0,1])$; cf. Assumption (F1) on p. 40 of [Hoo13]. We note that the convolution in Example 5.3.2 satisfies Assumption 5.3.1, but does not satisfy Assumption (F1) in [Hoo13]. They require a uniform Lipschitz constant because their Lemma 4.3 is an estimate in the $\|\cdot\|^*_{\mathrm{BL}}$-norm for which Part (ii) of our Lemma 4.2.2 is used. Our counterpart of Lemma 4.3 in [Hoo13] is Lemma 5.3.4. We give an estimate in terms of the $\|\cdot\|_{\mathrm{TV}}$-norm using (4.17) which does not involve the Lipschitz constant.

Our aim is to prove well-posedness (in some sense yet to be defined) of the following equation

$$\frac{\partial}{\partial t}\mu_t + \frac{\partial}{\partial x}(v[\mu_t]\,\mu_t) = f \cdot \mu_t. \tag{5.13}$$

As said in Section 5.2.2, we restrict ourselves to f that is bounded Lipschitz on $[0,1]$.

We now introduce the aforementioned forward-Euler-like approach to construct approximate solutions. Let $T > 0$ be given. For each $k \in \mathbb{N}$, define $t^k_j := jT/2^k$, $j \in \{0, \dots, 2^k\}$. Note in particular that $t^k_j = t^{k+1}_{2j}$ for each $j \in \{0, \dots, 2^k\}$.

Let $\mu_0 \in \mathcal{M}([0,1])$ be given. Define a sequence $(\mu^k)_{k\in\mathbb{N}} \subset C([0,T]; \mathcal{M}([0,1]))$ by

$$\mu^0_t = \mu_0, \ \text{ for all } t \in [0,T], \tag{5.14}$$

and

$$\begin{cases} \mu_t^k := Q^{v_j^k}_{t-t_j^k}\,\mu^k_{t_j^k}, & \text{if } t \in (t_j^k, t_{j+1}^k]; \\ v_j^k := v[\mu^k_{t_j^k}]; \\ \mu_0^k = \mu_0, \end{cases} \tag{5.15}$$

for $k \in \mathbb{N}^+$, where $(Q_t^v)_{t\geqslant 0}$ denotes the semigroup introduced in Section 5.2.2 associated to an arbitrary $v \in \mathrm{BL}([0,1])$.

We call this a forward-Euler-like approach, because it is the analogon of the forward Euler method for ODEs (cf. e.g. Chapter 2 in [But03]). Consider the ODE $dx/dt = v(x)$ on $\mathbb{R}$ for some (Lipschitz continuous) $v : \mathbb{R} \to \mathbb{R}$. The forward Euler method approximates the solution on some interval $(t_j, t_{j+1}]$ by evolving the approximate solution at time t_j, named x_j, due to a *constant* velocity $v(x_j)$. That is, $x(t) \approx x_j + (t - t_j) \cdot v(x_j)$ for all $t \in (t_j, t_{j+1}]$.
In (5.15), we introduce the approximation μ_t^k, where μ_t^k results from $\mu^k_{t_j^k}$ by the evolution due to the constant velocity field $v[\mu^k_{t_j^k}]$. The word *constant* here does not refer to v being the same for all $x \in [0,1]$, but to the fact that v corresponding to the same $\mu^k_{t_j^k}$ is used throughout $(t_j^k, t_{j+1}^k]$.

The conditions in Parts (ii)–(iv) of Assumption 5.3.1 are only required to hold for measures in a TV-norm bounded set, in view of the following lemma:

Lemma 5.3.4. *Let $\mu_0 \in \mathcal{M}([0,1])$ be given and let $v : \mathcal{M}([0,1]) \times [0,1] \to \mathbb{R}$ satisfy Assumption 5.3.1(i). Then*

$$\mathcal{A} := \{\mu_t^k : k \in \mathbb{N}, t \in [0,T]\},$$

i.e. the set of all timeslices corresponding to (5.15)*, is bounded in both $\|\cdot\|_{\mathrm{TV}}$ and $\|\cdot\|^*_{\mathrm{BL}}$.*

Proof. Fix $k \in \mathbb{N}^+$ and $j \in \{0, \dots, 2^k - 1\}$ and let $t \in (t_j^k, t_{j+1}^k]$. By Part (i) of Lemma 5.2.4, we have that

$$\begin{aligned} \|\mu_t^k\|_{\mathrm{TV}} = \|Q^{v_j^k}_{t-t_j^k}\,\mu^k_{t_j^k}\|_{\mathrm{TV}} &\leqslant \|\mu^k_{t_j^k}\|_{\mathrm{TV}}\, \exp(\|f\|_\infty\,(t - t_j^k)) \\ &\leqslant \|\mu^k_{t_j^k}\|_{\mathrm{TV}}\, \exp(\|f\|_\infty\, T/2^k) \end{aligned}$$

for all $t \in (t_j^k, t_{j+1}^k]$. Iteration of the right-hand side with respect to j yields

$$\|\mu_t^k\|_{\mathrm{TV}} \leqslant \|\mu_0\|_{\mathrm{TV}}\, \left(\exp(\|f\|_\infty\, T/2^k)\right)^{j+1}.$$

Hence, for all $t \in [0,T]$

$$\begin{aligned} \|\mu_t^k\|_{\mathrm{TV}} &\leqslant \|\mu_0\|_{\mathrm{TV}}\, \left(\exp(\|f\|_\infty\, T/2^k)\right)^{2^k} \\ &= \|\mu_0\|_{\mathrm{TV}}\, \exp(\|f\|_\infty\, T) \end{aligned}$$

This bound is in particular independent of t and k. The bound in $\|\cdot\|^*_{\mathrm{BL}}$ follows from the inequality $\|\mu\|^*_{\mathrm{BL}} \leqslant \|\mu\|_{\mathrm{TV}}$ that holds for all $\mu \in \mathcal{M}([0,1])$. □

We define a mild solution in this context as follows:

Definition 5.3.5 (Mild solution of (5.13))**.** *For each $k \in \mathbb{N}$, let $\mu^k \in C([0,T];\mathcal{M}([0,1]))$ be defined by* (5.15)*. Let $\mathcal{M}([0,1])$ be endowed with the topology induced by $\|\cdot\|^*_{\mathrm{BL}}$. Then, any limit of a subsequence of $(\mu^k)_{k\in\mathbb{N}}$ is called a (measure-valued) mild solution of* (5.13)*.*

The name *mild solutions* is appropriate, because they are constructed from piecewise mild solutions in the sense of Definition 4.2.4.

Remark 5.3.6. Consider the solution of (5.15) for any $k \in \mathbb{N}$. Mass that has accumulated on the boundary can move back into the interior of the domain whenever the velocity changes direction from one time interval to the next. This is due to the definition of the maximal interval of existence I_{x_0} and the hitting time $\tau_\partial(x_0)$ in Section 4.2.1.

We focus on *positive* measure-valued solutions, because these are physically relevant (cf. Remark 4.3.4). The main results of this chapter are the following two theorems.

Theorem 5.3.7. *For each $\mu_0 \in \mathcal{M}^+([0,1])$ and $v : \mathcal{M}([0,1]) \times [0,1] \to \mathbb{R}$ satisfying Assumption 5.3.1, there is a unique element of $C([0,T];\mathcal{M}^+([0,1]))$ with initial condition μ_0, that is a mild solution in the sense of Definition 5.3.5.*

Theorem 5.3.8 (Continuous dependence on initial data)**.** *For all $\tilde{R} > 0$ there is a constant $C_{\tilde{R}}$ such that for all $\mu_0, \nu_0 \in \mathcal{M}^+([0,1])$ satisfying $\|\mu_0\|_{\mathrm{TV}} \leqslant \tilde{R}$ and $\|\nu_0\|_{\mathrm{TV}} \leqslant \tilde{R}$, the corresponding mild solutions $\mu, \nu \in C([0,T];\mathcal{M}^+([0,1]))$ satisfy*

$$\sup_{t\in[0,T]} \|\mu_t - \nu_t\|^*_{\mathrm{BL}} \leqslant C_{\tilde{R}} \|\mu_0 - \nu_0\|^*_{\mathrm{BL}}.$$

The proofs of these two theorems are given in the next section, Section 5.4. The key idea of the proof of Theorem 5.3.7 is to show that the sequence $(\mu^k)_{k\in\mathbb{N}}$ is a Cauchy sequence in a complete metric space, hence converges. We use estimates between subsequent approximations μ^k and μ^{k+1}. Similar estimates are employed to obtain the result of Theorem 5.3.8.

5.4 Proofs of Theorem 5.3.7 and Theorem 5.3.8

In this section we prove the main results of this chapter: Theorem 5.3.7 and Theorem 5.3.8. The essential part of the proof of Theorem 5.3.7 is provided by the following lemma:

Lemma 5.4.1. *For fixed $\mu_0 \in \mathcal{M}^+([0,1])$, the sequence $(\mu^k)_{k\in\mathbb{N}}$ defined by* (5.14)–(5.15) *is a Cauchy sequence in $C([0,T];\mathcal{M}^+([0,1]))$. In particular, there is a constant c such that*

$$\sup_{\tau\in[0,T]} \|\mu^k_\tau - \mu^{k+1}_\tau\|^*_{\mathrm{BL}} \leqslant \frac{c}{2^k},$$

for all $k \in \mathbb{N}$.

Proof. Fix $k \in \mathbb{N}$ and let τ and j be given such that $\tau \in (t^k_j, t^k_{j+1}]$. We recall that $t^k_j = t^{k+1}_{2j}$.

Step 1: The case $\tau \in (t_j^k, t_{2j+1}^{k+1}]$. To simplify notation, we introduce $v := v_j^k = v[\mu_{t_j^k}^k]$ and $v' := v_{2j}^{k+1} = v[\mu_{t_{2j}^{k+1}}^{k+1}]$. Note that

$$\mu_\tau^k = Q^v_{\tau - t_j^k}\, \mu_{t_j^k}^k, \qquad \text{and} \qquad \mu_\tau^{k+1} = Q^{v'}_{\tau - t_{2j}^{k+1}}\, \mu_{t_{2j}^{k+1}}^{k+1}.$$

We estimate

$$\begin{aligned}
\|\mu_\tau^k - \mu_\tau^{k+1}\|_{\mathrm{BL}}^* &\leqslant \|Q^v_{\tau - t_j^k}(\mu_{t_j^k}^k - \mu_{t_j^k}^{k+1})\|_{\mathrm{BL}}^* + \|\big(Q^v_{\tau - t_j^k} - Q^{v'}_{\tau - t_j^k}\big)\mu_{t_j^k}^{k+1}\|_{\mathrm{BL}}^* \\
&\leqslant \|\mu_{t_j^k}^k - \mu_{t_j^k}^{k+1}\|_{\mathrm{BL}}^* \, \exp\left(|v|_{\mathrm{L}}\,(\tau - t_j^k) + \|f\|_{\mathrm{BL}}\,(\tau - t_j^k)\, e^{|v|_{\mathrm{L}}\,(\tau - t_j^k)} \right) \\
&\quad + \|v - v'\|_\infty \, \|\mu_{t_j^k}^{k+1}\|_{\mathrm{TV}} \, \exp\left(L\,(\tau - t_j^k) + \|f\|_{\mathrm{BL}}\,(\tau - t_j^k)\, e^{L\,(\tau - t_j^k)} \right) \cdot \\
&\quad \cdot \left[(\tau - t_j^k) + (\tau - t_j^k)^2 \|f\|_\infty \, e^{\|f\|_\infty\,(\tau - t_j^k)} \right],
\end{aligned} \tag{5.16}$$

using Corollary 5.2.5 and Lemma 5.2.6. Here, L denotes $\min(|v|_{\mathrm{L}}, |v'|_{\mathrm{L}})$. In view of Lemma 5.3.4, we define $R := \|\mu_0\|_{\mathrm{TV}} \cdot \exp(\|f\|_\infty T)$. From Parts (iii) and (iv) of Assumption 5.3.1 and the fact that $\tau - t_j^k \leqslant T/2^{k+1} < T$ it follows that

$$\begin{aligned}
\|\mu_\tau^k - \mu_\tau^{k+1}\|_{\mathrm{BL}}^* &\leqslant \|\mu_{t_j^k}^k - \mu_{t_j^k}^{k+1}\|_{\mathrm{BL}}^* \, \exp\left(L_R \, \frac{T}{2^{k+1}} + \|f\|_{\mathrm{BL}} \, \frac{T}{2^{k+1}} \, e^{L_R\, T} \right) \cdot \\
&\quad \cdot \left[1 + M_R\, R \, \frac{T}{2^{k+1}} + M_R\, R \, \left(\frac{T}{2^{k+1}} \right)^2 \|f\|_\infty \, e^{\|f\|_\infty\, T} \right].
\end{aligned}$$

Hence, there are positive constants $A_{1,1}$ and $A_{1,2}$, independent of j and k, such that the following estimate holds for all $\tau \in (t_j^k, t_{2j+1}^{k+1}]$:

$$\|\mu_\tau^k - \mu_\tau^{k+1}\|_{\mathrm{BL}}^* \leqslant \exp\left(A_{1,1} \, \frac{T}{2^{k+1}} \right) \cdot \left(1 + A_{1,2} \, \frac{T}{2^{k+1}} \right) \|\mu_{t_j^k}^k - \mu_{t_j^k}^{k+1}\|_{\mathrm{BL}}^*. \tag{5.17}$$

Here, we have estimated $(T/2^{k+1})^2 \leqslant T\,(T/2^{k+1})$ and incorporated the corresponding term in the term with prefactor $A_{1,2}$.

Step 2: The case $\tau \in (t_{2j+1}^{k+1}, t_{j+1}^k]$. We note that

$$\mu_\tau^k = Q^v_{\tau - t_{2j+1}^{k+1}} \, \mu_{t_{2j+1}^{k+1}}^k$$

holds, because of the semigroup property proved in Lemma 5.2.2. We define $v'' := v_{2j+1}^{k+1} = v[\mu_{t_{2j+1}^{k+1}}^{k+1}]$ and hence we have

$$\mu_\tau^{k+1} = \, Q^{v''}_{\tau - t_{2j+1}^{k+1}} \, \mu_{t_{2j+1}^{k+1}}^{k+1} \, .$$

We estimate the difference between the approximations at time τ like in (5.16). Applying the results of Corollary 5.2.5 and Lemma 5.2.6, we obtain

$$\|\mu_\tau^k - \mu_\tau^{k+1}\|_{\mathrm{BL}}^* \leqslant \|Q^v_{\tau - t^{k+1}_{2j+1}}(\mu^k_{t^{k+1}_{2j+1}} - \mu^{k+1}_{t^{k+1}_{2j+1}})\|_{\mathrm{BL}}^* + \|\big(Q^v_{\tau - t^{k+1}_{2j+1}} - Q^{v''}_{\tau - t^{k+1}_{2j+1}}\big)\mu^{k+1}_{t^{k+1}_{2j+1}}\|_{\mathrm{BL}}^*$$

$$\begin{aligned}
&\leqslant \|\mu^k_{t^{k+1}_{2j+1}} - \mu^{k+1}_{t^{k+1}_{2j+1}}\|_{\mathrm{BL}}^* \exp\left(L_R \frac{T}{2^{k+1}} + \|f\|_{\mathrm{BL}} \frac{T}{2^{k+1}} e^{L_R T}\right) \\
&\quad + \|v - v''\|_\infty \, R \exp\left(L_R \frac{T}{2^{k+1}} + \|f\|_{\mathrm{BL}} \frac{T}{2^{k+1}} e^{L_R T}\right) \cdot \\
&\qquad \cdot \left[\frac{T}{2^{k+1}} + \left(\frac{T}{2^{k+1}}\right)^2 \|f\|_\infty e^{\|f\|_\infty T}\right], \quad (5.18)
\end{aligned}$$

with $R := \|\mu_0\|_{\mathrm{TV}} \cdot \exp(\|f\|_\infty T)$ as before; cf. Lemma 5.3.4. We also used Part (iii) of Assumption 5.3.1 and the fact that $\tau - t^{k+1}_{2j+1} \leqslant T/2^{k+1} < T$. Using Part (iv) of Assumption 5.3.1, we treat the difference of velocities $\|v - v''\|_\infty = \|v^k_j - v^{k+1}_{2j+1}\|_\infty$ as follows:

$$\begin{aligned}
\|v - v''\|_\infty &\leqslant \| \, v[\mu^k_{t^k_j}] - v[\mu^{k+1}_{t^k_j}] \, \|_\infty + \| \, v[\mu^{k+1}_{t^k_j}] - v[\mu^{k+1}_{t^{k+1}_{2j+1}}] \, \|_\infty \\
&\leqslant M_R \, \|\mu^k_{t^k_j} - \mu^{k+1}_{t^k_j}\|_{\mathrm{BL}}^* + M_R \, \|\mu^{k+1}_{t^k_j} - \mu^{k+1}_{t^{k+1}_{2j+1}}\|_{\mathrm{BL}}^*, \quad (5.19)
\end{aligned}$$

in which we estimate the last term as

$$\begin{aligned}
\|\mu^{k+1}_{t^k_j} - \mu^{k+1}_{t^{k+1}_{2j+1}}\|_{\mathrm{BL}}^* &= \|\mu^{k+1}_{t^k_j} - Q^{v'}_{t^{k+1}_{2j+1} - t^k_j} \mu^{k+1}_{t^k_j}\|_{\mathrm{BL}}^* \\
&\leqslant \|\mu^{k+1}_{t^k_j}\|_{\mathrm{TV}} \left(\|f\|_\infty + \|v'\|_\infty\right) e^{\|f\|_\infty (t^{k+1}_{2j+1} - t^k_j)} \cdot (t^{k+1}_{2j+1} - t^k_j).
\end{aligned}$$

This inequality is due to Lemma 5.2.3 and the observation that $\mu^{k+1}_{t^k_j} = Q^{v'}_0 \, \mu^{k+1}_{t^k_j}$. Using the bound $(t^{k+1}_{2j+1} - t^k_j) \leqslant T/2^{k+1} < T$ and Assumption 5.3.1(ii), we obtain

$$\|\mu^{k+1}_{t^k_j} - \mu^{k+1}_{t^{k+1}_{2j+1}}\|_{\mathrm{BL}}^* \leqslant R \, (\|f\|_\infty + K_R) \, e^{\|f\|_\infty T} \cdot \frac{T}{2^{k+1}}. \quad (5.20)$$

We substitute (5.19) and (5.20) in (5.18) and note that (5.17) provides an upper bound on

$$\|\mu^k_{t^{k+1}_{2j+1}} - \mu^{k+1}_{t^{k+1}_{2j+1}}\|_{\mathrm{BL}}^*.$$

Hence, finally we obtain that for all $\tau \in (t^{k+1}_{2j+1}, t^k_{j+1}]$ the estimate

$$\begin{aligned}
\|\mu^k_\tau - \mu^{k+1}_\tau\|_{\mathrm{BL}}^* \leqslant \exp\left(A_{2,1} \frac{T}{2^{k+1}}\right) \cdot \left(1 + A_{2,2} \frac{T}{2^{k+1}}\right) \|\mu^k_{t^k_j} - \mu^{k+1}_{t^k_j}\|_{\mathrm{BL}}^* \\
+ A_{2,3} \left(\frac{T}{2^{k+1}}\right)^2, \quad (5.21)
\end{aligned}$$

holds for some positive constants $A_{2,1}$, $A_{2,2}$ and $A_{2,3}$ independent of j and k. Like we did with $A_{1,2}$, we have incorporated higher-order terms in $A_{2,2}$ and $A_{2,3}$.

Step 3: The entire interval $(t_{2j+1}^{k+1}, t_{j+1}^{k}]$**.** A suitable combination of (5.17) and (5.21) yields that there are positive constants A_1, A_2 and A_3, independent of j and k, such that

$$\sup_{\tau\in(t_j^k,t_{j+1}^k]} \|\mu_\tau^k - \mu_\tau^{k+1}\|_{\mathrm{BL}}^* \leqslant \exp\left(A_1\,\frac{T}{2^{k+1}}\right)\cdot\left(1+A_2\,\frac{T}{2^{k+1}}\right)\,\|\mu_{t_j^k}^k - \mu_{t_j^k}^{k+1}\|_{\mathrm{BL}}^* + A_3\left(\frac{T}{2^{k+1}}\right)^2 \tag{5.22}$$

holds. Note that $\|\mu_{t_j^k}^k - \mu_{t_j^k}^{k+1}\|_{\mathrm{BL}}^* = 0$ if $j = 0$. Applying (5.22) iteratively, we derive for each $j \in \{0,\dots,2^k-1\}$ the inequality:

$$\sup_{\tau\in(t_j^k,t_{j+1}^k]} \|\mu_\tau^k - \mu_\tau^{k+1}\|_{\mathrm{BL}}^* \leqslant \sum_{\ell=0}^{j} \exp\left(A_1\,\frac{\ell\,T}{2^{k+1}}\right)\cdot\left(1+A_2\,\frac{T}{2^{k+1}}\right)^{\ell} A_3\left(\frac{T}{2^{k+1}}\right)^2. \tag{5.23}$$

We take the supremum over j on both sides of the inequality and obtain

$$\begin{aligned}\sup_{\tau\in[0,T]} \|\mu_\tau^k - \mu_\tau^{k+1}\|_{\mathrm{BL}}^* &\leqslant \sum_{\ell=0}^{2^k-1} \exp\left(A_1\,\frac{\ell\,T}{2^{k+1}}\right)\cdot\left(1+A_2\,\frac{T}{2^{k+1}}\right)^{\ell} A_3\left(\frac{T}{2^{k+1}}\right)^2 \\ &\leqslant A_3\left(\frac{T}{2^{k+1}}\right)^2 \exp\left(A_1\,T/2\right)\,\sum_{\ell=0}^{2^k-1}\left(1+A_2\,\frac{T}{2^{k+1}}\right)^{\ell}. \end{aligned}\tag{5.24}$$

Including $\tau = 0$ in the supremum does not change the upper bound. Note that

$$\left(1+A_2\,\frac{T}{2^{k+1}}\right)^{\ell} = \sum_{i=0}^{\ell}\binom{\ell}{i}\left(A_2\,\frac{T}{2^{k+1}}\right)^{i},$$

while

$$\binom{\ell}{i} = \frac{\ell!}{i!\,(\ell-i)!} = \frac{1}{i!}\prod_{q=1}^{i}(\ell-i+q) \leqslant \frac{(2^k)^i}{i!},$$

because $\ell \leqslant 2^k - 1$. Hence,

$$\left(1+A_2\,\frac{T}{2^{k+1}}\right)^{\ell} \leqslant \sum_{i=0}^{\ell}\frac{(A_2\,T)^i}{i!} \leqslant e^{A_2\,T}. \tag{5.25}$$

A combination of (5.24) and (5.25) yields

$$\begin{aligned}\sup_{\tau\in[0,T]} \|\mu_\tau^k - \mu_\tau^{k+1}\|_{\mathrm{BL}}^* &\leqslant A_3\left(\frac{T}{2^{k+1}}\right)^2 \exp\left(A_1\,T/2\right)\,2^k\,e^{A_2\,T} \\ &\leqslant A_3\,\frac{T^2}{2^{k+1}}\,\exp\left(A_1\,T/2 + A_2\,T\right), \end{aligned}\tag{5.26}$$

which implies the statement of the lemma. Indeed, $(\mu^k)_{k\in\mathbb{N}}$ is a Cauchy sequence, since (5.26) provides a constant c such that for all $n \in \mathbb{N}^+$ and $m > n$

$$\sup_{\tau\in[0,T]} \|\mu_\tau^m - \mu_\tau^n\|_{\mathrm{BL}}^* \leqslant \sum_{k=n}^{m-1} \sup_{\tau\in[0,T]} \|\mu_\tau^k - \mu_\tau^{k+1}\|_{\mathrm{BL}}^* \leqslant \sum_{k=n}^{m-1} \frac{c}{2^k}$$
$$= c\left(\frac{1}{2^{n-1}} - \frac{1}{2^{m-1}}\right) \leqslant \frac{c}{2^{n-1}}.$$

Hence for all $\varepsilon > 0$, $\sup_{\tau\in[0,T]} \|\mu_\tau^m - \mu_\tau^n\|_{\mathrm{BL}}^* < \varepsilon$ for all $m > n \geqslant \bar{N} := \log_2(\frac{c}{\varepsilon})$. □

Remark 5.4.2. It is crucial that we use $\|\cdot\|_{\mathrm{BL}}^*$ and not $\|\cdot\|_{\mathrm{TV}}$ in Lemma 5.4.1. The factor $\|v - v'\|_\infty$ appears in (5.16) due to Lemma 5.2.6. Due to Assumption 5.3.1(iv) we subsequently obtain an estimate in which $\|\mu_{t_j^k}^k - \mu_{t_j^k}^{k+1}\|_{\mathrm{BL}}^*$ appears *as a factor*. This is essential for the result of the lemma. Note that Lemma 5.2.6 builds on Lemma 5.2.1. In (5.2) the Lipschitz property of the test functions is explicitly used and hence, there is no direct way to formulate the result of Lemma 5.2.1 in terms of $\|\cdot\|_{\mathrm{TV}}$. Consequently, we do not have an estimate of $\|\mu_\tau^k - \mu_\tau^{k+1}\|_{\mathrm{TV}}$ against $\|v - v'\|_\infty$ comparable to (5.16).

We recall and prove Theorem 5.3.7.

Theorem 5.3.7. *For each $\mu_0 \in \mathcal{M}^+([0,1])$ and $v : \mathcal{M}([0,1]) \times [0,1] \to \mathbb{R}$ satisfying Assumption 5.3.1, there is a unique element of $C([0,T];\mathcal{M}^+([0,1]))$ with initial condition μ_0, that is a mild solution in the sense of Definition 5.3.5.*

Proof. By definition, $\overline{\mathcal{M}}([0,1])$ is complete in the metric induced by the norm $\|\cdot\|_{\mathrm{BL}}^*$. In Lemma 4.1.1, $\mathcal{M}^+([0,1])$ is proved to be a closed subspace of $\overline{\mathcal{M}}([0,1])$, so $\mathcal{M}^+([0,1])$ is complete; cf. Lemma A.2 in Appendix A. Hence, due to Theorem A.3, the space

$$\{\nu \in C([0,T];\mathcal{M}^+([0,1])) \,:\, \nu(0) = \mu_0\}$$

is complete for the metric defined for all $\mu, \nu \in C([0,T];\mathcal{M}^+([0,1]))$ by

$$\sup_{t\in[0,T]} \|\mu_t - \nu_t\|_{\mathrm{BL}}^*.$$

For each initial measure $\mu_0 \in \mathcal{M}^+([0,1])$ and for each $k \in \mathbb{N}$, the Euler approximation defined by (5.15) is an element of $C([0,T];\mathcal{M}^+([0,1]))$, because the semigroup $(Q_t^v)_{t\geqslant 0}$ preserves positivity for all $v \in \mathrm{BL}([0,1])$. In Lemma 5.4.1, we showed that $(\mu^k)_{k\in\mathbb{N}}$ is a Cauchy sequence in $\{\nu \in C([0,T];\mathcal{M}^+([0,1])) \,:\, \nu(0) = \mu_0\}$, which is a complete space, as was argued above. Hence, the sequence $(\mu^k)_{k\in\mathbb{N}}$ converges in $\{\nu \in C([0,T];\mathcal{M}^+([0,1])) \,:\, \nu(0) = \mu_0\}$ and we have existence of a mild solution. Each subsequence as mentioned in Definition 5.3.5 converges to that same limit, thus uniqueness of the mild solution holds. □

Moreover, we recall Theorem 5.3.8:

Theorem 5.3.8 (Continuous dependence on initial data)**.** *For all $\tilde{R} > 0$ there is a constant $C_{\tilde{R}}$ such that for all $\mu_0, \nu_0 \in \mathcal{M}^+([0,1])$ satisfying $\|\mu_0\|_{\mathrm{TV}} \leqslant \tilde{R}$ and $\|\nu_0\|_{\mathrm{TV}} \leqslant \tilde{R}$, the corresponding mild solutions $\mu, \nu \in C([0,T]; \mathcal{M}^+([0,1]))$ satisfy*

$$\sup_{t\in[0,T]} \|\mu_t - \nu_t\|^*_{\mathrm{BL}} \leqslant C_{\tilde{R}} \, \|\mu_0 - \nu_0\|^*_{\mathrm{BL}}.$$

Proof. Each mild solution is the limit of a sequence defined by (5.15). Let $(\mu^k)_{k\in\mathbb{N}}$ and $(\nu^k)_{k\in\mathbb{N}}$ denote such sequences converging to μ and ν, respectively. It follows from Lemma 5.3.4 that all elements of

$$\{\mu^k_t : k \in \mathbb{N}, t \in [0,T]\} \cup \{\nu^k_t : k \in \mathbb{N}, t \in [0,T]\}$$

are bounded by $R := \tilde{R} \exp(\|f\|_\infty T)$ in both $\|\cdot\|_{\mathrm{TV}}$ and $\|\cdot\|^*_{\mathrm{BL}}$. Fix $k \in \mathbb{N}$, let $\tau \in (t^k_j, t^k_{j+1}]$ and consider the distance $\|\mu^k_\tau - \nu^k_\tau\|^*_{\mathrm{BL}}$. By an estimate in the spirit of (5.16)–(5.17), we obtain

$$\|\mu^k_\tau - \nu^k_\tau\|^*_{\mathrm{BL}} \leqslant e^{B_1 \, T/2^k} \left(1 + B_2 \, \frac{RT}{2^k}\right) \|\mu^k_{t^k_j} - \nu^k_{t^k_j}\|^*_{\mathrm{BL}}, \tag{5.27}$$

for some positive constants B_1 and B_2 independent of j and k. This estimate holds for all $\tau \in (t^k_j, t^k_{j+1}]$. We used that $\tau - t^k_j \leqslant T/2^k$ for all such τ. It follows from the recursive relation (5.27) that

$$\begin{aligned}\sup_{\tau\in[0,T]} \|\mu^k_\tau - \nu^k_\tau\|^*_{\mathrm{BL}} &\leqslant \left(\exp(B_1 \, T/2^k) \cdot \left(1 + B_2 \, \frac{RT}{2^k}\right)\right)^{2^k} \|\mu^k_0 - \nu^k_0\|^*_{\mathrm{BL}} \\ &\leqslant \exp(B_1 \, T + B_2 \, RT) \cdot \|\mu_0 - \nu_0\|^*_{\mathrm{BL}}, \end{aligned} \tag{5.28}$$

for all $k \in \mathbb{N}$, where the last step is based on the same arguments as the ones leading to (5.25). The triangle inequality yields

$$\sup_{\tau\in[0,T]} \|\mu_\tau - \nu_\tau\|^*_{\mathrm{BL}} \leqslant \sup_{\tau\in[0,T]} \|\mu^k_\tau - \nu^k_\tau\|^*_{\mathrm{BL}} + \underbrace{\sup_{\tau\in[0,T]} \|\mu^k_\tau - \mu_\tau\|^*_{\mathrm{BL}}}_{\to 0} + \underbrace{\sup_{\tau\in[0,T]} \|\nu^k_\tau - \nu_\tau\|^*_{\mathrm{BL}}}_{\to 0},$$

whence the same estimate as in (5.28) holds for $\sup_{\tau\in[0,T]} \|\mu_\tau - \nu_\tau\|^*_{\mathrm{BL}}$. □

Remark 5.4.3. We would have been inclined to use directly the result of Proposition 4.3.8, instead of deriving (5.27). We need, however, the exact dependence on $T/2^k$ of the prefactor, to make sure that the prefactor in (5.28) is bounded. This dependence is not (directly) provided by Proposition 4.3.8.

Remark 5.4.4. The result of Theorem 5.3.8 relies – via Corollary 5.2.5 and Lemma 5.2.6 – on Gronwall's Inequality. This is possible here because we restrict ourselves to Lipschitz perturbations. In Chapter 4 we considered the more general class of *piecewise* bounded Lipschitz perturbations. Hence, in the paragraph before Proposition 4.3.8 it was stated that the standard approach there does not work.

5.5 Discussion

In this chapter we have generalized the results of Chapter 4 to measure-dependent velocity fields via a forward-Euler-like approach. Our motivation was to derive flux boundary conditions for systems whose dynamics are driven by interactions. Such dynamics are in general more interesting than the dynamics that follow from prescribed velocity fields as in Chapter 4. We managed to obtain a converging procedure, but only for bounded Lipschitz continuous right-hand sides. Hence, our results hold for boundary layers in which mass decays, but not for the limit case of vanishing boundary layer. We start off this discussion section by commenting on the possibility to extend to piecewise bounded Lipschitz right-hand sides and to obtain the limit of vanishing boundary layer.

5.5.1 Piecewise bounded Lipschitz perturbations

To obtain the technical results in Section 5.2.2, we explicitly used the assumption that the perturbation f is bounded Lipschitz on $[0,1]$. Theorem 5.3.7 and Theorem 5.3.8 rely on the results in Section 5.2.2. We would have liked to obtain these results for piecewise bounded Lipschitz f, in particular to model decay of mass at one of the boundaries only. In Chapter 4 we circumvent the arising problems by providing the solution explicitly in (4.26). In the setting of Chapter 5, this explicit form would be given for each interval $(t_j^k, t_{j+1}^k]$, $k \in \mathbb{N}$, in (5.15) by

$$\mu_t^k := \int_{[0,1]} \exp\left(\int_0^{t-t_j^k} f(\Phi_s^{v_j^k}(x))\, ds \right) \cdot \delta_{\Phi_{t-t_j^k}^{v_j^k}(x)}\, d\mu_{t_j^k}^k(x). \tag{5.29}$$

In Chapter 4 we showed that it is possible to obtain the estimates needed to establish continuous dependence on initial data, because this explicit form has a regularizing effect on f and its discontinuities due to the integration in time. The key ingredient there, which is absent in the approach of this chapter, is the fact that the velocity field is the same for all time. If one wants to prove Theorem 5.3.8 using (5.29) instead of the properties of the semigroup Q, one encounters that at some point for any $\Delta t > 0$ fixed a Lipschitz estimate of the form

$$\| \int_0^{\Delta t} f(\Phi_s^v(\cdot))\, ds - \int_0^{\Delta t} f(\Phi_s^u(\cdot))\, ds \|_\infty \leqslant C \, \|u - v\|_\infty \tag{5.30}$$

is required, for all u and v taken from a class of admissible velocity fields. One would then proceed to estimate $\|u - v\|_\infty$ against the BL-distance of the corresponding measures, using Part (iv) of Assumption 5.3.1.

In view of Chapter 4, the restriction that the velocity should not be zero at discontinuities of f is reasonable. Even if we are willing to obey that condition, an estimate like (5.30) cannot be expected to hold. Let $f(x) = 0$ if $x \in [0,1)$ and $f(1) = 1$. Take $\varepsilon > 0$

and take $v \equiv \varepsilon$, $u \equiv -\varepsilon$. Then (for $\varepsilon < 1/\Delta t$)

$$\| \int_0^{\Delta t} f(\Phi_s^v(\cdot))\, ds - \int_0^{\Delta t} f(\Phi_s^u(\cdot))\, ds \|_\infty \geqslant | \int_0^{\Delta t} f(\Phi_s^v(1))\, ds - \int_0^{\Delta t} f(\Phi_s^u(1))\, ds |$$
$$= | \int_0^{\Delta t} f(1)\, ds - \int_0^{\Delta t} f(1 - \varepsilon\, s)\, ds | = \Delta t.$$

Since $\Delta t > 0$ is fixed and $\|u - v\|_\infty = 2\varepsilon$ can be made arbitrarily small, (5.30) cannot be satisfied.
An additional difficulty is that it remains to be seen how we can assure that a condition like $v(1) \neq 0$ is satisfied by a velocity field that depends on the solution itself.

5.5.2 Future directions

The extension of the results stated in Theorem 5.3.7 and Theorem 5.3.8 to functions f with discontinuities would clear the way for an approximation procedure like the one treated in Chapter 4. Apart from establishing the well-posedness of the problem for discontinuous f, there is an additional point to investigate: the question whether the Euler approximation limit and the boundary layer limit commute.

Let us focus on the vanishing boundary layer like in Chapter 4. Assume there are regions around 0 and 1 in which mass decays, and that these regions shrink to zero width. That is, there is a sequence $(f_n)_{n\in\mathbb{N}} \subset \mathrm{BL}([0,1])$ and there is an f satisfying $f(x) = 0$ if $x \in (0,1)$ and $f(0) = f(1) = 1$, such that $f_n \to f$ pointwise, and the Lebesgue measure of the set $\{x \in [0,1] : f_n(x) \neq f(x)\}$ tends to zero as $n \to \infty$. If we assume that we can extend the result of this chapter to piecewise bounded Lipschitz f, then well-posedness for the limit case is guaranteed. It remains to be proven however that the solution for finite boundary layer actually converges to the solution of the limit problem.
This is the same question as asking whether the two limits that we take, actually commute. The first limit is in the forward-Euler-like approach to obtain a mild solution. We assigned an index k to the elements in the approximating sequence and proved in Theorem 5.3.7 that the limit "$\lim_{k\to\infty}$" exists (for $f \in \mathrm{BL}([0,1])$). The second limit "$\lim_{n\to\infty}$" is the one introduced here involving the sequence $(f_n)_{n\in\mathbb{N}} \subset \mathrm{BL}([0,1])$. Proving the well-posedness for f piecewise bounded Lipschitz, is the same as proving that the limit "$\lim_{k\to\infty} \lim_{n\to\infty}$" exists. Proving that the sequence of solutions corresponding to each f_n actually converges to some limit in $C([0,T]; \mathcal{M}^+([0,1]))$ is equivalent to proving that "$\lim_{n\to\infty} \lim_{k\to\infty}$" exists. To conclude that the two limits commute, an additional argument is needed. It requires a characterization of "$\lim_{n\to\infty} \lim_{k\to\infty}$" that can be compared to "$\lim_{k\to\infty} \lim_{n\to\infty}$". Both proving that "$\lim_{n\to\infty} \lim_{k\to\infty}$" exists and characterizing the limit can be a difficult task, however, since our current results do not provide an explicit expression for "$\lim_{k\to\infty}$".

There are two reasons why we obtained uniqueness of mild solutions in this chapter. On the one hand, this is because the constructed approximating sequence converges, thus

inevitably each subsequence (cf. Definition 5.3.5) converges to the same limit. On the other hand, uniqueness holds because we constructed only one approximating sequence, namely by partitioning the interval $[0,T]$ into 2^k subintervals. We conjecture however that the same convergence result holds for a partitioning into q^k equal subintervals with arbitrary $q \in \mathbb{N}^+$. This claim remains to be proved, and if we manage to do so, then the question needs to be answered whether all limits obtained in this way are the same. We note that if $[0,T]$ is subdivided in intervals of unequal length, then most likely a uniformity condition on the interval length is needed. This can be understood if we consider (5.24), and replace the factors $T/2^{k+1}$ in the sum over ℓ by quantities d_ℓ representing the interval lengths. If we want the right-hand side to tend to zero as $k \to \infty$, then we have to make sure that *all* subintervals become small sufficiently fast as $k \to \infty$.
To apply the iterative argument that we used to obtain (5.23), one needs the partitioning for index $k+1$ to be a refinement of the partitioning for index k. The required calculations are substantially more complicated if subsequent partitionings are not refinements.

One step beyond the measure-dependent velocity fields proposed in this chapter, is to add anisotropy due to a field of vision. This would link the approach of Chapters 4 and 5 to Chapter 2.

An additional result to be derived concerns the stability with respect to parameters, in particular with respect to f and the specific form of v. This remark also applies to Chapter 4. In fact, Lemma 5.2.6 provides stability in v for the solution of Chapter 4, provided that $f \in \mathrm{BL}([0,1])$. Stability statements are essential in view of parameter *identification*. It is important to know how measurement errors in the parameters affect the solution of our model.

Chapter 6

Approximation of a mass-emitting object by a point source

We consider a linear diffusion equation for the mass density u on $\Omega := \mathbb{R}^2 \setminus \overline{\Omega_{\mathcal{O}}}$, where $\Omega_{\mathcal{O}}$ is a bounded domain. The time-dependent flux across the boundary $\Gamma := \partial\Omega_{\mathcal{O}}$ is prescribed. The aim of this chapter is to approximate the dynamics by the diffusion equation on the whole of $\mathbb{R}^2$ with a measure-valued point source in the origin. We denote by $\hat{u}$ the solution of the latter equation with a point source. The main question is:

Can we quantify the difference between the solutions u and $\hat{u}$ and their fluxes on Γ in a suitable Sobolev norm?

We use an $L^2([0,t];L^2(\Gamma))$-bound to estimate the difference in flux on the boundary. This estimate holds for all $t > 0$. Regarding the difference of the solutions to the two models an $L^2(\Omega)$-bound (for all time) and an $L^2([0,t];H^1(\Omega))$-bound are given. The chapter is closed by a conjecture that these bounds actually tend to zero.

6.1 Introduction

Our ultimate goal is to model a large number of small objects emitting or absorbing mass while moving in a bounded domain. We have in mind for instance the transport of chemical compounds by small vesicles within cells; cf. e.g. [LE97, BŠM03]. In this chapter we focus on a reduced scenario involving a single stationary vesicle.

Let $\Omega_{\mathcal{O}} \in \mathbb{R}^2$ be an open and bounded domain, such that its boundary $\Gamma := \partial\Omega_{\mathcal{O}}$ is C^2 and has finite length. This set denotes the interior of an object $\mathcal{O}$ with mass exchange

The work presented in this chapter is joint work with Sander Hille and Adrian Muntean, which started after fruitful discussions during the workshop "Modelling with Measures: from Structured Populations to Crowd Dynamics", organized at the Lorentz Center in Leiden, The Netherlands. It has been published in Mathematical Biosciences and Engineering [EHM15b].

through its boundary. We assume $0 \in \Omega_{\mathcal{O}}$. Let Ω denote the exterior of $\mathcal{O}$. That is, $\Omega := \mathbb{R}^2 \setminus \overline{\Omega_{\mathcal{O}}}$. See Figure 6.1a for a sketch of the geometry.

The quantity u is the concentration of mass in Ω. For given initial condition $u_0 : \Omega \to \mathbb{R}^+$ and given flux $\phi : \Gamma \times [0,T] \to \mathbb{R}$, we consider the problem

$$\begin{cases} \dfrac{\partial u}{\partial t} = D\Delta u, & \text{on } \Omega \times \mathbb{R}^+; \\ u(0) = u_0, & \text{on } \Omega; \\ D\nabla u \cdot n = \phi, & \text{on } \Gamma \times \mathbb{R}^+. \end{cases} \tag{6.1}$$

Here, $D > 0$ denotes the diffusion coefficient, which is fixed throughout this chapter. The vector n denotes the unit normal pointing outwards on Γ (so *into* $\Omega_{\mathcal{O}}$), and ϕ is the *influx* of u with respect to Ω. Positive ϕ corresponds to flux in the direction of $-n$.

Use $v_0 : \overline{\Omega_{\mathcal{O}}} \to \mathbb{R}^+$ to define $\hat{u}_0 : \mathbb{R}^2 \to \mathbb{R}^+$, given by

$$\hat{u}_0 := \begin{cases} u_0, & \text{on } \Omega; \\ v_0, & \text{on } \overline{\Omega_{\mathcal{O}}}, \end{cases} \tag{6.2}$$

which is an extension of u_0 to the whole of $\mathbb{R}^2$. Our target is to quantify the quality of approximation of the solution of (6.1) (with an appropriate solution concept, see Section 6.4 below) with the restriction to Ω of the *mild solution* of the problem

$$\begin{cases} \dfrac{\partial \hat{u}}{\partial t} = D\Delta \hat{u} + \bar{\phi}\delta_0, & \text{on } \mathbb{R}^2 \times \mathbb{R}^+; \\ \hat{u}(0) = \hat{u}_0, & \text{on } \mathbb{R}^2, \end{cases} \tag{6.3}$$

(see also Section 6.4).

Remark 6.1.1. Typically, the object $\mathcal{O}$ is *small*, but even if that is not the case, the approach of this chapter gives information about how much the solutions of the two problems deviate on Ω. In this chapter, it is not our objective to investigate the behaviour of (6.1) in the limit as $\mathcal{O}$ shrinks to the origin, so here $\mathcal{O}$ keeps physical proportions.

Remark 6.1.2. In (6.3), we have introduced a mapping $\bar{\phi} : \mathbb{R}^+ \to \mathbb{R}$ which represents the magnitude of the mass source. A measure-valued source was treated, for instance, in [SGTK12] (in the context of numerical approximation schemes) or in [BDGO97]; see also [LM72] for more background on the solvability of such evolution equations.

Remark 6.1.3. Problem (6.3) is posed on $\mathbb{R}^2$. The boundary Γ has no physical meaning in this problem; see Figure 6.1b. However, the flux on this imaginary curve will be used in later estimates.

In Section 6.2 we summarize the main results of this chapter, followed by some preliminaries in Section 6.3. In Section 6.5 we show the boundedness of the difference in the flux of the full problem (including the finite-size object) and the flux of the reduced problem (including the point source). This result is used in Section 6.6, where we estimate the difference between the two problems' solutions on the exterior domain. In the discussion section, Section 6.7, we state a conjecture about when we expect the differences in solutions and in flux to be small.

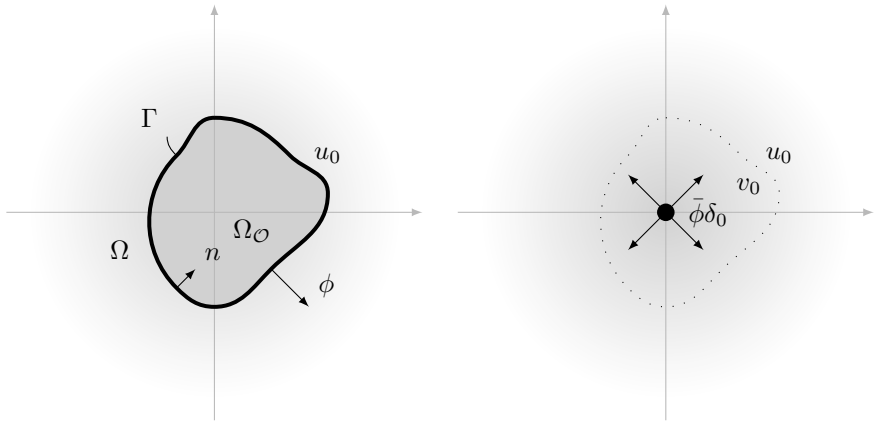

(a) Original domain (b) Extended domain

Figure 6.1: (a): Typical example of the original domain Ω outside the object $\mathcal{O}$, on which u evolves according to (6.1) starting from initial condition u_0. Also, ϕ and n, related to the boundary condition on Γ, are indicated. (b): Domain for the reduced problem associated to (a). Γ is now an imaginary curve within the domain (to be used later). The initial conditions u_0 and v_0 hold outside and inside Γ, respectively. The point source of magnitude $\bar{\phi}$ is indicated in the origin.

6.2 Summary of the main results

In Section 6.4 we use available results on maximal regularity that establish the existence of a unique solution u to Problem (6.1) in the sense of $L^2(\Omega)$-valued distributions, provided the initial condition $u_0 \in H^1(\Omega)$ and the prescribed flux $\phi \in H^1([0,T], L^2(\Gamma)) \cap L^2([0,T], H^1(\Gamma))$. Mild solutions to Problem (6.3) exist in a suitable Banach space containing the finite Borel measures for any initial *measure*, provided $\bar{\phi} \in L^1_{\mathrm{loc}}(\mathbb{R}^+)$ (see Section 6.4). We show that, for more regular initial condition $\hat{u}_0 \in H^1(\mathbb{R}^2)$ and flux from the source $\bar{\phi} \in H^1([0,T])$, the restriction of the mild solution $\hat{u}$ to Ω is as regular as u on Ω (Theorem 6.4.2), namely

$$u, \hat{u} \in H^1([0,T], L^2(\Omega)) \cap L^2([0,T], H^2(\Omega)).$$

Consequently, the time-integrated difference between the prescribed flux ϕ on Γ in Problem (6.1) and the flux on Γ generated by the solution to Problem (6.3) with flux $\bar{\phi}$ at 0, i.e.

$$c^*(t) := \int_0^t \|\phi(\tau) - D\nabla\hat{u}(\tau)\cdot n\|^2_{L^2(\Gamma)}\, d\tau \tag{6.4}$$

is finite for all $t \geqslant 0$. In Section 6.5 we derive an upper bound on $c^*(t)$, see Theorem 6.5.5 in terms of the data for Problems (6.1) and (6.3).

Our main result is the following:

Theorem 6.2.1. *Let $T > 0$ and let the data for Problems* (6.1) *and* (6.3) *satisfy $u_0 \in H^1(\Omega)$, $\phi \in H^1([0,T], L^2(\Gamma)) \cap L^2([0,T], H^1(\Gamma))$, $\bar{\phi} \in H^1([0,T])$ and $\hat{u}_0 \in H^1(\mathbb{R}^2)$ is such that $\nabla \hat{u}_0 \in L^p(\mathbb{R}^2)$ for some $2 < p < \infty$. Then the unique solutions u and $\hat{u}$ to* (6.1) *and* (6.3) *are such, that for all $\varepsilon \in (0, 2D)$ there are $c_1, c_2 > 0$ such that*

$$\|u(\cdot,t) - \hat{u}(\cdot,t)\|^2_{L^2(\Omega)} \leq c_1\, c^*(t)\, e^{\varepsilon t}, \text{ and} \tag{6.5}$$

$$\int_0^t \|u - \hat{u}\|^2_{H^1(\Omega)} \leq c_2\, c^*(t)\, e^{\varepsilon t}. \tag{6.6}$$

for all $0 < t \leq T$. The constants depend on Ω, D and ε.

Remark 6.2.2. Note that the initial condition $\hat{u}_0$ needs to be more regular than 'just' $H^1(\mathbb{R}^2)$ as needed in the regularity result for $\hat{u}$. The flux estimates in Section 6.5 require $\nabla \hat{u}_0 \in L^p(\mathbb{R}^2)$ with $2 < p < \infty$. The Sobolev Embedding Theorem (cf. [AF03], Thrm. 4.12, p. 85) yields that $\hat{u}_0 \in H^2(\mathbb{R}^2)$ is a sufficient condition to have the stronger result that $\hat{u}_0 \in H^1(\mathbb{R}^2) \cap W^{1,p}(\mathbb{R}^2)$ for any $2 < p < \infty$. In that case necessarily $u_0 \in H^2(\Omega)$ too.

An important characteristic of estimates (6.5) and (6.6) is that the upper bounds are linear in $c^*(t)$. This implies that, if we manage to enforce $c^*(t)$ to be small, then also the solutions u and $\hat{u}$ are close (in the sense described above) on Ω. At this point, we manage only to get a rough bound on $c^*(t)$, cf. Theorem 6.5.5, but we conjecture that a more sophisticated estimate is possible; see Section 6.7.

6.3 Preliminaries

Before we can discuss the properties of solutions (Section 6.4) and the details of our results (Section 6.5 and further), we need a few fundamental results. We summarize these preliminaries in this section.

Lemma 6.3.1 (Properties of the convolution, cf. [Fol99] Propositions 8.8 and 8.9, p. 241)**.** *Let $p, q \geq 1$ be such that $1/p + 1/q = 1$. If $f \in L^p(\mathbb{R}^d)$ and $g \in L^q(\mathbb{R}^d)$, then*

(i) $(f * g)(x)$ *exists for all $x \in \mathbb{R}^d$;*

(ii) $f * g$ *is bounded and uniformly continuous;*

(iii) $\|f * g\|_{L^\infty(\mathbb{R}^d)} \leq \|f\|_{L^p(\mathbb{R}^d)}\, \|g\|_{L^q(\mathbb{R}^d)}$.

If moreover $p, q \in (1, \infty)$, then

(iv) $f * g \in C_0(\mathbb{R}^d)$.

Let $p, q, r \in [1, \infty]$ satisfy $1/p + 1/q = 1 + 1/r$. If $f \in L^p(\mathbb{R}^d)$ and $g \in L^q(\mathbb{R}^d)$, then

(v) $f * g \in L^r(\mathbb{R}^d)$;

(vi) $\|f * g\|_{L^r(\mathbb{R}^d)} \leq \|f\|_{L^p(\mathbb{R}^d)}\, \|g\|_{L^q(\mathbb{R}^d)}$.

Proof. The proof can be found in [Fol99], p. 241. □

Statement (vi) of Lemma 6.3.1 is called Young's Inequality. It also holds for the convolution in time with upper bound t, which will appear in (6.13). This is shown in the following corollary:

Corollary 6.3.2. *Let T be fixed and let $p, q, r \in [1, \infty]$ satisfy $1/p + 1/q = 1 + 1/r$. If $f \in L^p([0,T])$ and $g \in L^q([0,T])$, then*

(i) $f *_t g := t \mapsto \int_0^t f(t-s)g(s)\,ds \in L^r([0,T])$;

(ii) $\|f *_t g\|_{L^r([0,T])} \leq \|f\|_{L^p([0,T])}\, \|g\|_{L^q([0,T])}$.

Proof. The statement of this corollary follows from extension to $\mathbb{R}$ of f and g by zero outside $[0,T]$ and applying Lemma 6.3.1, Parts (v) and (vi) (for $d = 1$). □

The Green's function of the diffusion operator on $\mathbb{R}^d$ is (for general dimension d) given by

$$G_t(x) := (4\pi D t)^{-d/2} \mathrm{e}^{-|x|^2/4Dt}, \tag{6.7}$$

for all $t \in (0, \infty)$ and $x \in \mathbb{R}^d$.

Lemma 6.3.3 (Properties of the Green's function)**.** *Consider the Green's function* (6.7) *for dimension $d = 2$.*

(i) The gradient of the Green's function satisfies

$$\|\nabla G_\cdot(x)\|_{L^\infty(0,\infty)} := \sup_{\tau \in (0,\infty)} \|\nabla G_\tau(x)\| = \begin{cases} 0, & x = 0; \\ \dfrac{8\mathrm{e}^{-2}}{\pi}\, |x|^{-3}, & x \in \mathbb{R}^2 \setminus \{0\}. \end{cases} \tag{6.8}$$

(ii) For all $1 \leq p \leq \infty$ there is a constant c such that for all $t \in \mathbb{R}^+$

$$\|G_t(\cdot)\|_{L^p(\mathbb{R}^2)} \leq c\, t^{\frac{1}{p}-1}. \tag{6.9}$$

The constant depends on p and D.

Proof. (i) For all $x \in \mathbb{R}^2$ and all $\tau \in \mathbb{R}^+$

$$\|\nabla G_\tau(x)\| = \frac{|x|}{8\pi D^2 \tau^2}\, \mathrm{e}^{-|x|^2/4D\tau}, \tag{6.10}$$

where $\|\cdot\|$ denotes the Euclidean norm on $\mathbb{R}^2$. For $x = 0$ we have that $\|\nabla G_\tau(0)\| = 0$ for all $\tau \in (0, \infty)$, thus the corresponding part of (6.8) follows.

Next, we consider $x \neq 0$. Note that for all such x

$$\lim_{\tau \to 0} \|\nabla G_\tau(x)\| = 0,$$
$$\lim_{\tau \to \infty} \|\nabla G_\tau(x)\| = 0.$$

Since the right-hand side in (6.10) is nonnegative and differentiable for all $\tau \in \mathbb{R}^+$, its maximum on $\mathbb{R}^+$ is attained where

$$\frac{\partial}{\partial \tau}\|\nabla G_\tau(x)\| = \frac{|x|}{4\pi D^2 \tau^3}\left(\frac{|x|^2}{8D\tau} - 1\right) \mathrm{e}^{-|x|^2/4D\tau} = 0,$$

i.e. at $\tau = |x|^2/8D$. Now the statement of the lemma follows:

$$\|\nabla G_\cdot(x)\|_{L^\infty(0,\infty)} = \|\nabla G_\tau(x)\|\Big|_{\tau=|x|^2/8D} = \frac{8\mathrm{e}^{-2}}{\pi}\,|x|^{-3}.$$

(ii) The proof is a direct consequence of the statement in [Hil08] at the bottom of p. 432.

□

6.4 Solution concepts and their regularity

For problem (6.1) we follow [DHP03, DHP07] by considering solutions in the sense of $L^2(\Omega)$-valued distributions on $[0,T]$. Our setting is a special case of the setting in [DHP07]. However, [DHP07] is one of the few works that we are aware of that consider maximal regularity issues for problems in *unbounded* domains. The seminal works by Solonnikov [Sol65] and Lasiecka [Las80] cover bounded domains Ω only.

We reformulate Theorem 2.1 in [DHP07] to obtain:

Theorem 6.4.1. *If*

- $\phi \in H^1([0,T]; L^2(\Gamma)) \cap L^2([0,T]; H^1(\Gamma))$, *and*
- $u_0 \in H^1(\Omega)$,

then Problem (6.1) *has a unique solution*

$$u \in H^1([0,T]; L^2(\Omega)) \cap L^2([0,T]; H^2(\Omega)).$$

Proof. The statement of this theorem is fully covered by Theorem 2.1 in [DHP07]. We now point out why we satisfy the assumptions of their result. Note that we use $p = 2$ and $m = 1$ in their setting. First, $\mathbb{R}$ is a so-called $\mathcal{HT}$-space, meaning that the Hilbert transform defines a bounded operator on $L^p(\mathbb{R})$ for $1 < p < \infty$ (cf. [Rie28], VII). The conditions (E), (LS), (SD) and (SB) from [DHP07] are easily verified for $\mathcal{A}u := -D\Delta u$ and $\mathcal{B}u := \nabla u \cdot n$. Regarding Condition (D) in [DHP07], we note that in our case $f \equiv 0$ and moreover, no compatibility condition (iv) is needed. In (iii), we use that $B^1_{2,2}(\Omega) = H^1(\Omega)$; see [AF03] p. 231. A sufficient condition for (ii) to hold, is the one on ϕ given in the hypotheses of this theorem. We avoid the use of fractional Sobolev spaces. □

Problem (6.3) has a measure-valued right-hand side. [BDGO97] provide regularity results for weak solutions of non-linear parabolic problems with such measure-valued right-hand side. These apply to *bounded* domains with Dirichlet boundary condition and zero initial

value.

We consider *mild solutions* to (6.3) in the Banach space of finite Borel measures on $\mathbb{R}^2$, completed for the dual bounded Lipschitz norm $\|\cdot\|^*_{\mathrm{BL}}$ or Fortet-Mourier norm: $\overline{\mathcal{M}}(\mathbb{R}^2)_{\mathrm{BL}}$ (cf. Chapter 4 of this thesis, or [HW09b] and references found there). First, the diffusion semigroup $(S_t)_{t\geqslant 0}$ on $\overline{\mathcal{M}}(\mathbb{R}^2)_{\mathrm{BL}}$ is defined for measures $\mu \in \mathcal{M}(\mathbb{R}^2)$ by convolution with the Green's function G_t defined by (6.7), i.e.

$$\langle S_t\mu, \varphi\rangle := \langle G_t * \mu, \varphi\rangle = \int_{\mathbb{R}^2}\int_{\mathbb{R}^2} G_t(x-y)\varphi(x)\, d\mu(y)\, dx \tag{6.11}$$

for $\varphi \in C_b(\mathbb{R}^2)$. Thus, for a positive μ, $S_t\mu$ defines a positive linear functional on $C_c(\mathbb{R}^2)$, which is represented by a unique Radon measure according to the Riesz Representation Theorem ([Fol99], Theorem 7.2). This measure $S_t\mu$ is a finite measure because of

$$(S_t\mu)(\mathbb{R}^2) = \langle S_t\mu, \mathbb{1}\rangle = \mu(\mathbb{R}^2) < \infty.$$

Using the Jordan decomposition (see e.g. [Hal59], p. 123), we see that $S_t\mu \in \mathcal{M}(\mathbb{R}^2)$ for any $\mu \in \mathcal{M}(\mathbb{R}^2)$. One can check using (6.11) that S_t is a bounded operator on $\mathcal{M}(\mathbb{R}^2)$ for $\|\cdot\|^*_{\mathrm{BL}}$. By continuity it extends to the completion $\overline{\mathcal{M}}(\mathbb{R}^2)_{\mathrm{BL}}$. Moreover, there exists $C > 0$ such that

$$\|S_t\nu\|^*_{\mathrm{BL}} \leq C\|\nu\|^*_{\mathrm{BL}}$$

for all $t \geqslant 0$ and $\nu \in \overline{\mathcal{M}}(\mathbb{R}^2)_{\mathrm{BL}}$. Strong continuity of $(S_t)_{t\geqslant 0}$ on $\overline{\mathcal{M}}(\mathbb{R}^2)_{\mathrm{BL}}$ can then be obtained from strong continuity on the dense subspace $\mathcal{M}(\mathbb{R}^2)$ that follows from (6.11) and [EN00], Proposition I.5.3.

The mild solution to (6.3) is now defined by

$$\hat{\mu}(t) := S(t)\mu_0 + \int_0^t S(t-s)[\bar{\phi}(s)\delta_0]\, ds, \tag{6.12}$$

for given initial measure $\mu_0 \in \mathcal{M}(\mathbb{R}^2)$ ([Paz83], Ch.4, Def. 2.3, p.106). One can show that $\hat{\mu} \in C(\mathbb{R}_+, \overline{\mathcal{M}}(\mathbb{R}^2)_{\mathrm{BL}})$ whenever $\bar{\phi} \in L^1_{\mathrm{loc}}(\mathbb{R}_+)$.

If μ_0 has density $\hat{u}_0$ with respect to Lebesgue measure dx on $\mathbb{R}^2$, then according to (6.11) solution $\hat{\mu}(t)$ can be identified with $\hat{u}(x,t)dx$ where the density function $\hat{u}$ is given by

$$\begin{aligned}\hat{u}(x,t) &= \int_{\mathbb{R}^2} G_t(x-y)\hat{u}_0(y)\, dy + \int_0^t G_{t-s}(x)\bar{\phi}(s)\, ds \\ &=: (G_t *_x \hat{u}_0)(x) + (G_\cdot(x) *_t \bar{\phi})(t).\end{aligned} \tag{6.13}$$

for all $(x,t) \in \mathbb{R}^2 \times \mathbb{R}^+$. Here the notation $*_x$ and $*_t$ emphasizes that one takes convolution with respect to the space or time variable. Both have a regularizing effect on the solution, that yields the following result for the restriction of $\hat{u}(t)$ to Ω, the domain on which we compare with solution $u(t)$ to Problem (6.1):

Theorem 6.4.2. *If $\hat{u}_0 \in H^1(\mathbb{R}^2)$ and $\bar{\phi} \in H^1([0,T])$, then $\hat{u}$ (restricted to Ω) satisfies*

$$\hat{u} \in H^1([0,T]; L^2(\Omega)) \cap L^2([0,T]; H^2(\Omega)).$$

Moreover, $\partial_t \hat{u}(t) = D\Delta\hat{u}(t)$ in $L^2(\Omega)$ for almost every t in $[0,T]$.

Proof. Note that for $\hat{u}_0 \in H^1(\mathbb{R}^2)$, the function $\hat{u}_1 := G *_x \hat{u}_0$ is a solution of

$$\begin{cases} \dfrac{\partial u}{\partial t} = D\Delta u, & \text{on } \mathbb{R}^2 \times \mathbb{R}^+; \\ u(0) = \hat{u}_0, & \text{on } \mathbb{R}^2, \end{cases}$$

which is unique and satisfies

$$\hat{u}_1 \in H^1([0,T]; L^2(\mathbb{R}^2)) \cap L^2([0,T]; H^2(\mathbb{R}^2))$$

due to [DHP07], Theorem 2.1, where the domain is taken to be $\mathbb{R}^2$.

Define $\hat{u}_2 := G *_t \bar{\phi}$. Then $\hat{u}_2$ satisfies

$$\begin{aligned} \|\hat{u}_2\|_{L^2(\Omega)} &= \left(\int_\Omega \left| \int_0^t G_{t-s}(x)\, \bar{\phi}(s)\, ds \right|^2 dx \right)^{1/2} \\ &\le \int_0^t \left(\int_\Omega \left| G_{t-s}(x)\, \bar{\phi}(s) \right|^2 dx \right)^{1/2} ds \\ &\le \int_0^t \|G_{t-s}\|_{L^2(\mathbb{R}^2)} |\bar{\phi}(s)|\, ds \\ &\le \int_0^t c\,(t-s)^{-1/2} |\bar{\phi}(s)|\, ds. \end{aligned} \tag{6.14}$$

In the second step we used Minkowski's Inequality for integrals (see [Ste70], p. 271), whereas the last inequality follows from Part (ii) of Lemma 6.3.3. Since $t \mapsto c\,t^{-1/2} \in L^1([0,T])$ and by assumption $\bar{\phi} \in L^2([0,T])$, Corollary 6.3.2 applied to (6.14) yields

$$\|\hat{u}_2\|_{L^2(\Omega)} \in L^2([0,T]). \tag{6.15}$$

Because $G_\cdot(x)$ and $\partial_t G_\cdot(x)$ are in $L^1_{\mathrm{loc}}(\mathbb{R}_+)$ for $x \neq 0$ and $\partial_t \bar{\phi} \in L^2(\mathbb{R}_+)$, one has in the sense of distributions

$$\partial_t \big(G_\cdot(x) * \bar{\phi} \big) = \big(\partial_t G_\cdot(x) \big) * \bar{\phi} = G_\cdot(x) * \big(\partial_t \bar{\phi} \big). \tag{6.16}$$

Thus we can repeat the argument leading to (6.15), replacing $\bar{\phi}$ by $\partial_t \bar{\phi}$, and obtain

$$\|\partial_t \hat{u}_2\|_{L^2(\Omega)} \in L^2([0,T]). \tag{6.17}$$

We conclude from (6.15) and (6.17) that

$$\hat{u}_2 \in H^1([0,T];L^2(\Omega)). \tag{6.18}$$

It follows from (6.7) with $d=2$ that

$$\begin{aligned}\partial_{x_i} G_t(x) &= \frac{x_i}{8\pi D^2 t^2} \mathrm{e}^{-|x|^2/4Dt}, \text{ and}\\ \partial_{x_i}\partial_{x_j} G_t(x) &= \frac{1}{8\pi D^2 t^2} \mathrm{e}^{-|x|^2/4Dt}\left[\delta_{ij} - \frac{x_i x_j}{2Dt}\right],\end{aligned}$$

where δ_{ij} denotes the Kronecker delta for $i,j \in \{1,2\}$. The gradient of the Green's function is bounded in the following way:

$$\begin{aligned}|\nabla G_t(x)|^2 &\le \sup_{t>0} |\nabla G_t(x)|^2\\ &= \sup_{t>0} \frac{|x|^2}{64\pi^2 D^4 t^4} \mathrm{e}^{-|x|^2/2Dt}\\ &= \frac{1}{|x|^6} \sup_{u>0} \frac{u^4}{4\pi^2} \mathrm{e}^{-u},\end{aligned}$$

for all $t>0$ and for all $x \in \Omega$, where we substituted $u := |x|^2/2Dt$ to obtain the constant $c_1 := \sup_{u>0} \frac{u^4}{4\pi^2}\mathrm{e}^{-u}$, which is independent of $|x|$, t, D. Thus

$$|\nabla G_t(x)|^2 \le \frac{c_1}{|x|^6}. \tag{6.19}$$

We use the Frobenius norm denoted by $\|\cdot\|_F$ and defined by

$$\|M\|_F := \sqrt{\sum_{i,j} |M_{ij}|^2},$$

for any matrix $M \in \mathbb{R}^{d\times d}$. In a similar way as for ∇G, we estimate from above the Frobenius norm of the Hessian matrix

$$\begin{aligned}\|\operatorname{Hess} G_t(x)\|_F^2 &\le \sup_{t>0} \left(\sum_{i=1}^{2}\sum_{j=1}^{2} \frac{1}{64\pi^2 D^4 t^4} \mathrm{e}^{-|x|^2/2Dt} \left[\delta_{ij} - \frac{x_i x_j}{2Dt}\right]^2 \right)\\ &= \sup_{t>0} \frac{1}{64\pi^2 D^4 t^4} \mathrm{e}^{-|x|^2/2Dt} \left(2 - \frac{|x|^2}{Dt} + \frac{|x|^4}{4D^2 t^2}\right)\\ &= \frac{1}{|x|^8} \sup_{u>0} \frac{u^4}{4\pi^2} \mathrm{e}^{-u} \left(2 - 2u + u^2\right)\\ &= \frac{c_2}{|x|^8},\end{aligned} \tag{6.20}$$

for all $t > 0$ and for all $x \in \Omega$. Now we show that $\partial_{x_i} G_t$ and $\partial_{x_i}\partial_{x_j} G_t$ are in $L^2(\Omega)$, both with uniform upper bound in t:

$$\begin{aligned}\|\partial_{x_i} G_t\|^2_{L^2(\Omega)} &= \int_\Omega |\partial_{x_i} G_t(x)|^2\,dx \\ &\le \int_\Omega |\nabla G_t(x)|^2\,dx \\ &\overset{(6.19)}{\le} \int_\Omega \frac{c_1}{|x|^6}\,dx =: C_1 < \infty, \end{aligned} \tag{6.21}$$

where we use that 0 is an interior point of $\Omega_{\mathcal{O}} = \mathbb{R}^2 \setminus \overline{\Omega}$. Also

$$\begin{aligned}\|\partial_{x_i}\partial_{x_j} G_t\|^2_{L^2(\Omega)} &= \int_\Omega |\partial_{x_i}\partial_{x_j} G_t(x)|^2\,dx \\ &\le \int_\Omega \|\operatorname{Hess} G_t(x)\|_F^2\,dx \\ &\overset{(6.20)}{\le} \int_\Omega \frac{c_2}{|x|^8}\,dx =: C_2 < \infty. \end{aligned} \tag{6.22}$$

For brevity, we now use the index notation for derivatives and, for $|\alpha| \in \{1,2\}$. Like in (6.14), using Minkowski's integral inequality, we obtain that

$$\|\partial_x^\alpha \hat{u}_2\|_{L^2(\Omega)} \le \int_0^t \|\partial_x^\alpha G_{t-s}\|_{L^2(\Omega)} |\bar{\phi}(s)|\,ds. \tag{6.23}$$

Due to (6.21)–(6.22), for each $|\alpha| \in \{1,2\}$ and for each $\tau > 0$

$$\|\partial_x^\alpha G_\tau\|_{L^2(\Omega)} \in L^\infty([0,T]) \subset L^1([0,T]).$$

Hence, the fact that $\bar{\phi} \in L^2([0,T])$ yields via Part (ii) of Corollary 6.3.2 that

$$\int_0^t \|\partial_x^\alpha G_{t-s}\|_{L^2(\Omega)} |\bar{\phi}(s)|\,ds \in L^2([0,T]), \tag{6.24}$$

for each $|\alpha| \in \{1,2\}$. It follows from (6.15), (6.23) and (6.24) that

$$\hat{u}_2 \in L^2([0,T]; H^2(\Omega)). \tag{6.25}$$

Together with (6.18), (6.25) finishes the proof of the first part.

The second statement of the theorem follows from (6.16) and a similar result that holds

for the spatial derivatives. For all $\psi \in C_c^\infty(\overline{\Omega})$ and $h \in C_c^\infty(\mathbb{R}_+)$, $\psi \otimes h(x,t) := \psi(x)h(t)$ is in $C_c^\infty(\overline{\Omega} \times \mathbb{R}_+)$ and one has

$$\begin{aligned}
\langle \partial_t \hat{u}, \psi \otimes h \rangle &= \left\langle \left(\partial_t G.\right) *_x \hat{u}_0, \psi \otimes h \right\rangle + \int_{\overline{\Omega}} \left\langle \partial_t \left[G.(x)\right] *_t \bar{\phi}, h \right\rangle \psi(x)\, dx \\
&= \langle D(\Delta G.) *_x \hat{u}_0, \psi \otimes h \rangle + \int_{\overline{\Omega}} \left\langle D[\Delta G.(x)] *_t \bar{\phi}, h \right\rangle \psi(x)\, dx \\
&= \langle D\Delta(G. *_x \hat{u}_0), \psi \otimes h \rangle + \left\langle D\Delta(G. *_t \bar{\phi}), \psi \otimes h \right\rangle \\
&= \langle D\Delta \hat{u}, \psi \otimes h \rangle .
\end{aligned}$$

By density of $C_c^\infty(\overline{\Omega}) \otimes C_c^\infty(\mathbb{R}_+)$ in the space of test functions $\mathcal{D}(\overline{\Omega} \times \mathbb{R}_+)$, we obtain $\partial_t \hat{u} = D\Delta \hat{u}$ in the sense of distributions on $\overline{\Omega} \times \mathbb{R}_+$. Since both are given by (locally integrable) functions according to the first part of the proof, $\partial_t \hat{u}(t) = D\Delta \hat{u}(t)$ for almost every t. □

Remark 6.4.3. The estimates (6.21)–(6.22) hinge on the fact that Ω is bounded away from 0, where the integrand is singular.

6.5 Flux estimates

In this section we present in Theorem 6.5.5 a bound on the difference between the fluxes on Γ in (6.1) and (6.3). According to Theorem 6.4.1 and Theorem 6.4.2, under the conditions for which these results hold, $c^*(t)$ defined by (6.4) is finite for every $t \in [0,T]$. The difference between the solutions u and $\hat{u}$ on Ω will be expressed in terms of $c^*(t)$, among others, in Section 6.6.

Throughout this section, we assume the conditions of Theorems 6.4.1 and 6.4.2 on the data. Note that $\bar{\phi} \in H^1([0,T])$ implies that

$$\int_0^t \|\bar{\phi}\|_{L^1(0,\tau)}^2 \, d\tau \le \tfrac{1}{2} t^2 \|\bar{\phi}\|_{L^2([0,T])}^2 < \infty$$

for all $0 \le t \le T$.

Before arriving at the main estimate for $c^*(t)$, we derive auxiliary results in Lemma 6.5.1 and Lemma 6.5.2.

Lemma 6.5.1. *Assume that $\hat{u}_0 \equiv 0$. Then, for all $t > 0$ we have*

$$\int_0^t \|D\nabla \hat{u} \cdot n\|_{L^2(\Gamma)}^2 \le D^2 C_\Gamma \int_0^t \|\bar{\phi}\|_{L^1(0,\tau)}^2 \, d\tau < \infty,$$

where

$$C_\Gamma := \int_\Gamma \|\nabla G.(x)\|_{L^\infty(0,\infty)}^2 \, d\sigma > 0$$

is independent of t.

Proof. For $\hat{u}_0 \equiv 0$, the solution (6.13) of (6.3) is given by

$$\hat{u}(x,t) = \int_0^t G_{t-s}(x)\bar{\phi}(s)\,ds.$$

Note that for $x \in \Gamma$ we have

$$\begin{aligned}
|D\nabla\hat{u}(x,\tau)\cdot n(x)| &= \left| D\int_0^\tau \nabla G_{\tau-s}(x)\bar{\phi}(s)\,ds\cdot n(x)\right| \\
&\le \left\| D\int_0^\tau \nabla G_{\tau-s}(x)\bar{\phi}(s)\,ds\right\| \\
&\le D\,\|\nabla G_\cdot(x)\|_{L^\infty(0,\infty)}\int_0^\tau |\bar{\phi}(s)|\,ds \\
&= D\,\|\nabla G_\cdot(x)\|_{L^\infty(0,\infty)}\,\|\bar{\phi}\|_{L^1(0,\tau)}. \qquad (6.26)
\end{aligned}$$

We emphasize here that the infinity norm $\|\nabla G_\cdot(x)\|_{L^\infty(0,\infty)}$ denotes the supremum in the time domain for fixed x, cf. (6.8). This observation leads to the following estimate

$$\begin{aligned}
\int_0^t \|D\nabla\hat{u}(x,\tau)\cdot n(x)\|^2_{L^2(\Gamma)}\,d\tau &= \int_0^t\int_\Gamma |D\nabla\hat{u}(x,\tau)\cdot n(x)|^2\,d\sigma\,d\tau \\
&\le D^2\int_0^t\int_\Gamma \|\nabla G_\cdot(x)\|^2_{L^\infty(0,\infty)}\,\|\bar{\phi}\|^2_{L^1(0,\tau)}\,d\sigma\,d\tau,
\end{aligned}$$

where (6.26) is used in the second step. Thus, we have

$$\int_0^t \|D\nabla\hat{u}(x,\tau)\cdot n(x)\|^2_{L^2(\Gamma)}\,d\tau \le D^2\int_0^t \|\bar{\phi}\|^2_{L^1(0,\tau)}d\tau\int_\Gamma \|\nabla G_\cdot(x)\|^2_{L^\infty(0,\infty)}\,d\sigma. \quad (6.27)$$

Since Γ has finite length and it is the boundary of a set of which 0 is an interior point, it follows from (6.8) in Lemma 6.3.3 that the second integral on the right-hand side of (6.27) is finite. This argument completes the proof. □

In the next lemma, we generalize this result to nonzero initial conditions.

Lemma 6.5.2. *If $\hat{u}_0$ is such that $\nabla\hat{u}_0 \in L^p(\mathbb{R}^2)$ for some $2 < p \le \infty$, then*

$$\int_0^t \|D\nabla\hat{u}\cdot n\|^2_{L^2(\Gamma)} \le D^2|\Gamma|Ct^{\frac{2}{q}-1}\|\nabla\hat{u}_0\|^2_{L^p(\mathbb{R}^2)} + 2D^2C_\Gamma\int_0^t \|\bar{\phi}\|^2_{L^1(0,\tau)}\,d\tau < \infty,$$

for all $t > 0$, where $q := p/(p-1)$, C depends on D and q and C_Γ is the constant from Lemma 6.5.1.

Proof. The solution of (6.3) is given by (6.13). We start off with the following estimate

$$\int_0^t \|D\nabla\hat{u}(x,\tau)\cdot n(x)\|^2_{L^2(\Gamma)}\,d\tau \le 2\int_0^t\int_\Gamma \left| D\nabla \int_{\mathbb{R}^2} G_\tau(x-y)\hat{u}_0(y)\,dy\cdot n(x)\right|^2 d\sigma\,d\tau + 2\int_0^t\int_\Gamma \left| D\nabla \int_0^\tau G_{\tau-s}(x)\bar{\phi}(s)\,ds\cdot n(x)\right|^2 d\sigma\,d\tau. \quad (6.28)$$

The second term on the right-hand side is covered by Lemma 6.5.1. Regarding the first term, we remark that, due to properties of the convolution,

$$\left| D\,\nabla \int_{\mathbb{R}^2} G_\tau(x-y)\hat{u}_0(y)\,dy\cdot n(x)\right| = \left| D\int_{\mathbb{R}^2} G_\tau(y)\nabla\hat{u}_0(x-y)\,dy\cdot n(x)\right|. \quad (6.29)$$

We use Part (iii) of Lemma 6.3.1 to estimate the right-hand side

$$\begin{aligned}\left| D\int_{\mathbb{R}^2} G_\tau(y)\nabla\hat{u}_0(x-y)\,dy\cdot n(x)\right| &\le D\left\|\int_{\mathbb{R}^2} G_\tau(y)\nabla\hat{u}_0(\cdot-y)\,dy\right\|_{L^\infty(\mathbb{R}^2)}\\ &\le D\,\|\nabla\hat{u}_0\|_{L^p(\mathbb{R}^2)}\,\|G_\tau\|_{L^q(\mathbb{R}^2)}, \end{aligned} \quad (6.30)$$

with $q := p/(p-1)$.

It follows from (6.29)–(6.30) and Part (ii) of Lemma 6.3.3 that

$$\begin{aligned}\int_0^t\int_\Gamma \left| D\nabla\int_{\mathbb{R}^2} G_\tau(x-y)\hat{u}_0(y)\,dy\cdot n(x)\right|^2 d\sigma\,d\tau &\le D^2\,\|\nabla\hat{u}_0\|^2_{L^p(\mathbb{R}^2)}\int_0^t\int_\Gamma \|G_\tau\|^2_{L^q(\mathbb{R}^2)}\,d\sigma\,d\tau\\ &\le c^2\,D^2\,|\Gamma|\,\|\nabla\hat{u}_0\|^2_{L^p(\mathbb{R}^2)}\int_0^t \tau^{\frac{2}{q}-2}\,d\tau\\ &= \frac{q\,c^2\,D^2\,|\Gamma|}{2-q}\,t^{\frac{2}{q}-1}\,\|\nabla\hat{u}_0\|^2_{L^p(\mathbb{R}^2)}, \end{aligned} \quad (6.31)$$

where c depends on q and D. We can perform the integration in time in the last step of (6.31) since the hypothesis $p > 2$ implies $q < 2$. The desired result follows by (6.28) and

the calculations in the proof of Lemma 6.5.1:

$$\int_0^t \|D\nabla\hat{u}(x,\tau)\cdot n(x)\|^2_{L^2(\Gamma)}\,d\tau \le \frac{2q\,c^2\,D^2\,|\Gamma|}{2-q}\,t^{\frac{2}{q}-1}\,\|\nabla\hat{u}_0\|^2_{L^p(\mathbb{R}^2)} + 2D^2\int_0^t \|\bar{\phi}\|^2_{L^1(0,\tau)}d\tau\int_\Gamma \|\nabla G_\cdot(x)\|^2_{L^\infty(0,\infty)}\,d\sigma,$$

of which the right-hand side is finite for all finite t. □

Remark 6.5.3. A sufficient condition for $\nabla\hat{u}_0 \in L^p(\mathbb{R}^2)$ to hold, is $\hat{u}_0 \in W^{1,p}(\mathbb{R}^2)$. To this aim, one may start from $u_0 \in W^{1,p}(\Omega)$ to hold for the *given* initial data. The remaining question is whether it is possible to find an extension v_0 on $\Omega_{\mathcal{O}}$ as in (6.2) such that $\hat{u}_0 \in W^{1,p}(\mathbb{R}^2)$. This, however is guaranteed by Theorem 5.22 on p. 151 of [AF03].

Remark 6.5.4. It is crucial that the gradient is applied to the initial condition in the computations starting at (6.29) and further. Instead of (6.29)–(6.30), we could have estimated

$$\left| D\,\nabla\int_{\mathbb{R}^2} G_\tau(x-y)\hat{u}_0(y)\,dy\cdot n(x)\right| \le D\;\|\hat{u}_0\|_{L^p(\mathbb{R}^2)}\;\|\nabla G_\tau\|_{L^q(\mathbb{R}^2)}\,,$$

which requires only a condition on $\hat{u}_0$, not on its gradient, for the lemma. It follows from [Hil08] (p. 432, bottom) that for some constant C

$$\|\nabla G_\tau\|_{L^q(\mathbb{R}^2)} \le C\,\tau^{\frac{1}{q}-\frac{3}{2}}.$$

This is a problem however, since similar arguments as in (6.31) would lead to

$$\int_0^t \|\nabla G_\tau\|^2_{L^q(\mathbb{R}^2)}\,d\tau \le C\int_0^t \tau^{\frac{2}{q}-3}\,d\tau,$$

of which the right-hand side is not integrable for any $1 \le q \le \infty$.

We can now give the main result of this section.

Theorem 6.5.5. *Assume that the hypotheses of Theorems 6.4.1 and 6.4.2 and Lemma 6.5.2 hold. Then, for all $t > 0$ the function c^* defined by* (6.4) *satisfies*

$$c^*(t) \le 2\int_0^t \|\phi\|^2_{L^2(\Gamma)} + 2D^2|\Gamma|Ct^{\frac{2}{q}-1}\|\nabla\hat{u}_0\|^2_{L^p(\mathbb{R}^2)} + 2C_\Gamma\int_0^t \|\bar{\phi}\|^2_{L^1(0,\tau)}\,d\tau. \qquad (6.32)$$

Proof. The statement of this theorem is a direct consequence of the observation

$$\int_0^t \|\phi - D\nabla\hat{u}\cdot n\|^2_{L^2(\Gamma)} \le 2\int_0^t \|\phi\|^2_{L^2(\Gamma)} + 2\int_0^t \|D\nabla\hat{u}\cdot n\|^2_{L^2(\Gamma)}\,. \qquad (6.33)$$

The assumptions of Theorem 6.4.1 imply that $\phi \in L^2([0,T];L^2(\Gamma))$ for all $T \in \mathbb{R}^+$. Hence, the first term in (6.33) is finite. The second term was estimated in Lemma 6.5.2. □

Remark 6.5.6. Estimate (6.32) is unsatisfactory for t close to zero. However, it shows for large t that on the long run the difference between the fluxes on Γ is dominated by the prescribed fluxes ϕ at Γ and $\bar{\phi}$ at the point source at 0, rather than the initial condition, which is clear intuitively. In Section 6.7 we provide a further discussion of the behaviour of $c^*(t)$.

6.6 Estimates in the exterior – Proof of Theorem 6.2.1

We can now prove our main result, an estimate for the difference between the solutions u of (6.1) and $\hat{u}$ of (6.3) (using the solution concept explained in Section 6.4):

Proof. (Theorem 6.2.1). Let $\psi \in C_c^\infty(\overline{\Omega})$ and $h \in C_c^\infty([0,T])$ be test functions. Define $(\psi \otimes h)(x,t) := \psi(x)h(t)$. Then according to Theorem 6.4.1 and Theorem 6.4.2 one has

$$\begin{aligned}\langle \partial_t u - \partial_t \hat{u}, \psi \otimes h\rangle &= D\,\langle \Delta u - \Delta \hat{u}, \psi \otimes h\rangle \\ &= \int_0^T \left\{ \int_\Gamma (\phi(t) - D\nabla \hat{u}(t)\cdot n)\,\psi \right\} h(t)dt \\ &\quad - D\int_0^T \left\{ \int_\Omega (\nabla u - \nabla \hat{u})\cdot \nabla \psi \right\} h(t)dt.\end{aligned} \tag{6.34}$$

Because of the regularity of the solutions u and $\hat{u}$ identity (6.34) extends to functions $f \in L^1([0,T],H^1(\Omega))$ by continuity:

$$\begin{aligned}\langle \partial_t u - \partial_t \hat{u}, f\rangle &= \int_0^T \int_\Gamma (\phi(t) - D\nabla \hat{u}(t)\cdot n)\, f(x,t)\, d\sigma(x)\, dt \\ &\quad - D\int_0^T \int_\Omega (\nabla u - \nabla \hat{u})\cdot \nabla f(x,t)\, dx\, dt.\end{aligned} \tag{6.35}$$

Now take $f(x,t) := (u(x,t) - \hat{u}(x,t))h(t)$ with $h \in C_c^\infty([0,T])$ arbitrary. Then the regularity of u and $\hat{u}$ and (6.35) imply that

$$\frac{1}{2}\frac{d}{dt}\|u-\hat{u}\|^2_{L^2(\Omega)} + D\|\nabla u - \nabla \hat{u}\|^2_{L^2(\Omega)} = \int_\Gamma (u-\hat{u})(\phi - D\nabla \hat{u}\cdot n)\,.$$

Add $D\|u-\hat{u}\|^2_{L^2(\Omega)}$ to both sides and integrate in time from 0 to an arbitrary t:

$$\frac{1}{2}\|u-\hat{u}\|^2_{L^2(\Omega)} + D\int_0^t \|u-\hat{u}\|^2_{H^1(\Omega)} = \int_0^t \int_\Gamma (u-\hat{u})(\phi - D\nabla \hat{u}\cdot n) + D\int_0^t \|u-\hat{u}\|^2_{L^2(\Omega)}\,, \tag{6.36}$$

where we have used that u and $\hat{u}$ are initially equal on Ω. Applying the Cauchy-Schwarz Inequality and using the result of Theorem 6.5.5, we obtain

$$\int_0^t \int_\Gamma (u-\hat{u})(\phi - D\nabla\hat{u}\cdot n) \;\le\; \left(\int_0^t \|u-\hat{u}\|^2_{L^2(\Gamma)}\right)^{1/2} \left(\int_0^t \|\phi - D\nabla\hat{u}\cdot n\|^2_{L^2(\Gamma)}\right)^{1/2}$$
$$= \sqrt{c^*(t)}\left(\int_0^t \|u-\hat{u}\|^2_{L^2(\Gamma)}\right)^{1/2}. \tag{6.37}$$

Since $H^1(\Omega) \hookrightarrow L^2(\Gamma)$, according to the Boundary Trace Imbedding Theorem (cf. [AF03], Theorem 5.36, p. 164) there is a constant $\bar{c} = \bar{c}(\Omega) > 0$ such that

$$\|u-\hat{u}\|_{L^2(\Gamma)} \le \bar{c}\,\|u-\hat{u}\|_{H^1(\Omega)},$$

which can be used to further estimate (6.37):

$$\int_0^t \int_\Gamma (u-\hat{u})(\phi - D\nabla\hat{u}\cdot n) \;\le \sqrt{c^*(t)}\,\bar{c}\left(\int_0^t \|u-\hat{u}\|^2_{H^1(\Omega)}\right)^{1/2}.$$

For arbitrary $\varepsilon > 0$, Young's inequality yields the following estimate on the right-hand side:

$$\sqrt{c^*(t)}\,\bar{c}\left(\int_0^t \|u-\hat{u}\|^2_{H^1(\Omega)}\right)^{1/2} \le \frac{1}{2\varepsilon}c^*(t)\bar{c}^2 + \frac{\varepsilon}{2}\int_0^t \|u-\hat{u}\|^2_{H^1(\Omega)}. \tag{6.38}$$

Take $\varepsilon \in (0, 2D)$. Then (6.36)–(6.38) together yield

$$\|u-\hat{u}\|^2_{L^2(\Omega)} + (2D-\varepsilon)\int_0^t \|u-\hat{u}\|^2_{H^1(\Omega)} \le \frac{1}{\varepsilon}c^*(t)\bar{c}^2 + 2D\int_0^t \|u-\hat{u}\|^2_{L^2(\Omega)}, \tag{6.39}$$

or

$$\|u-\hat{u}\|^2_{L^2(\Omega)} + \underbrace{(2D-\varepsilon)\int_0^t \|\nabla u - \nabla\hat{u}\|^2_{L^2(\Omega)}}_{\geqslant 0} \le \frac{1}{\varepsilon}c^*(t)\bar{c}^2 + \varepsilon\int_0^t \|u-\hat{u}\|^2_{L^2(\Omega)}. \tag{6.40}$$

It follows that

$$\|u-\hat{u}\|^2_{L^2(\Omega)} \le \frac{1}{\varepsilon}c^*(t)\bar{c}^2 + \varepsilon\int_0^t \|u-\hat{u}\|^2_{L^2(\Omega)},$$

and due to a version of Gronwall's Lemma:

$$\|u-\hat{u}\|^2_{L^2(\Omega)} \le \frac{1}{\varepsilon}c^*(t)\bar{c}^2\,\mathrm{e}^{\varepsilon t}, \tag{6.41}$$

where we use that $c^*(\cdot)$ is (by definition) non-decreasing. Note that $\varepsilon > 0$ is arbitrary but fixed, thus $1/\varepsilon < \infty$. We obtain (6.5) by defining $c_1 := \bar{c}^2/\varepsilon$.

From (6.39) it also follows that

$$\int_0^t \|u - \hat{u}\|^2_{H^1(\Omega)} \leq \frac{1}{\varepsilon(2D-\varepsilon)} c^*(t)\bar{c}^2 + \frac{2D}{2D-\varepsilon} \int_0^t \|u - \hat{u}\|^2_{L^2(\Omega)}\,.$$

The upper bound (6.41) now implies

$$\begin{aligned}\int_0^t \|u - \hat{u}\|^2_{H^1(\Omega)} &\leq \frac{1}{\varepsilon(2D-\varepsilon)} c^*(t)\bar{c}^2 + \frac{2D}{\varepsilon^2(2D-\varepsilon)} c^*(t)\bar{c}^2\,(e^{\varepsilon t} - 1) \\ &\leq \frac{2D}{\varepsilon^2(2D-\varepsilon)} c^*(t)\bar{c}^2\, e^{\varepsilon t}, \end{aligned} \tag{6.42}$$

where we use that $\varepsilon < 2D$ in the second step. The second statement of the theorem follows by taking $c_2 := 2D\bar{c}^2/(\varepsilon^2(2D-\varepsilon))$. □

Remark 6.6.1. In principle, (6.42) can be optimized in ε for every t separately, to get an optimal $\varepsilon = \varepsilon(t)$. After substitution of this $\varepsilon(t)$, (6.6) becomes independent of ε. However, its t-dependence obviously becomes more complicated. Further details on this aspect are omitted here.

Remark 6.6.2. The fact that the estimates in Theorem 6.2.1 are linear in c^* relates nicely to our conjecture formulated in Section 6.7 below. If indeed c^* is small or even goes to zero, then the same holds for $\|u(\cdot,t) - \hat{u}(\cdot,t)\|^2_{L^2(\Omega)}$ and $\int_0^t \|u - \hat{u}\|^2_{H^1(\Omega)}$.

6.7 Discussion

In this chapter we considered two problems involving the diffusion equation on $\mathbb{R}^2$. In the first problem a finite-size object was included with prescribed flux on its boundary. In the second problem this object was replaced by a mass-emitting point source. Our aim was to quantify the difference between the solutions and their fluxes on Γ in a suitable Sobolev norm. We managed to provide for all $t > 0$ an $L^2([0,t]; L^2(\Gamma))$-bound on the difference in flux on the boundary. For the difference in solutions we provided an $L^2(\Omega)$-bound (for all time) and an $L^2([0,t]; H^1(\Omega))$-bound.

The estimate (6.33) is a very crude way to find an upper bound on $c^*(t)$. In the following (deliberately vague) conjecture, we express under which conditions we expect $c^*(t)$ to be smaller than the upper bound of Theorem 6.5.5 suggests.

Conjecture. *The upper bound c^* can be much smaller than Theorem 6.5.5 suggests. In fact, it goes to zero.*

The following considerations support this conjecture:

- Once the geometry and ϕ on Γ are given, there still is a lot of freedom in dealing with the reduced problem (6.3). Choose $\bar{\phi}$ and v_0. Our conjecture is that a smart choice of $\bar{\phi}$ and v_0 can produce a flux on Γ that mimics well ϕ and gives more than merely a *bounded* difference.
- Initially, during a small time interval, the initial condition should induce a sufficiently close flux. To this aim an appropriate v_0 has to be provided.
- At a certain moment, mass originating from the source starts reaching the boundary. From then onwards, the mimicking flux should be – with some delay – mainly due to $\bar{\phi}$.
- Let $|\Omega_{\mathcal{O}}|$ denote a typical length scale of the object $\mathcal{O}$ (e.g. its diameter). The quantity $|\Omega_{\mathcal{O}}|^2/D$ is a typical timescale for points to travel the distance from source to boundary. This is also the timescale at which the transition between the above two bullet points takes place.
- The shape of object $\mathcal{O}$ is important. An intuitive guess is that a small object $\mathcal{O}$ can be better approximated. As the point source emits mass at the same rate in all directions, we expect a better approximation also to be possible if Γ is radially symmetric with respect to the origin, and ϕ is constant on Γ (in space, not necessarily in time). A generalization of the latter condition would be to have ϕ defined on a more general Γ, but to have an extension to a ball $B(0,R)$ such that $\Gamma \subset B(0,R) \subset \mathbb{R}^2$, and this extension is radially symmetric around the origin on $B(0,R)$.

The above statement was written under the assumption that in general the (normal component of the) flux is directed outward on Γ. For a mass sink, *mutatis mutandis* the same considerations hold.

One approach to prove that $c^* \to 0$ is to employ the limit "$|\mathcal{O}| \to 0$". This is one step further than the work presented in this chapter; cf. Remark 6.1.1. We point out at least one problem that is to be expected. In (6.27) we used explicitly that Γ is bounded away from the origin. If Γ shrinks towards the origin, then (6.8) no longer provides a useful upper bound. A formal asymptotic expansion with the object's size as a small parameter might provide an alternative approach here.

Chapter 7

Looking back and ahead

This chapter is an overview of the main achievements of this thesis and an outlook to possible future research based on the open ends that we identified.

7.1 Looking back

In Chapters 2 to 6 we obtain the following results:

- In Chapter 2 we introduce a field of vision in a first-order model for interacting individuals. Our objective is to guarantee the existence and uniqueness of solutions to this model with included field of vision. In our model the velocity is defined implicitly. Difficulties arise when a solution v has no continuous extension in time. We refer to this situation as root loss in the implicit equation. To extend the evolution of our system beyond root loss we provide a selection criterion for the velocity to jump to a different root. This criterion is based on an associated second-order system with a vanishing inertia term: the overdamped limit. Automatically, our approach selects a stable root. Details about the exact type of stability are given in Definition 2.3.2 and Theorem 2.3.4. In Chapter 2 we demonstrate our procedure by a combination of theoretical and numerical results.

- Chapter 3 is based on two questions. First, we answer the question how to derive particle schemes in a systematic way. We propose the following three-step procedure: (1) rewrite the equations in terms of measures and regularizing the density; (2) substitute a weighted sum of Dirac masses; (3) apply the principle of least action. The exact form of the resulting equation for the particle system depends on the order in which regularization and the principle of least action are applied. We also generalize this procedure to systems in which nonconservative forces are present.

  The second question concerns the many-particle limit $N \to \infty$ of the particle schemes. We give a convergence proof for general measure-valued equations (in the 1-Wasserstein distance) which is not restricted to particle approximations. Our

theorem provides convergence of solutions given a general sequence of corresponding initial measures approximating the initial condition of the limit problem. This result implies as a special case the convergence of particle solutions to the solution of the *regularized* continuum equation.

- We address the question how to define flux boundary conditions for measure-valued evolutions in Chapter 4. The model considered is an evolution problem for a measure with prescribed velocity field where the flow is restricted to the unit interval. The combination of the stopped flow and an absorption term in the right-hand side of the equation results in flux boundary conditions. Alternatively, we can model *influx* by including a production term. We also obtain these boundary conditions as the limit of an approximation by a vanishing absorptive boundary layer. While in each of the approximations mass is taken from the system in a zone of finite width, the limit corresponds to gating mass away only on the boundary.

- In Chapter 5 we generalize the results of Chapter 4 to measure-dependent velocity fields. This generalization makes interaction terms via convolution admissible. We introduce a forward-Euler-like approach. The time interval is partitioned into a number of subintervals. In each of these the velocity is prescribed based on the solution in the previous interval. Hence, the setting of Chapter 4 is applicable to each subinterval. We are driven by the same question about flux boundary conditions as in Chapter 4. In Chapter 5 we are able to answer this question for systems in which interactions govern the dynamics. The forward-Euler-like approach converges, but we manage to obtain this result only for bounded Lipschitz continuous right-hand sides. This means that we can deal with boundary layers in which mass is absorbed, but not (yet) with the limit of vanishing boundary layer.

- Chapter 6 is about two scenarios involving the diffusion equation in two-dimensional space. First, we consider an object with prescribed flux on its boundary, while on its exterior a mass density evolves due to diffusion. The exterior domain is called Ω. Secondly, we consider a point source that emits mass. We ask the question whether we can quantify the difference between the solutions of these two problems and their fluxes on Γ in a suitable Sobolev norm. We provide an $L^2([0,t];L^2(\Gamma))$-bound on the difference in flux on the boundary for all $t>0$, and moreover an $L^2(\Omega)$-bound (for all time) and an $L^2([0,t];H^1(\Omega))$-bound on the difference in solutions. We conjecture certain conditions under which these bounds go to zero.

We posed at the beginning of Chapter 1 the general mathematical guiding question: Can ideas from mathematical physics provide inspiration when modelling and analyzing systems of socially interacting individuals? The general spirit of this thesis is that it *is* possible to model living individuals as if they were non-living matter.

Chapter 1 provides the framework of modelling perspectives and equations in which the rest of the thesis fits. Many of the concepts that we describe are closely related to mathematical physics. For instance, the transition from the microscopic level to the meso- and macroscopic levels (the limit $N\to\infty$) are used to justify continuum descriptions of systems containing a large number of particles, molecules or atoms. Chapters 2 to 5 fit in the framework of Chapter 1. Moreover, interactions and anisotropy play a prominent

role. These chapters provide the answer to our guiding question. Chapter 3 in particular is physically oriented. There, social interactions are one of multiple ingredients.
Chapter 6 justifies in some sense some of the *ad hoc* approximation arguments used in physics. It is common practice in physics to describe small objects by points if their length scale is much smaller than other length scales in the system. Examples are point masses, point charges or point sources. Interactions are absent in Chapter 6. We regard this chapter as a first step towards modelling systems of interacting point sources. We note however that in view of the application we have in mind (vesicles transporting chemical compounds in cells), these interactions are not of a social nature.

7.2 Looking ahead

Let us summarize our main open issues.

- In Chapter 2 we derive a jump criterion for the velocity that is to be used when no continuous extension of the evolution is possible. This criterion makes use of the configuration $\mathbf{x}_+^*$ which denotes an infinitesimal extrapolation beyond root loss. We approximate this post-jump configuration by $\mathbf{x}^* + \delta \cdot \tilde{\mathbf{v}}$, where $\mathbf{x}^*$ is the pre-jump configuration, $\tilde{\mathbf{v}}$ is the pre-jump velocity and $\delta > 0$ is fixed. For each δ there is a corresponding post-jump velocity $\mathbf{v}_\delta^*$. The rigorous investigation of the limit $\lim_{\delta \downarrow 0} \mathbf{v}_\delta^*$ is a direction for future research. If this limit is well-defined, the corresponding jump should be compared to the jump that follows from the limit $\varepsilon \to 0$ in the second-order equation.

- Formally, the continuum limit of the anisotropic model used in Chapter 2 consists of the continuity equation completed with Equation (2.43) for the velocity; cf. Section 2.6. We would like to justify this continuum model in a rigorous way, possibly via a measure-valued formulation. The next step is to perform the overdamped limit $\varepsilon \to 0$ at the PDE level.

- We would like to support the claim that anisotropy is present, by evidence from experiments. A possible strategy is to analyze the data used in [CBMT14, CMV15]. This data consists of trajectories of people walking in a narrow passage between two staircases. One can extract from the data set all frames in which exactly two individuals are present, while the corresponding velocities are also recorded. Assume that the velocity of individual i in the presence of individual j is given by

$$v_i = v_{\mathrm{d},i} + v_{\mathrm{s}}\Big(|x_i - x_j|, \frac{x_i - x_j}{|x_i - x_j|} \cdot \frac{v_i}{|v_i|}\Big).$$

  Here, v_{d} denotes a *desired velocity* (cf. Section 2.6), which incorporates the target of an individual and restrictions due to the geometry. The first task is to estimate the desired velocity, which might be done using the collection of single pedestrian trajectories. Call this estimate $\bar{v}_{\mathrm{d}}$. We use this estimate to eliminate the effect of v_{d} from the data.
  The part v_{s} is the *social* part of the velocity. We assume it to have the same form

as the right-hand side of (2.4b). Define

$$R := |x_i - x_j| \quad \text{and} \quad \omega := \frac{x_i - x_j}{|x_i - x_j|} \cdot \frac{v_i}{|v_i|}.$$

Then in particular, v_{s} is of the form

$$v_{\mathrm{s}}(R, \omega) := f(R)\, g(\omega). \tag{7.1}$$

We wish to investigate (i) whether v_{s} indeed has this product structure; (ii) whether the data supports the claim that g encodes a field of vision.
We propose to deduce from the data an estimate of

$$\mathbb{E}\big[|v_{\mathrm{s}}| \,\big|\, (R, \omega)\big] \tag{7.2}$$

as a function of R and ω. In view of the available data, we approximate (7.2) by

$$\bar{v}_{\mathrm{s}}(R, \omega) := \mathbb{E}\big[|v - \bar{v}_{\mathrm{d}}| \,\big|\, (R, \omega)\big].$$

If the product structure (7.1) is present, then for each R, the cross-section

$$\bar{v}_{\mathrm{s}}(R, \cdot\,)/|f(R)|$$

should be approximately the same. If the cross-sections exhibit similarities, then the general shape indicates whether this g can be interpreted as a field of vision.
The described strategy is for the moment an idea and it has not been verified so far.

- In Section 3.7 of Chapter 3 we propose to investigate the many-particle limit $N \to \infty$ simultaneously with vanishing regularization $\gamma \rightharpoonup \delta_0$. It is common practice in the SPH community to obtain this simultaneous limit by introducing a typical length scale h called *smoothing length* in the smoothing kernel γ and subsequently taking $h \sim 1/\sqrt[d]{N}$. In [EZvdLD15] we support numerically the claim that solutions for N-dependent h converge as $N \to \infty$. We would like to investigate this limit theoretically.

- Chapters 4 and 5 deal with a problem on the unit interval. In Section 4.6 of Chapter 4 an interpretation in terms of a particle system is given with particles being gated away randomly from an absorption zone of finite width. We derive the limit as the width of this absorption zone goes to zero in Chapter 4. The generalization of this procedure to two or more spatial dimensions remains to be investigated. We note that in more than one dimension the shape and regularity of the boundary are factors that need to be taken into account.

- Our well-posedness proof involving measure-dependent velocities (see Chapter 5) only holds for right-hand sides with bounded Lipschitz continuous f. If we want to model the limit case of vanishing boundary layer, we need to extend this result to piecewise bounded Lipschitz f. Subsequently, we need to prove that the solution for finite boundary layer actually converges to the solution of the limit problem.
  As explained in Section 5.5, it is not clear whether two limits commute: the limit of

taking a finer and finer partitioning of $[0,T]$ in the forward-Euler-like approach, and the limit of vanishing zone of absorption. One of the key difficulties we currently face, is the fact that we do not have an explicit expression for the limit of the forward-Euler-like approach. Such expression would facilitate the comparison of the solutions obtained from taking the two aforementioned limits in either order. Note that we do have an explicit expression for the solution in Chapter 4.

- We constructed only one approximating sequence in Chapter 5, namely by partitioning the interval $[0,T]$ into 2^k subintervals. We expect that it is possible to obtain similar estimates as in Chapter 5 if we choose any $q \in \mathbb{N}^+$ and take a partitioning of $[0,T]$ in q^k subintervals. We expect moreover that these estimates can be used to prove that in this case the limit $k \to \infty$ is well-defined. These conjectures remain to be verified. Afterwards we need to answer the question whether all limits obtained in this way are the same; first for *uniform* partitionings with arbitrary q and later for general *non-uniform* partitionings.

- A possible extension to the model in Chapters 4 and 5 is to add anisotropy due to a field of vision. Such extension can also be viewed upon as placing the approach of Chapter 2 in a measure-valued framework and restricting the evolution to a bounded domain.

- Imagine that we want to determine (experimentally) the ingredients of our model, in particular f and v. In view of the inevitable errors that are made, it is important to know how these errors eventually affect the solution of our model. Therefore we need to derive stability estimates with respect to model ingredients and parameters. This is a first step in the direction of validating the model of Chapters 4 and 5 against real-life data.

- In Chapter 6 we compare the solutions of two problems, one involving flux through the boundary of an object and another involving mass emission from a point source. We provide bounds on the difference in fluxes and on the difference between the solutions. We conjecture that these bounds can become arbitrarily small. A seemingly straightforward strategy to achieve such vanishing upper bounds is simply to *provide* correctly both the magnitude of the source term and the initial condition inside Γ. These two model components need to be provided in such a way that they together produce the appropriate flux over the boundary Γ of the finite-size object. This is a nontrivial inverse problem. A possible second approach is to consider the limit "$|\mathcal{O}| \to 0$". We point out that if Γ shrinks towards the origin, then the upper bound provided by the combination of (6.8) and (6.27) tends to infinity. Instead of this estimate we can perhaps use a formal asymptotic expansion with the object's size as a small parameter.

- Chapter 6 treats a simple scenario related to a more complicated problem in which multiple point sources move around in a (bounded) domain and interact with each other. These point masses represent vesicles that transport material and exchange this material with their environment. Our ultimate goal is to model such systems with a discrete measure representing the point masses. In Chapter 6 the function

describing the emission of mass is prescribed. In a more realistic model, this function is one of the unknowns. A lot of progress is still to be made in this direction.

Appendix A

Completeness of spaces of continuous functions

This appendix provides completeness results for spaces of continuous functions from $[0,T]$ to a given complete metric space.

Lemma A.1. *Let (X, dist_X) be a complete metric space. For each $T > 0$, the space*

$$C([0,T];X),$$

endowed with the metric defined as

$$\sup_{\tau\in[0,T]} \mathrm{dist}_X(\mu_1(\tau),\mu_2(\tau)),$$

for all $\mu_1, \mu_2 \in C([0,T];X)$, is complete.

Proof. The proof mainly follows the lines of the proof of Theorem 1.5-5 in [Kre78] (which treats real-valued continuous functions).
Let $(\mu_n)_{n\in\mathbb{N}}$ denote a Cauchy sequence in $C([0,T];X)$. Fix $\varepsilon > 0$. There is a K such that for all $m, n \geqslant K$

$$\sup_{\tau\in[0,T]} \mathrm{dist}_X(\mu_m(\tau),\mu_n(\tau)) < \varepsilon.$$

For any fixed $t \in [0,T]$,

$$\mathrm{dist}_X(\mu_m(t),\mu_n(t)) \leqslant \sup_{\tau\in[0,T]} \mathrm{dist}_X(\mu_m(\tau),\mu_n(\tau)) < \varepsilon$$

holds, so $(\mu_n(t))_{n\in\mathbb{N}}$ is a Cauchy sequence in X. Since X is complete, $(\mu_n(t))_{n\in\mathbb{N}}$ converges to some $\tilde{\mu}_t \in X$. This pointwise limit exists for every $t \in [0,T]$, and we construct a mapping μ from $[0,T]$ to X by defining

$$\mu(t) := \tilde{\mu}_t$$

for all $t \in [0,T]$.
There is an N such that

$$\sup_{\tau\in[0,T]} \operatorname{dist}_X(\mu_m(\tau),\mu_n(\tau)) < \varepsilon/2 \tag{A.1}$$

for all $m,n \geqslant N$ (with the same ε as before!). In particular, for fixed $t \in [0,T]$,

$$\operatorname{dist}_X(\mu_m(t),\mu_n(t)) < \varepsilon/2 \tag{A.2}$$

holds for all $m,n \geqslant N$. Thus, for each fixed $t \in [0,T]$ and for each $m \geqslant N$,

$$\operatorname{dist}_X(\mu_m(t),\mu(t)) \leqslant \underbrace{\operatorname{dist}_X(\mu_m(t),\mu_n(t))}_{<\varepsilon/2} + \underbrace{\operatorname{dist}_X(\mu_n(t),\mu(t))}_{<\varepsilon/2} < \varepsilon, \tag{A.3}$$

for sufficiently large n. Here we use (A.2) to estimate the first term on the right-hand side. Due to the fact that $\mu(t)$ is defined as the pointwise limit of $\mu_n(t)$, the second term can be made arbitrarily small by increasing n. We conclude from (A.3) that $\operatorname{dist}_X(\mu_m(t),\mu(t)) < \varepsilon$ for all $m \geqslant N$. Due to (A.1), this estimate holds with the same ε and N for all $t \in [0,T]$, whence

$$\sup_{t\in[0,T]} \operatorname{dist}_X(\mu_m(t),\mu(t)) \leqslant \varepsilon$$

for all $m \geqslant N$, which proves the convergence of (μ_m) to μ.
The limit $\mu : [0,T] \to X$ is continuous since it is the uniform limit of continuous mappings (cf. [Kos04] Thm. 8.3.1 for a proof for real-valued functions that can be extended trivially to our situation), hence (μ_n) converges in $C([0,T];X)$. □

Lemma A.2 (cf. [Kre78] Thm. 1.4-7)**.** *If Y is a closed subset of a complete metric space $(Z,\operatorname{dist}_Z)$, then Y is complete.*

Proof. Let $(\xi_n) \subset Y$ be a Cauchy sequence. Since $Y \subset Z$ and Z is complete, there is a $\xi \in Z$ such that

$$\lim_{n\to\infty} \operatorname{dist}_Z(\xi_n,\xi) = 0.$$

Because (ξ_n) is a sequence in Y and Y is closed, ξ must be an element of Y. Thus, Y is complete. □

Theorem A.3. *Let $(X,\operatorname{dist}_X)$ be a complete metric space. Fix $\nu_0 \in X$ and $T > 0$, and define*

$$\mathcal{C} := \{\nu \in C([0,T];X) : \nu(0) = \nu_0\}.$$

Endowed with the metric

$$\sup_{\tau\in[0,T]} \operatorname{dist}_X(\mu_1(\tau),\mu_2(\tau)), \tag{A.4}$$

the space $\mathcal{C}$ is a complete metric space.

Proof. Due to Lemma A.1, $C([0,T];X)$ is complete with respect to the metric (A.4). Clearly, $\mathcal{C} \subset C([0,T];X)$. We now show that $\mathcal{C}$ is closed. Let $(\mu_n) \subset \mathcal{C}$ be a sequence that converges to $\mu \in C([0,T];X)$. That is,

$$\lim_{n\to\infty} \sup_{t\in[0,T]} \operatorname{dist}_X(\mu(t), \mu_n(t)) = 0.$$

We note that for every $n \in \mathbb{N}$

$$\operatorname{dist}_X(\mu(0), \nu_0) = \operatorname{dist}_X(\mu(0), \mu_n(0)) \leqslant \sup_{t\in[0,T]} \operatorname{dist}_X(\mu(t), \mu_n(t)).$$

Since the left-hand side is independent of n, while the right-hand side tends to 0 as $n \to \infty$, it holds that

$$\operatorname{dist}_X(\mu(0), \nu_0) = 0,$$

so $\mu(0) = \nu_0$. We conclude that $\mu \in \mathcal{C}$ and thus $\mathcal{C}$ is closed. It follows from Lemma A.2 that $\mathcal{C}$ is complete. □

Corollary A.4. *For each $R > 0$, define*

$$\mathcal{P}_R(\mathbb{R}^d) := \left\{ \mu \in \mathcal{P}(\mathbb{R}^d) : \operatorname{supp}\mu \subset \overline{B(R)} \right\},$$

with $\overline{B(R)} := \{x \in \mathbb{R}^d : |x| \leqslant R\}$. Fix $\nu_0 \in \mathcal{P}_R(\mathbb{R}^d))$ and $T > 0$. The space

$$\{\nu \in C([0,T];\mathcal{P}_R(\mathbb{R}^d)) : \nu(0) = \nu_0\},$$

endowed with the metric

$$\sup_{\tau\in[0,T]} W_1(\mu_1(\tau), \mu_2(\tau)),$$

is a complete metric space. Here, W_1 denotes the 1-Wasserstein distance.

Proof. The ball $\overline{B(R)}$ is complete. Hence, it follows from [AGS08], Proposition 7.1.5, that $\big(\mathcal{P}^1\big(\overline{B(R)}\big), W_1\big)$ is complete. Here, $\mathcal{P}^1\big(\overline{B(R)}\big)$ is the space of probability measures with bounded first moment. Observe that

$$\mathcal{P}^1\big(\overline{B(R)}\big) = \mathcal{P}\big(\overline{B(R)}\big).$$

The inclusion $\mathcal{P}^1\big(\overline{B(R)}\big) \subset \mathcal{P}\big(\overline{B(R)}\big)$ is trivial. The other inclusion follows from the fact that the first moment of each $\mu \in \mathcal{P}\big(\overline{B(R)}\big)$ is bounded by R. Thus, $\big(\mathcal{P}\big(\overline{B(R)}\big), W_1\big)$ is a complete metric space.

There is a one-to-one correspondence between elements of $\mathcal{P}\big(\overline{B(R)}\big)$ and elements of $\mathcal{P}_R(\mathbb{R}^d)$. Convergence in one of these spaces implies convergence in the other, and therefore $\mathcal{P}_R(\mathbb{R}^d)$ is complete too. Theorem A.3 now implies the statement of the corollary. □

Appendix B

Integration of measure-valued maps

Let (X, Σ) be a measurable space and S a Polish space. We refer to [DU77] for the basic results on Bochner integration. The following result shows that $\|\cdot\|^*_{\mathrm{BL}}$ is a good norm from the point of view of integration.

Proposition B.1. *For any map $p : X \to \mathcal{M}(S)$ the following statements are equivalent:*

(i) p is Bochner measurable as map into $\overline{\mathcal{M}}(S)_{\mathrm{BL}}$;

(ii) For each bounded measurable function φ on S, the map $x \mapsto \langle p(x), \varphi\rangle$ is measurable;

(iii) For each Borel measurable $E \subset S$, $x \mapsto p(x)(E)$ is measurable.

Proof. A detailed proof is given in [Wor10]. A version for positive measures is proven in [HW09a], Proposition 2.5. □

If μ is a σ-finite positive measure on (X, Σ), $x \mapsto p(x)$ is Bochner measurable and $x \mapsto \|p(x)\|^*_{\mathrm{BL}}$ is integrable with respect to μ, then p is Bochner integrable and

$$\Big\| \int_X p(x)\, d\mu(x) \Big\|^*_{\mathrm{BL}} \leqslant \int_X \|p(x)\|^*_{\mathrm{BL}}\, d\mu(x) \tag{B.1}$$

(see e.g. [DU77]). Because S is separable, $\overline{\mathcal{M}}(S)_{\mathrm{BL}}$ is separable. Therefore there exists a countable subset $\mathcal{N} \subset \overline{\mathcal{M}}(S)^*_{\mathrm{BL}}$ that is norming:

$$\|\varphi\|^*_{\mathrm{BL}} = \sup\big\{ |\, \langle \varphi, f\rangle \,| \;:\; f \in \mathcal{N} \big\}$$

for all $\varphi \in \overline{\mathcal{M}}(S)_{\mathrm{BL}}$. Since $\overline{\mathcal{M}}(S)^*_{\mathrm{BL}} \simeq \mathrm{BL}(S)$ ([HW09a], Theorem 3.7, p. 360), we may consider $\mathcal{N}$ as subset of $\mathrm{BL}(S)$. In particular, if $p : X \to \mathcal{M}(S)$ satisfies the conditions of Proposition B.1, then $x \mapsto \|p(x)\|^*_{\mathrm{BL}}$ is measurable.

Proposition B.2. *Let μ be a σ-finite positive measure on (X, Σ) and let $p : X \to \mathcal{M}(S)$ satisfy any of the equivalent conditions in Proposition B.1. Then $x \mapsto \|p(x)\|_{\mathrm{TV}}$ is Borel measurable. Moreover, if the latter function is in $L^1(X, \mu)$, then:*

(i) For each Borel set $E \subset S$, the set-wise integral $\nu(E) := \int_X p(x)(E)\, d\mu(x)$ is defined and yields a finite Borel measure ν.

(ii) The map $x \mapsto p(x)$ is Bochner integrable and the Bochner integral given by $\nu' := \int_X p(x)\, d\mu(x)$ in $\overline{\mathcal{M}}(S)_{\mathrm{BL}}$ equals ν. In particular, for any Borel set E in S,

$$\left(\int_X p(x)\, d\mu(x) \right)(E) = \int_X p(x)(E)\, d\mu(x). \tag{B.2}$$

(iii)

$$\Big\| \int_X p(x)\, d\mu(x) \Big\|_{\mathrm{TV}} \leqslant \int_X \|p(x)\|_{\mathrm{TV}}\, d\mu(x).$$

Proof. Because S is Polish, there exists a countable algebra $\mathcal{A}$ of Borel sets that generates the Borel σ-algebra $\mathcal{B}(S)$ (cf. [Bog07b], Example 6.5.2). Then for any Borel measure μ, every $\varepsilon > 0$ and Borel set E there exists $A \in \mathcal{A}$ such that $|\mu(E) - \mu(A)| < \varepsilon$. Therefore (cf. [Bog07a], p.176),

$$\|p(x)\|_{\mathrm{TV}} = \sup_{E \in \mathcal{B}(S)} p(x)(E) - \inf_{E \in \mathcal{B}(S)} p(x)(E) = \sup_{A \in \mathcal{A}} p(x)(A) - \inf_{A \in \mathcal{A}} p(x)(A).$$

The functions $p^{\mathcal{A}} : x \mapsto \sup_{A \in \mathcal{A}} p(x)(A)$ and $p_{\mathcal{A}} : x \mapsto \inf_{A \in \mathcal{A}} p(x)(A)$ are measurable as pointwise supremum of a countable collection of measurable functions (see Proposition B.1). So $x \mapsto \|p(x)\|_{\mathrm{TV}}$ is measurable.
(i): The integral defining ν converges, because $|p(x)(E)| \leqslant \|p(x)\|_{\mathrm{TV}}$. σ-Additivity of ν is obtained through Lebesgue's Dominated Convergence Theorem.
(ii): $x \mapsto \|p(x)\|^*_{\mathrm{BL}}$ is measurable and dominated by the μ-integrable function $\|p(x)\|_{\mathrm{TV}}$, so p is indeed Bochner integrable. For any $f \in \mathrm{BL}(S)$,

$$\langle \nu', f \rangle = \int_X \langle p(x), f \rangle \, d\mu(x) = \langle \nu, f \rangle .$$

The first step holds because f defines a continuous functional on $\overline{\mathcal{M}}(S)_{\mathrm{BL}}$, the second because f is the pointwise limit of a sequence of step functions. Two finite Borel measures that coincide on $\mathrm{BL}(S)$ are identical (e.g. [Dud66], Lemma 6). For ν, clearly

$$\int_S f\, d\nu = \int_X \langle p(x), f \rangle \, d\mu(x)$$

for any bounded measurable function f. Equation (B.2) follows by taking $f = \mathbb{1}_E$.
(iii): From part *(ii)* it follows that for any $A \in \mathcal{A}$ (introduced above),

$$\int_X p_{\mathcal{A}}(x)\, d\mu(x) \leqslant \nu(A) \leqslant \int_X p^{\mathcal{A}}(x)\, d\mu(x).$$

Therefore,

$$\|\nu\|_{\mathrm{TV}} = \sup_{A\in\mathcal{A}} \nu(A) - \inf_{A\in\mathcal{A}} \nu(A) \leqslant \int_X p^{\mathcal{A}}(x) - p_{\mathcal{A}}(x)\, d\mu(x) = \int_X \|p(x)\|_{\mathrm{TV}}\, d\mu(x).$$

□

Moreover, for any continuous map $P : \mathcal{M}^+(S)_{\mathrm{BL}} \to \mathcal{M}^+(S)_{\mathrm{BL}}$ that is additive and positively homogeneous, i.e. $P(a\mu) = aP(\mu)$ for $a \geqslant 0$, one has

$$P\big(\int_X p(x)\, d\mu(x)\big) = \int_X P[p(x)]\, d\mu(x). \tag{B.3}$$

Appendix C

Equivalence of dual norms on bounded Lipschitz functions

Let S be a Polish space. Recall from Section 4.1.1 the bounded Lipschitz or Dudley norm, defined by

$$\|\phi\|_{\mathrm{BL}} := \|\phi\|_\infty + |\phi|_{\mathrm{L}}, \tag{C.1}$$

and the Fortet-Mourier norm, defined by

$$\|\phi\|_{\mathrm{FM}} := \max\{\|\phi\|_\infty, |\phi|_{\mathrm{L}}\},$$

for all $\phi \in \mathrm{BL}(S)$. We show now that both norms are equivalent.

Lemma C.1 (Equivalence of norms)**.** *The norms $\|\cdot\|_{\mathrm{BL}}$ and $\|\cdot\|_{\mathrm{FM}}$ are equivalent. In particular, we have*

$$\|\phi\|_{\mathrm{FM}} \leqslant \|\phi\|_{\mathrm{BL}} \leqslant 2\,\|\phi\|_{\mathrm{FM}} \tag{C.2}$$

for all $\phi \in \mathrm{BL}(S)$. Moreover, the given bounds are sharp.

Proof. The first inequality follows from the fact that

$$\begin{aligned}\|\phi\|_{\mathrm{FM}} &= \max\{\|\phi\|_\infty, |\phi|_{\mathrm{L}}\}\\ &\leqslant \min\{\|\phi\|_\infty, |\phi|_{\mathrm{L}}\} + \max\{\|\phi\|_\infty, |\phi|_{\mathrm{L}}\}\\ &= \|\phi\|_\infty + |\phi|_{\mathrm{L}}\\ &= \|\phi\|_{\mathrm{BL}}.\end{aligned}$$

The second inequality follows from

$$\begin{aligned}\|\phi\|_{\mathrm{BL}} &= \|\phi\|_\infty + |\phi|_{\mathrm{L}}\\ &\leqslant 2\max\{\|\phi\|_\infty, |\phi|_{\mathrm{L}}\}\\ &= 2\|\phi\|_{\mathrm{FM}}.\end{aligned}$$

If we choose $\phi \in \mathrm{BL}(S)$ to be a constant, then $|\phi|_{\mathrm{L}} = 0$. Hence, $\|\phi\|_{\mathrm{BL}} = \|\phi\|_\infty = \|\phi\|_{\mathrm{FM}}$ and thus there is an element of $\mathrm{BL}(S)$ for which the first inequality in (C.2) is

really an equality. If we choose $\phi \in \mathrm{BL}(S)$ such that $\|\phi\|_\infty = |\phi|_\mathrm{L}$ then $\|\phi\|_\infty = |\phi|_\mathrm{L} = \max\{\|\phi\|_\infty, |\phi|_\mathrm{L}\}$. Consequently, $\|\phi\|_\mathrm{BL} = 2\max\{\|\phi\|_\infty, |\phi|_\mathrm{L}\} = 2\|\phi\|_\mathrm{FM}$, and we have a ϕ for which equality holds in the second half of (C.2). □

Let $\mathrm{BL}(S)^*$ be the dual of $\mathrm{BL}(S)$, with duality pairing $\langle \phi^*, \phi \rangle$ for all $\phi^* \in \mathrm{BL}(S)^*$ and $\phi \in \mathrm{BL}(S)$. We define dual norms on $\mathrm{BL}(S)^*$, which – completely in line with the above – we do in two ways. First, for any $\phi^* \in \mathrm{BL}(S)^*$ we define the bounded Lipschitz or Dudley *dual* norm as

$$\|\phi^*\|^*_\mathrm{BL} := \sup\{|\langle \phi^*, \phi \rangle| \,:\, \phi \in \mathrm{BL}(S),\, \|\phi\|_\mathrm{BL} \leqslant 1\}. \tag{C.3}$$

The Fortet-Mourier *dual* norm is given by

$$\|\phi^*\|^*_\mathrm{FM} := \sup\{|\langle \phi^*, \phi \rangle| \,:\, \phi \in \mathrm{BL}(S),\, \|\phi\|_\mathrm{FM} \leqslant 1\}. \tag{C.4}$$

Lemma C.2 (Equivalence of dual norms)**.** *The norms $\|\cdot\|^*_\mathrm{BL}$ and $\|\cdot\|^*_\mathrm{FM}$ are equivalent. In particular, we have*

$$\|\phi^*\|^*_\mathrm{BL} \leqslant \|\phi^*\|^*_\mathrm{FM} \leqslant 2\,\|\phi^*\|^*_\mathrm{BL} \tag{C.5}$$

for all $\phi^* \in \mathrm{BL}(S)^*$. The given lower bound is sharp. If there are $x, y \in S$ such that $d(x,y) = 2$, then also the given upper bound is sharp.

Proof. To prove the estimates, let $\phi^* \in \mathrm{BL}(S)^*$ be given. Define the following subsets of $\mathbb{R}$:

$$\begin{aligned} A_\mathrm{BL} &:= \{|\langle \phi^*, \phi \rangle| \,:\, \phi \in \mathrm{BL}(S),\ \|\phi\|_\mathrm{BL} \leqslant 1\}, \\ A_\mathrm{FM} &:= \{|\langle \phi^*, \phi \rangle| \,:\, \phi \in \mathrm{BL}(S),\ \|\phi\|_\mathrm{FM} \leqslant 1\}, \\ A_{\mathrm{FM},\frac{1}{2}} &:= \left\{|\frac{1}{2}\langle \phi^*, \phi \rangle| \,:\, \phi \in \mathrm{BL}(S),\ \|\phi\|_\mathrm{FM} \leqslant 1\right\}. \end{aligned}$$

Note that these sets depend on ϕ^*. By definition of the dual norms (C.3) and (C.4), $\|\phi^*\|^*_\mathrm{BL} = \sup A_\mathrm{BL}$ and $\|\phi^*\|^*_\mathrm{FM} = \sup A_\mathrm{FM}$ hold.

1. Assume that $\alpha \in A_\mathrm{BL}$, then there is a $\phi \in \mathrm{BL}(S)$ satisfying $\|\phi\|_\mathrm{BL} \leqslant 1$ such that $|\langle \phi^*, \phi \rangle| = \alpha$. Since $\|\phi\|_\mathrm{FM} \leqslant \|\phi\|_\mathrm{BL}$ (Lemma C.1), we know that $\|\phi\|_\mathrm{FM} \leqslant 1$ and thus $\alpha \in A_\mathrm{FM}$. Hence, $A_\mathrm{BL} \subset A_\mathrm{FM}$ and consequently $\sup A_\mathrm{BL} \leqslant \sup A_\mathrm{FM}$. The latter statement can be written as

$$\|\phi^*\|^*_\mathrm{BL} \leqslant \|\phi^*\|^*_\mathrm{FM}.$$

2. Assume that $\alpha \in A_{\mathrm{FM},\frac{1}{2}}$, then there is a $\phi \in \mathrm{BL}(S)$ satisfying $\|\phi\|_\mathrm{FM} \leqslant 1$ such that $\frac{1}{2}|\langle \phi^*, \phi \rangle| = \alpha$. Define $\tilde{\phi} := \frac{1}{2}\phi$. Since $\|\phi\|_\mathrm{BL} \leqslant 2\|\phi\|_\mathrm{FM}$ (Lemma C.1), we know that $\|\tilde{\phi}\|_\mathrm{BL} \leqslant 2\|\frac{1}{2}\phi\|_\mathrm{FM} = \|\phi\|_\mathrm{FM} \leqslant 1$. This implies that $\tilde{\phi}$ satisfies the conditions in A_BL and thus $|\langle \phi^*, \tilde{\phi} \rangle| \in A_\mathrm{BL}$. Because $|\langle \phi^*, \tilde{\phi} \rangle| = \alpha$, it follows that $A_{\mathrm{FM},\frac{1}{2}} \subset A_\mathrm{BL}$ and consequently $\sup A_{\mathrm{FM},\frac{1}{2}} \leqslant \sup A_\mathrm{BL}$. The observation $\sup A_{\mathrm{FM},\frac{1}{2}} = \frac{1}{2}\sup A_\mathrm{FM}$ finally leads to

$$\|\phi^*\|^*_\mathrm{FM} \leqslant 2\|\phi^*\|^*_\mathrm{BL}.$$

To prove sharpness of the bounds, consider the following:

1. Fix $x \in S$ and take ϕ^* such that $\langle \phi^*, \phi \rangle = \phi(x)$. This ϕ^* is a bounded linear functional. For each $\phi \in \mathrm{BL}(S)$ we have that $|\langle \phi^*, \phi \rangle| = |\phi(x)| \leqslant \|\phi\|_\infty$.

   (i) The inequality $\|\phi\|_\infty \leqslant \|\phi\|_{\mathrm{FM}}$ is trivially satisfied. For each $\phi \in \mathrm{BL}(S)$ with $\|\phi\|_{\mathrm{FM}} \leqslant 1$ we therefore have that $|\langle \phi^*, \phi \rangle| \leqslant 1$. The upper bound is attained by $\phi \equiv 1$, thus $\|\phi^*\|^*_{\mathrm{FM}} = 1$.

   (ii) Because $\|\phi\|_\infty \leqslant \|\phi\|_{\mathrm{BL}}$ holds, $|\langle \phi^*, \phi \rangle| \leqslant 1$ for all $\phi \in \mathrm{BL}(S)$ satisfying $\|\phi\|_{\mathrm{BL}} \leqslant 1$. This upper bound is attained by $\phi \equiv 1$. Consequently, $\|\phi^*\|^*_{\mathrm{BL}} = 1$.

   We thus have that
   $$\|\phi^*\|^*_{\mathrm{FM}} = 1 = \|\phi^*\|^*_{\mathrm{BL}},$$
   which proves the sharpness of the first inequality.

2. Take $x, y \in S$ such that $d(x, y) = 2$ and let ϕ^* be the bounded linear functional given by $\langle \phi^*, \phi \rangle = \phi(x) - \phi(y)$.

   (i) For each $\phi \in \mathrm{BL}(S)$ with $\|\phi\|_{\mathrm{FM}} \leqslant 1$ we have that $|\langle \phi^*, \phi \rangle| = |\phi(x) - \phi(y)| \leqslant |\phi|_{\mathrm{L}}\, d(x, y) = 2|\phi|_{\mathrm{L}} \leqslant 2$. The upper bound is attained by some $\phi \in \mathrm{BL}(S)$ satisfying $\|\phi\|_{\mathrm{FM}} \leqslant 1$, namely by $\phi : z \mapsto (d(x, z) - d(y, z))/2$, thus $\|\phi^*\|^*_{\mathrm{FM}} = 2$.

   (ii) If for $\phi \in \mathrm{BL}(S)$ we have $\|\phi\|_{\mathrm{BL}} \leqslant 1$, then $|\langle \phi^*, \phi \rangle| \leqslant 2|\phi|_{\mathrm{L}}$ and moreover $|\langle \phi^*, \phi \rangle| = |\phi(x) - \phi(y)| \leqslant 2\|\phi\|_\infty$. Adding these conditions and dividing by 2, we obtain $|\langle \phi^*, \phi \rangle| \leqslant \|\phi\|_{\mathrm{BL}}$. For any $\phi \in \mathrm{BL}(S)$ satisfying $\|\phi\|_{\mathrm{BL}} \leqslant 1$ we thus have the upper bound $|\langle \phi^*, \phi \rangle| \leqslant 1$. This upper bound is attained by $\phi : z \mapsto (d(x, z) - d(y, z))/4$, which also satisfies $\|\phi\|_{\mathrm{BL}} \leqslant 1$. Consequently, $\|\phi^*\|^*_{\mathrm{BL}} = 1$.

   In this case
   $$\|\phi^*\|^*_{\mathrm{FM}} = 2 = 2\|\phi^*\|^*_{\mathrm{BL}}.$$

□

We conclude from Lemma C.2 that the dual space consists of the same elements, independently of our choice for $\|\cdot\|_{\mathrm{BL}}$ or $\|\cdot\|_{\mathrm{FM}}$ as the norm on $\mathrm{BL}(S)$. A linear functional that is bounded with respect to one of the two associated dual norms, is also bounded in the other, due to their equivalence.

Appendix D

Flat metric for signed discrete measures

Let S be a Polish space and $\mathcal{M}(S)$ be the space of finite Borel measures on S. The natural pairing between measures $\mu \in \mathcal{M}(S)$ and bounded measurable functions ϕ is

$$\langle \mu, \phi \rangle := \int_S \phi \, d\mu.$$

Using the Fortet-Mourier dual norm, we define a *distance* between two measures μ and ν (also called *flat metric*)

$$F(\mu, \nu) := \|\mu - \nu\|^*_{\mathrm{FM}} = \sup \left\{ \int_S \phi \, d(\mu - \nu) \, : \, \phi \in \mathrm{BL}(S), \, \|\phi\|_{\mathrm{FM}} \leqslant 1 \right\}.$$

Note that the absolute value within the supremum is omitted. This does not change the value of the supremum, since if $\phi \in \mathrm{BL}(S)$ satisfies $\|\phi\|_{\mathrm{FM}} \leqslant 1$, then also $-\phi \in \mathrm{BL}(S)$ and $\|-\phi\|_{\mathrm{FM}} \leqslant 1$. The value $|\int_S \phi \, d(\mu - \nu)|$ is then attained by $\int_S \psi \, d(\mu - \nu)$ for either $\psi = \phi$ or $\psi = -\phi$.

In the sequel we restrict ourselves to $S = \mathbb{R}$ (where all our results can also be obtained easily for an interval $S \subset \mathbb{R}$). Moreover, we only consider $\mu - \nu$ of the form

$$\mu - \nu = \sum_{k=1}^{N} a_k \delta_{x_k},$$

where $N \in \mathbb{N}$ is fixed, $\{a_k\}_{k=1}^N \subset \mathbb{R}$ and $\{x_k\}_{k=1}^N \subset \mathbb{R}$. Without loss of generality, we can assume that $a_k \neq 0$ for all k and that $x_1 < \ldots < x_N$.

It is clear that for this particular type of measures $\mu - \nu$

$$\int_{\mathbb{R}} \phi \, d(\mu - \nu) = \sum_{k=1}^{N} a_k \, \phi_k,$$

where $\phi_k := \phi(x_k)$. The condition $\phi \in \mathrm{BL}(\mathbb{R})$, with $\|\phi\|_{\mathrm{FM}} \leqslant 1$, translates to $|\phi_k| \leqslant 1$ for all $k \in \{1, 2, \ldots, N\}$ and $|\phi_k - \phi_j| \leqslant |x_k - x_j|$ for all pairs $j, k \in \{1, 2, \ldots, N\}$. We formalize this statement in the following lemma, showing also that it is sufficient to have the condition $|\phi_k - \phi_j| \leqslant |x_k - x_j|$ only for $j = k - 1$.

Lemma D.1. *For any measure on $\mathbb{R}$ of the form $\mu - \nu = \sum_{k=1}^{N} a_k \delta_{x_k}$, satisfying $x_1 < \ldots < x_N$, the following equality holds*

$$\sup\left\{\int_{\mathbb{R}} \phi \, d(\mu - \nu) \,:\, \phi \in \mathrm{BL}(\mathbb{R}),\, \|\phi\|_{\mathrm{FM}} \leqslant 1\right\}$$
$$= \sup\left\{\sum_{k=1}^{N} a_k \, \phi_k \,:\, |\phi_k| \leqslant 1, |\phi_k - \phi_{k-1}| \leqslant |x_k - x_{k-1}| \, \forall k\right\}.$$

Proof. The proof requires a two-step approach.

1. We show that:

$$\overbrace{\sup\left\{\int_{\mathbb{R}} \phi \, d(\mu - \nu) \,:\, \phi \in \mathrm{BL}(\mathbb{R}),\, \|\phi\|_{\mathrm{FM}} \leqslant 1\right\}}^{=:B_1}$$
$$= \underbrace{\sup\left\{\sum_{k=1}^{N} a_k \, \phi_k \,:\, (\phi_1, \ldots, \phi_N)^T \in \mathbb{R}^N,\, |\phi_k| \leqslant 1, |\phi_k - \phi_j| \leqslant |x_k - x_j| \, \forall j, k\right\}}_{=:B_2}.$$

   (i) Let $\beta \in B_1$, with $\phi \in \mathrm{BL}(\mathbb{R})$, satisfying $\|\phi\|_{\mathrm{FM}} \leqslant 1$, such that $\int_{\mathbb{R}} \phi \, d(\mu - \nu) = \beta$. Define $\phi_k := \phi(x_k)$ for all k. Then $\sum_{k=1}^{N} a_k \, \phi_k = \int_{\mathbb{R}} \phi \, d(\mu - \nu) = \beta$, $|\phi_k| = |\phi(x_k)| \leqslant 1$ for all k and $|\phi_k - \phi_j| = |\phi(x_k) - \phi(x_j)| \leqslant |x_k - x_j|$ for all j, k. Thus $\beta \in B_2$, which implies $B_1 \subset B_2$.

   (ii) Let $\beta \in B_2$, with $(\phi_1, \ldots, \phi_N)^T \in \mathbb{R}^N$, $|\phi_k| \leqslant 1$ and $|\phi_k - \phi_j| \leqslant |x_k - x_j|$ for all j, k, such that $\sum_{k=1}^{N} a_k \, \phi_k = \beta$. Define a function $\phi : \mathbb{R} \to \mathbb{R}$ as:

$$\phi(x) := \begin{cases} \phi_1, & x < x_1; \\ \phi_{k-1} + \dfrac{x - x_{k-1}}{x_k - x_{k-1}}(\phi_k - \phi_{k-1}), & x_{k-1} \leqslant x < x_k,\ k \in \{2, \ldots, N\}; \\ \phi_N, & x \geqslant x_N. \end{cases}$$

   Then $\phi(x_k) = \phi_k$ for all k and thus $\int_{\mathbb{R}} \phi \, d(\mu - \nu) = \sum_{k=1}^{N} a_k \, \phi_k = \beta$. For $x_{k-1} \leqslant x < x_k$, we have that $|\phi(x)| \leqslant \max\{|\phi_{k-1}|, |\phi_k|\}$, thus $\|\phi\|_\infty \leqslant \max_k\{|\phi_k|\} \leqslant 1$. Note that ϕ is differentiable almost everywhere, and its weak derivative is bounded: $\|\phi'\|_\infty \leqslant \max_{2 \leqslant k \leqslant N}(\phi_k - \phi_{k-1})/(x_k - x_{k-1})$. Hence, ϕ is Lipschitz continuous and $|\phi|_{\mathrm{L}} \leqslant \|\phi'\|_\infty$, due to [Eva10], Theorem 4, p. 294. By assumption on $\{\phi_k\}$, for each k: $(\phi_k - \phi_{k-1})/(x_k - x_{k-1}) \leqslant 1$, hence $|\phi|_{\mathrm{L}} \leqslant 1$. We conclude that $\phi \in \mathrm{BL}(\mathbb{R})$ and $\|\phi\|_{\mathrm{FM}} \leqslant 1$, which implies that $B_2 \subset B_1$.

The inclusions $B_1 \subset B_2$ and $B_2 \subset B_1$ yield that $\sup B_1 = \sup B_2$.

2. We show that:

$$\sup\left\{\sum_{k=1}^{N} a_k\,\phi_k \,:\, |\phi_k| \leqslant 1, |\phi_k - \phi_j| \leqslant |x_k - x_j|\,\forall j,k\right\}$$
$$= \sup \underbrace{\left\{\sum_{k=1}^{N} a_k\,\phi_k \,:\, |\phi_k| \leqslant 1, |\phi_k - \phi_{k-1}| \leqslant |x_k - x_{k-1}|\,\forall k\right\}}_{=:B_3}.$$

It is clear that $B_2 \subset B_3$.
Assume that $(\phi_1, \ldots, \phi_N)^T \in \mathbb{R}^N$ satisfies $|\phi_k - \phi_{k-1}| \leqslant |x_k - x_{k-1}|$ for all $2 \leqslant k \leqslant N$. As the elements of $\{x_k\}$ are ordered, $|x_k - x_{k-1}| = x_k - x_{k-1}$ for each k. Let $j, \ell \in \{1, \ldots, N\}$ be arbitrary, and assume without loss of generality $j \leqslant \ell$. Due to the triangle inequality

$$|\phi_\ell - \phi_j| \leqslant \sum_{k=j+1}^{\ell} |\phi_k - \phi_{k-1}| \leqslant \sum_{k=j+1}^{\ell} (x_k - x_{k-1}) = x_\ell - x_j = |x_\ell - x_j|.$$

Hence $B_3 \subset B_2$.
It follows that $B_2 = B_3$ and thus $\sup B_2 = \sup B_3$.

□

Appendix E

Algorithm for computing the flat metric for signed discrete measures

In this appendix we describe an algorithm for computing the flat metric, based on its characterization given in Lemma D.1. We present here the results of [JMC13] and use the same notation as in Appendix D. The algorithm works for discrete measures on $\mathbb{R}$ as well as on intervals $S \subset \mathbb{R}$.

Define

$$F^m(\psi) := \sup \left\{ \sum_{k=1}^{m} a_k \, \phi_k \, : \, \phi_m = \psi, |\phi_k| \leqslant 1, |\phi_k - \phi_{k-1}| \leqslant |x_k - x_{k-1}| \, \forall k \leqslant m \right\}$$

for any $m \leqslant N$ and $\psi \in [-1, 1]$. By definition $F(\mu, \nu) = \sup_{\psi \in [-1,1]} F^N(\psi)$. Define $\Delta_k := |x_k - x_{k-1}|$ for all $k \in \{2, \ldots, N\}$. Note that

$$F^1(\psi) = a_1 \, \psi, \text{ and} \tag{E.1}$$

$$F^m(\psi) = a_m \, \psi + \sup_{\phi_{m-1} \in [\psi - \Delta_m, \psi + \Delta_m] \cap [-1,1]} F^{m-1}(\phi_{m-1}). \tag{E.2}$$

Our aim is to exploit this recursive relation for F^m to construct F^N. As we will see in Lemmas E.1 and E.2, the functions F^m are all concave and piecewise linear, and the supremum (in fact: maximum) of F^N is hence easily found. The algorithm that we present in Section E.1, follows the same philosophy.

Lemma E.1. *For each $m \in \{1, \ldots, N\}$, the function F^m is concave.*

Proof. We use a mathematical induction argument with respect to m. Since $F^1(\psi) = a_1 \, \psi$, the statement is true for $m = 1$. Now, assume that F^{m-1} is concave for some $1 < m \leqslant N$. Define, for any $\psi \in [-1, 1]$,

$$\bar{F}^{m-1}(\psi) := \sup_{z \in [\psi - \Delta_m, \psi + \Delta_m] \cap [-1,1]} F^{m-1}(z). \tag{E.3}$$

Choose $\psi^1, \psi^2 \in [-1,1]$. By definition of the supremum, (E.3) implies that for each $i \in \{1,2\}$ there is a sequence $(\psi^i_j)_{j\in\mathbb{N}} \subset [\psi^i - \Delta_m, \psi^i + \Delta_m] \cap [-1,1]$ such that

$$\bar{F}^{m-1}(\psi^i) = \lim_{j\to\infty} F^{m-1}(\psi^i_j).$$

For each $j \in \mathbb{N}$ and each $\theta \in [0,1]$,

$$\theta\,\psi^1_j + (1-\theta)\,\psi^2_j \;\in\; \overline{B}\big(\theta\,\psi^1 + (1-\theta)\,\psi^2\,,\,\Delta_m\big) \cap [-1,1] \tag{E.4}$$

is satisfied. Hence, for $\theta \in [0,1]$, we have

$$\begin{aligned}\theta\,\bar{F}^{m-1}(\psi^1) + (1-\theta)\,\bar{F}^{m-1}(\psi^2) &= \lim_{j\to\infty} \theta\,F^{m-1}(\psi^1_j) + (1-\theta)\,F^{m-1}(\psi^2_j)\\ &\leqslant \lim_{j\to\infty} F^{m-1}(\theta\,\psi^1_j + (1-\theta)\,\psi^2_j)\\ &\leqslant \bar{F}^{m-1}(\theta\,\psi^1 + (1-\theta)\,\psi^2),\end{aligned} \tag{E.5}$$

where we use in the second step that F^{m-1} is concave and that $\psi^1_j, \psi^2_j \in [-1,1]$ for each $j \in \mathbb{N}$. The third step is due to a combination of (E.3) and (E.4). It follows from (E.5) that $\bar{F}^{m-1}$ is concave. Since $F^m(\psi) := a_m\,\psi + \bar{F}^{m-1}(\psi)$ is the sum of a linear function and a concave function, F^m itself is concave. □

Lemma E.2. *For all $m \in \{1,\dots,N\}$ the function F^m is continuous and piecewise linear, and it is determined by its function values in at most $m+1$ points. If $m \in \{2,\dots,N\}$, then the function F^m satisfies*

$$F^m(\psi) = a_m\,\psi + \begin{cases} F^{m-1}(\psi + \Delta_m), & \psi \in [-1, \tilde{\psi}_m - \Delta_m] \cap [-1,1];\\ F^{m-1}(\tilde{\psi}_m), & \psi \in [\tilde{\psi}_m - \Delta_m, \tilde{\psi}_m + \Delta_m] \cap [-1,1];\\ F^{m-1}(\psi - \Delta_m), & \psi \in [\tilde{\psi}_m + \Delta_m, 1] \cap [-1,1];\end{cases} \tag{E.6}$$

where $\tilde{\psi}_m := \max\{\tilde{\psi} \in [-1,1] \,:\, F^{m-1}(\psi) \leqslant F^{m-1}(\tilde{\psi})$ for all $\psi \in [-1,1]\}$.

Proof. Again we use mathematical induction. F^1 is a linear function, and hence determined by its values in -1 and 1. Now assume that F^{m-1} satisfies the statement of the lemma (with $m \geqslant 2$). Since F^{m-1} is continuous and concave (Lemma E.1) on a compact interval, $\tilde{\psi}_m$ exists. Since F^{m-1} is piecewise linear, its maximum is attained at the endpoint of an interval. In case the maximum is attained at an internal point, F^{m-1} is constant on the corresponding interval, and hence we can choose $\tilde{\psi}_m$ to be the right endpoint (it is important to make a choice, although it is arbitrary which choice we make). Hence, if $[\psi_1, \psi_2]$ is an interval on which F^{m-1} is linear, then

- if $\psi_2 \leqslant \tilde{\psi}_m$: F^{m-1} is nondecreasing on the interval and takes its maximum in ψ_2;
- if $\psi_1 \geqslant \tilde{\psi}_m$: F^{m-1} is decreasing on the interval and takes its maximum in ψ_1.

Fix $\psi \in [-1,1]$. If $\psi \in [\tilde{\psi}_m - \Delta_m, \tilde{\psi}_m + \Delta_m]$, then $\tilde{\psi}_m \in [\psi - \Delta_m, \psi + \Delta_m]$ and

$$\sup_{\phi \in [\psi-\Delta_m, \psi+\Delta_m]\cap[-1,1]} F^{m-1}(\phi) = F^{m-1}(\tilde{\psi}_m);$$

the left-hand side occurs in (E.2). If $\psi < \tilde{\psi}_m - \Delta_m$ then

$$\sup_{\phi \in [\psi - \Delta_m, \psi + \Delta_m] \cap [-1,1]} F^{m-1}(\phi) = F^{m-1}(\psi + \Delta_m),$$

since F^{m-1} is nondecreasing on $[-1, \tilde{\psi}_m]$. Analogously, we have

$$\sup_{\phi \in [\psi - \Delta_m, \psi + \Delta_m] \cap [-1,1]} F^{m-1}(\phi) = F^{m-1}(\psi - \Delta_m),$$

if $\psi > \tilde{\psi}_m - \Delta_m$. Summarizing, we obtain

$$\sup_{\phi} F^{m-1}(\phi) = \begin{cases} F^{m-1}(\psi + \Delta_m), & \psi \in [-1, \tilde{\psi}_m - \Delta_m] \cap [-1,1]; \\ F^{m-1}(\tilde{\psi}_m), & \psi \in [\tilde{\psi}_m - \Delta_m, \tilde{\psi}_m + \Delta_m] \cap [-1,1]; \\ F^{m-1}(\psi - \Delta_m), & \psi \in [\tilde{\psi}_m + \Delta_m, 1] \cap [-1,1], \end{cases} \tag{E.7}$$

where the supremum is taken over all $\phi \in [\psi - \Delta_m, \psi + \Delta_m] \cap [-1,1]$. Via (E.2), the expression in (E.7) implies the desired result for F^m as stated in (E.6). Note that one or more of the three intervals in (E.7) may be empty.
It is easily checked in (E.6) that F^m is continuous if F^{m-1} is continuous. In particular, continuity holds at $\psi = \tilde{\psi}_m \pm \Delta_m$. By assumption, F^{m-1} is piecewise linear and determined by its function values in at most m points. By construction $\tilde{\psi}_m$ is one of these points. F^m is constructed by translating the graph of F^{m-1} on the left-hand (right-hand) side of $\tilde{\psi}_m$ to the left (right) over a distance Δ_m, and interpolating linearly on the interval $[\tilde{\psi}_m - \Delta_m, \tilde{\psi}_m + \Delta_m]$. The addition of the linear term $a_m \psi$ preserves the piecewise linearity. This construction adds a degree of freedom, making a total of at most $m+1$, because F^{m-1} had at most m degrees of freedom. Note that the number of degrees of freedom might decrease by points determining F^{m-1} that end up outside the interval $[-1,1]$ after translation over $\pm\Delta_m$. □

Note that ψ is comparable to an element from the *range* of the test function $\phi \in \mathrm{BL}(\mathbb{R})$. The fact that ψ always comes from the interval $[-1,1]$ is compatible with the demand $\|\phi\|_{\mathrm{FM}} \leqslant 1$. Although ψ is the argument of F^m and it occurs on the horizontal axis in the above, it should not be confused with the positions of the Dirac masses, which can be anywhere in $\mathbb{R}$.

We have derived in Lemma E.2 the relation between the subsequent F^ms. From now on, we can 'forget' *why* (E.6) is true, and simply apply it recursively as basis for our algorithm, ultimately to obtain F^N. See also Figure E.1 for a schematic illustration of one of the recursive steps. The fact that we deal with piecewise linear functions (of which the lemma gives the maximum number of degrees of freedom) makes that we can store and build the whole function efficiently: per recursion step we only need to trace the positions and function values of the endpoints of the linear subintervals. In fact, what we store (see Section E.1) are the value at -1, the endpoints of the intervals – and even only those in the interior: $(-1,1)$ – and the slopes on the linear subintervals.

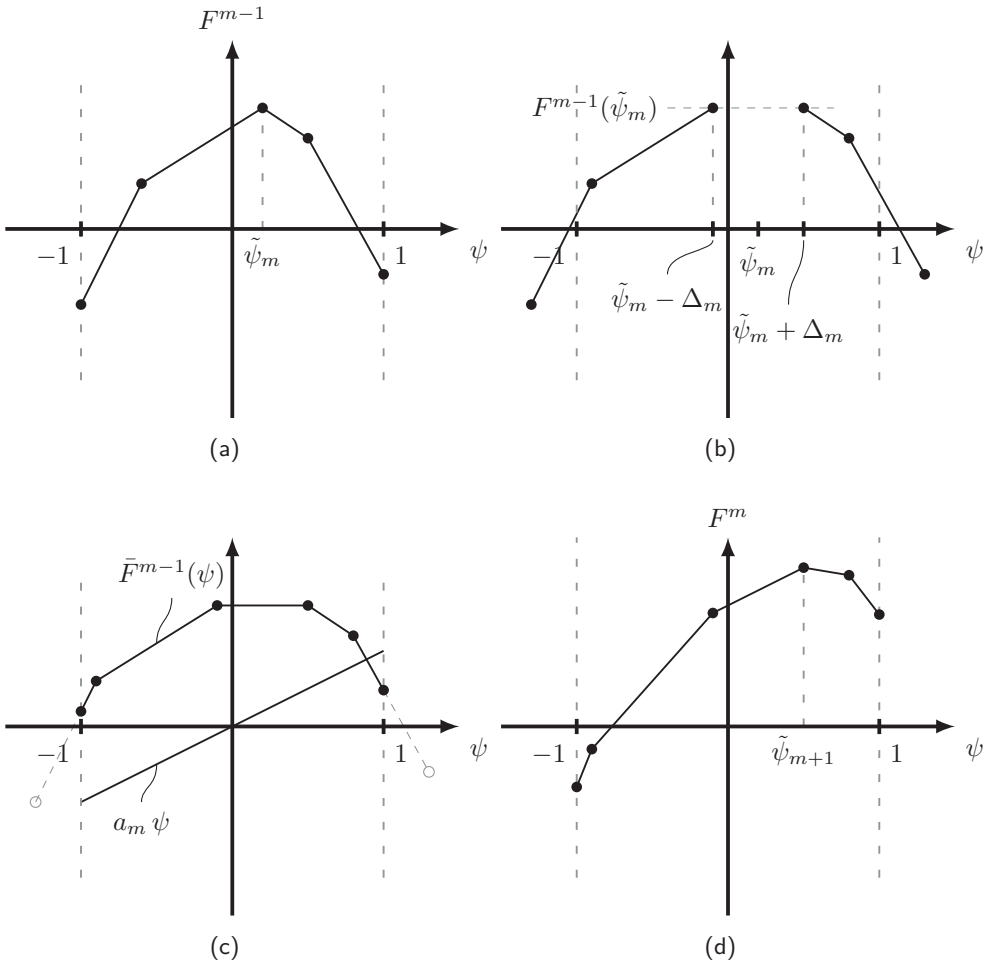

Figure E.1: (a): Previous piecewise linear, concave function F^{m-1}. (b): Split at the maximum and translate over distance Δ_m to the left/right at either side of the maximum. (c): Interpolate by a constant on the interval $[\tilde{\psi}_m - \Delta_m, \tilde{\psi}_m + \Delta_m]$ and restrict the function to $[-1, 1]$; introduce the linear function $\psi \mapsto a_m\,\psi$. (d): Addition of $\bar{F}^{m-1}$ and the linear function yields F^m; its maximum is attained at $\tilde{\psi}_{m+1}$ which is used in the next step.

E.1 The actual algorithm

The way the algorithm is described in this section is influenced by MATLAB syntax.

Initialization

Assume that the arrays `x` and `a` are given. If `x(i)` $=$ `x(j)` (`i` $\neq$ `j`), then replace `a(i)` by `a(i)` $+$ `a(j)` and remove element `j` from `x` and `a`. Remove element `i` from `x` and `a` if `a(i)` $= 0$. Sort `x` in increasing order, and sort `a` accordingly. Start the algorithm thus with `N`-dimensional arrays `a` and sorted `x`.

Since $F^1(\psi) = a_1\,\psi$ we initialize `leftVal` $= -a_1$, the variable for $F^m(-1)$, and

$$\texttt{funcDes} = \begin{pmatrix} -1 & a_1 \\ 1 & -\infty \end{pmatrix},$$

where the first column denotes the endpoints of the subintervals, and the second column the slope of F^1 in the interval to the right of the corresponding value in the first column. The variable `leftVal` and the array `funcDes` will be updated every step, where the number of columns in `funcDes` increases by at most 1. The value $-\infty$ in the bottom right entry is added for technical reasons: the entry needs to be filled, and in such a way that concavity is preserved (i.e. slopes decrease).

For each `m` from `2` to `N` repeat the following:

Define `d` $=$ `x(m)` $-$ `x(m-1)`. Identify nondecreasing segments, store them in the array `funcLeft` after translating the corresponding endpoints over a distance `d` to the left:

```
idxBool  =  funcDes(:,2)>=0
funcLeft  =  [funcDes(idxBool,1)-d, funcDes(idxBool,2)]
```

Analogously, for the decreasing intervals:

```
 idxBool  =  funcDes(:,2)<0
funcRight  =  [funcDes(idxBool,1)+d, funcDes(idxBool,2)]
```

Store $\tilde{\psi}_m + \Delta_m$:

```
yTop = min(funcRight(:,1))
```

Intermediate step: store the information about $\bar{F}^{m-1}$ (before adding the linear function):

```
funcDes = [funcLeft; [yTop-2*d, 0]; funcRight]
```

Note that `yTop-2*d` $= \tilde{\psi}_m - \Delta_m$. Determine the indices of those points that were shifted out of the interval $[-1, 1]$ on the left-hand side (at least one, as `d` > 0 by construction of `x`):

```
idxBool  =  funcDes(:,1)<-1
    idx  =  1:size(funcDes,1)
    idx  =  idx(idxBool)
```

Calculate the new `leftVal` after translation of the graph to the left and addition of $a_m\,\psi$. This depends on the endpoints that were shifted beyond -1.

```
for j=idx
    leftVal = leftVal +...
                (min(funcDes(j+1,1),-1)-funcDes(j,1))*funcDes(j,2)
end
leftVal = leftVal - a(m)
```

Find the new subinterval with left endpoint -1:

```
idxBool  =  funcDes(:,1)<=-1
    idx  =  1:size(funcDes,1)
    idx  =  idx(idxBool)
 maxIdx  =  max(idx)
   yMin  =  funcDes(maxIdx,1)
   pMin  =  funcDes(maxIdx,2)
```

Create F^m by deleting the points outside the interval $[-1, 1)$, and adding a_m to the slope of each subinterval:

```
idxBool  =  (funcDes(:,1)>=-1).*(funcDes(:,1)<1)
    idx  =  1:size(funcDes,1)
    idx  =  idx(idxBool)
```

```
if yMin<-1
    funcDes = [[-1, pMin+a(m)];...
                [funcDes(idx,1),funcDes(idx,2)+a(m)]; [1,-Inf]]
else
    funcDes = [[funcDes(idx,1),funcDes(idx,2)+a(m)]; [1,-Inf]]
end
```

After the above loop over `m`

Determine on which subintervals F^N is increasing:

```
idxBool  =  funcDes(:,2)>0
    idx  =  1:size(funcDes,1)
    idx  =  idx(idxBool)
```

Calculate the maximum (i.e. the final answer) using the slopes on those intervals where F^N is increasing:

```
distance = leftVal
for j=idx
    distance = distance + (funcDes(j+1,1)-funcDes(j,1))*funcDes(j,2)
end
```

Return the value of `distance`. This completes the algorithm.

Remark E.1. The algorithm does not generalize to higher dimensions, because it uses the ordering of the positions, e.g. in the proof of Lemma D.1, to obtain

$$\sum_{k=j+1}^{\ell} |x_k - x_{k-1}| = \sum_{k=j+1}^{\ell} (x_k - x_{k-1}) = x_\ell - x_j = |x_\ell - x_j|.$$

The natural ordering is lost in dimension higher than 1.

Summary

Evolution Equations for Systems Governed by Social Interactions

In this thesis, ideas from mathematical physics are used to model systems of socially interacting individuals, e.g. crowds of pedestrians, flocks of birds or schools of fish. The work presented includes modelling, analysis and numerical computations. Our main techniques are taken from partial differential equations, measure theory, semigroup theory, continuum mechanics, functional analysis and singular perturbation theory. Chapter 1 provides the framework of modelling perspectives and equations in which the rest of the thesis fits.

In Chapter 2 we introduce a field of vision in a first-order model for interacting individuals. Our objective is to guarantee existence and uniqueness of solutions to this model with included field of vision. In our model the velocity is defined implicitly. Problems arise when a solution v has no continuous extension in time. We refer to this situation as root loss in the implicit equation. To extend the evolution of our system beyond root loss we provide a selection criterion for the velocity to jump to a different root. This criterion is based on an associated singularly-perturbed second-order system. We demonstrate our procedure by a combination of theoretical and numerical results.

In Chapter 3 we derive particle schemes for continuum equations in a systematic way via a three-step approach. The exact form of the resulting equation for the particle system depends on the order in which these steps are executed.

The derivation of these schemes involves a transition to measure-valued equations. To prove convergence of solutions in the many-particle limit we use the Wasserstein distance on the space of probability measures. Solutions converge at the same rate as the one at which the initial condition is approximated. This result is not restricted to particle approximations, but holds for a general sequence of approximations to the initial condition of the limit problem.

We define flux boundary conditions in terms of measures in Chapter 4. The model considered is an evolution problem for a measure with prescribed velocity field where the flow is restricted to the unit interval. The combination of this stopped flow and an absorption term in the right-hand side of the equation results in flux boundary conditions. We also obtain these boundary conditions as the limit of an approximation by a vanishing absorptive boundary layer. While in each of the approximations mass is taken from the system in a zone of finite width, the limit corresponds to gating mass away only on the

boundary. We give the convergence rate for this approximation procedure. The analysis takes place in a framework of semigroups on measures and uses the distance induced by the dual bounded Lipschitz norm.
In Chapter 5 we generalize the results of Chapter 4 to measure-dependent velocity fields. This generalization makes interaction terms via convolution admissible. We introduce a forward-Euler-like approach. The time interval is partitioned into a number of subintervals. In each of these the velocity is prescribed based on the solution in the previous interval. Hence, the setting of Chapter 4 is applicable to each subinterval. We obtain a convergence result for the forward-Euler-like approach when the sink right-hand side is a bounded Lipschitz continuous function. This means that we can deal with boundary layers in which mass is absorbed, but not (yet) with the limit of vanishing boundary layer.
Chapter 6 is about two scenarios involving the diffusion equation in two-dimensional space. First, we consider diffusion outside of an object with prescribed flux on its boundary Γ. The exterior domain is called Ω. Secondly, we consider a point source that emits mass. We obtain mild solutions that are in principle measures, but have a density due to the regularizing effect of diffusion. To quantify the difference between the solutions of these two scenarios and their fluxes on Γ, we provide an $L^2([0,t];L^2(\Gamma))$-bound on the difference in flux on the boundary for all $t > 0$, and moreover an $L^2(\Omega)$-bound (for all time) and an $L^2([0,t];H^1(\Omega))$-bound on the difference in solutions. We conjecture at the end of Chapter 6 certain conditions under which these bounds go to zero.

Samenvatting

Evolutievergelijkingen voor systemen die worden gedreven door sociale interacties

In dit proefschrift worden ideeën uit de mathematische physica gebruikt om systemen te modelleren waarin deeltjes interacties met elkaar aangaan, bijvoorbeeld mensenmassa's, zwermen vogels of scholen vissen. Het hier gepresenteerde werk omvat modellering, analyse en numerieke berekeningen. De belangrijkste technieken zijn afkomstig uit de deelgebieden partiële differentiaalvergelijkingen, maattheorie, halfgroepentheorie, continuümmechanica, functionaalanalyse en singuliere storingsrekening. Hoofdstuk 1 geeft het algemene raamwerk van modelleerperspectieven en vergelijkingen waarin de rest van dit proefschrift past.

In Hoofdstuk 2 introduceren wij een gezichtsveld in een eerste-ordemodel voor individuën met interacties. Ons doel is om existentie en eenduidigheid te garanderen van oplossingen van het model waarin dit gezichtsveld is meegenomen. In ons model is de snelheid impliciet gedefinieerd. Er ontstaan problemen wanneer de oplossing v niet continu kan worden voortgezet in de tijd. We noemen deze situatie het verlies van een wortel in de impliciete vergelijking. Om de evolutie van ons systeem voort te zetten voorbij het punt waar we een wortel kwijtraken, geven we een selectiecriterium voor de sprong die de snelheid moet maken naar een andere wortel. Dit criterium is gebaseerd op een gerelateerd singulier verstoord tweede-ordesysteem. We zetten onze werkwijze uiteen met behulp van theoretische en numerieke resultaten.

In Hoofdstuk 3 leiden we in drie stappen systematisch deeltjesschema's af voor continuümvergelijkingen. De exacte vorm van de uiteindelijke vergelijking voor het deeltjessysteem hangt af van de volgorde waarin deze stappen worden uitgevoerd.

Om deze schema's af te leiden, is een overgang naar maatwaardige vergelijkingen nodig. We gebruiken de Wassersteinafstand op de ruimte van kansmaten om aan te tonen dat de oplossingen convergeren als het aantal deeltjes naar oneindig gaat. Oplossingen convergeren met een snelheid van gelijke orde als waarmee de beginvoorwaarde benaderd wordt. Dit resultaat beperkt zich niet tot deeltjessystemen, maar geldt voor een algemene rij benaderingen van de beginvoorwaarde van het limietprobleem.

We leiden fluxrandvoorwaarden in termen van maten af in Hoofdstuk 4. Het beschouwde model is een evolutieprobleem voor een maat met voorgeschreven snelheidsveld, waarbij de stroom is beperkt tot het eenheidsinterval. Deze gestopte stroom resulteert samen met een absorptieterm aan de rechterkant van de vergelijking in fluxrandvoorwaarden.

Dezelfde randvoorwaarden kunnen we ook verkrijgen als de limiet van een rij benaderingen waarbij de dikte van een absorberende laag naar nul gaat. Terwijl in elk van deze benaderingen massa het systeem verlaat via een gebied van eindige dikte rond de rand, wordt in de limiet alleen massa van de rand weggehaald. We geven de convergentiesnelheid voor deze approximatie. Voor de analyse gebruiken we halfgroepen op de ruimte van maten en de afstand die voortkomt uit de duale begrensde-Lipschitznorm.
In Hoofdstuk 5 veralgemeniseren we de resultaten van Hoofdstuk 4 naar maatafhankelijke snelheidsvelden. Deze veralgemenisering staat interactietermen in de vorm van een convolutie toe. We introduceren een aanpak die lijkt op de voorwaartse methode van Euler. Het tijdsinterval wordt onderverdeeld in een aantal deelintervallen. In elk van deze deelintervallen is de snelheid voorgeschreven, afhankelijk van de oplossing in het vorige interval. Derhalve zijn de resultaten uit Hoofdstuk 4 van toepassing binnen elk deelinterval. We tonen de convergentie van deze Euler-voorwaarts-geïnspireerde methode aan in het geval dat de rechterkant van de vergelijking een begrensde, Lipschitz-continue functie is. Dit betekent dat we wel absorberende gebieden van eindige dikte rond de rand kunnen beschrijven, maar (nog) niet de limiet waarin de dikte van deze laag naar nul is gegaan.
Hoofdstuk 6 gaat over twee scenario's waarin de diffusievergelijking op een twee-dimensionaal domein een rol speelt. Eerst beschouwen we diffusie aan de buitenkant van een object met voorgeschreven flux door de rand Γ. Het buitengebied heet Ω. Als tweede beschouwen we een puntbron van waaruit massa het domein binnenstroomt. We vinden milde oplossingen, die in principe maten zijn, maar die een dichtheid hebben door het regulariserende effect van de diffusie. Om het verschil tussen de oplossingen van deze twee scenario's en de bijbehorende flux door Γ te kwantificeren, geven we een $L^2([0,t];L^2(\Gamma))$-bovengrens voor alle $t>0$ voor dit verschil in flux over de rand, en een $L^2(\Omega)$-grens (voor alle tijd) en een $L^2([0,t];H^1(\Omega))$-grens voor het verschil tussen de oplossingen. Aan het einde van Hoofdstuk 6 formuleren we een vermoeden dat zegt onder welke voorwaarden deze bovengrenzen naar nul gaan.

Notation

$\mathbb{R}^+$	$(0, \infty)$
$\mathbb{R}_0^+$	$[0, \infty)$
$B(x, R)$	Open ball of radius $R > 0$ around x (in an arbitrary metric space)
$B(R)$	Short form of $B(0, R)$ (in a normed vector space)
$\mathbb{1}_E$	Indicator of the set E
$\lvert \cdot \rvert$	Absolute value of a number, Euclidean norm on $\mathbb{R}^d$, Lebesgue measure of a set, determinant of a matrix or total variation of a measure
$[\cdot]^+$	Positive part of its argument
f_t	Time-slice of f at time t (not: time-derivative of f)
JF	Jacobian matrix of $F : \mathbb{R}^d \to \mathbb{R}^d$
$\operatorname{Hess} f$	Hessian matrix of $f : \mathbb{R}^d \to \mathbb{R}$
$C_b^k(X; Y)$	Space of bounded and continuous functions from X to Y with bounded and continuous derivatives up to order k, where X can be $\mathbb{R}^d$, $\mathbb{R}_0^+$ or $[0, T] \times \mathbb{R}^d$
$C_b^k(X)$	$C_b^k(X; Y)$ with $Y = \mathbb{R}$
S	General Polish space (separable, completely metrizable topological space)
$C_b(S)$	Space of continuous and bounded functions on S, i.e. $C_b^k(S)$ with $k = 0$
$\mathrm{BL}(S)$	Space of bounded Lipschitz functions on S
$\mathcal{M}(S)$	Space of finite Borel measures on S
$\overline{\mathcal{M}}(S)$	Completion of $\mathcal{M}(S)$ in $\lVert \cdot \rVert_{\mathrm{BL}}^*$ (see below), short form of $\overline{\mathcal{M}}(S)_{\mathrm{BL}}$
$\mathcal{M}^+(S)$	Cone of positive finite Borel measures on S
$\mathcal{P}(S)$	Space of probability measures on S
$\mathcal{P}_r(\mathbb{R}^d)$	Space of probability measures on $\mathbb{R}^d$ with support in $\overline{B(r)}$
$\langle \cdot, \cdot \rangle$	Duality pairing
$\lvert \cdot \rvert_{\mathrm{L}}$	Lipschitz constant
$\lVert \cdot \rVert_{\mathrm{BL}}$	Bounded Lipschitz norm (Dudley norm): $\lVert \cdot \rVert_\infty + \lvert \cdot \rvert_{\mathrm{L}}$
$\lVert \cdot \rVert_{\mathrm{FM}}$	Fortet-Mourier norm: $\max\{\lVert \cdot \rVert_\infty, \lvert \cdot \rvert_{\mathrm{L}}\}$
$\lVert \cdot \rVert_{\mathrm{BL}}^*$	Dual bounded Lipschitz norm
$\lVert \cdot \rVert_{\mathrm{FM}}^*$	Dual Fortet-Mourier norm, induces the flat metric
$\Phi \# \mu$	Push-forward of μ by Φ
$\Pi(\mu, \nu)$	Space of joint representations of $\mu, \nu \in \mathcal{P}(\mathbb{R}^d)$
$W_p(\mu, \nu)$	p-Wasserstein distance between measures μ and ν

Index

Curriculum Vitae

Joep Evers was born on February 14, 1988 in Roermond, The Netherlands, and grew up in the nearby village of Swalmen. After finishing pre-university education (*gymnasium*) in 2006 at Bisschoppelijk College Broekhin in Roermond, he studied Industrial and Applied Mathematics at Eindhoven University of Technology. He obtained his bachelor's and master's degrees (both *cum laude*) in 2009 and 2011, respectively. His graduation project titled "Modelling Crowd Dynamics: A Multiscale, Measure-theoretical Approach" was awarded the TU/e Final Project Award 2012. In 2011 he started a PhD project at Eindhoven University of Technology, as a member of the Institute for Complex Molecular Systems (ICMS) within the NWO Graduate Programme. His daily work took place at the Centre for Analysis, Scientific computing and Applications (CASA) of the Department of Mathematics and Computer Science. The results of this research are presented in this thesis.

List of publications

Preprints:

1. J.H.M. Evers, I.A. Zisis, B.J. van der Linden and M.H. Duong. From continuum mechanics to SPH particle systems and back: Systematic derivation and convergence. `arXiv:1501.04512` (submitted), 2015.

2. J.H.M. Evers, R.C. Fetecau and L. Ryzhik. Anisotropic interactions in a first-order aggregation model: a proof of concept. `arXiv:1406.0967` (submitted), 2014.

Refereed journal papers:

3. J.H.M. Evers, S.C. Hille and A. Muntean. Mild solutions to a measure-valued mass evolution problem with flux boundary conditions. *Journal of Differential Equations*, 2015. doi:10.1016/j.jde.2015.02.037

4. J.H.M. Evers, S.C. Hille and A. Muntean. Modelling with measures: Approximation of a mass-emitting object by a point source. *Mathematical Biosciences and Engineering*, 12(2):357–373, 2015.

5. P.L. Curşeu, O. Krehel, J.H.M. Evers and A. Muntean. Cognitive distance, absorptive capacity and group rationality: A simulation study. *PLoS ONE*, 9(10):e109359, 2014.

6. J.H.M. Evers, S.C. Hille and A. Muntean. Well-posedness and approximation of a measure-valued mass evolution problem with flux boundary conditions. *Comptes Rendus Mathématique*, 352:51–54, 2014.

7. L. Gulikers, J.H.M. Evers, A. Muntean and A.V. Lyulin. The effect of perception anisotropy on particle systems describing pedestrian flows in corridors. *Journal of Statistical Mechanics: Theory and Experiment*, P04025, 2013.

8. J.H.M. Evers and A. Muntean. Modeling micro-macro pedestrian counterflow in heterogeneous domains. *Nonlinear Phenomena in Complex Systems*, 14(1):27–37, 2011.

Refereed conference proceedings papers:

9. J.H.M. Evers, A. Muntean and A.A.F. van de Ven. Crowds reaching targets by maximizing entropy: a Clausius-Duhem inequality approach. In *Proceedings of the 1st IFAC Workshop on Control of Systems Governed by Partial Differential Equations (Paris, France, September 25-27, 2013)*, pages 263–268, 2013.

Non-refereed proceedings papers:

10. C.J. Budd, J.H.M. Evers, J.E. Frank, S.W. Gaaf, R. Hoogwater, D.J.P. Lahaye, C. Meerman, E. Siero and T. van Zalen. Effective water storage as flood protection: The Rijnstrangen study case. In *Proceedings of the 90th European Study Group Mathematics with Industry, 2013*, pages 79–114, 2014.

11. J.B. van den Berg, R. Castro, J. Draisma, J.H.M. Evers, M. Hendriks, O. Krehel, I. Kryven, K. Mora, B. Szabó and P.W. Zwiernik. Non-imaging optics for LED-lighting. In *Proceedings of the 84th European Study Group Mathematics with Industry (SWI 2012)*, pages 70–103, 2013.

12. J.H.M. Evers, D. Kiss, W. Kowalczyk, T. Navilarekallu, D.R.M. Renger, L. Sella, V. Timperio, A. Viorel, A.C.C. van Wijk and A.N. Yzelman. Node counting in wireless ad-hoc networks. In *Proceedings of the 79th European Study Group Mathematics with Industry, January 24-28, 2011*, pages 49–73, 2012.

Acknowledgements

> He now flashed on an old adage from early Grecian free divers who hunted lobsters in the coral caves of the Aegean Islands. *When swimming into a dark tunnel, there arrives a point of no return when you no longer have enough breath to double back. Your only choice is to swim forward into the unknown. . . and pray for an exit.*
>
> – Dan Brown, *Inferno*,
> Transworld Publishers (2014), p. 158

There were moments in which I wondered where this 'PhD tunnel' was leading, and how I would reach the exit. However, it never even crossed my mind to swim back or give up. This is mainly due to the people mentioned here.

I wish to express my gratitude to my supervisors Adrian Muntean and Mark Peletier for encouraging, shaping and inspiring me. Whenever I was insecure or indecisive, you would readily give me a gentle push in the right direction, or a firm kick if needed. I thank you for that.

I sincerely thank the Institute for Complex Molecular Systems for giving me the opportunity to do this PhD research within the NWO Graduate Programme. In particular I acknowledge the support of managing director Sagitta Peters and the current and previous secretaries. The ICMS Animation Studio contributed to the illustrations of my thesis.

I am grateful to Razvan Fetecau for hosting me so generously at Simon Fraser University for two months and for our pleasant cooperation. Thank you, Sander Hille, for all our meetings in Leiden and Eindhoven. You are a source of knowledge, from which I benefitted to the most. I am indebted to all other committee members (Prof. José Antonio Carrillo, Prof. Barry Koren and Dr. Hans Wyss) for their efforts and for their input to improve this thesis. I thank my collaborators without whom it would not have been possible to achieve the various parts of this thesis.

I acknowledge the kind permission of the M.C. Escher Company to use the photo on the cover of this thesis and I thank Giovanni Bonaschi, Bart Gubbels and Math Reumers

for their practical help.

I wish to thank Fons van de Ven, who has seen me in this university since I was a bachelor's student. I appreciate your interest during all those years in what I was doing, your willingness to share your huge experience and your humorous, down-to-earth view on things. I thank my present and former office mates (Carlo, Oleh, Patrick and Alessandro), my co-organizers of our CASA Wednesday morning sessions (Kundan, Michiel, Corien, Sarah, Hong and Upanshu), the 'India crew' (Jeroen, Giovanni, Patrick, Upanshu and Deepesh: *Shukriya!*) and my paranymphs (Jeroen and Patrick). Of course, many thanks also go to Marèse Wolfs and Enna van Dijk: each of you is a true 'mamma di CASA'. I thank you for all your help and kindness. I thank all present and former CASA members for their suggestions and comments at various occasions and for making work feel like a home.

I am grateful for the support I received from my family (danke daoveur, Janneke, Willem en aanhang), and from my friends and relatives.

Es lètste wil ich (netuurlik) pap en mam bedanke: geur höbt mich altied laote gewaere, ich dink döks zónger zuuver te weite wo ich eigelik mit bezig woor. Zónger uch sjteun (al den neet ónger wäörd gebrach) zooj ich neet zin waem en wo ich noe bön. Ich draag dit proofsjrif den ouch op aan uch.

Bibliography

[AF03] R.A. Adams and J.J.F. Fournier. *Sobolev Spaces*. Academic Press, 2nd edition, 2003.

[AGS08] L. Ambrosio, N. Gigli, and G. Savaré. *Gradient Flows in Metric Spaces and in the Space of Probability Measures*. Birkhäuser Verlag, Basel, 2nd edition, 2008.

[AI05] A.S. Ackleh and K. Ito. Measure-valued solutions for a hierarchically size-structured population. *Journal of Differential Equations*, 217(2):431 – 455, 2005.

[AJCRB08] J.M. Arrieta, A. Jimenez-Casas, and A. Rodriguez-Bernal. Flux terms and Robin boundary conditions as limit of reactions and potentials concentrating at the boundary. *Rev. Mat. Iberoamericana*, 24:183 – 211, 2008.

[AM13] T. Aiki and A. Muntean. A free-boundary problem for concrete carbonation: Front nucleation and rigorous justification of the $\sqrt{t}$-law of propagation. *Interfaces and Free Boundaries*, 15(2):167–180, 2013.

[AP13] G. Albi and L. Pareschi. Binary interaction algorithms for the simulation of flocking and swarming dynamics. *Multiscale Model. Simul.*, 11(1):1–29, 2013.

[Bal04] P. Ball. *Critical Mass*. Farrar, Straus and Giroux, New York, 2004.

[BCC+08] M. Ballerini, N. Cabibbo, R. Candelier, A. Cavagna, E. Cisbani, I. Giardina, V. Lecomte, A. Orlandi, G. Parisi, A. Procaccini, M. Viale, and V. Zdravkovic. Interaction ruling animal collective behaviour depends on topological rather than metric distance: evidence from a field study. *Proc. Natl. Acad. Sci.*, 105:1232–1237, 2008.

[BCDP15] G.A. Bonaschi, J.A. Carrillo, M. DiFrancesco, and M.A. Peletier. Equivalence of gradient flows and entropy solutions for singular nonlocal interaction equations in 1D. *ESAIM: Control, Optimisation and Calculus of Variations*, 21(2):414–441, 2015.

[BCL09] A.L. Bertozzi, J.A. Carrillo, and T. Laurent. Blow-up in multidimensional aggregation equations with mildly singular interaction kernels. *Nonlinearity*, 22(3):683–710, 2009.

[BCLR13a] D. Balagué, J.A. Carrillo, T. Laurent, and G. Raoul. Dimensionality of local minimizers of the interaction energy. *Arch. Ration. Mech. Anal.*, 209(3):1055–1088, 2013.

[BCLR13b] D. Balagué, J.A. Carrillo, T. Laurent, and G. Raoul. Nonlocal interactions by repulsive-attractive potentials: radial ins/stability. *Physica D*, 260:5–25, 2013.

[BDF08] M. Burger and M. Di Francesco. Large time behavior of nonlocal aggregation models with nonlinear diffusion. *Netw. Heterog. Media*, 3(4):749–785, 2008.

[BDGO97] L. Boccardo, A. Dall'Anglio, Th. Gallouët, and L. Orsina. Nonlinear parabolic equations with measure data. *J. Funct. Anal.*, 147:237–258, 1997.

[Ben06] B. Ben Moussa. On the convergence of SPH mehods for scalar conservation laws with boundary conditions. *Meth. Appl. Analysis*, 13(1):29–62, 2006.

[Ber09] V.L. Berdichevsky. *Variational Principles of Continuum Mechanics; Volume I. Fundamentals*. Springer Verlag, Berlin, 2009.

[BHW13] M. Burger, J. Haškovec, and M.-Th. Wolfram. Individual based and mean-field modeling of direct aggregation. *Physica D*, 260:145–158, 2013.

[BL07] A.L. Bertozzi and T. Laurent. Finite-time blow-up of solutions of an aggregation equation in $\mathbf{R}^n$. *Comm. Math. Phys.*, 274(3):717–735, 2007.

[BLH+12] K.J.M. Boot, K.R. Libbenga, S.C. Hille, R. Offringa, and B. van Duijn. Polar auxin transport: An early invention. *Journal of Experimental Botany*, 63:4213–4218, 2012.

[BLR11] A.L. Bertozzi, T. Laurent, and J. Rosado. L^p theory for the multidimensional aggregation equation. *Comm. Pur. Appl. Math.*, 64(1):45–83, 2011.

[Bog07a] V.I. Bogachev. *Measure Theory; Volume I*. Springer, Berlin, 2007.

[Bog07b] V.I. Bogachev. *Measure Theory; Volume II*. Springer, Berlin, 2007.

[Bol08] F. Bolley. Separability and completeness for the Wasserstein distance. In *Séminaire de probabilités XLI*, volume 1934 of *Lecture Notes in Mathematics*, pages 371–377. 2008.

[BŠM03] F. Baluška, J. Šamaj, and D. Menzel. Polar transport of auxin: Carrier-mediated flux across the plasma membrane or neurotransmitter-like secretion? *Trends in Cell Biology*, 13:282–285, 2003.

[BSO12] A. Bompadre, B. Schmidt, and M. Ortiz. Convergence analysis of meshfree approximation schemes. *SIAM J. Numer. Anal.*, 50(3):1344–1366, 2012.

[But03] J.C. Butcher. *Numerical Methods for Ordinary Differential Equations*. John Wiley and Sons Ltd., 2003.

[BV05] M. Bodnar and J.J.L. Velázquez. Derivation of macroscopic equations for individual cell-based models: a formal approach. *Math. Meth. Appl. Sci.*, 28(15):1757–1779, 2005.

[BV06] M. Bodnar and J.J.L. Velázquez. An integro-differential equation arising as a limit of individual cell-based models. *J. Differential Equations*, 222(2):341–380, 2006.

[CB13] E. Cancès and C. Le Bris. Mathematical modeling of point defects in material science. *Mathematical Models and Methods in Applied Sciences*, 23:1795–1859, 2013.

[CBMT14] A. Corbetta, L. Bruno, A. Muntean, and F. Toschi. High statistics measurements of pedestrian dynamics. *Transportation Research Procedia*, 2:96–104, 2014. The Conference on Pedestrian and Evacuation Dynamics 2014 (PED 2014), 22-24 October 2014, Delft, The Netherlands.

[CC08] V. Coscia and C. Canavesio. First-order macroscopic modelling of human crowd dynamics. *Math. Mod. Meth. Appl. Sci.*, 18(suppl.):1217–1247, 2008.

[CCC13] J.A. Cañizo, J.A. Carrillo, and S. Cuadrado. Measure solutions for some models in population dynamics. *Acta Applicandae Mathematicae*, 123(1):141–156, 2013.

[CCGU12] J.A. Carrillo, R.M. Colombo, P. Gwiazda, and A. Ulikowska. Structured populations, cell growth and measure valued balance laws. *Journal of Differential Equations*, 252:3245–3277, 2012.

[CCH14] J.A. Carrillo, Y.P. Choi, and M. Hauray. The derivation of swarming models: Mean-field limit and Wasserstein distances. In *Collective Dynamics from Bacteria to Crowds*, volume 553 of *CISM International Centre for Mechanical Sciences: Courses and Lectures*, pages 1–46. Springer Vienna, 2014.

[CCR11] J.A. Cañizo, J.A. Carrillo, and J. Rosado. A well-posedness theory in measures for some kinetic models of collective motion. *Mathematical Models and Methods in Applied Sciences*, 21(3):515–539, 2011.

[CDF+03] S. Camazine, J.-L. Deneubourg, N.R. Franks, J. Sneyd, G. Theraulaz, and E. Bonabeau. *Self-Organization in Biological Systems*. Princeton Studies in Complexity. Princeton University Press, Princeton, NJ, 2003. Reprint of the 2001 original.

[CDF+11] J.A. Carrillo, M. DiFrancesco, A. Figalli, T. Laurent, and D. Slepčev. Global-in-time weak measure solutions and finite-time aggregation for nonlocal interaction equations. *Duke Math. J.*, 156:229–271, 2011.

[CDM+07] Y.-L. Chuang, M.R. D'Orsogna, D. Marthaler, A.L. Bertozzi, and L.S. Chayes. State transitions and the continuum limit for a 2D interacting, self-propelled particle system. *Physica D*, 232(1):33–47, 2007.

[CDP09] J.A. Carrillo, M.R. D'Orsogna, and V. Panferov. Double milling in self-propelled swarms from kinetic theory. *Kinet. Relat. Models*, 2(2):363–378, 2009.

[CFTV10] J.A. Carrillo, M. Fornasier, G. Toscani, and F. Vecil. Particle, kinetic, and hydrodynamic models of swarming. In *Mathematical Modeling of Collective Behavior in Socio-Economic and Life Sciences*, Model. Simul. Sci. Eng. Technol., pages 297–336. Birkhäuser Boston, Inc., Boston, MA, 2010.

[CG09] R.M. Colombo and G. Guerra. Differential equations in metric spaces with applications. *Discrete and Continuous Dynamical Systems A*, 23(3):733–753, 2009.

[CGP14] A. Colagrossi, G. Graziani, and M. Pulvirenti. Particles for fluids: SPH versus vortex methods. *Mathematics and Mechanics of Complex Systems*, 2(1):45–70, 2014.

[CH99] Th. Cazenave and A. Haraux. *An Introduction to Semilinear Evolution Equations*. Oxford University Press, Oxford, revised edition, 1999.

[Cha76] P. Chadwick. *Continuum Mechanics*. George Allen & Unwin, London, 1976.

[Cha03] P.-H. Chavanis. Generalized thermodynamics and Fokker-Planck equations: Applications to stellar dynamics and two-dimensional turbulence. *Phys. Rev. E*, 68:036108, 2003.

[CKEM14] P.L. Curşeu, O. Krehel, J.H.M. Evers, and A. Muntean. Cognitive distance, absorptive capacity and group rationality: A simulation study. *PLoS ONE*, 9(10):e109359, 2014.

[CKP10] A. Chavarría-Krauser and M. Ptashnyk. Homogenization of long-range auxin transport in plant tissues. *Nonlinear Analysis: Real World Applications*, 11:4524–4532, 2010.

[CL71] M. Crandall and T. Liggett. Generation of semi-groups of nonlinear transformations on general banach spaces. *Amer. J. Math.*, 93:265–298, 1971.

[CMV03] J.A. Carrillo, R.J. McCann, and C. Villani. Kinetic equilibration rates for granular media and related equations: Entropy dissipation and mass transportation estimates. *Rev. Mat. Iberoamericana*, 19:971–1018, 2003.

[CMV06] J.A. Carrillo, R.J. McCann, and C. Villani. Contractions in the 2-Wasserstein length space and thermalization of granular media. *Arch. Ration. Mech. Anal.*, 179(2):217–263, 2006.

[CMV15] A. Corbetta, A. Muntean, and K. Vafayi. Parameter estimation of social forces in pedestrian dynamics models via a probabilistic method. *Mathematical Biosciences and Engineering*, 12(2):337–356, 2015.

[CPT11] E. Cristiani, B. Piccoli, and A. Tosin. Multiscale modeling of granular flows with application to crowd dynamics. *Multiscale Model. Simul.*, 9(1):155–182, 2011.

[CPT14] E. Cristiani, B. Piccoli, and A. Tosin. *Multiscale Modeling of Pedestrian Dynamics*, volume 12 of *Modeling, Simulation & Applications*. Springer International Publishing Switzerland, 2014.

[DH13] W. Daamen and S.P. Hoogendoorn. Estimating model parameters for bottlenecks in evacuation conditions. In *Traffic and Granular Flow '11*, pages 121–127, 2013.

[Dho96] J.K.G. Dhont. *An Introduction to Dynamics of Colloids*, volume 2 of *Studies in Interface Science*. Elsevier, Amsterdam, 1996.

[DHP03] R. Denk, M. Hieber, and J. Prüss. $\mathcal{R}$-boundedness, Fourier multipliers and problems of elliptic and parabolic type. *Mem. Am. Math. Soc.*, 166(788):viii+114 pp., 2003.

[DHP07] R. Denk, M. Hieber, and J. Prüss. Optimal L^p-L^q-estimates for parabolic boundary value problems with inhomogeneous data. *Math. Z.*, 257:193–224, 2007.

[DL00] R. Dautray and J.-L. Lions. *Mathematical Analysis and Numerical Methods for Science and Technology; Volume 6, Evolution Problems II*. Springer, Berlin Heidelberg, 2000.

[DPZ14] M.H. Duong, M.A. Peletier, and J. Zimmer. Conservative-dissipative approximation schemes for a generalized Kramers equation. *Math. Meth. Appl. Sci.*, 37(16):2517–2540, 2014.

[DU77] J. Diestel and J.J. Uhl jr. *Vector Measures*. Amer. Math. Soc., Providence, 1977.

[Dud66] R.M. Dudley. Convergence of Baire measures. *Stud. Math.*, 27:251–268, 1966.

[Dud74] R.M. Dudley. Correction to: "Convergence of Baire measures". *Stud. Math.*, 51:275, 1974.

[Dud04] R.M. Dudley. *Real Analysis and Probability*. Cambridge University Press, 2004.

[DZ03] Q. Du and P. Zhang. Existence of weak solutions to some vortex density models. *SIAM J. Math. Anal.*, 34(6):1279–1299 (electronic), 2003.

[EFR14] J.H.M. Evers, R.C. Fetecau, and L. Ryzhik. Anisotropic interactions in a first-order aggregation model: a proof of concept. `arXiv:1406.0967` (submitted), 2014.

[EHM14] J.H.M. Evers, S.C. Hille, and A. Muntean. Well-posedness and approximation of a measure-valued mass evolution problem with flux boundary conditions. *Comptes Rendus Mathématique*, 352:51–54, 2014.

[EHM15a] J.H.M. Evers, S.C. Hille, and A. Muntean. Mild solutions to a measure-valued mass evolution problem with flux boundary conditions. *Journal of Differential Equations*, 2015. doi:10.1016/j.jde.2015.02.037.

[EHM15b] J.H.M. Evers, S.C. Hille, and A. Muntean. Modelling with measures: Approximation of a mass-emitting object by a point source. *Mathematical Biosciences and Engineering*, 12(2):357–373, 2015.

[EM11] J.H.M. Evers and A. Muntean. Modeling micro-macro pedestrian counterflow in heterogeneous domains. *Nonlinear Phenomena in Complex Systems*, 14(1):27–37, 2011.

[EMvdV13] J.H.M. Evers, A. Muntean, and A.A.F. van de Ven. Crowds reaching targets by maximizing entropy: a Clausius-Duhem inequality approach. In *Proceedings of the 1st IFAC Workshop on Control of Systems Governed by Partial Differential Equations*, pages 263–268, 2013.

[EN00] K.-J. Engel and R. Nagel. *One-Parameter Semigroups for Linear Evolution Equations*. Springer-Verlag, New York, 2000.

[Eva10] L.C. Evans. *Partial Differential Equations*, volume 19 of *Graduate Studies in Mathematics*. American Mathematical Society, Providence, RI, 2nd edition, 2010.

[EZvdLD15] J.H.M. Evers, I.A. Zisis, B.J. van der Linden, and M.H. Duong. From continuum mechanics to SPH particle systems and back: Systematic derivation and convergence. `arXiv:1501.04512` (submitted), 2015.

[FGHS07] G. Fibich, I. Gannot, A. Hammer, and S. Schochet. Chemical kinetics on surfaces: A singular limit of a reaction-diffusion system. *SIAM J. Math. Anal.*, 38(5):1371–1388, 2007.

[FH13] R.C. Fetecau and Y. Huang. Equilibria of biological aggregations with nonlocal repulsive-attractive interactions. *Physica D*, 260:49–64, 2013.

[FHK11] R.C. Fetecau, Y. Huang, and T. Kolokolnikov. Swarm dynamics and equilibria for a nonlocal aggregation model. *Nonlinearity*, 24(10):2681–2716, 2011.

[Fil88] A. F. Filippov. *Differential Equations with Discontinuous Righthand Sides*, volume 18 of *Mathematics and its Applications (Soviet Series)*. Kluwer Academic Publishers Group, Dordrecht, 1988. Translated from Russian.

[FM53] R. Fortet and E. Mourier. Convergence de la répartition empirique vers la répartition théorique. *Ann. Sci. E.N.S.*, 70(3):276–285, 1953.

[Fol99] G.B. Folland. *Real Analysis: Modern Techniques and Their Applications*. John Wiley and Sons, New York, 2nd edition, 1999.

[FR10] K. Fellner and G. Raoul. Stable stationary states of non-local interaction equations. *Math. Models Methods Appl. Sci.*, 20(12):2267–2291, 2010.

[Fri44] K.O. Friedrichs. The identity of weak and strong extensions of differential operators. *Trans. Amer. Math. Soc.*, 55:132–151, 1944.

[Fro12] A. Frouvelle. A continuum model for alignment of self-propelled particles with anisotropy and density-dependent parameters. *Math. Models Methods Appl. Sci.*, 22(7):1250011, 40, 2012.

[FS14] R.C. Fetecau and W. Sun. First-order aggregation models and zero inertia limits. `arXiv:1410.7095` (submitted), 2014.

[FW14] D. Florea and H.M. Wyss. Towards the self-assembly of anisotropic colloids: Monodisperse oblate ellipsoids. *Journal of Colloid and Interface Science*, 416:30–37, 2014.

[GEML13] L. Gulikers, J.H.M. Evers, A. Muntean, and A.V. Lyulin. The effect of perception anisotropy on particle systems describing pedestrian flows in corridors. *Journal of Statistical Mechanics: Theory and Experiment*, page P04025, 2013.

[GJMC12] P. Gwiazda, G. Jamróz, and A. Marciniak-Czochra. Models of discrete and continuous cell differentiation in the framework of transport equation. *SIAM J. Math. Anal.*, 44(2):1103–1133, 2012.

[GLMC10] P. Gwiazda, T. Lorenz, and A. Marciniak-Czochra. A nonlinear structured population model: Lipschitz continuity of measure-valued solutions with respect to model ingredients. *Journal of Differential Equations*, 248:2703–2735, 2010.

[GM78] R.A. Gingold and J.J. Monaghan. Binary fission in damped rotating polytropes. *Monthly Notices of the Royal Astronomical Society*, 184:481–499, 1978.

[GPF+15] A. Garcimartín, J.M. Pastor, L.M. Ferrer, J.J. Ramos, C. Martín-Gómez, and I. Zuriguel. Flow and clogging of a sheep herd passing through a bottleneck. *Phys. Rev. E*, 91:022808, 2015.

[GPK12] B.D. Goddard, G.A. Pavliotis, and S. Kalliadasis. The overdamped limit of dynamic density functional theory: rigorous results. *Multiscale Model. Simul.*, 10(2):633–663, 2012.

[GPPS13] M.G.D. Geers, R.H.J. Peerlings, M.A. Peletier, and L. Scardia. Asymptotic behaviour of a pile-up of infinite walls of edge dislocations. *Arch. Rational Mech. Anal.*, 209:495–539, 2013.

[GPS01] H. Goldstein, C.P. Poole, and J.L. Safko. *Classical Mechanics*. Addison-Wesley, 3rd edition, 2001.

[Gua] Festivalgoers killed in stampede at Love Parade in Germany. *The Guardian*. Published online 24 July 2010. URL: `http://www.theguardian.com/world/2010/jul/24/love-parade-festival-tunnel-stampede`.

[Gur93] M. Gurtin. *Thermomechanics of Evolving Phase Boundaries in the Plane*. Oxford University Press, Oxford, 1993.

[Hai92] J.M. Haile. *Molecular Dynamics Simulation: Elementary Methods*. John Wiley and Sons, New York, 1992.

[Hal59] P.R. Halmos. *Measure Theory*. D. van Nostrand, Princeton, NJ, 1959.

[Har10] S. Haret. *Mécanique sociale*. Gauthier-Villars, Paris, 1910.

[HB10] Y. Huang and A.L. Bertozzi. Self-similar blowup solutions to an aggregation equation in $\mathbb{R}^n$. *SIAM J. Appl. Math.*, 70(7):2582–2603, 2010.

[HB11] D. Hull and D.J. Bacon. *Introduction to Dislocations*. Elsevier, 5th edition, 2011.

[HD07] S.P. Hoogendoorn and W. Daamen. Microscopic calibration and validation of pedestrian models: cross-comparison of models using experimental data. In *Traffic and Granular Flow '05*, pages 329–340, 2007.

[Hil05] S.C. Hille. Continuity of the restriction of C_0-semigroups to invariant banach subspaces. *Integr. Equ. Oper. Theory*, 53:597–601, 2005.

[Hil08] S.C. Hille. Local well-posedness of kinetic chemotaxis models. *Journal of Evolution Equations*, 8:423–448, 2008.

[HM95] D. Helbing and P. Molnár. Social force model for pedestrian dynamics. *Phys. Rev. E*, 51(5):4282–4286, 1995.

[HNT10] N. Hirokawa, S. Niwa, and Y. Tanaka. Molecular motors in neurons: Transport mechanisms and roles in brain function, development, and disease. *Neuron*, 68:610–638, 2010.

[Hoo13] R. Hoogwater. Non-linear Structured Population Models: An Approach with Semigroups on Measures and Euler's Method. Master's thesis, Leiden University, February 2013.

[HP06] D.D. Holm and V. Putkaradze. Formation of clumps and patches in selfaggregation of finite-size particles. *Physica D.*, 220(2):183–196, 2006.

[HW09a] S.C. Hille and D.T.H. Worm. Continuity properties of Markov semigroups and their restrictions to invariant L^1-spaces. *Semigroup Forum*, 79:575–600, 2009.

[HW09b] S.C. Hille and D.T.H. Worm. Embedding of semigroups of Lipschitz maps into positive linear semigroups on ordered Banach spaces generated by measures. *Integr. Equ. Oper. Theory*, 63:351–371, 2009.

[IK10] K. Ishijima and M. Kimura. Truncation error analysis of finite difference formulae in meshfree particle methods. *Trans. Japan Soc. Indust. Appl. Math.*, 20(3):165–182, 2010. (in Japanese).

[Jac75] J.D. Jackson. *Classical Electrodynamics*. John Wiley and Sons, New York-London-Sydney, 2nd edition, 1975.

[JCRB11] A. Jimenez-Casas and A. Rodriguez-Bernal. Dynamic boundary conditions as limit of singularly perturbed parabolic problems. *DCDS Supplements, Special issue*, pages 737–746, 2011.

[JMC13] J. Jablonski and A. Marciniak-Czochra. Efficient algorithms computing distances between Radon measures on $\mathbb{R}$. `arXiv:1304.3501v1` (submitted), 2013.

[JN82] H.M. Jäger and S.R. Nagel. Physics of the granular state. *Science*, 255:1523–1531, 1982.

[KH12] H. Kunz and C.K. Hemelrijk. Simulations of the social organization of large schools of fish whose perception is obstructed. *Appl. Anim. Behav. Sci.*, 138:142–151, 2012.

[Kos04] W.A.J. Kosmala. *A Friendly Introduction to Analysis*. Pierson Prentice Hall, Upper Saddle River, 2nd edition, 2004.

[Kra40] H.A. Kramers. Brownian motion in a field of force and the diffusion model of chemical reactions. *Physica*, 7(4):284–304, 1940.

[Kra08] E.M. Kramer. Computer models of auxin transport: A review and commentary. *Journal of Experimental Botany*, 59:45–53, 2008.

[Kre78] E. Kreyszig. *Introductory Functional Analysis with Applications*. John Wiley and Sons, New York, 1978.

[KS07] L.B. Koralov and Y.G. Sinai. *Theory of Probability and Random Processes*. Springer-Verlag, Berlin Heidelberg, 2nd edition, 2007.

[KSUB11] T. Kolokolnikov, H. Sun, D. Uminsky, and A.L. Bertozzi. Stability of ring patterns arising from two-dimensional particle interactions. *Phys. Rev. E, Rapid Communications*, 84:015203(R), 2011.

[Las80] I. Lasiecka. Unified theory for abstract boundary problems – a semigroup approach. *Appl. Math. Optim.*, 6:287–333, 1980.

[LE97] Y. Liu and R.H. Edwards. The role of vesicular transport proteins in synaptic transmission and neural degeneration. *Ann. Rev. Neurosci.*, 20:125–156, 1997.

[LGP97] R. Di Lisio, E. Grenier, and M. Pulvirenti. On the regularization of the pressure field in compressible Euler equations. *Ann. Scu. Norm. Sup. Pisa*, 24(2):227–238, 1997.

[LGP98] R. Di Lisio, E. Grenier, and M. Pulvirenti. The convergence of the SPH method. *Computers Math. Applic.*, 35:95–102, 1998.

[LM72] J.D. Lions and E. Magenes. *Non-Homogeneous Boundary Value Problems and Applications*. Springer Verlag, 1972.

[LMS02] A. Lasota, J. Myjak, and T. Szarek. Markov operators with a unique invariant measure. *J. Math. Anal. Appl.*, 276:343–356, 2002.

[LRS96] B.J. Leimkuhler, S. Reich, and R.D. Skeel. Integration methods for molecular dynamics. In *Mathematical Approaches to Biomolecular Structure and Dynamics*, volume 82 of *The IMA Volumes in Mathematics and its Applications*, pages 161–185. Springer, New York, 1996.

[LRS10] T. Lelièvre, M. Rousset, and G. Stoltz. *Free Energy Computations: A Mathematical Perspective*. Imperial College Press, London, 2010.

[LT04] H. Li and G. Toscani. Long-time asymptotics of kinetic models of granular flows. *Archive for Rational Mechanics and Analysis*, 172(3):407–428, 2004.

[LTB09] A.J. Leverentz, C.M. Topaz, and A.J. Bernoff. Asymptotic dynamics of attractive-repulsive swarms. *SIAM J. Appl. Dyn. Syst.*, 8(3):880–908, 2009.

[Lun95] A. Lunardi. *Analytic Semigroups and Optimal Regularity in Parabolic Problems*. Birkhäuser, Basel, 1995.

[Löw10] H. Löwen. Particle-resolved instabilities in colloidal dispersions. *Soft Matter*, 6:3133–3142, 2010.

[MB09] A. Muntean and M. Böhm. A moving-boundary problem for concrete carbonation: global existence and uniqueness of weak solutions. *Journal of Mathematical Analysis and Applications*, 350(1):234–251, 2009.

[McC97] R.J. McCann. A convexity principle for interacting gases. *Advances in Mathematics*, 128:153–179, 1997.

[MCKB14] A. Muntean, E.N.M. Cirillo, O. Krehel, and M. Böhm. Pedestrians moving in the dark: Balancing measures and playing games on lattices. In *Collective Dynamics from Bacteria to Crowds*, volume 553 of *CISM International Centre for Mechanical Sciences: Courses and Lectures*, pages 75–103. Springer Vienna, 2014.

[MCO05] D. Morale, V. Capasso, and K. Oelschläger. An interacting particle system modeling aggregation behavior: from individuals to populations. *J. Math. Biol.*, 50:49–66, 2005.

[MdPIB07] R.M.H. Merks, Y. Van de Peer, D. Inzé, and G.T.S. Beemster. Canalization without flux sensors: A traveling-wave hypothesis. *Trends in Plant Science*, 12:384–390, 2007.

[MEK99] A. Mogilner and L. Edelstein-Keshet. A non-local model for a swarm. *J. Math. Biol.*, 38:534–570, 1999.

[Mon05] J.J. Monaghan. Smoothed particle hydrodynamics. *Rep. Prog. Phys.*, 68:1703–1759, 2005.

[Mon12] J.J. Monaghan. Smoothed particle hydrodynamics and its diverse applications. *Annu. Rev. Fluid Mech.*, 44:323–346, 2012.

[MR13] J.J. Monaghan and A. Rafiee. A simple SPH algorithm for multi-fluid flow with high density ratios. *International Journal for Numerical Methods in Fluids*, 71:537–561, 2013.

[MRtT05] R.M.M. Mattheij, S.W. Rienstra, and J.H.M. ten Thije Boonkkamp. *Partial Differential Equations: Modeling, Analysis, Computation*. SIAM Monographs on Mathematical Modeling and Computation. SIAM, Philadelphia, 2005.

[MS08] C. Muratov and S. Shvartsman. Boundary homogenization for periodic arrays of absorbers. *Multiscale Model. Simul.*, 7(1):44–61, 2008.

[Nel67] E. Nelson. *Dynamical Theories of Brownian Motion*. Princeton University Press, Princeton, New Jersey, 1967.

[Oel90] K. Oelschläger. Large systems of interacting particles and the porous medium equation. *Journal of Differential Equations*, 88:294–346, 1990.

[Oel91] K. Oelschläger. On the connection between Hamiltonian many-particle systems and the hydrodynamical equations. *Arch. Rational Mech. Anal.*, 115:297–310, 1991.

[Pav14] G.A. Pavliotis. *Stochastic Processes and Applications: Diffusion Processes, the Fokker-Planck and Langevin Equations*, volume 60 of *Texts in Applied Mathematics*. Springer, New York, 2014.

[Paz83] A. Pazy. *Semigroups of Linear Operators and Applications to Partial Differential Equations*. Springer-Verlag, New York, New York, 1983.

[PK99] J.K. Parrish and L.E. Keshet. Complexity, pattern, and evolutionary trade-offs in animal aggregation. *Science*, 284:99–101, 1999.

[Por12] A. Portuondo y Barceló. *Apuntes sobre Mecánica Social*. Establecimiento Topográfico Editorial, Madrid, 1912.

[PR13] B. Piccoli and F. Rossi. Transport equation with nonlocal velocity in Wasserstein spaces: convergence of numerical schemes. *Acta Applicandae Mathematicae*, 124(1):73–105, 2013.

[Pri12] D.J. Price. Smoothed particle hydrodynamics and magnetohydrodynamics. *Journal of Computational Physics*, 231(3):759–794, 2012.

[QBL06] N.J. Quinlan, M. Basa, and M. Lastiwka. Truncation error in mesh-free particle methods. *Int. J. Numer. Meth. Engng.*, 66:2064–2085, 2006.

[Rav85] P.A. Raviart. An analysis of particle methods. In *Numerical Methods in Fluid Dynamics*, volume 1127 of *Lecture Notes in Mathematics*, pages 243–324. 1985.

[Rav13] J.A. Raven. Polar auxin transport in relation to long-distance transport of nutrients in the Charales. *Journal of Experimental Botany*, 64:1–9, 2013.

[Ren13] D.R.M. Renger. *Microscopic Interpretation of Wasserstein Gradient Flows*. PhD thesis, Eindhoven University of Technology, 2013.

[Rie28] M. Riesz. Sur les fonctions conjuguées. *Math. Z.*, 27:218–244, 1928.

[RKM03] U. Rüde, H. Köstler, and M. Mohr. Accurate multigrid techniques for computing singular solutions of elliptic problems. In *Eleventh Copper Mountain Conference on Multigrid Methods*, 2003.

[Sch02] T. Schlick. *Molecular Modeling and Simulation: An Interdisciplinary Guide*, volume 21 of *Interdisciplinary Applied Mathematics*. Springer, New York, 2002.

[Sch14] B. Schmidt. On the infinite particle limit in Lagrangian dynamics and convergence of optimal transportation meshfree methods. *Multiscale Model. Simul.*, 12(1):265–289, 2014.

[SGTK12] T.I. Seidman, M.K. Gobbert, D.W. Trott, and M. Kružík. Finite element approximation for time-dependent diffusion with measure-valued source. *Numer. Math.*, 122:709–723, 2012.

[SK81] R. Seidl and W. Kaiser. Visual field size, binocular domain and the ommatidial array of the compound eyes in worker honey bees. *J. Comp. Physiol. A*, 143:17–26, 1981.

[Sol65] V.A. Solonnikov. On boundary value problems for linear parabolic systems of differential equations of general form. *Trudy Mat. Fust. Steklov*, 83:3–163, 1965. In Russian; Engl. Transl.: *Proc. Steklov Inst. Math.*, 83:1–184, 1965.

[Ste70] E.M. Stein. *Singular Integrals and Differentiability Properties of Functions*. Princeton University Press, Princeton, New Jersey, 1970.

[Sue] Die Ohnmacht der Masse. *Süddeutsche Zeitung*. Published online 27 July 2010. URL: `http://www.sueddeutsche.de/panorama/tragoedie-bei-der-loveparade-die-ohnmacht-der-masse-1.979439`.

[SW68] R.L. Seliger and G.B. Whitham. Variational principles in continuum mechanics. *Proc. Roy. Soc. A*, 305:1–25, 1968.

[Tag] Loveparade-Ermittlungen: Einige Tote wurden doch im Tunnel gefunden. *Der Tagesspiegel*. Published online 30 July 2010. URL: `http://www.tagesspiegel.de/weltspiegel/loveparade-ermittlungen-einige-tote-wurden-doch-im-tunnel-gefunden/1893462.html?view=print`.

[Tai04] K. Taira. *Semigroups, Boundary Value Problems and Markov Processes*. Springer Verlag, Berlin, 2004.

[Tay06] M.E. Taylor. *Measure Theory and Integration*, volume 76 of *Graduate Studies in Mathematics*. American Mathematical Society, Providence, RI, 2006.

[TBL06] C.M. Topaz, A.L. Bertozzi, and M.A. Lewis. A nonlocal continuum model for biological aggregation. *Bull. Math. Bio.*, 68:1601–1623, 2006.

[Tes12] G. Teschl. *Ordinary Differential Equations and Dynamical Systems*, volume 140 of *Graduate Studies in Mathematics*. American Mathematical Society, Providence, RI, 2012.

[TGCD03] G. Theraulaz, J. Gautrais, S. Camazine, and J.-L. Deneubourg. The formation of spatial patterns in social insects: from simple behaviors to complex structures. *Phil. Trans. R. Soc. Lond.*, 361:1263–1282, 2003.

[Tik52] A. N. Tikhonov. Systems of differential equations containing small parameters in the derivatives. *Mat. Sb. (N.S.)*, 31(73):575–586, 1952.

[Vas63] A.B. Vasil′eva. Asymptotic behaviour of solutions of certain problems for ordinary non-linear differential equations with a small parameter multiplying the highest derivatives. *Uspekhi Mat. Nauk*, 18(3(111)):15–86, 1963.

[vBdBStT13] K. van Berkel, R.J. de Boer, B. Scheres, and K. ten Tusscher. Polar auxin transport: Models and mechanisms. *Development*, 140:2253–2268, 2013.

[vBU12] J.H. von Brecht and D. Uminsky. On soccer balls and linearized inverse statistical mechanics. *J. Nonlinear Sci.*, 22(6):935–959, 2012.

[vBUKB12] J.H. von Brecht, D. Uminsky, T. Kolokolnikov, and A.L. Bertozzi. Predicting pattern formation in particle interactions. *Math. Models Methods Appl. Sci.*, 22(Supp. 1):1140002, 2012.

[Vil03] C. Villani. *Topics in Optimal Transportation*, volume 58 of *Graduate Studies in Mathematics*. American Mathematical Society, Providence, RI, 2003.

[Vil09] C. Villani. *Optimal Transport: Old and New*. Springer, Berlin-Heidelberg, 2009.

[vMM14] P. van Meurs and A. Muntean. Upscaling of the dynamics of dislocation walls. *Advances in Mathematical Sciences and Applications*, 24(2):401–414, 2014.

[vMMP14] P. van Meurs, A. Muntean, and M.A. Peletier. Upscaling of dislocation walls in finite domains. *Eur. J. Appl. Math.*, 25:749–781, 2014.

[vS06] M. von Smoluchowski. Zur kinetischen Theorie der Brownschen Molekularbewegung und der Suspensionen. *Annalen der Physik*, 326(14):756–780, 1906.

[vS17] M. von Smoluchowski. Versuch einer mathematischen Theorie der Koagulationskinetik kolloider Lösungen. *Zeitschrift f. physik. Chemie*, 92:129–168, 1917.

[Š94] H. Šikić. Nonlinear perturbations of positive semigroups. *Semigroup Forum*, 48:273–302, 1994.

[VWR+11] T. Vissers, A. Wysocki, M. Rex, H. Löwen, C.P. Royall, A. Imhof, and A. van Blaaderen. Lane formation in driven mixtures of oppositely charged colloids. *Soft Matter*, 7:2352–2356, 2011.

[Wor10] D.T.H. Worm. *Semigroups on Spaces of Measures*. PhD thesis, Leiden University, 2010.

[Zah00] R. Zaharopol. Fortet-Mourier norms associated with some iterated function systems. *Stat. Prob. Letters*, 50:149–154, 2000.

[ZKSS12] J. Zhang, W. Klingsch, A. Schadschneider, and A. Seyfried. Ordering in bidirectional pedestrian flows and its influence on the fundamental diagram. *Journal of Statistical Mechanics: Theory and Experiment*, page P02002, 2012.

[ZvdLGK14] I. Zisis, B. van der Linden, C. Giannopapa, and B. Koren. On the derivation of SPH schemes for shocks through inhomogeneous media. (Submitted), 2014.